UTS UNIVERSITY OF TECHNOLOGY SYDNEY

MODELLING SOIL EROSION HAZARDS AND CROP DIVERSITY CHANGES DUE TO CLIMATE VARIATION IN FARMING SYSTEMS AT CENTRAL HIGHLANDS IN SRI LANKA USING GEO- INFORMATICS TECHNOLOGIES

by Sumudu Sangeethika Senanayake

Thesis submitted in fulfilment of the requirements for the degree of

Doctor of Philosophy

under the supervision of

Distinguished Professor Biswajeet Pradhan

Distinguished Professor Alfredo Huete

Dr Jane Brennan

University of Technology Sydney
Faculty of Engineering and Information Technology

July 2023

CERTIFICATE OF ORIGINAL AUTHORSHIP

I, ***Sumudu Sangeethika Senanayake*** declare that this thesis, is submitted in fulfilment of the requirements for the award of ***Doctor of Philosophy***, in the School of Civil and Environmental Engineering, Faculty of Engineering and Information Technology at the University of Technology Sydney.

This thesis is wholly my own work unless otherwise referenced or acknowledged. In addition, I certify that all information sources and literature used are indicated in the thesis.

This document has not been submitted for qualifications at any other academic institution.

This research is supported by the Australian Government Research Training Program.

Signature: Production Note:
Signature removed prior to publication.

Date: 07/07/2023

DEDICATION

THIS WORK IS DEDICATED TO

MY LOVING MOTHER AND MY LATE MOTHER IN-LAW

ACKNOWLEDGMENT

It is a great pleasure to give my gratitude those who support to achieve this work. First of all, I am thankful to University of Technology Sydney providing opportunity and financial support to carry out my research in Australia during this pandemic period.

I would like to express my deep and sincere gratitude to my principal supervisor Distinguished Professor Biswajeet Pradhan for giving me the opportunity to research under his guidance. His, great supervision, encouragement and invaluable knowledge directed me to achieve the best outcome for this research. Further to this I would like to extend my heartfelt gratitude my co-supervisors Distinguished Professor Alfredo Huete and Dr Jane Brennan for their scholarly advices, great support and encouraging words throughout this time.

Most importantly, I would like to thank my husband Dr Haritha Wedathanthirige for his greatest support during my PhD journey. He always encouraged and helped me to come out of critique and uncertainties. His love, encouragement, and understanding gave a real achievement in this journey.
I also like to sincerely thank my beloved mother and our family members in Sri Lanka who always gave caring and affection at every time.

I would like to give special thanks to my senior officers in my workplace in Sri Lanka, Mr. Wattuhewa, Dr Ajantha De Silva, Dr Wickramasinghe, Mr Munasinghe, Mr Kandaragamage and staff of the Natural Resources Management Center, Department of Agriculture, Sri Lanka.

There are many other people I should thanks in my school at UTS. My thesis committee; Dr Chakraborthi, and Professor Babak Abedin, Professor Andrea Trianni, Distinguished Professor T.M. Indra Mahalia Professor Ghassan Beydoun, and Ms Indrawathi, staff of the Schools of Information Systems and Modelling and Civil engineering, the IT section and Graduate Research School. Thank you very much for all the advice and support during this journey.

I am thankful to my friends Sahar, Abhirup, Ratirangan, Hossein, Mariym, Husam, Ahamad, Abdulfasar, Nuwan and Kavidi. Sahar thank you very much for being with me all the time.

Last but not least to our family friends in Australia Ravi Ayya and Thushari, Upil ayya and Nangi, Thushara and Rohini thank you so much being with us, especially during the hard pandemic situation.

PUBLICATIONS

Journal articles

1. **Senanayake, S.,** Pradhan, B., Huete, A., Brennan, J., 2020a. Assessing Soil Erosion Hazards Using Land-Use Change and Landslide Frequency Ratio Method: A Case Study of Sabaragamuwa Province, Sri Lanka. Remote Sens. 12, 1483. https://doi.org/10.3390/rs12091483

2. **Senanayake, S.,** Pradhan, B., Huete, A., Brennan, J., 2020b. A Review on Assessing and Mapping Soil Erosion Hazard Using Geo-Informatics Technology for Farming System Management. Remote Sens. 12, 4063. https://doi.org/10.3390/rs12244063

3. **Senanayake, S.,** Pradhan, B., Huete, A., Brennan, J., 2021. Proposing an ecologically viable and economically sound farming system using a matrix-based geo-informatics approach. Sci. Total Environ. 794, 148788. https://doi.org/10.1016/j.scitotenv.2021.148788

4. **Senanayake, S.,** Pradhan, B., Huete, A., Brennan, J., 2022. Spatial modeling of soil erosion hazards and crop diversity change with rainfall variation in the Central Highlands of Sri Lanka. Sci. Total Environ. 806, 150405. https://doi.org/10.1016/j.scitotenv.2021.150405

5.**Senanayake, S.,** Pradhan, B., 2022. Predicting soil erosion susceptibility associated with climate change scenarios in the Central Highlands of Sri Lanka. J. Environ. Manage. 308, 114589. https://doi.org/10.1016/j.jenvman.2022.114589

6. **Senanayake, S.,** Pradhan, B., Alamri, A., Park, H.-J., 2022. A new application of deep neural network (LSTM) and RUSLE models in soil erosion prediction. Sci. Total Environ. 845, 157220. https://doi.org/10.1016/j.scitotenv.2022.157220

Conference presentations

Senanayake, S., Pradhan, B., 2022. Soil erosion susceptibility to rainfall variation in the farming systems of the Central Highlandsof Sri Lanka, in: Soil Erosion Workshop 2022- Soil Erosion for the EU- Technical Working Groups: WG Erosion. European Soil Data Centre (ESDAC), p. 101.

Senanayake. S., 2022. Soil erosion monitoring in support of achieving SDGs | Agriculture Conferences 2022 | Agriculture and Horticulture Conference | Agri 2022 [WWW Document]. 2nd Ed. Glob. Conf. Agric. Hortic. URL https://agri-conferences.com/program/scientific-program/2022/soil-erosion-monitoring-in-support-of-achieving-sdgs (accessed 7.26.22).

Senanayake, S., Pradhan, B., Huete, A., Brennan, J., 2019, Poster presentation in 23rd international congress on modelling and simulation (MODSIM) Canberra, Australia from 1-6 December 2019 (https://modsim2019.exordo.com)

Awards

Women in AI awards 2023 Asia-Pasific Climate in AI award finalist.
(https://www.womeninai.co/waiawards2023apac)

Post Thesis Scholarship winner, Round 4, 2022, Faculty of Engineering and Technology, University of Technology Sydney, Sydney.

All the aforementioned papers have been published during my Ph.D. candidature.

TABLE OF CONTENTS

CERTIFICATE OF ORIGINAL AUTHORSHIP i

ACKNOWLEDGMENT iii

PUBLICATIONS v

TABLE OF FIGURES x

LIST OF TABLES xiv

ACRONYMS xvi

ABSTRACT xvii

CHAPTER 1 1

INTRODUCTION 1

1.1 Overview 1
1.2 Research background 1
1.3 Problem statement 2
1.4 Motivation behind the thesis 3
1.5 Research aims and objectives 6
1.6 Research questions 6
1.7 Research significance 6
1.8 Scope of the study 7
1.9 Thesis organisation 8

CHAPTER 2 10

LITERATURE REVIEW 10

2.1 Overview 10
2.2 Soil erosion in farming systems 10
2.2.1 Water erosion 11
2.2.2 Major causative factors of water erosion 13
2.3 Soil erosion hazards 16
2.4 Soil erosion assessment 17
2.4.1 Traditional soil erosion models 18
2.4.2 Advancement of soil erosion assessment using geo-informatics techniques 20
2.5 Spatial and temporal detection and predictions of soil erosion hazards 31
2.5.1 Gully Erosion vulnerability assessment 31
2.5.2 Landslides vulnerability assessment 34
2.6 Land use change detection in Farming systems 37
2.6.1 Land transformation model 39
2.6.2 Spectral angle mapper 39
2.6.3 Terrestrial laser scanning 39

2.6.4 Decision tree model 39
2.7 Crop diversity changes and soil erosion 40
2.7.1 Crop diversity change assessment in geo-informatics environment 41
2.8 Validation methods 46
2.9 Soil erosion management strategies in farming systems 47
2.10 Challenges, innovations and future directions 49
2.11 Gaps in the literature and summary 50

CHAPTER 3 54

MATERIALS AND METHODOLOGY 54

3.1 Overview 54
3.2 Study area 54
3.3 Data and software 56
3.4 Overall methodology 57
3.5 Implementation of the methodology 58
3.5.1 Objective 1: 58
3.5.2 Objective 2 80
3.5.3 Objective 3 88
3.5.4 Objective 4 101
3.6 Summary 117

CHAPTER 4 119

RESULTS AND DISCUSSION 119

4.1 Overview 119
4.2 Objective 1 119
4.2.1 Land-use and land-cover change in the Central Highlands 119
4.2.2 Demarcation of farming systems 121
4.2.3 Soil erosion in the Central Highlands 123
4.2.4 Soil erosion hazards in the Central Highlands 126
4.2.5. The case study on assessing soil erosion hazards in Sabaragamuwa Province 128
4.2.6 Crop diversity change in the farming systems 139
4.3 Objective 2 154
4.3.1 The extreme rainfall analysis 154
4.3.2 Standard precipitation index 157
4.5.3 Rainfall anomaly index 158
4.5.4 Innovative trend analysis 159
4.5.5 The relationship between rainfall variation and soil erosion hazards 163
4.6 Objective 3 166
4.6.1 Determination of criteria indicators 166
4.6.2 Determination of weights for criteria indicators 169
4.6.3 Assessing ecologically viable farming systems 170
4.6.4 Assessing economically sound farming systems 172

4.6.5 Classification of ecologically viable and economically sound farming systems 174
4.7 Objective 4 179
4.7.1 Soil erosion susceptibility mapping and model performance in RUSLE method 179
4.7.2 Frequency ratio method 182
4.7.3 Artificial neural network method 184
4.7.4 Support vector machine learning method 185
4.7.5 Adaptive neuro-fuzzy inference system method 185
4.7.6 Validation of susceptibility maps 187
4.7.7 Relative importance of the soil erosion conditioning factors 189
4.7.8. LSTM model 192
4.9 Summary 200

CHAPTER 5 203

CONCLUSION AND RECOMMENDATIONS 203

5.1 Overview 203
5.2 Conclusion of objective 1 205
5.3 Conclusion of objective 2 206
5.4. Conclusion of objective 3 207
5.5. Conclusion of objective 4 208
5.6 Implication of the study 209
5.7. Research limitations 211
5.8. Recommendation for future work 212
References 213

TABLE OF FIGURES

Figure 2. 1 The mechanisms of water erosion. 12
Figure 2. 2. Soil erosion assessment models. 18
Figure 2. 3. Various remote sensing platforms for soil erosion hazard assessment. 23
Figure 2. 4 The typical architecture of neural networks model. 29
Figure 2. 5 Explaining the principles of the architecture of SVM. 29
Figure 2. 6 A typical architecture of an ANFIS structure. 31
Figure 2. 7 Image classification methods for land-use change detection and soil erosion hazard assessment. 38
Figure 2. 8 Spectral signature of a plant detected by four different sensors: 42
Figure 2. 9 Spectral signature of different vegetation types and soil (source: Ustin & Gamon (2010). 43
Figure 3. 1 Location of the Central Highlands in Sri Lanka 55
Figure 3. 2 Land-use distribution with elevation in the Central Highlands in 2015 (source: LUPPD_SL). 55
Figure 3. 3 Overall methodology used in this research. 58
Figure 3. 4.The flowchart of the methodology used for objective 1. 59
Figure 3. 5 Landslides inventory map of the Central Highlands of Sri Lanka. 70
Figure 3. 6 (a) Location map of Sabaragamuwa Province in Sri Lanka; (b) digital elevation map; (c) slope angle map; (d) river distribution map. 71
Figure 3. 7 The overall methodology of the study. 73
Figure 3. 8 Soil erosion hazard classes and landslide distribution in each AER. 76
Figure 3. 9. (a) Average soil erosion rate, (b) the number of landslides occurred, (c) agricultural cropping area in the farming system, and (d) selected farming systems for three case studies. 77
Figure 3. 10 The flowchart of the methodology used for objective 2 of this study. 81
Figure 3. 11 Selected five agro-meteorological stations at the Central Highlands. 81
Figure 3. 12 The autocorrelation results of a) rain gauge data and b) satellite rainfall data. 86
Figure 3. 13 Overall methodology used for identifying ecologically viable and economically sound farming systems in the study area. 89
Figure 3. 14 The overall flowchart of the process for objective 4 of this study. 102
Figure 3. 15 Condition factor maps (a) aspect, (b) distance to stream, ... 106

Figure 3. 16 (Continue). Condition factor maps (c) slope length and steepness, (d) P factor (e) soil erodibility, (f) C factor. 107
Figure 3. 17 (Continue) Condition factor maps (g) steam power Index (h) rainfall erosivity RCP 8.5, (I) rainfall erosivity RCP 2.6 (j) rainfall gauge erosivity (k) satellite-based rainfall erosivity. 108
Figure 3. 18 Multilayered perceptron (MLP) with feed-forward network. 109
Figure 3. 19 The structure of the multilayer ANN method from MATLAB. 110
Figure 3. 20 The architecture of ANFIS model. 111
Figure 3. 21 The architecture of repeating module in the LSTM neural network. 114
Figure 4. 1. LULC maps in the Central Highlands: (a) 2000, (b) 2010, and (c) 2019.. 120
Figure 4. 2 Farming systems of the Central Highlands of Sri Lanka. 122
Figure 4. 3. Factor maps (a) K- factor, (b) LS factor, (c)P- factor, (d) R- factor 2000, (e) R- factor 2010, and (f) R- factor 2019. 124
Figure 4. 4 C-Factor maps (a) 2000, (b) 2010, and (c) 2019. 125
Figure 4. 5 Soil erosion map for (a) 2000, (b) 2010, and (c) 2019. 126
Figure 4. 6 Land-use land-cover (LULC) maps: (a) 2000; (b) 2010; (c) 2019. 129
Figure 4. 7 Factor maps of Sabaragamuwa Province: (a) slope length and steepness (LS)-factor; (b) rainfall erosivity (R)-factor; (c) soil erodibility (K)-factor; (d,e) crop management (C) -factor and conservation practice (P)-factor; (f) soil erosion hazard map. 131
Figure 4. 8 The percentage of land-use change and landslide frequency ratio () over the river distribution zones (RDZs). 134
Figure 4. 9 (a) River distribution zones map; (b) landslide inventory map; (c) soil erosion hazard map with landslide locations. 134
Figure 4. 10 (a) Landslide frequency ratio of each RDZ; (b) the area covered by soil erosion hazard classes of each RDZ. 136
Figure 4. 11 (a) NDVI, EVI and SAVI distribution (b) MODIS derived over the period in the Central Highlands. 140
Figure 4. 12 NDVI maps in the Central Highlands for (a) 2000 (b) 2010 and (c) 2019. 141
Figure 4. 13 EVI maps for the Central Highlands (a) 2000 (b) 2010 and (c) 2019. 141
Figure 4. 14 SAVI maps for the Central Highlands (a) 2000 (b) 2010 and (c) 2019. .. 142

Figure 4. 15 MODIS-derived: NDVI and EVI distribution over the period with annual average rainfall (ARF- satellite and gauge) in Ratnapura area (WL1a). 143
Figure 4. 16 MODIS (a) NDVI (b) EVI indices distribution from 2000 to 2019. 144
Figure 4. 17 NDVI values (within the year and over the years) for WM1a farming system. 144
Figure 4. 18 NDVI values (within the year and over the years) for WL1a farming system. 144
Figure 4. 19 NDVI values (within the year and over the years) for IU3e farming system. 144
Figure 4. 20 RUE variation with rainfall (a) WL1a (b) WM1a and (c) IU3e farming systems. 149
Figure 4. 21 The trend of RUE in three farming systems: (a) WL1a, (b) WM1a, and . 150
Figure 4. 22 RESTREND over the years: (a) WM1a, (b) WL1a, and (c) IU3e farming systems 152
Figure 4. 23 Extreme rainfall events in the Central Highlands (a). ARF (b) SDII (c) R99 (d) CWD and (e) CDD. 156
Figure 4. 24 The rainfall variation over the period in five stations. 158
Figure 4. 25 Annual average rainfall and rainfall anomaly in five agro-met stations. . 159
Figure 4. 26 Results of the innovative trend analysis from satellite-based rainfall data. 161
Figure 4. 27 Results of the innovative trend analysis from gauged rainfall data in five stations. 162
Figure 4. 28 The details of the relationship between (a) Average soil erosion and average annual rainfall and b) average annual soil erosion rate and landslide frequency. 164
Figure 4. 29 (countinue) The details of the relationship between (c) Average rainfall erosivity and landslides frequency ratio in each farming system. 165
Figure 4. 30 Maps of ecological indicators: (a) Aspect, (b) Drainage density, (c) Slope, (d) Precipitation, (e) Vegetation cover, (f) Distance to stream, (g) Landslides, (h) Soil quality, and (i) Soil erosion classes. 167
Figure 4. 31 Maps of economic indicators: (a) Cost of production, (b) Distance to market, (c) Distance to the main road, and (e) Population density. 168
Figure 4. 32 Ecological viability maps for (a) AERs, and (b) farming systems. 170

Figure 4. 33 Maps showing economically sound WLC for (a) AER, and (b) farming systems. 172
Figure 4. 34 Map of ecologically viable and economically sound (a) AERs, and (b) farming systems. 174
Figure 4. 35 Field photographs showing some eroded areas in WL1a farming system (rubber plantation converted to pineapple cultivation) 177
Figure 4. 36 Average annual rainfall in Rathnapura area 180
Figure 4. 37 Soil erosion susceptibility maps (a) 2020 based on gauged rainfall data, (b) 2020 based on satellite rainfall data (c) RCP 2.6, and (d) RCP 8.5 in 2040 respectively. 181
Figure 4. 38 (a) The best validation process and (b) performance curve of the ANN method. 184
Figure 4. 39 (a) Predicted vs actual (b) Comparison between target and SVM output. 185
Figure 4. 40 Soil erosion susceptibility map for (a) 2020 based on gauged rainfall data, (b) 2020 based on satellite rainfall data (c) RCP 2.6 and (d) RCP 8.5 in 2040 respectively. 186
Figure 4. 41 The areas vulnerable for soil erosion by different erosion models. 187
Figure 4. 42 Model validation from ROC curve. 188
Figure 4. 43 The relative importance of soil erosion conditioning factors. 189
Figure 4. 44 The root means squire error (RMSE) values of LSTM different training datasets. 193
Figure 4. 45 Observed and LSTM predicted rainfall at five gauge stations (a) Bandarawela (b) Nuwara Eliya (c) Kundasale. 194
Figure 4. 46 (continue) Observed and LSTM predicted rainfall at five gauge stations (d) Peradeniya and (e) Ratnapura. 195
Figure 4. 47 The spatial distribution of (a) observed mean annual rainfall and (b) corresponding predicted rainfall erosivity map for 2024 using the LSTM dataset. 196
Figure 4. 48 Spatial distribution of soil erosion susceptibility map in 2024. 197
Figure 4. 49 The figure illustrates the area under the curve (AUC) of the Soil erosion susceptibility map for the year 2024. 199

LIST OF TABLES

Table 2. 1 Integrated soil erosion modelling approaches with remote sensing-based methods. 22
Table 2. 2 Summary of temporal and spatial resolution adapted from Vrieling (2006). 24
Table 2. 3 Gully erosion assessment and mapping models. 32
Table 2. 4 Landslide susceptibility assessment and mapping models. 35
Table 2. 5 Summary of popular vegetation indices 44
Table 2. 6 Some applications of crop diversity assessment using remote sensing. 46
Table 3. 1 Summary of the data sources 56
Table 3. 2 Downloaded Landsat satellite datasets 57
Table 3. 3 The details of land-use classes. 60
Table 3. 4. SVM basic kernel, formulas and parameters 62
Table 3. 5. Details of meteorological stations 66
Table 3. 6. Details of the soil erodibility values (t ha h $MJ^{-1}mm^{-1}$) 67
Table 3. 7. P-factor and C-factor values for land-use classes. 69
Table 3. 8. Details of selected five agro-meteorological stations at the Central Highlands. 82
Table 3. 9. Details of extreme indices 83
Table 3. 10. Wet and dry classification based on the *Z* index and SPI value. 84
Table 3. 11. Soil characteristics in the Central Highlands of Sri Lanka. 91
Table 3. 12. Soil quality indicators. 92
Table 3. 13. Summary of ecological indicators and classification 95
Table 3. 14. Summary of economic indicators and classification 97
Table 3. 15. The scale of relative importance (Wind and Saaty, 1980). 98
Table 3. 16 Average random inconsistency indicators (RCI). 100
Table 4. 1. LULC change from 2000 to 2019. 121
Table 4. 2. Results of three LULC accuracy assessments using a confusion matrix. 122
Table 4. 3. Details of farming systems in the Central Highlands. 123
Table 4. 4. The details of soil erosion classes, rates, and area distribution in the Central Highlands 125
Table 4. 5. Details of the farming systems 127
Table 4. 6. Confusion matrix between ground truths and land-use classes. 128

Table 4. 7. Respective values of commission, omission, producer accuracy, and user's accuracy for classified land-use classes for 2019. 128
Table 4. 8. Land-use change between 2000 and 2019. 129
Table 4. 9. The details of soil erosion category, rates, and land area. 131
Table 4. 10. The landslide frequency ratio for each land-use type. 132
Table 4. 11. The major land-use change in each zone. 133
Table 4. 12. Landslide frequency ratios of the RDZ. 135
Table 4. 13. Prioritization of RDZ in Sabaragamuwa Province. 137
Table 4. 14. Details of Shannon index- richness and evenness during the period. 146
Table 4. 15. The Pearson's correlation matrix. 147
Table 4. 16. The KGE index for NDVI and rainfall. 147
Table 4. 17. The vegetation indices and rainfall in three farming systems. 148
Table 4. 18. Details of R^2 of EVI and NDVI, for RUE and RESTREND values. 151
Table 4. 19. Results of Mann-Kendall and Sen's slope tests for extreme rainfall indices. 157
Table 4. 20. Results for innovative trend test of annual rainfall in the Central Highlands. 160
Table 4. 21. KGE index for rain gauge measured rainfall in five stations. 161
Table 4. 22. KGE index: soil erosion, rainfall erosivity and landslides frequency ratio. 163
Table 4. 23. Pair-wise comparison for ecological indicators. 169
Table 4. 24. Pair-wise comparison for economic indicators. 169
Table 4. 25. Total score and final ratings for ecologically viable farming systems. 171
Table 4. 26. Total score and final ratings for economically sound farming systems. 173
Table 4. 27. Classes of the overall index. 175
Table 4. 28. Final matrix with the overall index. 175
Table 4. 29. Area covered by the soil erosion category from the RUSLE model. 182
Table 4. 30. Frequency ratios analysis and weight for each factor. 182
Table 4. 31. Area covered by the soil erosion category from the ANFIS model. 187
Table 4. 32. The model performance using AUC 188
Table 4. 33. LSTM summary results of five agro metrological stations. 196
Table 4. 34. The details of soil erosion hazard classes, rates, and area distribution in 2024. 198

ACRONYMS

AHP- Analytic hierarchy process

ANFIS -Adaptive network-based fuzzy inference system

ANN- Artificial neural networks

AUC - Area Under Curve

DEM- Digital Elevation Model

FAO – Food and Agriculture Organization of United Nation

GHG - Greenhouse gas

IPCC – Intergovernmental Panel on Climate Change

ITA -Innovative trend analysis test

LFR/ FR – Landslides frequency ratio / Frequency ratio

LSTM- Long short term memory neural network

LULC – Land-use land-cover

RCP- Representative Concentrative Pathway

RDZ – River distribution zones

RF – Random forest

RUSLE - Revised Universal Soil Loss Equation

SDGs - Sustainable development goals

SPI - Standard Precipitation Index

SVM - Support vector machine

LUPPD- Land use policy planning department

ABSTRACT

Healthy farming systems play a vital role in sustainable food production. Soil erosion hazard is one of the prominent climate hazards that negatively affect farming systems, economies, and livelihoods. Spatial and temporal variations of soil erosion hazards are crucial in providing timely information on climate risk prediction, and managing risk in food production especially in hazards vulnerable tropical countries like Sri Lanka. This research investigates the soil erosion hazards vulnerability in different farming systems using a geo-informatics modelling approach with soil erosion, plant diversity, and rainfall variation to achieve sustainable food production. The study employed a time-series analysis of several variables, such as land-use land-cover (LULC) and crop diversity and rainfall variation, to detect the spatial variability of soil erosion in farming systems. Rain-use efficiency (RUE) and residual trend analysis (RESTREND) combined with a regression approach were applied to partition the soil erosion caused by human-induced and climate-induced land degradation. A novel matrix-based analytic hierarchy process (AHP) and weighted linear combination method with geo-informatics tools were proposed to identify ecologically viable and economically sound farming systems. Five models including machine learning and deep learning models were employed to predict the soil erosion susceptibility. Results showed that soil erosion has increased from 9.08 Mg/ha/yr to 11.08 Mg/ha/yr from 2000 to 2019 in the Central Highlands of Sri Lanka. However, crop diversity had decreased in farming systems, namely low country (WL1a) and mid-country (WM1a) wet zone, in the western part of the Central Highlands. The RUE and RESTREND analyses revealed that climate-induced soil erosion is responsible for land degradation in these farming systems and threatens sustainable food production. The matrix-based AHP framework results indicated that more than 50% of farming systems demonstrated moderate status in terms of ecological and economic aspects. Results of prediction models indicate the WL1a and WM1b farming systems, have a very-poor status and will worsen under the climate scenario RCP 8.5 by 2040. The thesis concluded that the farming systems in the western part of the Central Highlands are ecologically and economically degraded and highly vulnerable to future climate hazards. Therefore, priority should go to restoration and resilience development through adaptation and mitigation to improve the present condition and reduce future vulnerability. This study provides a comprehensive framework and implementation strategies to manage future soil erosion hazards for sustainable land management and

food security. Finally, the implications of this research contribute to achieving Sustainable Development Goals by 2030.

CHAPTER 1

INTRODUCTION

1.1 Overview

Food and nutritional security through promoting sustainable agriculture has been one of the most important aspects to achieving the sustainable development goal of zero hunger by 2030. According to the United Nations 2030 agenda for sustainable development, it is imperative to ensure sustainable food production systems by increasing productivity throughout the world. Healthy farming systems play a vital role in improving agricultural productivity and sustainable food production. Developing resilient agriculture helps to maintain ecosystems and strengthen the capacity for adaptation to climate change: extreme weather events such as drought, intensive rains, floods, and other disasters, as well as progressively improve land and soil quality to create prosperity for all. This study focuses on soil erosion hazards and crop diversity change in different farming systems due to rainfall variation and resilience development towards sustainable food production. Chapter 1 presents the overview of the study, research background, problem statement, motivation behind the thesis, research questions, specific objectives and significance of the research. Finally, the scope of the thesis and thesis organisation.

1.2 Research background

Land degradation changes the soil's physical, chemical, and biological processes, which ultimately affects food security. Soil erosion is one of the forms of land degradation, defined as a gradual process of detachment and transport top layer of soil due to mechanical force or by an agent such as water, wind or snow. Soil erosion by water is known as water erosion that has been identified as the major form of land degradation (Montgomery et al., 2016). Food production in farmlands decreases with an increase in water erosion (Almagro et al., 2017). The process of water erosion may be accelerated due to explosion, mining, excavations for infrastructure and building construction, and agricultural activities such as soil tillage, crop harvesting, land levelling, quarrying and trench digging (Poesen, 2018). When the erosion rate is accelerated beyond the level of the permissible rate, it leads to a hazard. Rahman et al. (2015) defined a hazard as “a threatening situation to human life, property or environment”. The soil erosion hazard

influences the landscape processes such as land productivity, hydrological processes, and eventual human well-being. Water erosion assessment is very complex due to its multifactorial influences (Lal, 1988; Ananda and Herath, 2003). Hence, climatic, biophysical, topographic and human interference factors (such as socio, economic and political factors) are needed to be considered for water erosion assessment to take measures of risk minimisation for food security.

1.3 Problem statement

Global (macro and micro) climate variations inevitably influence agricultural food production. It has been identified that human-induced land-use and changes in climate greatly contribute to land degradation (Lal, 2011; Borrelli et al., 2020). Furthermore, the agricultural land area per head of population is continuing to shrink globally with increasing population. Borrelli et al. (2017) reported that each year 75 billion tons of soil are eroded from the croplands globally. According to the Global Soil Partnership led by FAO, this is equal to an estimated financial loss of US$ 400 billion per year. Tropical regions are more vulnerable in terms of reducing land productivity due to increasing temperature and monsoon rainfall variation (Borrelli et al., 2017). Water erosion is one of the most prominent land degradation forms in tropical farming systems and reduces agricultural productivity and ecosystem services (Han et al., 2020). Water erosion in farmlands reduces crop yield (Lal, 2014) and changes in land-use patterns that may lead to food insecurity (Rodríguez Sousa et al., 2019; Han et al., 2020). Every year 10 million hectares of cropland are lost due to water erosion (Pimentel and Burgess, 2013). The soil's productivity in terms of its biological, chemical, and physical structure has been changed due to long-term cultivation, intensification of cropping practices, and receiving high intensity rainfalls (Maitima et al., 2009; Hunt et al., 2019). García-Ruiz et al. (2015) observed the highest soil erosion rates in croplands due to significant land-use change effects and a positive relationship with increasing slope and precipitation. Moreover, the expansion of agricultural areas led to increasing water erosion rates (Khaledian et al., 2017) and decreased soil quality (Lal, 2014; Keesstra et al., 2016). Further to this, Poesen (2018) has pointed out that water erosion may induce environmental hazards such as gully and landslides in tropical hillslopes.

The vegetation cover plays a major role in soil erosion in terms of run-off and infiltration, and it effectively prevents excessive surface run-off (Hou et al., 2016; Liu et al., 2018).

However, plant diversity can positively impact on soil erosion. Hunt et al. (2019) investigated the interaction between plant functional diversity and soil erosion. They found that increasing plant diversity inhibits soil erosion under heterogeneous vegetation cover. Plant species diversity helps protect against soil erosion on slopes (Pohl et al., 2009). Furthermore, Berendse et al. (2015) found a strong impact of soil erosion on crop diversity. Liu et al. (2018) examined a quantitative relationship between soil loss and plant diversity. However, changes in species composition or diversity are unavoidable due to the continuous change in LULC and climate (John et al., 2008). In addition, crop diversity may change according to the cropping pattern in the agricultural landscape, e.g. highly intensive monoculture shows less crop diversity. It is, not surprising researchers have revealed that mono-cropping encourages soil erosion (Hunt et al., 2019) and reduces plant diversity, which causes further soil erosion.

Scholars continuously struggle to understand the impact of climate and land-use change and to find solutions and adaptation measures to meet the growing food demand (Borrelli et al., 2017; Panagos and Katsoyiannis, 2019). Modelling spatial and temporal variation of soil erosion and land-use change is important for predicting future impacts and taking mitigation measures to secure food supply (Lal, 2011; Panagos and Katsoyiannis, 2019). However, in terms of risk reduction, the development of adaptation and mitigation strategies are becoming more challenging due to variations in climate day by day (Campbell et al., 2016). Lal (2011) emphasised that understanding the impact of climate change, vulnerability, and successful adaptation measures will reduce the impact of the unexpected events of climate variation.

1.4 Motivation behind the thesis

South Asian countries are highly vulnerable to soil erosion in their tropical regions due to climate hazards, such as droughts, floods, and other extreme rainfall events (Lal, 2011). Poesen (2018) reported that water erosion induces environmental hazards such as landslides in tropical regions, creating poverty, particularly in developing counties. For instance, tropical countries in South Asia, such as Sri Lanka, have experienced intensive rains, floods, and landslides in the recent past (Ratnayake and Herath, 2005; Dang et al., 2019). In recent, Sri Lanka was ranked the second country on the global climate risk index in 2019 (Eckstein et al., 2019). This index ranked the countries that suffered from climate extremes such as storms, floods, drought, and landslides and their adverse impacts. These

undesirable consequences will make the farming systems more vulnerable and low productivity.

Soil erosion is one of the main problems of agricultural development in Sri Lanka (Hewawasam and Illangasinghe 2015). Researchers found that the Central region of the country is more vulnerable to soil erosion hazards (Ratnayake and Herath, 2005; Perera et al., 2019). Understanding crop diversity changes may be an important indicator for detecting the degree of soil erosion and hazard levels in terms of understanding soil fragility (Carlsson et al., 2017). Soil erosion assessment and mapping have been conducted using different models combined with geo-informatics techniques (Vrieling et al., 2010; Zeng et al., 2013) because of geo-informatics' capabilities such as efficient data collection, analysis, and validation techniques (Tralli et al., 2005; Regmi and Meade, 2013; Pradhan et al., 2014). Many studies have evaluated agricultural land use changes and soil erosion assessment using geo-informatics technology (Bakker et al., 2005; Leh et al., 2013; Borrelli et al., 2017). Other studies have investigated land degradation and plant diversity using various remote sensing technologies with time-series observation using geo-informatics (Wessels et al., 2007; Burrell et al., 2017; Mondal et al., 2020). However, none of these studies introduced a method to identify farming systems using geo-informatics.

The rainfall variation is emerging as a significant threat to national food production in Sri Lanka. A study conducted by Hewawasam and Illangasinghe (2015) showed that rainfall variation heavily contributes to soil erosion and crop productivity losses in Sri Lanka. The cropping seasons are based on the monsoonal rainfall pattern. Irregular and intense precipitation induces water erosion (Puente et al., 2019). Furthermore, rainfall variation and extreme weather events significantly induce soil erosion hazards such as gully erosion and landslides (Dang et al., 2019). Thus, the people and their livelihoods are highly vulnerable to the impact of climate change. Hence, the farming systems of Sri Lanka, particularly in the Central Highlands, are increasingly vulnerable to the adverse impact of climate change (Esham and Garforth, 2013). The evidence shows that these rainfall variations heavily impact major economic crops such as tea and paddy crops, which are rain-fed crops that is 66% of total agricultural croplands (Esham and Garforth, 2013). Thus, understanding the interdependence of soil erosion hazards, rainfall variation and other factors helps formulate climate risk management strategies and their implementation for better management and rainfall variation-related risk reduction.

Therefore, it is more practicable to identify the vulnerability to soil erosion and predict soil erosion hazards with rainfall variation in the Central Highland of Sri Lanka to reduce future damages. None of the previous approaches attempted to employ spatial modelling of soil erosion hazards and plant diversity change concerning rainfall variation using geo-informatics tools with time-series analysis.

Identifying and prioritising critical areas can be utilised to implement land development activities that help to reduce the impact of soil erosion to a certain level (Alilou et al., 2019; Montgomery et al., 2016; Elsheikh et al., 2013). The high economic cost of on-site and off-site conservation measures would result in market failures (Dabi et al., 2017). Resource allocation efficiency can enhance land productivity by implementing soil conservation measures for prioritising critical farming systems where there might be sufficient financial incentives for soil conservation. In addition, the outcome of this research will be beneficial for several government organizations in Sri Lanka, such as the Ministry of Agriculture, the Department of Agriculture, the National Building Research Organization, the Disaster Management Centre and the Department of Meteorology.

Modelling soil erosion to evaluate the present situation and examine potential vulnerability using future climate scenarios are crucial for reducing potential environmental hazards and maintaining sustainable land resources (Panagos et al., 2021). Continuous observation and predictions are essential to detect vulnerability to soil erosion (Li and Fang, 2016; Mullan et al., 2012). A proper understanding of the spatial locations and magnitude of erosion at present and future situations is required to achieve the United Nations Sustainable Development Goals (SDGs): 2-zero hunger, 6- clean water and sanitation, and 15 - life on land (Lal et al., 2021). Hence, there is a need to select an appropriate method to predict soil erosion vulnerable hotspots due to future climate variability. In the case of the Central Highlands of Sri Lanka, there was limited knowledge regarding soil erosion predictions concerning various climate scenarios.

1.5 Research aims and objectives

This research study aims to identify soil erosion hazards and crop diversity changes for different farming systems due to rainfall variation using geo-informatics technology in the Central Highlands of Sri Lanka.

The specific objectives of this research are to:

1. Assess the soil erosion hazard and crop diversity changes for different farming systems in the Central Highlands of Sri Lanka.
2. Investigate the relationship between soil erosion hazard and rainfall variation across the Central Highlands.
3. Identify ecologically viable and economically sound farming systems using an erosion hazard status.
4. Develop a spatiotemporal process to predict the vulnerability of different farming systems to soil erosion hazards.

1.6 Research questions

The following research questions were developed more precisely to achieve the research objectives.

1. What is the impact of soil erosion hazards and crop diversity change in different farming systems during the last 20 years (2000 – 2019)?
2. What is the relationship between soil erosion hazard and rainfall variation in the Central Highlands?
3. How can the status of erosion hazards be used to identify ecologically viable and economically sound farming systems?
4. How to develop a predictive model based on soil erosion hazards used to identify the vulnerability of farming systems?

1.7 Research significance

It is imperative to investigate the impact of soil erosion hazards and crop diversity changes due to rainfall variation in farming systems to develop adaptation strategies and mitigation measures for sustainable agricultural land use management. This study aimed to contribute new theoretical and methodological insights with research outcomes.

Understanding soil erosion hazards and crop diversity changes with rainfall variation through a geo-informatics approach helped formulate climate risk management strategies and mitigation measures for better management in terms of rainfall variation-related risk reduction. The methodology introduced in this thesis on farming systems delineation is a practical method that can be used in any country. It can be inferred that this research developed a novel spatiotemporal process to predict the vulnerability of farming systems using the soil erosion hazard status and crop diversity changes to enable resilience development for sustainable land management. This novel spatiotemporal process to predict the vulnerability of farming systems can be utilised elsewhere to develop climate-related risk reduction strategies for food security.

This research would potentially provide guidelines for the government to identify and prioritize ecologically viable and economically sound farming systems in the Central Highlands. The modelling approaches presented in this thesis help to identify the vulnerability to soil erosion, forecast the soil erosion hazards with rainfall variation and take necessary actions to reduce future damages. Furthermore, the outcomes of this enhance the capability of forecasting potential soil erosion in farming systems, thus allowing the necessary steps to ensure the sustainability of food crop production systems against adverse effects of rainfall variation to be taken in advance. Hence, this research project significantly contributes to the knowledge on vulnerability in farming systems and to resilience agriculture development, thereby ensuring sustainable farming systems and food security in Sri Lanka, where limited knowledge was available on these aspects. Adaptation strategies and mitigation measures for resilient agriculture development are significantly important for Sri Lanka and other tropical countries that are highly vulnerable to extreme rainfall events and other types of climate variations.

1.8 Scope of the study

This research study intends to examine the soil erosion hazards and crop diversity changes in farming systems using geo-informatics technology. A spatiotemporal process executes to identify the vulnerability of soil erosion hazards for making necessary steps in advance to ensure the sustainability of food crop production systems against adverse effects of rainfall variation. The scope of this research is presented as follows:

1. Conducting LULC change using SVM, Interactive supervised classification, and RF techniques (in section 3.5.1.1.1-3.5.1.1.3 for more details).

2. Assessing soil erosion hazards using RUSLE model combined with geo-informatics.

2. Implementing time-series analyses to estimate soil erosion hazards' spatial and temporal patterns with rainfall variation from 2000 to 2019.

3. Investigating crop diversity change with rainfall variation in farming systems using remote sensing satellite images and vegetation indices.

4. Data sourcing for vegetation indices from the freely available remote sensing satellite images (Landsat and MODIS).

5. Implementing rainfall trend analysis with a combination of Innovative trend analysis, Modified Mann–Kendall test and Sens' slope test to observe the rainfall variation.

6. Implementing ecological and economic indicators to identify ecologically viable economically sound farming systems.

7. Using machine learning, statistical techniques and future climate scenarios to predict soil erosion vulnerability to 2040.

8. Calibrating and validating simulated soil erosion susceptibility maps, soil erosion hazards maps and land-use change maps with google maps by evaluating metrics of root mean square error (RMSE), receiver operative characteristic (ROC) and confusion matrix.

1.9 Thesis organisation

This research dissertation consists of five chapters. The thesis commences with chapter one, the introduction, which provides an overview, research background, problem statement, motivation behind the thesis, research objectives and questions, significance and scope of the study. The second chapter provides a comprehensive literature review to identify the gaps in the literature. It briefly discusses soil erosion in farming systems, different methods of soil erosion assessments, advancement of soil erosion assessment using geo-informatics technology, spatial and temporal detection and predictions of soil erosion hazards. Further crop diversity changes with soil erosion and crop diversity change assessment using geo-informatics are studied. Then, there is a discussion of validation methods, climate change and future challenges, management strategies, chapter summary and gaps in the literature. Chapter three provides a general introduction,

an outline of the study area, the data and software that were used, and the overall methodology. Then LULC assessment was conducted for farming system demarcation and implementation of the methods to achieve each research question. Each methodology provides sufficient details by means of a flow diagram. Chapter four presents the results of each methodology and how it addressed the research questions. Finally, chapter five provides the conclusion and future directions. It consists of a brief overview of findings and study contribution, conclusions, research limitations and implications, and recommendations for future works.

CHAPTER 2

LITERATURE REVIEW

2.1 Overview

This chapter reviews soil erosion in farming systems, soil erosion assessment and prediction methods and advanced modelling techniques in geo-informatics. The chapter is organised as follows: a brief description of water erosion in farming systems, major causative factors of water erosion followed by traditional and advanced methods of soil erosion assessment, spatial and temporal detection and predictions of soil erosion hazards. Further, crop diversity assessment, the impact of soil erosion on crop diversity, soil erosion management strategies, challenges, innovations and future directions are discussed. The chapter concludes with gaps in the literature and chapter summary.

2.2 Soil erosion in farming systems

Soil erosion is a natural phenomenon. The natural soil erosion process is induced by heavy rainfall, runoff, drought, snowfall, wind, fire and gravity. Intensification of soil erosion causes environmental, economic and social disturbances and hazardous situations (Pradhan et al., 2012). It deteriorates the soil quality through loss of nutrients (Lal, 2003), changes in physical, chemical and biological processes (Lal, 2001); resulting in the reduction of agriculture productivity (Lal et al., 1999) and thereby causing resulting global food insecurity (Pimentel and Burgess, 2013). Soil erosion creates severe impacts on downslopes and downstream such as siltation in water bodies (Dube et al., 2020). Human interference and climate variation lead to the intensification of soil erosion (Poesen, 2018). Many studies show that agricultural landscapes, mainly farming systems, are more vulnerable to soil erosion due to present climate variation (Thornton et al., 2014; Borrelli and Panagos, 2020).

Keating and McCown (2001) described the farming system as an entire production system and management system on a particular farm or similar farms. The Food and Agriculture Organization (FAO) defined the farming system as “a population of individual farm systems that have broadly similar resource bases, enterprise patterns, household livelihoods and constraints for which similar development strategies and interventions would be appropriate. Thus a farming system can encompass a few dozen or many millions of households” (FAO, 2020).

2.2.1 Water erosion

Soil erosion by water is the most significant factor of land degradation (Rahman et al., 2009; Panagos et al., 2017a). Water erosion has been identified as a major threat to the agricultural landscape and farming systems (Angima et al., 2003; Montanarella et al., 2015). Water erosion in farmlands dramatically reduces land productivity and accessibility which may induce a risk of food insecurity (Pham et al., 2018; Zhang et al., 2019; Dube et al., 2020). The erosion process is threatening to agricultural productivity, ecosystem functionality and sustainability (Pimentel, 2006; Allen et al., 2011). Water erosion induces loss of soil carbon and nutrient decline; and highly influences soil biological processes, changes in Carbon and Nitrogen cycling, acid-sulphate soils and soil acidification, thus changing the soil structure and nutrient availability. Soil erosion reduces the organic matter by diminishing the availability of major nutrient elements such as nitrogen, phospherous and potassium (N, P, K) and minor nutrient elements. Water erosion damages the physical and chemical structure of the soil due to decreasing nutrient levels and increasing toxic levels due to acidification and salinisation (Maitima et al., 2009).

Water erosion can be observed throughout the world as one of the most important factors that can induce mass soil movement. For instance, United States agricultural land has an average annual water erosion of 5–170 t ha^{-1} yr^{-1}, China 150–200 t ha^{-1} yr^{-1}, Australia 0.1–150 t ha^{-1} yr^{-1}, India 0.3–40 t ha^{-1} yr^{-1}, Belgium 3–30 t ha^{-1} yr^{-1}, Ethiopia 8–42 t ha^{-1} yr^{-1}, Colombia 0.2–61 t ha^{-1} yr^{-1}, Brazil 60 t ha^{-1} yr^{-1} Europe 2.46 t ha^{-1} yr^{-1} and Russia 4.58 t ha^{-1} yr^{-1} (Panagos et al., 2015; Li and Fang, 2016; Guerra et al., 2017; Maltsev and Yermolaev, 2020). The tolerable threshold value of soil erosion depends on soil production functions to maintain ecosystem service. Therefore, the rate of soil production varies in different regions (FAO, 2019). Borrelli et al. (2017) found that the generic tolerable soil erosion threshold value is 10 t ha^{-1} yr^{-1}. However, the United States Department of Agriculture proposed a tolerable range between 4.5 and 11.2 t ha^{-1} yr^{-1}. The European Environment Agency sets the threshold value between 1 t ha^{-1} yr^{-1} for shallow sandy soils and 5 t ha^{-1} yr^{-1} for deeper, well-developed soils. Bui et al. (2011) provided a value of 0.85 t ha^{-1} yr^{-1} for Australia as reported by the Food and Agriculture Organization (FAO, 2019). The most commonly quoted tolerable soil loss rate is 1 t $ha^{-1}yr^{-1}$ (Verheijen et al., 2009), and an average annual soil erosion rate higher than 1t $ha^{-1}yr^{-1}$ can be considered irreversible over 50–100 years.

Research supports the assumption that rainfall accelerates soil erosion in hilly areas and watersheds because soil erosion is highly sensitive to precipitation (Labrière et al., 2015; Li and Fang, 2016). The process of water erosion consists of detachment, transportation and deposition

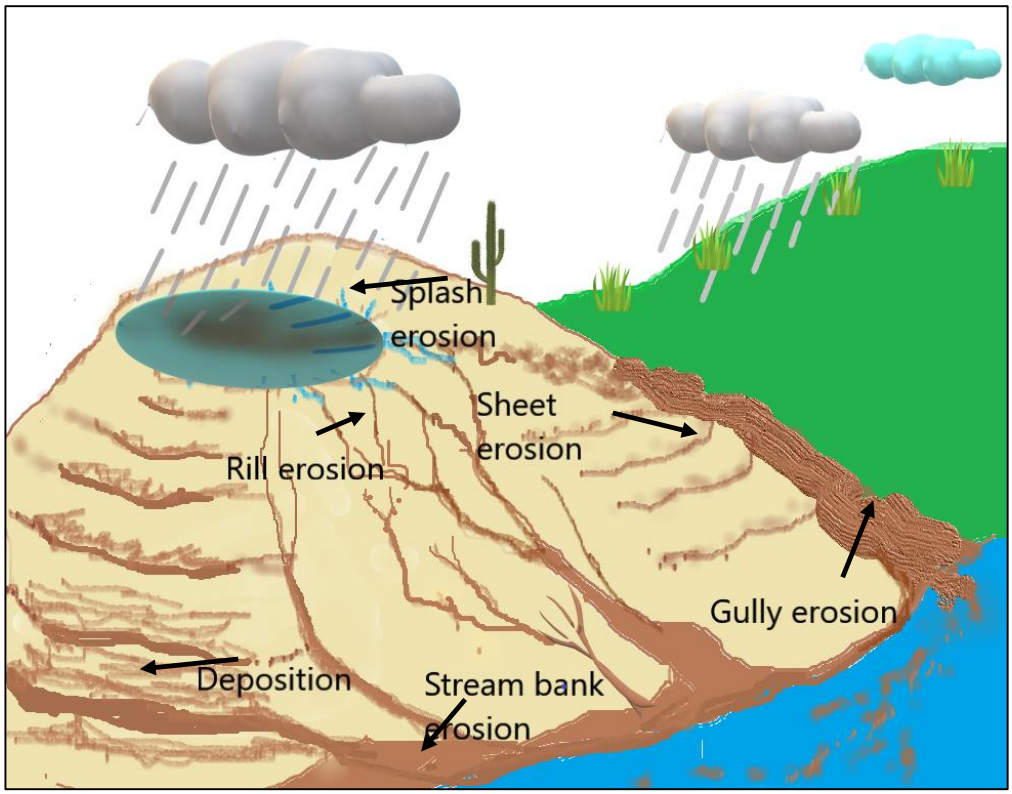

Figure 2. 1 The mechanisms of water erosion.

of sediment in a separate location (Foster et al., 1977; Wischmeier and Smith, 1978; Lal, 2001). There are several types of water erosion such as splash erosion, sheet or inter-rill, rill, and gully or ravine erosion (Wischmeier and Smith, 1978; Poesen et al., 2003). Figure 2.1 shows the types of soil erosion by water. The kinetic energy of water drops detaches the soil surface into soil particles, known as splash erosion. These soil particles move with runoff water flow. These runoff water flows create tiny channels (rills) in hill slopes. When these water flows of rills connect, they cause the formation of gullies. This process can be described as gully erosion. The removal of soil layers is called sheet erosion. The rate of soil erosion depends on several key factors such as rainfall intensity, soil infiltration, amount of runoff water and slope length (Drzewiecki et al., 2014). However, soil erosion may also depend on other factors, such as anthropogenic activities.

Understanding the process of soil erosion and impacting factors to selecting an effective monitoring method for water erosion is important for sustainable land management.

2.2.2 Major causative factors of water erosion

Water erosion accelerates due to several factors such as rainfall, topography, soil erodibility, slope characteristics, crop factors and land management practices. Wischmeier and Smith (Wischmeier and Smith, 1978) identified that soil erosion depends on several key factors rainfall, slope length and steepness, crop and land management. In addition, snow covers the land's surface in winter and spring seasons in most of the arable land of the humid and temperate zones. Hence, the soil contains a large degree of moisture, making it more vulnerable to erosion due to repeated freezing and melting (Raman et al., 2018). Furthermore, soil erosion occurs with less ground cover due to snowmelt runoff, usually during late winter or spring (Chakrabortty et al., 2020). The permeability of the soil increases by repeated freezing and melting, thereby increasing the chances of soil erosion (Edwards et al., 2007). Researchers have also considered various other factors for modelling such as land-use change, lithology, distance to the river and distance to the road. The following paragraphs discuss in detail the key factors affecting water erosion and relevant research that are still required to be done in future to understand these factors fully.

2.2.2.1 Rainfall

The capability of rainfall to cause soil erosion is defined as the erosive power of rainfall or rainfall erosivity. It has been observed that rainfall amount, intensity and spatiotemporal distribution may vary with climate variation (Turner et al., 2003; Mullan et al., 2012). Besides, irregular and intense precipitation is the leading cause of water erosion (Almagro et al., 2017; Panagos et al., 2017b). The impact of rainfall intensity and rainfall patterns on soil erosion, such as surface ceiling, runoff water, erosion hazard, loss of organic matter and soil fertility has been studied, and it has become clear that rapid changes take place during rainfall, affecting infiltration and runoff in the erosion processes (Arshad and Mermut, 1988; Remley and Bradford, 1989). The increasing rainfall reduces the nutrient level (Pimentel and Burgess, 2013) and enhances the acidification in the soil.

Almagro et al. (2017) reported warming climates and intense rainfalls will increase significantly due to an increase in global mean temperature by one degree Celsius. As a

result, the moisture retention capacity of the atmosphere will increase by 7%. Water vapour in the atmosphere influences the circulation patterns of the hydrological cycle and initiates high intensity and extreme rainfall events (Nearing et al., 2005). In a recent paper, Poesen (2018) highlighted that more research should be done on rainfall characteristics such as rainfall amount, rainfall intensity, rainfall depth, erosivity and the number of rainy days with present climate variation in different regions. For example: in Europe, researchers have predicted that the relative mean rain erosivity may increase by 18% in 2050 (compared to 2010) due to the large spatial variability of rainfall (Teng et al., 2018). Hence, understanding the impact of the extreme situations of precipitation is important, and it can be used to study rainfall erosivity and soil erosion for shorter time intervals. The expansion of erosion features based on precipitation events can also be examined through high temporal resolutions. Hence, more research is needed to investigate rainfall variation in hill-slope against various crop management practices with present rainfall variation. Special attention should be paid to soil erosion hazards caused by physical changes in the soil due to rainfall variation.

2.2.2.2 Slope length and steepness factor

Terrain characteristics such as slope steepness and slope length play a major role in soil loss (De La Rosa et al., 1999; Kayet et al., 2018). In a hilly area, when the slope length increases, soil runoff in the downslope direction per unit area also increases. While the slope steepness increases, the runoff velocity is increases. When the slope increases, runoff water will find a path nearby, increasing soil erosion and reducing infiltration (Ganasri and Ramesh, 2016). The slope length and steepness would increase the runoff velocity by reducing infiltration, which causes severe damage to the soil and livelihoods. The ground cover from plants or mulch helps to reduce the runoff velocity. Hence, it is vital to make policy changes for land-use and soil conservation measures to minimize the severity of damages in terms of the effect of rainfall variation in hillslopes.

2.2.2.3 Soil erodibilty

Soil erodibility reflects the soil susceptibility to erosion. Mainly, it depends on the organic matter content, soil texture (silt, very fine sand, sand and organic matter), permeability and aggregate stability (Yang et al., 2018a). Soil erodibility values for different types of soil can be obtained from nomographs (Wischmeier and Smith, 1978). However, runoff plots under the standard conditions of fallow soil is a reliable way to measure the soil

erodibility for local soil types. Studies should be carried out for a period of more than five years to obtain satisfactory values from field plot experiments (Loch et al., 1998). Hence, researchers commonly assume that once the soil erodibility value has been established for the soil in a particular area, this soil erodibility value is permanent. Nonetheless, Poesen (2018) indicated that soil erodibility also depends on climate variation, however the relationship between soil erodibility and climate variation were not fully understood. Therefore, more research is needed to study rainfall variation, topography and vegetation impacts on soil erodibility.

2.2.2.4 Ground cover

Vegetation cover helps to protect the soil from the disintegration of soil particles by rainfall and acts as a barrier for the detachment of soil particles (De Rouw and Rajot, 2004; Wibowo et al., 2012). Hence, if vegetation cover is dense enough, the impact of the rainfall on the erosion rate will be reduced the erosion rate. Plant root systems also play a significant role in soil erosion, where the above-ground mass is not prominent due to grazing, drought or fire. A major contribution from a plant root system for erodibility is the ability of mechanical soil binding. Although plant roots do not have a prominent effect on splash erosion, some plants have better-rooting patterns, so they hold the soil in better and prevent the formation of rills, gully and shallow landslides (Gyssels et al., 2005; Dube et al., 2020). Therefore, Poesen (2018) suggests that more attention should be given to examining the effect of root characteristics and soil erosion rates in different soil types.

2.2.2.5 Soil conservation practices

Water erosion leads to land degradation in farming systems and low productivity of crop production. Soil and water conservation structures help to reduce water erosion (Fu et al., 2020), increase soil moisture, soil fertility and improve the response to commercial fertilizer that contributes to increase crop yield (Dabi et al., 2017). According to Udayakumara et al. (2010), soil conservation measures improve soil health and help to improve the ecosystem services in every aspect. Agricultural practices, such as multiple cropping and agroforestry, also increase soil organic matter and soil carbon sequestration. Thus, multiple cropping and agroforestry practices reduce soil erosion through cover crops, deep-rooted crops and verities (West and Post, 2002; Hajjar et al., 2008). Poor crop management practices are directly related to inducing water erosion. This situation can be improved by implementing crop management strategies, such as planting cover crops,

minimum tillage, and adding organic matter to enhance water infiltration by improving soil moisture availability (Büchi et al., 2018). In addition, these strategies may also help to mitigate the impacts of severe rainfall and drought events or from water erosion (Lal, 1995; Sanchis et al., 2008). Research is still required on new strategies for mitigation the climate impacts on the soil.

2.3 Soil erosion hazards

Water erosion greatly contributes to soil erosion hazards (Poesen, 2018). A hazard is a situation or potential condition that causes harm or threat to life or, health or damage to property or the environment (Cutter, 1996). According to the United Nations International Strategy for Disaster Reduction (UNISDR), soil erosion is a geomorphological and geological hazard that may cause property damage, loss of livelihoods and services, social and economic disruption or environmental damage (Poesen, 2018). Research found that increasing rainfall intensities and prolonged seasonal dry periods due to climate variation had triggered an intensification of soil erosion and temporal probability of hazard occurrence such as mass movements (García-Ruiz et al., 2013). The extent, frequency and magnitude of soil erosion and its associated temporal probability of occurrence can potentially be increased due to future climate change (Mullan et al., 2012; Borrelli et al., 2020). Anthropogenic factors such as land-use change and forest fires further exacerbated the soil erosion hazard situation (García-Ruiz et al., 2013; Borrelli et al., 2017). Moreover, water erosion caused by environmental hazards was reported by many scholars (Pradhan et al., 2012; Farhan and Nawaiseh, 2015; Vergari, 2015). The mass movement of soil is an indicator of a soil erosion hazard. That includes gully erosion, riverbank erosion, rock-falls, debris-falls and landslides that can create damage to the environment and livelihoods. More than thousands of lives are lost annually due to mass soil movement worldwide (Li and Mo, 2019), and according to, Blaschke et al. (2000) these impacts of mass movement on soil erosion and land productivity are under-rated in the literature. Thus, less research attention was given to soil erosion due to the mass movement. Most of the soil erosion hazards prevail during a rainy season or after heavy rain (Dang et al., 2019; Maltsev and Yermolaev, 2020). Tropical agricultural lands are mostly vulnerable to gully erosion and landslides due to heavy water erosion (Hewawasam, 2010 ; Pradhan et al., 2012). Researchers have identified that landslides and other types of mass movement are responsible for the loss of thousands of lives and hundreds of millions of US dollars' worth of property and agricultural yield losses every year (Guerra et al.,

2017). Therefore, understanding the potential risk or susceptibility to soil erosion is very important for mitigation and risk minimisation.

Several studies have highlighted sediment deposition in water sources and its impact on water quality, biodiversity and natural resources (Hewawasam, 2010; Bartley et al., 2015). Wilkinson et al. (2018) pointed out that understanding of driving factors of gully initiation and assessing water erosion dynamics in the river basin of northeast Australia is important due to its impact on the Great Barrier Reef lagoon. Therefore, it is vital to estimate flow discharge and corresponding erosion rates on steep-slope lands using runoff and water erosion models. This resulted model outcomes are needed to map for conserving natural resources, preventing and controlling soil erosion by aiming for a sustainable land management process (Buttafuoco et al., 2012). Furthermore, Poesen (2018) highlighted that more research is needed on soil erosion runoff and sediment deposition related to present rainfall variation on sloping lands to identify sustainable conservation plans.

2.4 Soil erosion assessment

Water erosion assessment methods can be categorised into three main approaches: (i) the field plot experiment or fallout radionuclides methods using average soil loss measurements (Hurni, 1988), (ii) the field survey method by visible soil erosion indicators and identification of soil erosion influencing factors (Whitlow, 1988) and (iii) soil erosion modelling (Wischmeier and Smith, 1978). The classification of soil erosion assessment methods shows in Figure 2.2. Soil erosion assessment using field experiments was done by many researchers over several decades (Hurni, 1988; Hewawasam, 2010). Most of the methods were executed as field plot scale or watershed base experiments. Poesen (2018) identified hydrological discharges on the hill slopes or catchments are dependent on the area and cannot generalize from a field plot experiment. The realistic runoff should be measured according to the relief and corresponding erosion rates on hill slopes. These understandings of soil erosion runoff are important for better predicting sheet and rill erosion rates in different environments. Ganasri and Ramesh (2016) indicated that most of these conventional methods of soil erosion assessments are expensive and time-consuming. However, soil erosion modelling approaches provide a quantitative and reliable estimation for the erosion process and sediment yield in a diverse environment (de Vente and Poesen, 2005). Numerous soil erosion models have been developed by

utilising different scientific methods and modelling approaches. In general, three categories of traditional soil erosion models based on the nature of the basic algorithms exist (a) physics-based, (b) empirical and (c) conceptual models (Hewawasam, 2010; Labrière et al., 2015). These three categories of soil modelling will be discussed briefly in the following sections.

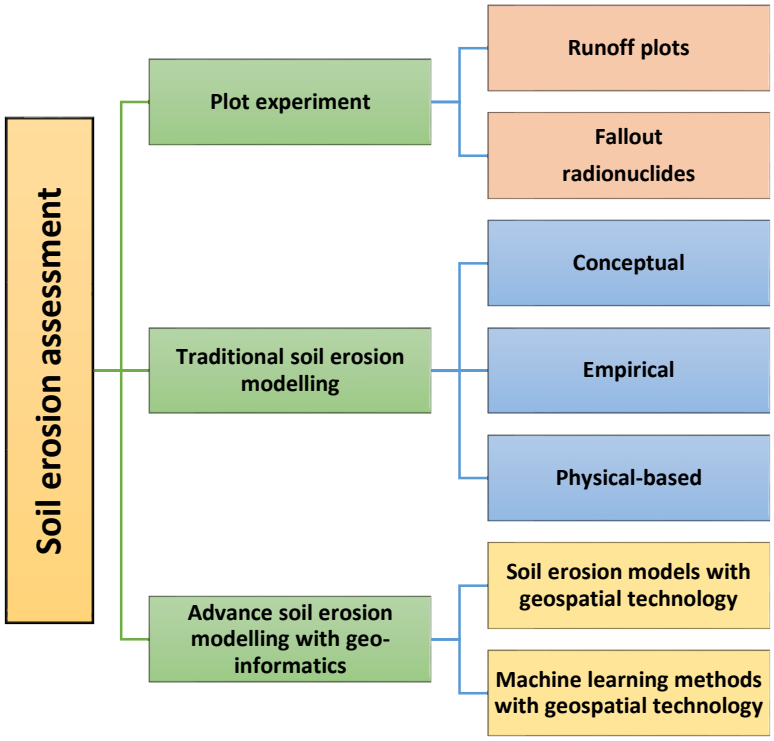

Figure 2. 2. Soil erosion assessment models.

2.4.1 Traditional soil erosion models

a) Physical-based models

Physics-based models are built on field-based research and simulate climate, runoff, infiltration, water balance, plant growth and decomposition, tillage and consolidation. These models are on the basis of the physics of flow and sediment transport processes and their interaction on the transfer of mass, momentum and energy (Kandel et al., 2005). It can be applied for a range of experiments, such as from a field plot scale to small watersheds and different time periods, including individual storm events, monthly, yearly or as an average annual value, based on the data from several decades. The major limitations of these models are high complexity and computational costs. The Water

Erosion Prediction Project (WEPP) model is an example of a commonly used physical process-based water erosion model (Renard et al., 1997). It was developed as a system modelling approach for predicting and assessing soil loss and identifying watershed management practices for soil conservation.

b) Empirical models

Empirical models are a simplified representation of natural processes based on experimental observations. Argent (2005) investigated the models that calibrate the relationship between input and output without a detailed description of the causes of each process. These models are based on observations of the environment that can be statistically quantified and proven (Nearing et al., 1994). Hence, empirical models are frequently employed for soil erosion modelling and are useful for identifying the sources of sediments and quantifying the erosion rates (Merritt et al., 2003). Empirical-based models have been widely used in soil erosion assessments. The Universal soil loss equation (USLE), the revised universal soil loss equation (RUSLE) and the modified universal soil loss equation (MUSLE) are commonly employed empirical-base models for soil erosion assessments (Sepuru and Dube, 2018; Yang et al., 2018a). Alewell et al. (2019) compared runoff and soil loss amounts by RUSLE and WEPP models. They found RUSLE and WEPP models satisfactorily predicted soil loss for the analysed conditions, and RUSLE performance was better than WEPP.

c) Conceptual models

Conceptual models are a combination of empirical and physical-based models. General descriptions of catchment processes can incorporate conceptual models without stipulating process interactions since detailed catchment information would require process interactions (Merritt et al., 2003). Therefore, conceptual models provide measurements on quantitative and qualitative processes within an area such as a watershed and consist with inherent limitations of empirical models such as a wide range of data set are needed for calibration. The conceptual soil erosion model AGNPS (agricultural non-point sources pollution model) combines SCS (Soil conservation service) method and RUSLE that predicts runoff with SCS and soil erosion loss. The SWAT (soil and water assessment tool) model predicts runoff with SCS curve number and MUSLE for soil loss prediction (Renard et al., 1997).

This review highlights several models that researchers have employed to monitor factors of water erosion. Researchers have made huge progress in the process of soil erosion, identifying the causative factors and their controlling mechanisms through modelling approaches. The USLE (Wischmeier and Smith, 1978) and RUSLE (Morgan et al., 1984) are widely employed to assess long-term soil erosion rates from farmlands due to different management practices (Sepuru and Dube, 2018). Several studies have analysed soil erosion and soil erosion hazards in different agricultural sloping lands using the models of USLE and RUSLE around the world. Although empirical models do not tend to be event responsive, instead they estimate soil erosion annually. Integration of different models is used to identify and estimate soil erosion and soil erosion hazard vulnerability in recent literature. Initially, USLE/RUSLE models had limitations with spatial distribution, which have been overcome by integrating geo-spatial technology (Sepuru and Dube, 2018). In this context, geo-informatics played a vital role in advanced methodological development in estimating soil erosion and soil erosion hazards (Zeng et al., 2013).

2.4.2 Advancement of soil erosion assessment using geo-informatics techniques

Since the 1930s, several soil erosion models have been developed and tested; however, it is still challenging for researchers to assess and predict soil erosion accurately due to its complex nature (Lal, 2003; Rahman et al., 2009). Karydas et al. (2014) identified 82 soil erosion models and classified them under eight geo-spatial categories. They identified the integration of geo-spatial techniques as a landmark change for soil erosion assessment. In recent decades, soil erosion assessment integrated with geo-spatial technology has enabled the development of simplified models to assess complex situations. Geo-informatics is a field of study on the scientific investigation of economic, social, environmental, health & safety and security challenges in multiple disciplines by analysing big geo-spatial and temporal data and interpretation of results for better understanding and decision-making (Ayanlade et al., 2014). It is widely applied in various disciplines of engineering, earth science, climate science & meteorology, agriculture, public health, archaeology, oceanography, military and so forth. Geo-informatics helps in the acquisition of different types of data on socio-economic and biophysical parameters using geo-spatial technology geographic information systems (GIS), remote sensing (RS) and global positioning systems (GPS). It also facilitates data storage, management,

analysis and visualisation to develop new theories and methodological tools to address complex social and environmental challenges. Geo-informatics has great potential for soil erosion assessment (Maltsev and Yermolaev, 2020) and benefited from combining soil erosion modelling in the recent past.

The geo-informatics technologies, that is, remote sensing, geographic information systems (GIS) and global positioning systems (GPS), have been integrated with various soil erosion models for soil erosion assessment and risk evaluation (Rahman et al., 2015). Many studies have been conducted using different soil erosion models combined with geo-informatics techniques (Pradhan et al., 2012; Ganasri and Ramesh, 2016; Seutloali et al., 2017). The capabilities of geo-informatics, such as efficient data collection, analysis and validation techniques, provide valid information on dynamics and intensity of soil erosion over time and space for controlling and forecasting (Argent, 2005; Brits et al., 2014). Brits et al. (2014) believe that the use of geo-informatics technology has been widely expanded due to its rapid development and capabilities with new tools and software. The application of geo-informatics to soil erosion studies has been popularised as a robust, low cost and high accuracy method (Seutloali et al., 2017). It offers a significant strength for soil erosion assessment at a larger spatial scale, particularly the land areas where difficult to reach for field investigations (Sepuru and Dube, 2018). Soil erosion assessments have been conducted based on different territorial units of spatial analysis (raster grid basis) such as a watershed or river basin, country, regional and global scale levels. Most parameters of water erosion are scale-dependent. For example, a smaller geographical scale (plot experiment) mostly is used to study on-site impacts of soil erosion, while a larger geographical scale is employed to investigate off-site impacts of soil erosion. Because the same scale is not always appropriate for realistic soil erosion assessments (Karydas et al., 2014).

The integrated use of remote sensing, GIS and soil erosion modelling has been widely applied by researchers for soil erosion assessment. Table 2.1 provides a few examples of recent research on integrating remote sensing-based soil erosion assessment in a GIS environment.

Table 2. 1 Integrated soil erosion modelling approaches with remote sensing-based methods.

Soil Erosion Model	Remote Sensing-Based Methods	Data Sources	Study Area	References
RUSLE	Normalized Difference Vegetation Index (NDVI) for vegetation cover	Multi-source remotely sensed data (MODIS, Gaofen (GF)-1)	China	(Yan et al., 2020)
RUSLE	Land use/land cover classes generation	Indian remote sensing (IRS) satellite 1D-LISS-3 image	India	(Ganasri and Ramesh, 2016)
Soil plots and RUSLE	Digital erosion Model (DEM) Rainfall depths and intensity, Ground cover	Light Detection and Ranging (LiDAR) and Shuttle Radar Topography Mission (SRTM), radar rain-field data in NetCDF, Landsat-8 imagery Rapideye, Aerial photograph	Australia	(Yang et al., 2018a)
USLE	Land use/cover classification for C-factor generation using Supervised classification	SPOT 5 and Landsat ETM+	Malaysia	(Pradhan et al., 2012)
RUSLE and Land- use change	Object-based image classification for land-use land cover change detection	SPOT-5	Malaysia	(Nampak et al., 2018)
Field plot method	NDVI for vegetation cover	ALOS data	Sri Lanka	(Udayakumara et al., 2011)
and AHP	NDVI Different land use/land cover classification	IRS-P6 LISS III	China	(Rahman et al., 2009)
Biophysical factors derivation	Vegetation cover, DEM and topographic variables (slope, stream erosivity-SPI, topographic wetness index TWI)	Landsat TM images ASTER DEM	South Africa	(Seutloali et al., 2017)
RUSLE and Sediment yield	NDVI for C-factor generation	Landsat TM images	Iran	(Fathizad et al., 2014)
Gully erosion detection	NDVI for vegetation cover	Unmanned Aerial Vehicles (UAVs)	Morocco	(d'Oleire-Oltmanns et al., 2012)

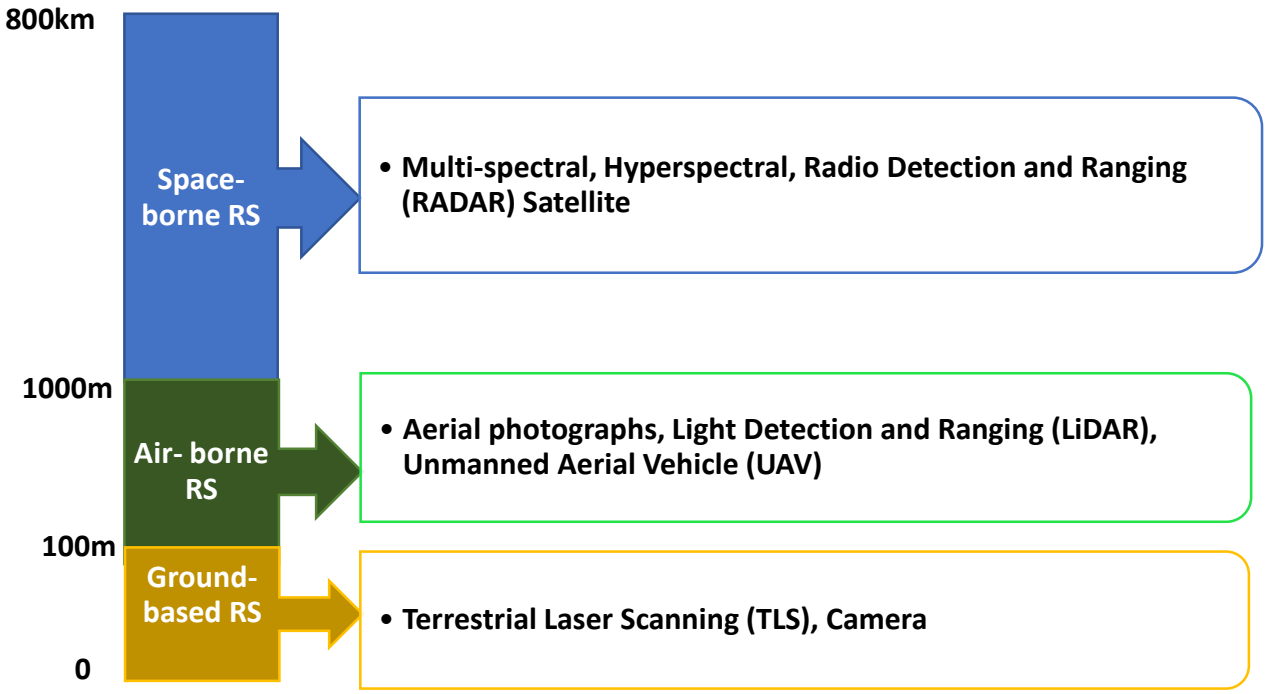

Figure 2. 3. Various remote sensing platforms for soil erosion hazard assessment.

The remote sensing-based airborne and space-borne sensors such as multi-spectral, hyperspectral, Radio Detection and Ranging (RADAR) and Light Detection and Ranging (LiDAR) and their wide range of applications have been used to detect soil erosion in different scales of landscape throughout the world. The remote sensing platforms for soil erosion hazard assessment is illustrated below in Figure 2.3.

Das et al. (2015) suggested that these methods could be used on rapid assessments without disturbing the soil surface and have vast spatial coverage. In addition, these remote sensing technologies help with a time-period assessment with less cost (Seutloali et al., 2017). Although high spatial resolution satellite imagery such as IKONOS, QuickBird and Spot 5 are available at high cost, coarse resolution satellite imagery: Landsat, Moderate Resolution Imaging Spectrometer (MODIS), National Oceanic and Atmospheric Administration Advanced Very High-Resolution Radiometer (NOAA-AVHRR), and Advance Space-borne Thermal Emission and Reflectance Radiometer (ASTER) are freely available for researchers and can be utilised for the time series analysis. A summary of temporal and spatial resolution is given in Table 2.2.

Table 2. 2 Summary of temporal and spatial resolution adapted from Vrieling (2006).

Satellite	Temporal Resolution	Spatial Resolution
IKONOS	24 h	0.82 m panchromatic; 3.28 m multispectral,
QuickBird	3.5 days	2.4 m spatial resolution and a panchromatic band at a 0.6 m
Spot 5	26 days	2.5 to 5 m in panchromatic mode and 10 m in multispectral mode
Landsat 3-8,	16 days	15 m panchromatic 30 m multispectral
MODIS	1–2 days	250 m at nadir, with five bands at 500 m, provides global coverage
NOAA-AVHRR	twice per day	1.1 km
ASTER	6 days at the equator	60 km
Sentinel-2A	5 days	10–60 m

The digital elevation model (DEM) is one of the essential inputs required for soil erosion modelling. DEM can be generated by analysis of remotely sensed spectral data such as stereoscopic optical (ASTER), microwave (synthetic aperture radar- SAR), Shuttle Radar Topography Mission (SRTM) and terrestrial LiDAR for 3D representation in a various resolutions for landform recognition (Mulder et al., 2011; Mullan et al., 2012). The radar has the capability of penetrating through the canopy cover and is independent from weather and daylight to retrieve high resolution, remotely sensed data (Scaioni et al., 2014). LiDAR can produce high-resolution topographic data, which can be used to generate Digital Terrain Models (DTM) and Digital Surface Models (DSM) for detailed terrain analysis (Tarolli, 2014). There are several global geo-spatial databases available for soil erosion assessments. Global Historical Climatology Network-Daily provides global daily rainfall data (Menne et al., 2012). GTOPO30 provides a digital elevation model (DEM) with resolutions of 1000, 500 and 250 m (Danielson and Gesch, 2011). Global soil degradation data are available at GLASOD (Oldeman, 1992) and GLADIS (Masoudi et al., 2006; Borrelli et al., 2017). Data of land degradation in dryland areas can be accessible in LADA of FAO, UNEP-GEF (Masoudi et al., 2018). However, these models have limited predictive power due to coarse resolution (Borrelli et al., 2017).

The majority of freely available satellite image sources have a limitation of being low-resolution cloud contaminated and with uncertainties is surface reflectance retrievals. Thus, land cover change detection is limited. A number of radiometric correction techniques have been developed to address this limitation (Hall et al., 1991). In contrast, NASA's Earth Observing System (EOS) and Moderate Resolution Imaging Spectroradiometer (MODIS) are equipped with surface reflectance products for land cover change detection (Vermote et al., 2002). Further to this, the availability and low cost of images are major benefits of Landsat series data. Hence, Landsat data can be used for long term monitoring purposes. However, there are several limitations with Landsat series data: the low spectral resolution of the sensor and limited capability of soil erosion parameters estimation such as vegetation cover, outlining of bare surfaces, calculation of vegetation indices and change of topography (Alatorre and Beguería, 2009).

Sentinel 2 and Landsat 8 series data provide improved spatial, spectral radiometric and temporal resolutions as the most required spatial tool for continuous monitoring Sepuru and Dube (2018). The vegetation indices have been identified as a simple and quick feature extraction technique for soil erosion by assessing and mapping from satellite data (Sepuru and Dube, 2018). A number of researchers have suggested that soil erosion classes could be delineated based on vegetation cover interpretation and multi-temporal images allow to assess its expansion (Alatorre and Beguería, 2009). Research shows that vegetation cover is depressed with the occurrence of land degradation (De Rouw and Rajot, 2004). The vegetation indices, such as The Normalized Difference Vegetation Index (NDVI), have been used for many studies of soil erosion (Udayakumara et al., 2011; Wessels et al., 2012; Sepuru and Dube, 2018; Puente et al., 2019). NDVI is a vegetation index derived based on remote sensing techniques mostly applied with above-ground net productivity and dynamics with spatial and temporal distribution of vegetation cover (Myeong et al., 2006). This index can be used to obtain information about not only plant growth characteristics but also site-specific qualities such as prevailing climate, ecosystem, terrain and physical soil properties (Sommer et al., 2003; Sumfleth and Duttmann, 2008). Puente et al. (2019) have indicated that NDVI is a commonly used vegetation index for extraction of the vegetation information from satellite data. This index identifies healthy and green vegetation. A number of studies have examined soil erosion patterns by analysing the changes on NDVI values using time series analysis in

growing seasons and the onset of the dry seasons (Lozano-García et al., 1991; Wessels et al., 2012). In addition, soil properties have been studied by several researchers using NDVI images, such as, soil color (Mukherjee and Singh, 2020; Singh et al., 2020), soil texture and water holding capacity (Sumfleth and Duttmann, 2008), root zone soil moisture (Wang et al., 2007) and soil carbon and nitrogen content (Sumfleth and Duttmann, 2008).

Unmanned Aerial Vehicles (UAV) derived data is becoming more popular due to its rapid development in sensor technology (Valavanis and Vachtsevanos, 2015), low cost and risk (Tarolli et al., 2011; Anderson and Gaston, 2013). The UAV-based LiDAR and hyperspectral images provide much more detailed estimates of earth surface processes and patterns for geomorphological and hydrological modelling, including soil erosion estimates and river channel morphology changes (Hutton and Brazier, 2012). In addition, UAV well performs in DTM, biodiversity monitoring and land-cover change detection (Koh and Wich, 2012). UAV data can be used to derive vegetation indices such as NDVI, which are correlated with biophysical characteristics of vegetation cover (Lelong et al., 2008; Sankey et al., 2017).

The advances of geo-informatics and erosion models help to develop systematic and integrated approaches in soil erosion hazard and risk evaluation. Due to the complex nature of the soil erosion hazard process, several integrated approaches were applied. This literature review found that the capability of geo-informatics techniques could be utilised as a novel approach due to its vast application of potential and promising characteristics. Some of the studies examined focused on the development of a set of criteria and indexes which can be spatially represented as information layers to quantitative and qualitative assessment (Rahman et al., 2009; Drzewiecki et al., 2014). In many recent research studies, soil erosion hazard models were combined with several statistical approaches and algorithms in a geo-spatial environment to quantify the assessment (Arabameri et al., 2018; Arabameri et al., 2019b). These approaches included expert decision tree and artificial neural-network evaluation methods (De La Rosa et al., 1999), geo-statistical multivariate approaches (Conoscenti et al., 2008; Garosi et al., 2019), sensitivity analysis approaches (Mendicino, 1999), soft computing method (Lisboa et al., 2018) and analytical risk evaluation methods (Masoudi et al., 2006; Wu and Wang, 2007).

These models can be categorised into four types; expert knowledge-based models, data-driven models, machine learning models and hybrid methods. The following sections describe some of these model approaches.

2.4.2.1 Knowledge-based models

The analytic hierarchy process (AHP) of the multi-criteria decision-making method, is described as a simplified method for pair-wise comparison of homogenous elements (Saaty and Vargas, 2013). This method has been applied to the qualitative assessment of soil erosion (Xue and Su, 2017). The AHP method was proposed by Thomas L Saaty in 1980 based on the criteria evaluation procedure to determine the weights of the factors through a matrix that compared all the identified attributes against one another. The main advantage of the AHP method is its ability to work with available data and limited resources.

2.4.2.2 Fuzzy logic model

The fuzzy logic model is a qualitative analysis method that can be implemented with a more flexible combination of weighted maps based on the GIS environment. This model can be employed with relatively limited input variables to a large extent with considerable accuracy for soil erosion prediction (Mitra et al., 1998). This model is widely applied in soil erosion assessment (Saha et al., 2019; Sinshaw et al., 2021), landslide susceptibility mapping (Razifard, Shoaei & Zare 2019) land-use changes (Einheuser et al. 2013) soil quality (Wu et al. 2019) due to its simplicity of understanding and implication.

2.4.2.3 Data-driven models- Frequency ratio method

The frequency ratio (FR) model is a statistics-based bivariate approach, that can quantify the spatial relationship between independent and dependent variables (Rahmati et al., 2017). This method can be employed to analyse the probability of the occurrence of an event for probability mapping by Bonham-Carter (1994). Many researchers have frequently used this method for flood susceptibility, and landslide susceptibility mapping (Jebur et al., 2014; Gayen and Saha, 2017). Combining the FR with multivariate methods enables analysis that is more precise (Gayen et al., 2019).

2.4.2.4 Machine learning-based models

Machine learning techniques are engaged with a set of different equations and mathematical models to represent complex systems and interactions. These models study the algorithms that learn from the existing dataset to implement processing tasks such as classification, prediction or clustering. These analyses generate results that cannot identify even by the eyes of experts (Puente et al. 2019). Golhani et al. (2018) reported that machine-learning techniques have two major drawbacks. These models highly depend on the pattern of variables, and in the classification process, they may require training the model many times for better accuracy. Researchers have widely employed the following machine learning approaches.

2.4.2.4.1 Artificial Neural Network

Artificial Neural Network (ANN) is a computer machine-learning model and has been used for pattern recognition in many applications, such as data mining (Rizeei et al. 2016). This model helps to acquire, represent, and compute a set of data into information, which can be presented as maps. This model operates input mode from input layers and feeds forward to output mode through hidden layers (Golhani et al. 2018). This approach has several advantages, for example it is independent of the statistical distribution of the training data and allows defining the relationship to their distribution for each data source. Therefore, the integration of remote sensing or GIS data is very convenient. Pradhan & Lee (2010) found that the ANN method is a more positive approach for landslide susceptibility mapping than the logistic regression analysis method. Melchiorre et al. (2008) improved the predictive capability and strength of ANNs by introducing a cluster analysis. For instance, the architecture of the ANN model is given in Figure 2.4.

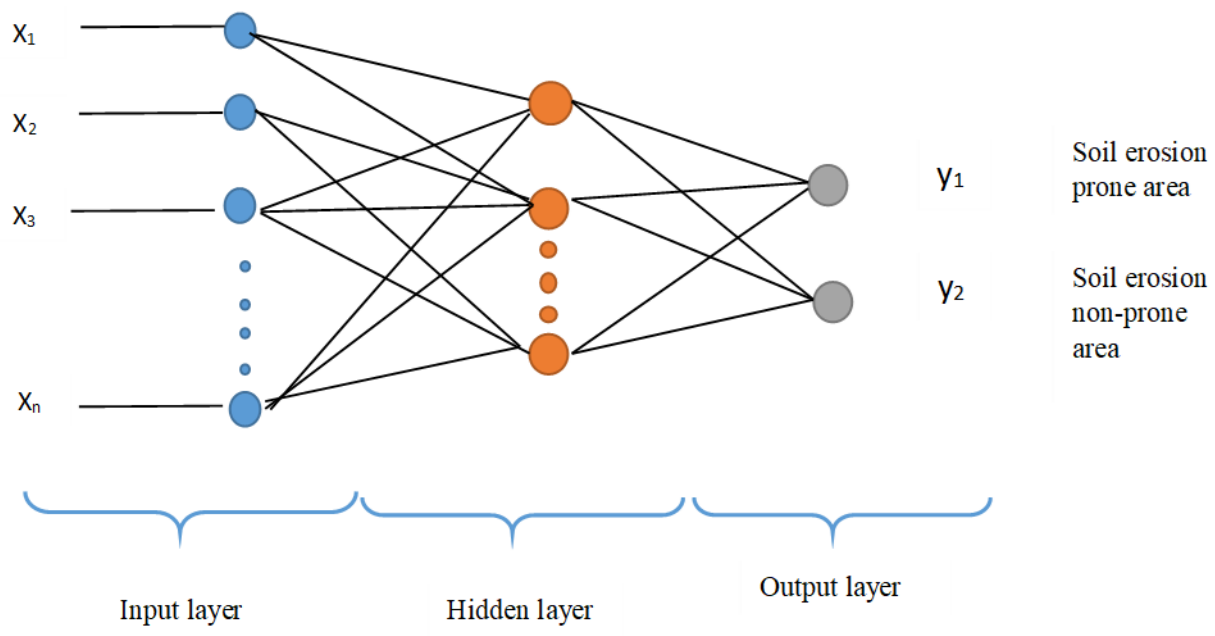

Figure 2. 4 The typical architecture of neural networks model.

2.4.2.4.2 Support vector machine

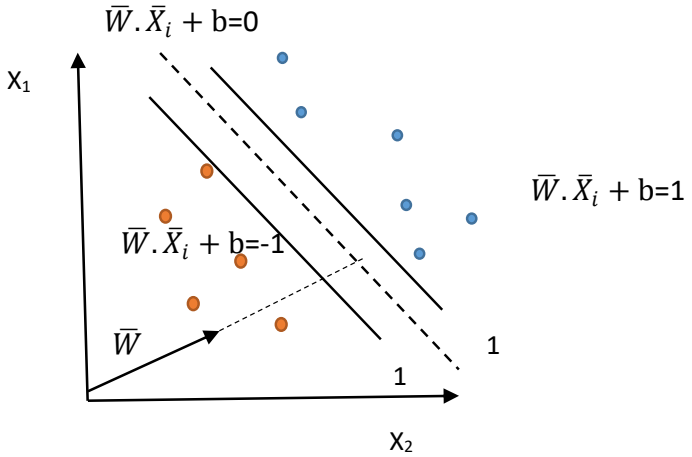

Figure 2. 5 Explaining the principles of the architecture of SVM.

Support vector machine (SVM) is one of the most popular machine learning algorithms and is considered a high-performing technique. The SVM algorithm is a supervised pattern classification technique that was proposed by Cortes and Vapnik (1995). SVM is one of the best land-use classification methods with high accuracy (Jozdani et al., 2019;

Lee et al., 2017). The primary basis of the SVM method is to find an optimal separation hyper-plane from the dataset (Lee et al., 2017; Hong and Jung, 2017). The principles of the architecture of SVM are explained in Figure 2.5.

The goal of the SVM is to search an n-dimensional hyperplane, differentiating the two classes by their maximum gap (Figure 2.5). This is expressed as:

$$\frac{1}{2} \| \omega \|^2 \qquad (2.1)$$

2.4.2.5. Hybrid method -Neuro-fuzzy interface system

The adaptive neuro-fuzzy inference system (ANFIS) uses a hybrid-learning algorithm by a combination of gradient descent and the least square method. This method was developed by Jang (1993) using the Takagi–Sugeno rule format, which is the combination of an optimized premise membership function (gradient descent) with an optimized consequent equation (linear least squares estimator). ANFIS is a process of both fuzzy logic and artificial neural network methods and uses for driving the fuzzy If-then rules into the artificial neural network with high computational power (Tien Bui et al., 2012). Fuzzy rules are executed along with suitable membership functions of training paired and further lead to an interface (Islam et al., 2018). This model has been applied in many environmental hazards applications such as floods, landslides and soil erosion assessment. Figure 2.6 shows a typical architecture of an ANFIS model.

A combined approach of Land Transformation Model –(LTM), Artificial Neural Networks algorithm – (ANN), SCS-CN model and autoregressive integrated moving average (ARIMA) model have been applied to soil erosion assessment by Rizeei et al. (2018). Arabameri et al. (2018) employed AHP and multi-criteria decision-making approach in the GIS environment to investigate erosion-prone areas. LTM, together with ANN and USLE models have been used to predict soil erosion and land cover dynamics (Rizeei et al., 2016). Weights-of-evidence (WoE) and evidential belief function (EBF) models were used by Gayen and Saha (2017) to identify the soil erosion in vulnerable areas. Another recent study employed ANN, geographically weighted regression (GWR) and GWR–ANN ensemble model to predict soil erosion (Mosavi et al., 2020).

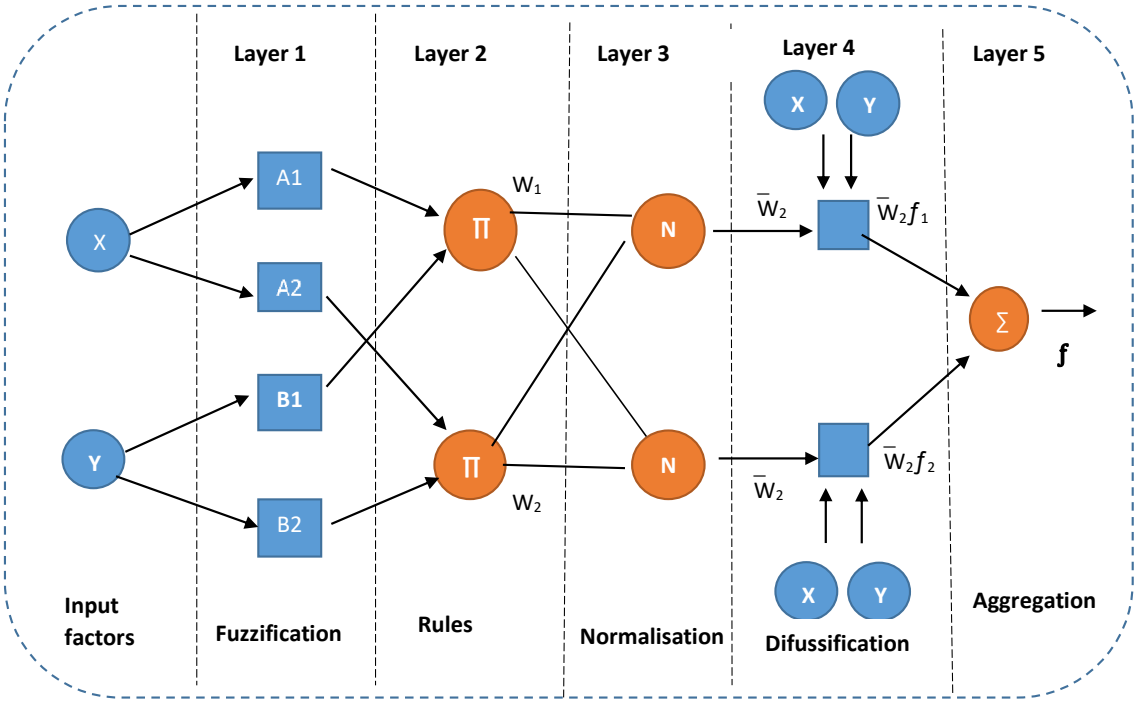

Figure 2. 6 A typical architecture of an ANFIS structure.

2.5 Spatial and temporal detection and predictions of soil erosion hazards

The spatiotemporal pattern of soil erosion hazards has been studied and predicted by several researchers (Zhu et al., 2014; Nampak et al., 2018; Yang et al., 2018a: Abdulkareem et al., 2019). Many researchers used remote sensing and GIS tools to monitor, map and forecast soil erosion hazards and land-use/land-cover changes (Rizeei et al., 2016; Rizeei et al., 2018). In addition, geo-informatics technology provides a better understanding of the spatiotemporal relationship in soil erosion hazards: gully erosion susceptibility and landslide vulnerability mapping. This review further focuses on geo-informatics involvement in two of the major types of soil erosion hazards, that is, gully erosion and landslides, in detail.

2.5.1 Gully Erosion vulnerability assessment

Gully erosion is one of the important indicators of soil erosion hazards. It has been a great threat to agriculture by reducing soil fertility worldwide, especially in arid and semi-arid regions in tropical and sub-tropical countries (Gayen et al., 2019). Gully erosion has become more common due to the impact of climate change effect (Poesen, 2018). The high intense rainfall events in a bare landscape create gully incisions (Guerra et al., 2017;

Lisboa et al., 2018). Furthermore, they discharge a high amount of sediment into water sources (Garosi et al., 2018; Gayen et al., 2019). The studies conducted in Australia have identified land-use change such as vegetation clearance, animal grazing and alternating periods of extreme rainfall events and drought events, heavily induced gully erosion (Bui et al., 2011; Wilkinson et al., 2018). Li et al. (2015) have also claimed that the reduction of vegetation cover greatly contributes to gully development.

Remote sensing and GIS-based models have been applied to identify spatial and temporal distribution, investigate susceptibility to gully erosion and map the risk classes in order to minimize soil erosion (García-Ruiz and Lana-Renault, 2011). Numerous studies have incorporated image analysis techniques in satellite remote sensing such as object-based analysis into detecting and mapping gullies. In addition, several scientists have adapted advanced statistical, knowledge-based and machine learning models for gully erosion assessment. Most of these research studies attempt to find out gully susceptibility using soil, terrain, climatic and land use aspects with geo-informatics technology for the landscape evaluations. Several recent studies with adapted geo-informatics technology for gully erosion mapping are summarised in Table 2.3 below.

Table 2. 3 Gully erosion assessment and mapping models.

Model Type	Country	Attributes	Techniques	References
Knowledge-based model	Iran	Elevation, slope degree, slope–length (LS), slope aspect, plan curvature, lithology, distance from the river, drainage density, distance from the road, use/land cover, topography wetness index (TWI), stream power index (SPI), land normalized difference vegetation index (NDVI),	Analytic Hierarchy Process (AHP)	(Arabameri et al., 2019b)
Statistical Models	Iran	Soil texture, lithology, altitude, slope angle, slope aspect, plan curvature, land use, topographic wetness index (TWI), drainage density and distance from rivers	Certainty Factor (CF), a bivariate statistical model;	(Azareh et al., 2019)

Model Type	Country	Attributes	Techniques	References
Machine learning model	India	Soil type, altitude, Slope gradient, slope aspect, plan curvature, land use, slope length (LS), drainage density, topographical wetness index (TWI), distance from the river and road, distance from the lineament,	Flexible discriminant analysis (FDA), Random forest (RF), Multivariate additive regression splines (Jin et al.) and Support Vector Machine (SVM).	(Gayen et al., 2019)
Machine learning model	Iran	Elevation, slope degree, slope aspect, plan curvature, profile curvature, catchment area, stream power index, topographic position index, topographic wetness index, land use and normalized difference vegetation index	Generalized linear model, boosted regression tree (BRT), multivariate adaptive regression spline and artificial neural network (ANN).	(Garosi et al., 2019)
Machine learning model	Australia	Digital elevation model, Annual precipitation, Geology, Temperature, land-use, soil characteristics, distance to the river and so on	Random forest (RF)	(Kuhnert et al., 2010)
Knowledge-based model	China	Topographic factors, Vegetation cover and land use	Remote sensing techniques with visual interpretations	Li et al. (2015)
Knowledge-based model	Morocco	Slop, Specific catchment area, Flow direction, stream power index, Sediment transport capacity index, NDVI	Object-based image analysis	(Shruthi et al., 2015)
Hybrid method	Iran	Elevation, slope, soil type, lithology, plan curvature, stream power index (SPI), topographic wetness index (TWI), distance to road, distance to stream, drainage density, land use/land cover and rainfall	Weighted regression (GWR), Certainty factor (CF) and Random forest (RF)	(Arabameri et al., 2019b)

2.5.2 Landslides vulnerability assessment

A number of research studies were conducted for landslide risk mapping by integrating new models, theories and geo-informatics tools (Oštir et al., 2003; Perotto-Baldiviezo et al., 2004). Landslide susceptibility zoning is denoted as the "division of land into somewhat homogeneous areas or domains and their ranking according to the degrees of actual or potential landslide susceptibility, hazard or risk" (Bobrowsky and Couture, 2014, p 65). Landslide susceptible maps can be developed with various geo-spatial data: including slope, aspect, soil, lithology, vegetation indices, land cover, distance to drainage, precipitation, distance to a fault, and distance to road extracted from synthetic aperture radar (SAR) data for better planning and risk reduction (Shahabi and Hashim, 2015). This method is widely employed for landslide mapping (Corsini et al., 2006; Tarolli, 2014; Shahabi and Hashim, 2015). Some of these landslide susceptibility assessment models were summarised in Table 2.4.

Ashournejad et al. (2019) claimed that data-driven methods perform better than knowledge-based methods based on expert opinion. In contrast, Zhu et al. (2018) concluded that the expert knowledge-based model is more suitable for landslide susceptibility mapping over large areas. For instance: the application of this model in two landslides areas; Kaixian and Three Gorges in China, has provided evidence with satisfactory outcomes. Furthermore, researchers have adapted several combinations of models for different research studies. However, every combination of methods has its own advantages and limitations.

Table 2. 4 Landslide susceptibility assessment and mapping models.

Model Type	Method	References
Knowledge-based model/ Expert knowledge model	Simple additive weighting (SAW)	(Ashournejad et al., 2019)
	Fuzzy gamma operation	
	Multi-criteria evaluation techniques	(Zhu et al., 2014)
	Fuzzy logic	
	Boolean logic	
	Simple overlay	
	Analytic hierarchy process (AHP)	
Data-driven models/ Statistical model	Frequency ratio (FR)	(Arabameri et al., 2019a)
	Evidential belief function (EBF)	(Chen et al., 2019) (Ashournejad et al., 2019)
	Radial basis function Link Network (RBFLN)	
	Probabilistic Neural Network (PNN)	
	Single and bivariate statistics Analysis (BSA)	(Pradhan and Lee, 2010a)
	Multivariate analysis(MSA)	(Arabameri et al., 2019b)
	Bivariate Logistic regression	(Abedini and Tulabi, 2018)
	landslide nominal risk factor (LNRF)	(Pradhan, 2013)
	Weights-of evidence (WoE)	
	Decision tree (DT)	
Machine Learning model	Artificial neural network (ANN)	(Pradhan and Lee, 2010a) (Youssef et al., 2016)
	Boosted regression tree (BRT)	(Tien Bui et al., 2017)
	Least squares support vector machines (LSSVM)	
	Random forest (RF)	
Hybrid method	Bayesian logistic regression (BLR)	(Tien Bui et al., 2012)
	Adaptive neuro-fuzzy inference systems (ANFIS)	
	Back-propagation neural networks (BPNNs) and rough sets	(Wu et al., 2013)
	Least square SVM	(Abedini et al., 2019)
	Statistical and Artificial intelligent techniques FR-RF integrated	(Althuwaynee et al., 2014)
	Expert knowledge base (AHP) and Multivariate and Bivariate analysis	

As previously mentioned, a sufficient level of research attention was given in the literature to gully erosion and landslide susceptibility mapping. However, soil erosion susceptibility mapping has received less attention compared to other natural hazard assessments (Tehrany et al., 2017). According to Tehrany et al. (2017), a variety of statistical and advanced methods such as evidential belief function (EBF), weights-of-evidence (WoE) and adaptive neuro-fuzzy inference system (ANFIS) have been applied and tested in the field situations of flooding and landslides but not in soil erosion modelling. However, recent studies were conducted on soil erosion susceptibility mapping using weights-of-evidence (WoE), evidential belief function (EBF) models (Saha et al., 2019) and ANFIS (Islam et al., 2018).

Despite the above soil erosion modelling, recent studies have introduced several new approaches on the model application, such as combining approaches and scenario-based simulations to predict the impacts of land use and climate change on soil erosion. Nampak et al. (2018) employed remote sensing technology to predict land-use change and its impact on soil erosion. They predicted land-use changes and soil erosion in the Cameron Highlands of Malaysia by 2025. Tehrany et al. (2017) explored soil erosion hazard susceptibility mapping using evidential belief function and the frequency ratio by using nine conditioning factors based on A2 climate scenario (IPCC, 2007) which was an for the present situation and predictions for 2100. The recent works of soil erosion assessment at a global scale have provided new knowledge about future soil erosion rates and predictions. Borrelli et al. (2017) predicted the future rate of soil erosion by modelling potential global soil erosion risks by employing shared socioeconomic pathway and representative concentrative pathways of the Inter-governmental panel on climate change's (IPCC) climate scenarios (SSP-RCP). Furthermore, Dube et al. (2020) have conducted an assessment on linear erosion features of rills and gullies erosion at a global scale.

Agriculture is highly dependent on climate (Holzkämper, 2017). Climate variation greatly influences crop production systems (Vermeulen et al., 2012), threatening ecosystems functions and ecosystem services: soil formation, hydrological cycle and nutrient cycling (Vermeulen et al., 2012), which leads to a decrease in biodiversity and food security (Campbell et al., 2016). Recent research studies have claimed that rainfall and land-use change play a major role in soil erosion hazards of different regions (Mwaniki et al., 2015;

Zhu et al., 2018). Rainfall data is crucial for several applications such as soil erosion assessment, risk evaluation and forecasting (Brocca et al., 2012). There are also satellite sensors that can provide spatially contiguous soil moisture data (soil moisture active passive (SMAP) or advanced scatterometer (ASCAT) and spatial rainfall data (Zappa et al., 2019).

This review provided erosion modelling and spatial assessment of land susceptibility to concentrated flow erosion for the restoration of ecosystems. However, continuous attention is required to find potential best solutions and strategies to prevent these hazard situations in order to maintain sustainable landscapes and farming systems. The spatial and temporal distribution of hazards is important to assess the causative factors, vulnerability and to study its correlation with future incidents. Implementation of sustainable landscape management policies and strategies depends on the basis of the spatial and temporal distribution of soil erosion hazard levels and risk assessment. However, it is still a challenge to analyse, understand and predict the situation with dynamic factors such as rainfall, land-use and land cover with the present climate variation.

2.6 Land use change detection in Farming systems

The dynamics of land use and land cover can be studied using remote sensing data such as space and airborne imageries (Bakker et al., 2005) with different classification methods. Govender et al. (2007) revealed satellite and airborne hyperspectral data can be used for classification and mapping purposes such as land-use classes and vegetation change detection. Yang et al. (2017) reviewed landscape classification systems and realized that these classifications were important to understand the landscape change patterns for cross-comparison or validation. The satellite image classification algorithms can be categorised as supervised, unsupervised and hybrid methods (Figure 2.7). Recently, advanced non-parametric classifiers such as neural networks, regression trees, fuzzy set classification logic, support vector machines (SVM) and mahalanobis distance classifier (MDC) have been used over the traditional parametric classification methods (Mulder et al., 2011). Temporal comparison has also been used to find land use changes and enlargement of eroded lands by using satellite data (Landsat TM) and aerial photos (Dwivedi et al., 1997). Individual features such as gullies and large rills can be identified by using satellite data. However, there are limitations with satellite data due to clouds and

canopy covers. Hence, aerial photography is a common method for detecting individual gullies as it provides better differentiation (Vrieling, 2006). Moreover, the Terrestrial laser scanning (TLS) method can be applied for a variety of applications such as land-use changes (Olsoy et al., 2014; Orwig et al., 2018), landslide susceptibility, rock-fall (Li et al., 2019) and gully erosion assessment (Goodwin et al., 2016). GIS-based TLS provides an accurate method for collecting a much higher density dataset (Olsoy et al., 2014). Figure 2.7 provides an image classification method.

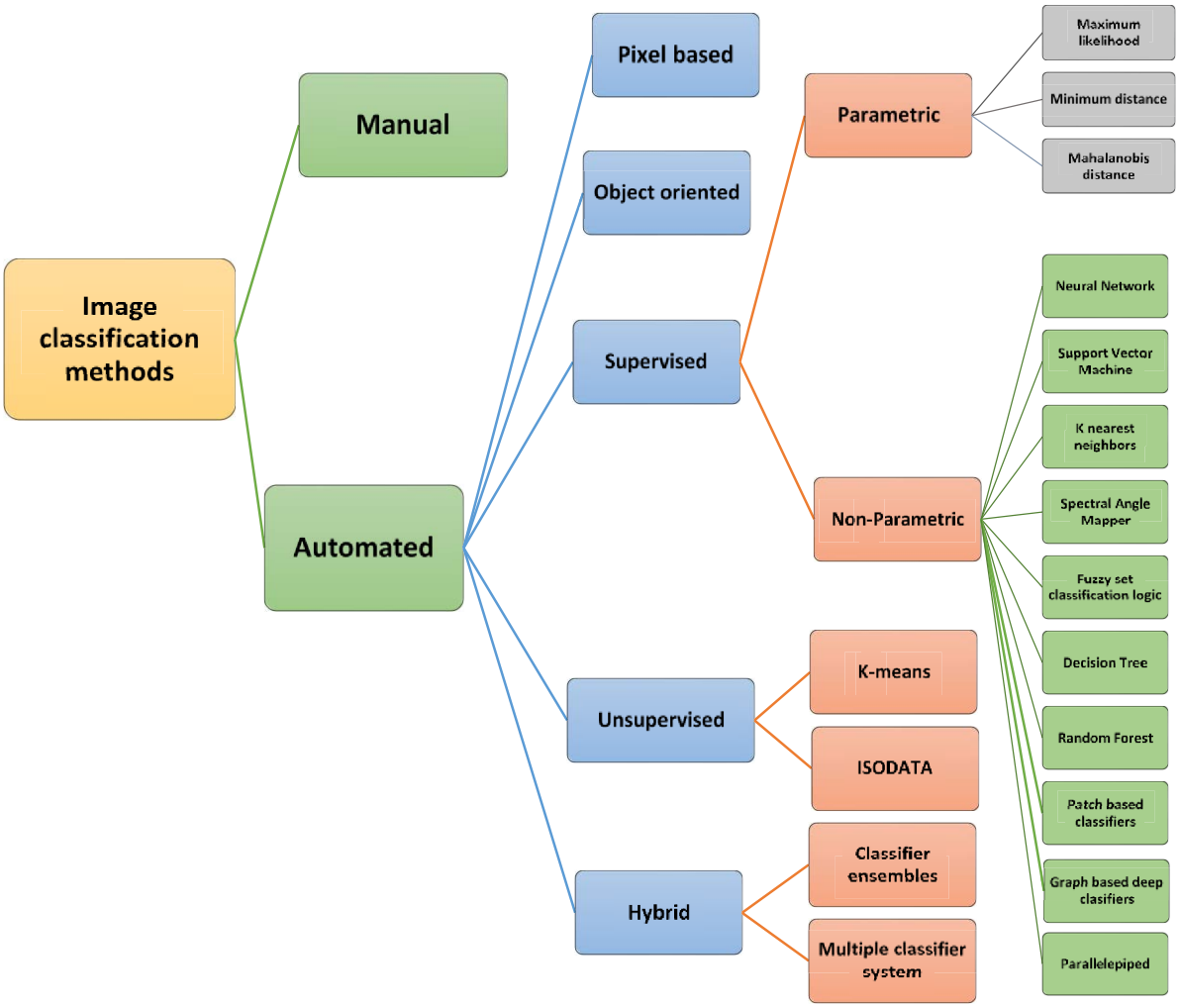

Figure 2. 7 Image classification methods for land-use change detection and soil erosion hazard assessment.

Some of the important GIS-based land-use change models are described below.

2.6.1 Land transformation model

The land transformation model (LTM) is a GIS-based model that can predict land-use change in a large area. It can be combined with several parameters such as political, socio-economic and environmental issues (Pijanowski et al., 2002; Rizeei et al., 2016). The LTM combines with GIS technology and can connect with other land-use models to predict and guide for better planning in local and regional level applications.

2.6.2 Spectral angle mapper

Spectral angle mapper (SAM) is an automated method for the comparison of image spectra with a known spectrum. Many researchers have used spectral indices to emphasise certain physiological features and can be used to differentiate between one vegetation within a mosaic of other land uses (Galvao et al., 2005; Underwood et al., 2003). Wibowo et al. (2012) proposed depressing the vegetation cover is an indicator of land degradation. SAM describes as the difference between one object and the reference spectra of vegetation.

2.6.3 Terrestrial laser scanning

The terrestrial laser scanning (TLS) method can be applied for a variety of applications such as land-use changes **(**Olsoy et al., 2014; Orwig et al., 2018), landslide susceptibility (Zieher et al., 2018), rock fall (Li et al., 2019) gully erosion assessment (Goodwin et al. 2016). The GIS-based TLS method provides an accurate method for collecting a much higher density dataset (Olsoy et al., 2014). It has a role in quantitative monitoring and continuous improvement of methods (Decuyper et al., 2018).

2.6.4 Decision tree model

The decision trees (DT) model has been used for classification and prediction analysis, such as land-use change (Gounaridis et al., 2019; Kadavi et al., 2019) and natural hazards in several studies (Pradhan, 2013; Tehrany et al., 2013). This model is a non-parametric supervised learning method and can be used for classification and regression datasets. The DT helps find the set of decision rules by creating independent variables into

homogeneous zones according to multistage or hierarchical decision-making schemes (Pradhan, 2013).

2.7 Crop diversity changes and soil erosion

Agricultural biodiversity or agrobiodiversity helps to enhance agricultural sustainability and food security (Brookfield et al., 2002). Diversity helps maintain different ecosystem functions and respond in various ways to environmental changes (Lin, 2011) such as buffering against extreme climatic events (Reusch et al., 2005). Increased diversity improves the maximum utilization of nutrients in the soil, which in turn increases biomass (Wilby and Thomas, 2002). Researchers have shown that plant diversity enhances soil water storage capacity, reduces soil erosion, and improves other ecosystem services (Hou et al., 2016; Hunt et al., 2019). The plant diversity represents the number of different plant species in a unit land area that increases with the plant density and plant cover while improving the functional diversity and indirectly reduces soil erosion (Wang et al., 2012). Hou et al. (2016) researched plant functional diversity and soil erosion. They found increasing plant diversity inhibits soil erosion under heterogynous vegetation cover. Scholars identified that plant species diversity helps reduce soil erosion on slopes (Pohl et al., 2009). Nevertheless, plant diversity makes a different response to soil erosion. Berendse et al. (2015) found a strong impact of soil erosion on crop diversity. They concluded that protecting and restoring diverse plant communities on slopes are vital to reducing soil erosion. Liu et al. (2018) examined a quantitative relationship between soil loss and plant diversity.

Maitima et al. (2009) conducted a series of studies in East Africa regarding the linkages of different land uses on biodiversity and land degradation with comparison trends in multiple sites. They examined different land uses in Kenya, Tanzania, Uganda in three different countries. The findings showed a negative correlation between soil erosion severity and plant species number. This research further compared different land uses and biodiversity measures at the same location with soil fertility measures and soil erosion indicators with a statistical evaluation. As a result, Maitima et al. (2009) found that the level of soil productivity can be categorised according to the soil characteristic and plant species composition: crop species diversity becomes low due to poor soil condition, and some plant species become more prominent such as *Digitaria scalarum, Launea Ananas comosus* (pineapple), *Helianthus annuus* (sunflower) and *Carica papaya* (pawpaw)

Oxalis corniculata, Bidens pilosa, Senecio abyssinica, and *Setaria homonyma* (Maitima et al., 2009).

The changes in species composition or diversity are unavoidable due to the continuous change in land use and land cover, and climate (John et al., 2008). In addition, crop diversity may change according to the cropping pattern in the agricultural landscape, e.g. highly intensive monoculture shows less crop diversity. Researchers have revealed that mono-cropping encourages soil erosion and reduces plant diversity, which causes more soil erosion (Hunt et al., 2019). Although there was no strong evidence, Shrestha (2011) pointed out that a negative correlation was observed with soil erosion of land uses and their respective plant diversity subject to further research. Studies on the effect of vegetation, ecosystem process and soil erosion are very limited. Most geo-informatics attempts were made to determine the effects of above-ground biomass properties such as canopy cover and height. Limited attention has been taken to examining the role of below ground biomass such as roots and soil organic matter using geo-informatics (Bardgett et al., 2014; Poesen, 2018). Therefore, crop diversity assessment against soil erosion hazards is important to identify the relationship, soil erosion susceptibility to introduce mitigation measures.

2.7.1 Crop diversity change assessment in geo-informatics environment

Estimating plant diversity by using remote sensing techniques has been conducted through direct and indirect methods (Turner et al., 2003; John et al., 2008). Direct methods use spectral reflectance values and various spatial resolutions from different sensors (Warren et al., 2014). Indirect methods estimate environmental parameters or biophysical characteristics such as primary productivity, habitat structure and climate variables which are derived by remote sensing techniques (Turner et al., 2003; John et al., 2008).

2.7.1.1 Remote sensing direct techniques

Many researchers have used remote sensing techniques for several decades due to its rewarding factors; efficiency and cost-effectiveness, detecting areas that cannot be reachable, and time-series studies (Asner et al., 2009). Different crop/plant species have different spectral signatures. Spectral reflectance may vary with the crop/plant condition, such as health, stress condition, species type and canopy state (Smith et al., 2002).

Researchers have found a positive relationship between spectral reflectance with species richness (Wang et al., 2018). Active and passive sensors in remote sensing have been used to study vast different areas, and the visible/near-infrared (VNIR) to shortwave infrared (SWIR) wavelength region (0.4–2.50μm) provide reflectance measurements in diagnostic information (Grebby et al., 2014). The satellite images can be differentiated according to their specifications for instance, various spatial (what area and how detailed), spectral (what colours – bands), temporal (time of day/ season/year) and radiometric (colour depth) resolutions.

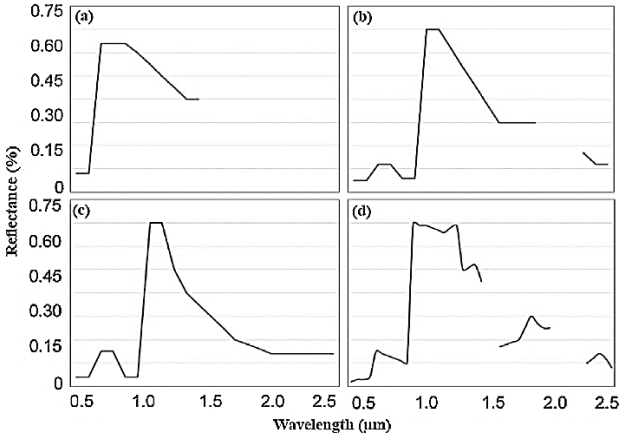

Figure 2. 8 Spectral signature of a plant detected by four different sensors: (a) Advanced Very High-Resolution Radiometer (AVHRR) (b) Landsat, (c) MODIS and (d) Airborne Visible Infrared Imaging Spectrometer (AVIRIS) source: Ustin & Gamon (2010).

A suitable type of remote sensing sensor is needed to detect specific characteristics of vegetation. The main types of remote sensing sensors such as Multi-spectral, Hyperspectral, Radio Detection and Ranging (RADAR) and Light Detection and Ranging (LiDAR) and their wide range of applications have been used to detect different types of vegetation. The spectral signature of a plant detection by four different sensors are illustrated in Figure 2.8.

Spectral diversity metrics have the potential to predict species richness by quantifying the variation in spectral data caused by biochemical, structural, or phonological properties of plants'(Gholizadeh et al., 2018). For example, the spectral signature of different vegetation types and soil is illustrated in Figure 2.9. Some studies reported a negative relationship between spectral diversity and species richness due to background effects from bare soil (Lucas and Carter, 2008).

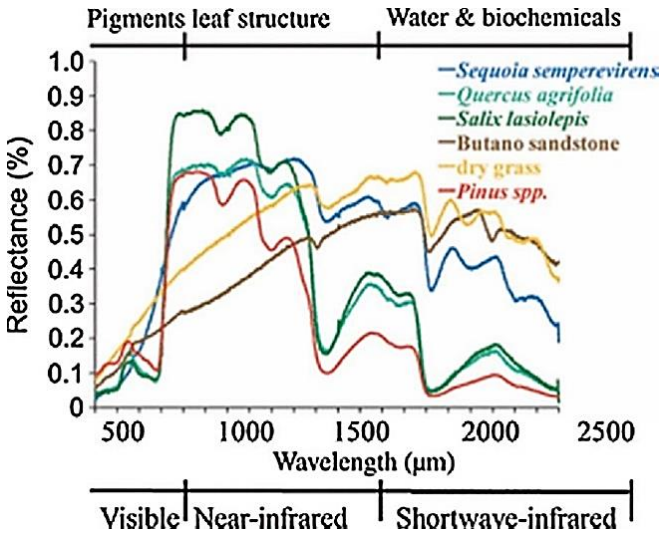

Figure 2. 9 Spectral signature of different vegetation types and soil (source: Ustin & Gamon (2010).

The hyperspectral remote sensing method is an efficient and fast-developing technology that can capture the data from hundreds of narrow spectral bands ranging from visible to near infra-red. This technique has been applied for various applications such as detection, classification, discrimination, identification and characterization (Golhani et al. 2018). Schmidt and Skidmore (2003) show that the hyperspectral analysis can identify detailed information to different wetland plant species. In addition, this study highlighted the importance of hyperspectral imagery and the potential use of vegetation spectral indices with remote sensing data (Becker et al., 2005).

2.7.1.2 Remote sensing indirect methods (Vegetation index)

A number of methods are employed by researchers for crop diversity assessments in indict method. Wang et al. (2018) studied biodiversity by using remote sensing and compared with seven diversity metrics; Planted species richness, Observed species richness, Shannon's index, Simpson's index, Evenness, Phylogenetic species variability, Phylogenetic species evenness. A strong relationship has been observed with Simpsons' index and Wang et al. (2018) pointed out more research on 'spectral diversity-biodiversity relationship' due to scale dependence.

Vegetation Indices have been used to detect land-use change and soil erosion susceptibility. The most popular general equations for vegetation indices are summarized in Table 2.5. The value of NDVI may deviate due to noises in the satellite data due to cloud cover, water, snow, shadow, sources of errors, false highs or scan angles or transmission errors (Oldeman, 1992). Hence, the soil-adjusted vegetation index (SAVI) (Huete, 1988), the Transformed SAVI (TSAVI) (Rondeaux et al., 1996), the Modified SAVI (MSAVI) and the Global Environment Monitoring Index (GEMI) (Qi et al., 1994; Rogan and YooL, 2001) are used to reduce soil background reflectance. Furthermore, the Enhanced Vegetation Index (EVI) can be used to minimize the contamination problems of NDVI images (canopy background and residual aerosol influences) and provides complementary information about the spatial and temporal variation of the vegetation cover and plant diversity (Qi et al., 1994).

Table 2. 5 Summary of popular vegetation indices.

Vegetation Index	Equation formula	Reference
NDVI	$\text{NDVI} = \frac{(NIR - RED)}{NIR + RED}$	(Rouse et al., 1974)
SAVI	$\text{SAVI} = \frac{(NIR - RED)(1 + L)}{NIR + RED + L}$ Where L= correction factor between 0 and 1	(Huete, 1988)
EVI	$\text{EVI} = G\frac{(NIR - RED)}{(NIR + C1.RED - C2.B + L)}$ G = 2.5; C1 = 6; C2 = 7.5; L = 1	(Huete et al., 2002)
TSAVI	$\text{TSAVI} = \frac{s(NIR - sRED - a)}{(aNIR + RED - as + X(1 + s2)}$ s = the soil line slope a = the soil line intercept X = an adjustment factor that is set to minimize soil noise	(Rondeaux et al., 1996)
MSAVI	$\text{MSAVI} = \frac{(2 * \text{NIR} + 1 - \text{sqrt}((2 * \text{NIR} + 1)\text{^}2 - 8 * (\text{NIR} - \text{R})))}{2}$	(Rogan and YooL, 2001)
GEMI	$\text{GEMI} = h(1 - 0.25h)\frac{(RED - 1.125)}{1 - RED}$ Where $h = \frac{2(NIR.NIR - RED.RED)(1.5NIR + 0.5RED)}{NIR + RED + 0.5}$	(Rondeaux et al., 1996)

Many researchers have studied plant diversity using vegetation indices, such as NDVI and EVI indices (Waring et al., 2006; Levin et al., 2007; Chitale et al., 2019). Several researchers have reported that there is a strong relationship between plant species diversity with vegetation indices such as NDVI (Levin et al., 2007; Pouteau et al., 2018), enhanced vegetation index (EVI) (Waring et al., 2006; Morisette et al., 2006). Levin et al. (2007) revealed that average NDVI values were strongly correlated with the percentage of tree cover. Previous studies indicate that Landsat derived vegetation indices are highly sensitive to plant abundance and species richness in tropical landscapes (Nagendra et al., 2010). Nagendra et al. (2010) found that vegetation indices have low, non-significant relationships with stand density (the number of trees per unit area). Alternatively, they found stronger relationships with species richness and diversity. The standard deviation (SD) of NDVI was positively correlated with total species richness and annual plant richness. Furthermore, SD of gross primary production (GPP) and NDVI values were positively correlated with the total species richness (John et al., 2008; Levin et al., 2007). Pau et al. (2012) researched that NDVI values have increased by 30%- to 60% due to the variance of tree species richness in a tropical forest (Pau et al., 2012). In addition, they found NDVI was positively correlated with the tree cover, and NDVI values can be used to distinguish between dense forests, non-forested areas, such as agricultural fields and savannahs. NDVI values range from −1 and +1. NDVI values become above zero in vegetated areas, and below zero can assume to be non-vegetated (Warren et al., 2014). Further to this, atmospheric conditions are another aspect that must be considered when using the NDVI (Willers et al., 2012).

Many investigations were conducted to identify the relationship associated with EVI index and the plant species richness (Waring et al., 2006; Morisette et al., 2006). Scholars revealed there is also a positive relationship between EVI and species richness. The EVI is independent from climate drives such as rainfall, sunlight intensity (Waring et al., 2006). It was developed to optimize the vegetation signal to improve vegetation monitoring by removing the background soil signal and atmospheric influences (Huete et al., 2002). The difference between the EVI and NDVI of MODIS products is an adjustment for the atmosphere and soil background (Huete et al., 2002). Therefore, it is worth to note that NDVI and EVI can be used for mapping and predicting patterns of species richness in large areas. These applications are relatively low cost (Levin et al.,

2007; Nagendra et al., 2010). Table 2.6 indicates some applications of crop diversity assessment using remote sensing in the recent past.

Table 2. 6 Some applications of crop diversity assessment using remote sensing.

Reference	Sensor type	Spectral variation measure	Spectral resolution	Response variable
Rocchini et al. (2014)	MODIS	Natural logarithm of the number of different NDVI values per polygon	250 m	Plant species counts
Schmidtlein & Fassnacht (2017)	Sentinel-2A 2B and Landsat 8 OLI	Reo Q index	30m	Tree species
Wang et al. (2019)	Landsat	Vegetation Index and machine learning	30m	Agricultural Crop types
Mishra & Singh (2019)	Landsat	NDVI and crop diversity index	30m	Cropping pattern

2.8 Validation methods

There are several methods of model evaluation and validation. Some of them are Mean Absolute Error (MAE) and the area under the receiver operating characteristic curve (AUROC). Soil erosion maps were frequently validated from ROC/AUC analysis. The AUC value equal to 1 indicates the perfect prediction. The ROC curve was employed for the validation of soil erosion susceptibility maps using training datasets. The ROC curve was developed based on the false positive rate (1-specificity) in respect to the true positive rate (sensitivity) with the various cut-off thresholds. With regard to this ROC curve, 30% of soil erosion locations are used for the model validation.

$$\text{RMSE} = \sqrt{\frac{\sum_{i=1}^{N}[\bar{X} - X]^2}{N}} \qquad (2.2)$$

$$\text{MAE} = \frac{1}{N}\sum_{i=1}^{N}[\bar{X} - X] \qquad (2.3)$$

Where N is the sample size, $\bar{X}$ is means predicted values, and X means observed values. The means absolute error is described as the sum of the deviation between the predicted

values of a variable and the real observed values. A lower RMSE (closer to zero) means a higher prediction rate.

2.9 Soil erosion management strategies in farming systems

The farming systems are vulnerable to the impacts of climate variability and extreme weather events (Thornton et al., 2014). Climate variation also causes several adverse impacts on infiltration, runoff and soil erosion, consequently reduction of crop biomass and land-use change in farming systems (Li and Fang, 2016). Therefore, reliable measures and investment in climate and environment monitoring actions are required to address these issues effectively. Soil erosion and runoff assessment, along with predictions, are essential to implement conservation measures as well as rehabilitation planning for improving sustainable productivity on a long-term basis (Hajkowicz and Young, 2005; Lu et al., 2006). Pradhan and Lee (2010b) described soil erosion susceptibility and hazard assessment with prediction models that significantly reduce future damages. Hence, a better understanding of soil erosion rates and the effects of climate variables are important for the revision of land-use policies and better soil and water conservation measures in farming systems. Persichillo et al. (2017) emphasized that maintenance of man-made mechanical structures are very important to prevent mass movement. In addition, more efforts are needed to develop or improve effective erosion control techniques and strategies for soil erosion-prone areas using biological conservation methods such as live vegetation cover.

The soil erosion hazard maps are important to identify erosion-prone areas with its magnitude for detection of the vulnerability (Rahman et al., 2009). Rahman et al. (2015) observed that soil erosion hazard and risk assessment are key factors in risk management. Although a significant number of techniques are available, Ashournejad et al. (2019) noted geo-informatics technology such as aerial and satellite images, GIS techniques, satellite and ground-based geodetic techniques, a global positioning system (GPS) provide a better understanding of risk reduction. In addition, soil erosion hazard maps provide a foundation for a further analytical tool for gully erosion, landslide susceptibility and risk identification (Tehrany et al., 2017). Hence, continuous monitoring and evaluation of mass movement using geo-informatics technology are important for risk reduction and damage prevention.

Accurate mapping of susceptibility to erosion hazards is crucial to avoid economic losses and life losses. To improve the land resources through hazard mitigation in regional development planning, conservationists and policy-makers must understand how landforms, soil types, farming practices are interacting with rainfall and water runoff affect on soil erosion process. Vrieling (2006) highlighted the importance of the validation process of data and maps, and Ganasri and Ramesh (2016) indicated that validation could be done with ground-level data. However, when ground-level data and previous research data were absent, it was very difficult. It is vital to compile and analyse valuable metadata before they are lost for future generations (Poesen, 2018). Hence, large-scale data collection (data mining) of published data on soil erosion rates, causative factors, and sediment yield can be utilised for future benefits.

Few studies have been conducted using different methods and criteria to develop indices and metrics to evaluate the sustainability of the agricultural landscape. Metrics enable a quantitative and objective analysis of the different types of agricultural landscape (Sertel et al., 2018). A quantitative model was proposed on land planning and management scenarios to identify the sustainability of olive farms in Andalusia, Spain (Sousa et al., 2019). This study used different conditions of soil erosion and management practices as criteria for modelling of abandonment, production and economic benefits of Olive farms. In addition, a multi-criteria evaluation method was used by several other researchers to identify land capability and suitability for agricultural activities by utilizing physical characteristics such as soil depth, soil texture, soil drainage, erosion hazard, land-use, altitude, slope and slope direction (Salari et al., 2019; Yohannes and Soromessa, 2019). Montgomery et al. (2016) utilised the GIS-based Logic Scoring of Preference (LSP) method as an effective tool for decision-making on agricultural land capability and land suitability assessment in Colorado, USA. It was an improved multi-criteria evaluation method, which comprises social, economic and physical characteristics as evaluation criteria: soil, topographic, climatic, economic, land-use and accessibility attributes for the analysis.

Furthermore, Gray et al. (2015) developed a new matrix scheme to guide sustainable land management in New South Wales, Australia. This scheme was used to identify the potential impact of various land degradation hazards and to promote sustainable land management practices across the region. Hence, the development of sustainable

landscape indices and a matrix with a proper monitoring system will guide scientific land management under the context of climate variation to minimize its adverse impacts on land resources. Therefore, landscape indices and matrices can be developed using geo-informatics technology to evaluate the land capability and identify sustainable land-uses. Moreover, it is important to identify ecologically viable and economically sound farming systems with future climate scenarios for sustainability. Therefore, this review provides important directions on geo-informatics applications for agricultural land vulnerability assessment and developing models for future climatic variation that help to formulate management strategies for climate-related risk reduction in farming systems. Furthermore, this review provides significant insights to assess ecologically viable and economically sound farming systems against soil erosion hazards for future implications.

2.10 Challenges, innovations and future directions

The complexity of morphological and other parameters in larger land area is a more significant challenge for soil erosion assessment and risk evaluation. Soil erosion assessment models as such RUSLE/ USLE have some drawbacks when predicting sediment pathways from hill slopes to water bodies and gully erosion assessment (Cohen et al., 2005). When combined with geo-informatics techniques: geo-spatial modelling and image fusion techniques can obtain successful research outcomes from soil erosion assessment. Hence, it has been suggested that remote sensing-based soil erosion assessment is more innovative and practicable for larger landscapes (Sepuru and Dube, 2018). Although high-resolution commercial remote sensing data have more potential, freely available Landsat archive data have been commonly used for remote sensing-based soil erosion modelling studies. Freely available Sentinel satellite data from the European Space Agency also has great potential for future soil erosion studies with its high temporal resolution and SAR sensor. The SAR (microwave/radar) sensor of the Sentinel satellite avoids misclassification due to clouds and haze. SAR is an ‘active’ remote sensing method and can collect real-time data in day and night under all weather conditions (Mizuochi et al., 2019). For example, multi-temporal X-band SAR (TerraSAR-X) (Gorrab et al., 2015; Huang et al., 2020) and GF-3 (Yang et al., 2018b) have been used for soil moisture retrieval studies. Sepuru and Dube (2018) suggested that Sentinel data have a high potential for temporal scale soil erosion assessment with 10 m resolution and 5-day repeat coverage. Similarly, the short revisit time satellites data of the Canadian

RADARSAT, the Japanese ALOS PALSAR-2 and the Himawari-8 have a great potential for temporal analysis, which can be facilitated to detect potential soil erosion hazards: emerging gullies in farmlands and susceptibility for landslide in the larger extent of a landscape. Moreover, detailed and extensive monitoring and quantification of soil erosion using the above satellite data will help to prevent and control soil erosion in a sustainable manner. The multi-temporal topographic data provide a better opportunity to detect geomorphological changes such as landslide movements, gully erosion and detection of faults in theearth surface (Tarolli, 2014). Furthermore, cloud-based geo-spatial data platforms such as the Google Earth engine and Land Viewer can support time series data analysis.

In addition, many studies indicate rainfall erosivity is highly correlated with soil erosion and soil erosion hazards (Panagos et al., 2017a). Moreover, spatially adjoining soil moisture data (SMAP) and radar/microwave base spatial rainfall data (PR-Precipitation Radar) such as TRMM (Tropical Rainfall Measurement Mission), AMSR (Advanced Microwave Scanning Radiometer) can be utilised as reliable data sources (Scaioni et al., 2014) for future research on rainfall intensity and variation and potential soil erosion hazard in farming systems, spatial-temporal assessment and prediction of climate scenarios.

However, increasing the availability of satellite data is also challenging, as the processing period may also increase in data analysis. The capabilities of remote sensing-based and GIS software can be utilised for processing satellite data. Artificial Intelligence GIS techniques (AIGIS) such as GIS incorporated with machine learning and deep learning techniques such as data mining software have an excellent opportunity for satellite data handling.

2.11 Gaps in the literature and summary

Key findings and gaps in the literature reviewed here can be summarised as follows:

- Lack of research attention on the spatial and temporal pattern of soil erosion along with rainfall characteristics such as rainfall amount, rainfall intensity, rainfall depth, erosivity and the number of rainy days with present climate variation in some parts of countries.

- There is a need to select an appropriate method for identifying farming systems using geo-informatics tools.
- The relationships between rainfall variation and potential soil erosion hazards in different climatic regions are still far from clear in the literature.
- Limited attention has been taken to examine the role of below ground biomass such as organic matter using geo-informatics.
- Much work to be done in developing spatial and temporal patterns of soil erosion, innovative techniques, and strategies for landscape evaluation to enhance productivity in a sustainable manner.
- Limited research studies were conducted to examine the correlation with soil erosion hazard, rainfall variation and crop diversity changes in farming systems.
- No proper analysis was found on the combined approach on soil erosion hazards, crop diversity and rainfall variation in farming systems.

Soil erosion has generated several issues in the agriculture landscape and farming systems worldwide. As a result, crop production losses and economic losses are countless. This review provides evidence from the literature that soil erosion has been a great threat to land productivity: in terms of damages to the soil physical, chemical and biological structure, resulting in erosion hazards which lead to low agricultural productivity, economic damages and threats to human lives.

Continuous soil erosion assessments and monitoring are essential with the present climate variation in the farming systems for sustainable land management. The combined approach of soil erosion assessment, such as empirical soil erosion modelling with geo-informatics, provide a better understanding of soil erosion and facilitate continuous monitoring. Fast-growing technologies and increasingly freely available data sources provide valid measurements for planning and implementation.

The review emphasizes that more research is required on the spatial and temporal pattern of soil erosion with present rainfall variation and as well as the development of new techniques and strategies for landscape evaluation to improve the environmental condition sustainably. It further reveals a lack of research attention on the spatial and temporal pattern of soil erosion along with rainfall characteristics such as rainfall amount, rainfall intensity, rainfall depth, erosivity and the number of rainy days with present

climate variation. The relationships between rainfall variation and potential soil erosion hazards in different climatic regions are still far from clear in the literature.

Geo-informatics technology provides a platform with advanced capabilities and potential of real-time hazard detection with a spatiotemporal distribution and soil erosion hazard predictions. Thus, geo-informatics can be applied to continuously monitor and evaluate soil erosion hazards for risk reduction and to prevent damage in farming systems. However, there is a need to select an appropriate method for identifying farming systems using geo-informatics tools.

Geo-informatics provides real-time data for analysis and solving prevailing issues using machine learning algorithms. The knowledge generated from these techniques can be used to evaluate erosion rates, develop new indices and matrices to assess the farming systems and gain a better understanding of the effects of climate variation. In addition, only a few numbers of studies have conducted in soil erosion probability and mapping using the knowledge base, data-driven and machine learning technologies for the current study area in Sri Lanka. Applications of machine learning techniques are yield better results in soil erosion hazards assessments for predicting vulnerable farming areas. The literature indicates that there is much work to be done in developing spatial and temporal patterns of soil erosion, innovative techniques, and strategies for landscape evaluation to enhance productivity in a sustainable manner.

This extended review showed limited research studies were conducted to examine the correlation with soil erosion hazard, rainfall variation and crop diversity changes in farming systems. In addition, findings of past research studies did not adequately address how crop diversity changes could be utilised to identify soil erosion hazards. A number of models with geo-spatial techniques have been employed by focusing on land uses changes and forecasting, biodiversity assessments, vegetation characteristics and environmental monitoring studies. However, no proper analysis was found on a combined approach to soil erosion hazards, crop diversity and rainfall variation in farming systems. These gaps indicate the literature undermined the importance of extending research to examine the correlation between soil erosion hazards and crop diversity changes with rainfall variation in farming systems.

Finally, this review identified several research needs pertaining to future research for academics, researchers and policy planners. Soil erosion rates and soil erosion hazard susceptibility maps provide information for vulnerable areas and their determinants, which will be useful to develop new models and applications in future research for predictions and sustainable farming systems development. Policy planners could utilise the outcomes of soil erosion hazard assessment to guide appropriate actions such as soil and water conservation measures and recommendations for sustainable landscape development and natural resource management in the future. A combination of multi-temporal data: commonly used optical satellite data, microwave short revisit satellite data, and UAV data have enormous potential to predict soil erosion hazards in farming systems against future climate scenarios.

CHAPTER 3

MATERIALS AND METHODOLOGY

3.1 Overview

This chapter provides the materials and methodology employed to investigate soil erosion hazards and crop diversity changes for different farming systems due to rainfall variation in the Central Highlands of Sri Lanka. This study examined four aspects of soil erosion hazards: soil erosion hazards with crop diversity changes, rainfall variation, ecologically viable and economically sound farming systems, and soil erosion hazards susceptibility associated with climate change scenarios. Comprehensive methodological approaches were employed to address four research questions. This chapter first describes the study area and the location and data sources. This is followed by a discussion of overall methodology and its implementation: LULC change assessments, the soil erosion hazards, and crop diversity change assessments in different farming systems in the Central Highlands of Sri Lanka. Secondly, the analyses of rainfall variation and soil erosion hazards are described. The assessment of ecologically viable and economically sound farming systems using a matrix-based geo-informatics approach and predicting soil erosion susceptibility associated with climate change scenarios are described in the following sections, respectively. Furthermore, a summary of the materials and methodology is provided.

3.2 Study area

Sri Lanka is an island in the Indian Ocean situated at 6° 55'' N - 9º50'N longitudes and 79º42' E to 81º52' E latitudes (Rathnayake, 2011). The Central Highlands of Sri Lanka were selected for this study (Figure 3.1). The central region of the country consists of hilly and mountainous terrain with highly fractured and folded basement rock overlaid by residual soil and colluviums. The Central Highlands mainly cover three provinces, i.e. Central, Uva and Sabaragamuwa. The Central Highland was declared a protected area under the soil conservation act (Act No 25: 1951) of Sri Lanka due to potential soil erosion. The total land area of the Central Highlands is about 10,618 km^2. Sri Lanka has divided into three distinct climatic zones: the dry zone, intermediate zone and wet zone, according to the temporal and spatial variation of rainfall. The majority of the landmass in the Central Highlands is situated in the wet zone. The higher elevation areas receive

over 4,000 mm of annual rainfall. The elevation of the Central Highlands ranges from about 300 to 2,500 m (the highest elevation is at 2,524 m in Pidurutalaga). The annual average rainfall in the Central Highlands area is 4000mm (de Silva and Sonnadara, 2016). The Central Highlands is occupied about 35% of the total population in Sri Lanka. Agricultural land use with the elevation of the Central Highlands is given in Figure 3.2.

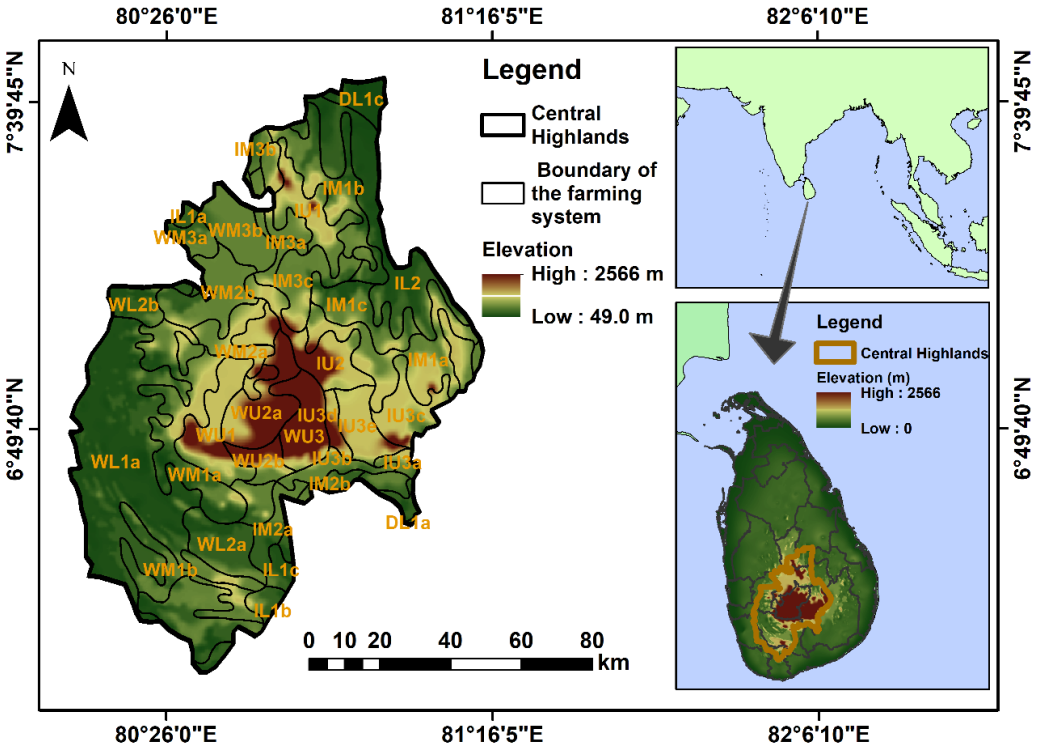

Figure 3. 1 Location of the Central Highlands in Sri Lanka

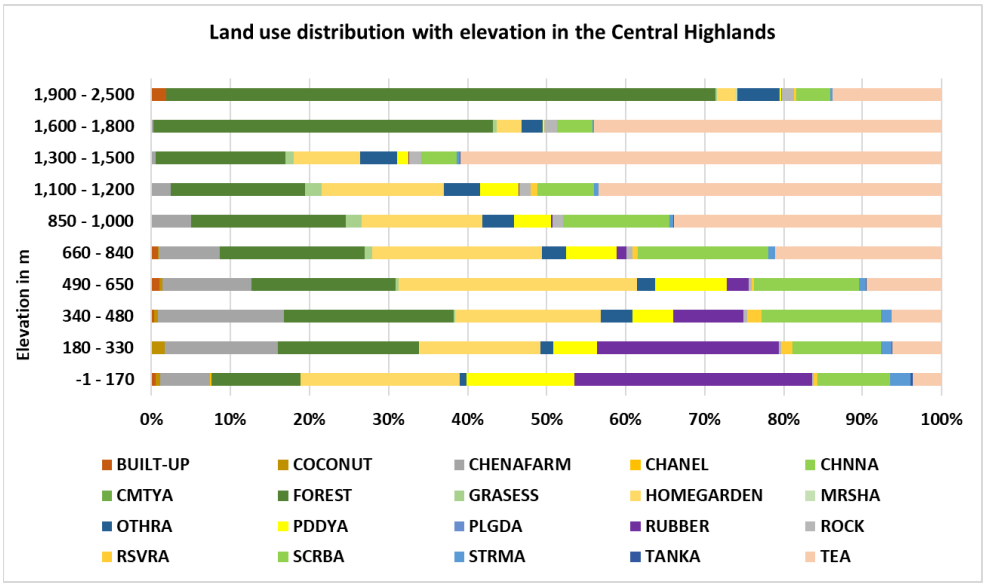

Figure 3. 2 Land-use distribution with elevation in the Central Highlands in 2015 (source:LUPPD_SL).

3.3 Data and software

Respective data for this study were gathered from different sources (Table 3.1). The Landsat imageries (freely available) for the respective period of 2000 - 2020 were downloaded (Table 3.2) from the USGS website (https://earthexplorer.usgs.gov). Land-use maps were obtained for 2000, 2008, and 2015 from the Department of Land use policy planning of Sri Lanka, rainfall data from the Department of Meteorological and Department of Agriculture, Sri Lanka, soil and contour maps from the Survey Department of Sri Lanka. Furthermore, the past landslide incidents were collected from the Disaster Management Centre and National Research Building Organization of Sri Lanka and other data sources such as the "Desinventar" disaster information system of UNISDR (United Nations International Strategy for Disaster Reduction). The statistically downscaled Community Climate System Model (CCSM) projections' precipitation dataset (RCP precipitation projection) were downloaded from National Center for Atmospheric Research (NCAR) (https://gisclimatechange. ucar.edu/ inspector) in GIS formats at global 1-degree (Hoar and Nychka, 2008).

Table 3. 1 Summary of the data sources

Data	Resolution	Source
Landsat images	30m	USGS Earth explore https: earthexplorer.usgs.gov
MODIS data MOD13Q1	250/500m	Global Subsets Tool: MODIS/VIIRS Land Products. https://modis.ornl.gov/globalsubset/
Soil data	30m	Natural Resources Management Center www.doa.gov.lk, http://nrmc.lk/NRMC/
Precipitation data from Five agrometeorological stations from 2000 to 2019		Natural Resources Management Center https://www.doa.gov.lk/NRMC/index.php/en/
Topographic data	30m	Survey Department of Sri Lanka
Past landslide incidence		United Nations International Strategy for Disaster Reduction (UNISDR) http://www.desinventar.lk:8081/DesInventar/index.jsp
Satellite rainfall data (PERSIANN-CDR)		Center for Hydrometeorology and Remote Sensing (CHRS) (https://chrsdata.eng.uci.edu/)
Economic and social statistics		Central bank report-2019 https://www.cbsl.gov.lk/en/publications/economic-and-financial-reports/annual-reports/annual-report-2019
Climate System Model (CCSM) projections		https://gisclimatechange. ucar.edu/ inspector https://gisclimate change.ucar.edu http://www. worldclim.org/

Table 3. 2 Downloaded Landsat satellite datasets

Satellite image	Date	Cloud cover (%)	Resolution (m)
LE07_L1TP_141055_20000123_20170213_01_T1.tar LE07_L1TP_141056_20000123_20170213_01_T1.tar	23-01-2000	2.04	30
LT05_L1TP_141055_20100126_20161017_01_T1.tar LT05_L1TP_141056_20100126_20161017_01_T1.tar	26-01-2010	11.00	30
LC08_L1TP_141055_20190324_20190403_01_T1.tar LC08_L1TP_141056_20190324_20190403_01_T1.tar	24- 03-2019	8.23	30

Software used for this research:

ArcGIS, QGIS, ENVI – Spatial analysis and mapping

SPSS, R studio - Statistical analysis

Matlab, Python, - Machine learning and deep learning programing

MS Office package, Past 4.03, Power BI desktop- Report writing, data analysis, and data visualization

3.4 Overall methodology

Soil erosion hazard assessments in the Central Highland were conducted by estimating using RUSLE and GIS and remote sensing techniques. Several researchers, including Dissanayake et al. (2019), have confirmed that combined use of GIS and erosion models, such as RUSLE, is an effective approach to estimating the magnitude and spatial distribution of soil erosion in the Central Highlands. Factors causing soil erosion (rainfall erosivity, soil erodibility, land slope and length, land use and land management practices) were geographically analysed, and the risk maps were generated.

LULC and soil erosion assessments were carried out in different farming systems to investigate erosion hazards. Agricultural land-use changes during the past two decades were assessed by remotely sensed image data. Crop diversity changes with soil erosion and rainfall over the past two decades were examined using vegetation indices and spatiotemporal distribution using the knowledge of remote sensing and geo-informatics technology. The site-specific erosion hazards and crop diversity changes were investigated using RUSLE integrated GIS and remote sensing data. Land capability indices were developed to identify the ecologically viable and economically sound farming systems in the Central Highlands. Statistical and machine learning models were employed to predict agricultural land vulnerability for future rainfall variation based on

RCP climate scenarios. The schematic diagram of the overall methodology of this research to achieve the research objectives is shown in Figure 3.3.

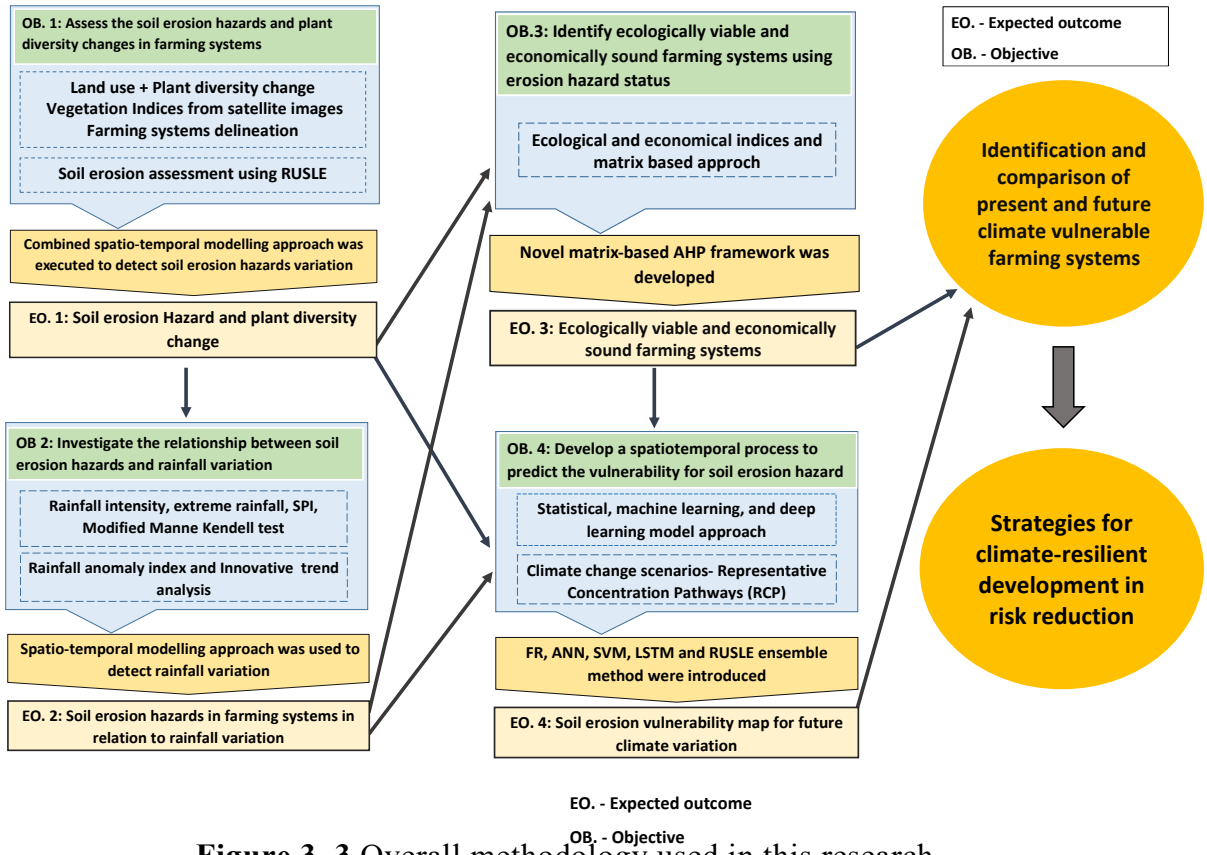

Figure. 3 Overall methodology used in this research.

3.5 Implementation of the methodology

3.5.1 Objective 1:

The first objective of this study was to examine soil erosion hazards and crop diversity changes. Remote sensing data provides useful information to monitor long-term changes in ecosystems and agricultural land management for sustainable food production. Several studies investigated land degradation and plant diversity using various remote sensing technologies with time-series observation (Wessels et al., 2007; Burrell et al., 2017; Mondal et al., 2020). Landsat data does not serve the purpose of time-series analysis. However, MODIS data serves for the purpose (see chapter 5.7, page 197). Therefore, we used both Landsat and MODIS data. Remote sensing and geographical information systems (GIS) have been widely applied to soil erosion and land-use change analyses (Fenta et al., 2021). However, none of the studies attempted to employ spatial modelling

of the soil erosion hazards and plant diversity change using time-series analysis with geo-informatics tools. LULC assessment was conducted for the farming system demarcation based on agro-ecological regions in the Central Highlands. Soil erosion, soil erosion hazards and crop diversity change were analysed to achieve objective 1. The case study approach was employed for further analysis.

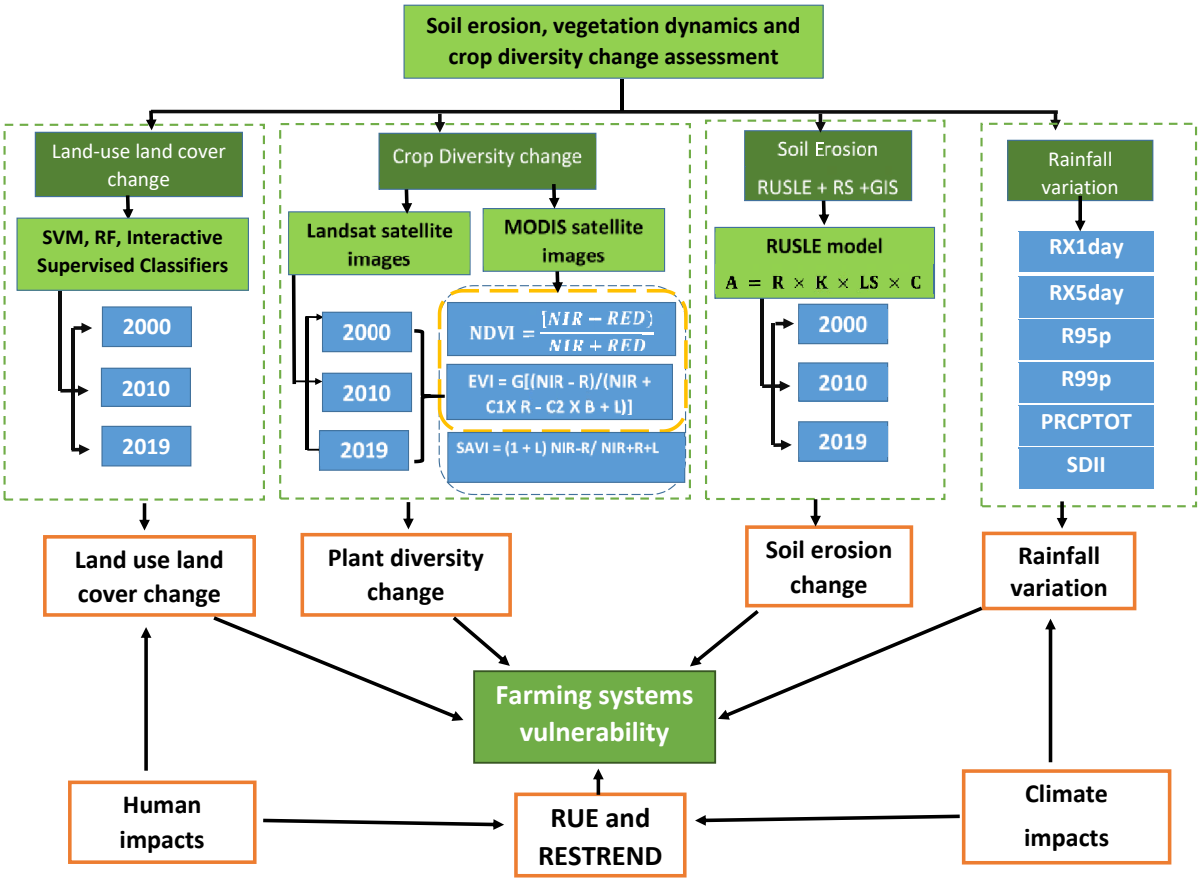

Figure 3. 4. The flowchart of the methodology used for objective 1.

The current study provides a ***novel approach*** by integrating land-use and land-cover change, soil erosion hazards, crop diversity change and rainfall variation for early detection of soil erosion in the farming systems. This combined spatial modelling approach is further employed to do partition between human and climate-induced land degradation. The schematic diagram of the overall methodology for objective 1 is shown in Figure 3.4.

3.5.1.1 LULC assessment

The land-use land-cover (LULC) classification was carried out through support vector machine algorithm (SVM), random forest (RF) and the interactive supervised classification methods using Landsat satellite images from 2000, 2010, and 2019. The SVM and RF are a widely used machine-learning method (Thanh Noi and Kappas, 2017; Ahmad et al., 2018), SVM was introduced by Cortes and Vapnik (1995) and RF was introduced by (Breiman, 2001). The Environment for Visualizing Images (ENVI), ArcGIS and QGIS software were used for image processing. An interactive supervised classification method was employed in ArcGIS. The random forest method is a robust and efficient machine learning algorithm that was employed in QGIS software. Each acquired image was geometrically corrected and registered into WGS 84 datum and UTM zone 44N projection. The radiometric and atmospheric corrections are prerequisites for generating high-quality images (Chander et al., 2009). The dark object subtraction method was applied to all images (Chavez, 1996) using the ENVI software. LULC time-series analyses were conducted after pan sharpening. The land use maps were developed for 2000, 2010 and 2019. Five land-use classes were identified from the satellite images using land-use maps of the Land Use Policy Planning Department (LUPPD) of Sri Lanka.

Table 3. 3 The details of land-use classes.

Land-use Type	Description
Dense forest	Primary forest in Sabaragamuwa Province: lowland evergreen rainforest, lower montane forest, and upper montane forest such as part of "Sinharaja" Forest and part of "SriPadha" Peak wildness sanctuary.
Less dense forest	The forest shorter than the primary forest or secondary forest such as shrubs and bushes.
Cropping area	The area used to cultivate agricultural crops such as tea, rubber, coconut export agriculture crops, horticultural crops, and home gardens.
Urban area	The urban area including roads, buildings, and settlements.
Water bodies	The area consists of tanks and reservoirs.

Olofsson et al. (2013) highlighted the importance of accuracy assessment: user's, producer's and overall accuracy. Therefore, on average, 7500 training pixels were considered for each image to conduct a validation process using a confusion matrix. Finally, Kappa coefficients were derived for each classified image for 2000, 2010, and 2019. The Kappa coefficient is commonly used by researchers in accuracy assessment

(Qi et al., 2012; Rizeei et al., 2016; Nampak et al., 2018). The Kappa coefficient is given in equation 3.1 (Bishop et al., 2007),

$$Kappa = \frac{N\sum_{i=1}^{r} X_{ii} - \sum_{i=1}^{r}(x_{i+})(x_{i+})}{N^2 - \sum_{i=1}^{r}(x_{i+})(x_{i+})} \qquad (3.1)$$

where N is the total number of pixels of the ground truth (Singh et al., 2014) land-use classes, X_{ii} denotes the confusion matrix diagonals, $(x_{i+})(x_{i+})$ are the ground truth pixels in a class and the sum of the classified pixels in that class and the sum of overall classes.

3.5.1.1.1 Support vector machine learning classification

Support vector machine algorithm (SVM) is one of the most popular machine learning algorithms and is considered a high-performing technique. SVM algorithm was used to classify land-use classes from downloaded satellite images. Two Landsat satellite images were downloaded from earth explore to cover the study area. The ENVI software was used for image processing as well as radiometric and atmospheric corrections. Each acquired image was geometrically corrected and registered into WGS 84 datum and UTM zone 44 N projection. Researchers revealed SVM is one of the best land-use classification methods with high accuracy (Jozdani et al., 2019**;** Lee et al., 2017). The primary basis of the SVM method is to find optimal separation hyper-plane from the dataset (Lee et al., 2017) and the training points that are closer to hyper-plane called support vectors (Pradhan, 2013). When considering the training vectors (X_i, Y_i) corresponding influencing factor if $X_i \in R^n$, and $Y_i \in \{+1,-1\}$, i= 1……m the optimal separating hyperplane can separate two classes, i.e. eroded areas and non-eroded areas can be determined as in equation (3.2).

$$Y = (W \times X_i + \mathrm{b}) \geq 1 - \zeta_i \qquad (3.2)$$

where w is a coefficient vector that determines the orientation of the hyper- plane in the pace of the feature, b is the offset of the hyper plane from the origin, $\zeta_i > 0$ is the positive lack variables (Cortes and Vapnik, 1995). Slack variables were introduced due to the effects of misclassification (Samui, 2008).

The determination of an optimal hyper plane leads to the solving of the following optimization problem using Lagrangian multipliers (Samui, 2008)

$$\text{Minimize} \qquad \sum_{i=1}^{n} \alpha_i - \frac{1}{2}\sum_{i=1}^{n}\sum_{j=1}^{n} \alpha_i \alpha_j x_i x_j j(x_i\ x_j) \qquad (3.3)$$

Subject to $\sum_{i=1}^{n} \alpha_j y_j = 0 \; and \; 0 \leq x_i \leq C$ (3.4)

The decision function, which is used for the classification of new data, can then be written as in equation (3.5),

$$G(x) = \text{sign}(\sum_{i=1}^{n} y_i \alpha_i x_i + b \qquad (3.5)$$

when the separating hyper plane is not a linear kernel function, the original input data can transfer into some nonlinear kernel functions. The classification decision function is written as in equation (3.6);

$$G(x) = \text{sign}(\sum_{i=1}^{n} a_1 \times y \times K \times (X, X_1) + C) \qquad (3.6)$$

Where, C, α_1, are the offset from the origin, K (X,X_i), is the kernel function. There are several other kernel functions for SVM (Table 3.4) for optimisation: linear, polynomial, radial basis function (RBF), and sigmoid (Lee et al., 2017) The RBF function was used for this analysis. A successful classification and optimisation are influenced by the choice of kernel type and the parameters (Damaševičius, 2010). The different kernel types and their equations are as follows:

Table 3. 4. SVM basic kernel, formulas and parameters

Kernel	Equation	Parameter
Linear	$K(X_i, X_j) = x_i^T x_j$	-
Polynomial	$K(X_i, X_j) = (yx_i^T x_j + r)^d$	y, r, d
Radial basis	$K(X_i, X_j) = \exp(-\Upsilon \parallel X_i X_j \parallel^2)$	Υ
Sigmoid	$K(X_i, X_j) = tanh(yx_i^T x_j + r)$	Υ r

3.5.1.1.2. Random forest method

The Random forest (RF) algorithm was introduced by (Breiman, 2001). RF is a nonparametric ensemble method that has been successfully used in many areas due to its ability to deal with different forms of data. It is an integrated method of decision tree and supervised learning algorithm. Random forest is a collection of tree predictors that are grown independently. Individual trees are built from bootstrapping training datasets. The method has been mainly applied to classification and regression problems. RF has been increasingly used for remotely sensed satellite image processing due to its higher accuracy.

3.5.1.1.3 Interactive supervised classification method

The interactive supervise classifier technique was applied to delineate the LULC classes from the satellite images. The image analysis algorithms can be divided into two categories: pixel-based image classifiers and object-based image classifiers (Nampak et al., 2018). The object-based image classification method has been used as a robust and accurate method for image classification (Leh et al., 2013). The selection of optimum segmentation is one of the challenges in the object-based image classification method (Rizeei et al., 2018). Hence, the mixed method was used to classify the images (Leh et al., 2013). The images' multi-temporal Landsat 7 (ETM+) and 8 (OLI) bands (5, 4, and 3) and Landsat 5 (TM) bands (4, 3, and 2) with false-colour composites were used to distinguish the different land-cover types and classify the land area into homogenized groups. An interactive supervised classification method was used to classify the images initially. The tool entails a supervised classification method that can speed up the classification process. On average, 80 training data sets were considered for each LULC class. Seven land-use classes were defined from the classified images, prior knowledge of the area, and the LULC map of the Land Use Policy Planning Department (LUPPD) of Sri Lanka. The land-use classes were classified according to the Anderson classification scheme, as in Burian et al. (2002). Table 3.3 shows the details of the land use classes.

The same methodology was employed to create other image layers for land-use change detection. The time-series of the multispectral datasets of the study area were analysed. The land-use classes were retrieved for 2000, 2010, and 2019, respectively, from the Landsat images. The LULC change was investigated from 2000 to 2019 and quantified the change during this period. An accuracy assessment is required to ensure the correctness of the information on the LULC change driven from the Landsat images. Olofsson et al. (2013) emphasized the importance of a validation process to achieve good study outcomes. Thus, an image classification accuracy assessment was performed using approximately 289 ground control points for each image. The field data, google map, and land-use maps produced by the LUPPD were used for further validation and verification by the above land-use classes generated from the Landsat satellite image dataset. The image accuracy was quantified with a confusion matrix by computing user's accuracy (accounting for errors of commission), producer's accuracy (accounting for errors of

omission), overall accuracy, and the Kappa coefficient for each corresponding image. This method for the accuracy assessment is widely used by other researchers in similar studies (Dissanayake et al., 2019).

3.5.1.2 Farming systems demarcation

The food and agriculture organization of the United Nations (FAO) defines a farming system as a "population of individual farm systems that have broadly similar resource bases, enterprise patterns, household livelihoods and constraints, and for which similar development strategies and interventions would be appropriate. Thus, a farming system can encompass a few dozen or many millions of households" (FAO, 2020). Farming systems in the Central Highlands of Sri Lanka consist of different cropping systems, including plantation agriculture, horticultural crops, and homegardens. The cropping pattern of farming systems is mainly based on the characteristics of agro-ecological regions. There are 46 agro-ecological regions (AERs) in Sri Lanka (Punyawardena et al., 2003). Panabokke (1996) described, "an AER represents a particular combination of the natural characteristics of climate, soil, and relief, and as such, each AER would support a particular farming system where a certain range of crops and farming practices find their best expression".

This research derives the operational definition of the farming system as the cropping area under each AER. A land-use land-cover classification was carried out with SVM using ENVI software to identify the cropping areas in the Central Highlands. A detailed description of this method is given in above (section 3.5.1.1.2**)**. The cropping areas were extracted in the GIS environment based on the classified land-use map. Finally, the AERs map of the Central Highlands was overlaid on extracted cropping areas to demarcate the farming systems.

3.5.1.3 Soil erosion assessment

The soil erosion vulnerability of each farming system in the Central Highlands was derived to determine the spatial and temporal variation of soil erosion. Although there are several approaches used to estimate soil erosion, Revised Universal Soil Loss Equation (RUSLE) has been used in this study (see equation 3.7). The RUSLE method was used due to its easy integration of geo-informatics techniques as well as a practical method of considering a large land area and data-scarce situation. The RUSLE is a widely accepted attractive tool and has been used under different climatic conditions worldwide (Angima et al., 2003; Fernández and Vega, 2018; Alewell et al., 2019). This model has been successfully employed in several applications in tropical counties such as India, Sri Lanka (Ganasri and Ramesh, 2016: Wijesundara et al., 2018) and Malaysia (Nampak et al., 2018).

$$A = R \times K \times L \times S \times C \times P \qquad (3.7)$$

The annual soil loss per unit area (A) is measured in tons per hectare per year. The rainfall erosivity factor (R) (MJ mm ha^{-1} $h^{-1}yr^{-1}$) was calculated with rainfall data from the past 30 years (1990-2019). The soil erodibility factor (K) (t ha h $MJ^{-1}mm^{-1}$), slope length and steepness factor (LS) (dimensionless), crop factor (C) (dimensionless) and conservation practices factor (P) (dimensionless) were derived from data gathered from different sources. The R, K, LS, C, and P factor layers were computed in 30m gridded raster format. The raster calculator tool in the spatial analysis was used to estimate the annual soil loss in the study area. The final soil erosion raster map was classified into five classes to identify the most vulnerable regions. The soil erosion hazards maps were generated for 2000, 2010 and 2019.

The geo-spatial layers were generated in 30 m resolution in GIS environment. Rainfall erosivity (R-factor) was calculated using 30 years of precipitation data, whilst soil erodibility (K-factor) was derived using a soil map with the local soil conditions prepared by the survey department of Sri Lanka. The L and S factors were derived from the digital elevation model (DEM) from the contour maps developed by the Sri Lanka survey department. The crop management (C-factor) was generated from the NDVI value, and conservation practices (P-factor) were computed from the values using the recent literature by Dissanayake et al. (2019).

The rainfall erosivity (R-factor) represents the influence of rainfall on soil erosion (Wischmeier and Smith, 1978). Thirty years of daily rainfall data (1990–2019), from nine rain-gauge stations (Bandarawela, Badulla, Ambewella, Nuwara Eliya, Katugastota, Ehaliyagoda, Watawala, Ratnapura, Aranayake) were collected from the Department of Meteorology and the Agro-meteorological stations of the Department of Agriculture in Sri Lanka.

Table 3. 5. Details of meteorological stations

FID	Station	Longitude	Latitude	Duration	ARF	Duration1	ARF2
1	Bandarawela	80.96	6.82	1970-2000	1468.08	1985-2015	1609.52
2	Badulla	81.5	6.95	1970-2000	1699.6	1978-2007	1687.52
3	Ambewella	80.8	6.88	1970-2000	2252.53	1975-2005	2091.19
4	Nuwara Eliya	80.76	6.96	1970-2000	1928.45	1975-2005	1883.86
5	Katugastota	80.63	7.33	1970-2000	1872.39	1977-2007	1788.21
6	Ehaliyagoda	80.27	6.85	1970-2000	4085.7	1975-2005	4033.03
7	Watawala	80.53	6.96	1970-2000	5174.1	1975-2005	5187.22
8	Ratnapura	80.38	6.7	1970-2000	3717.31	1975-2005	3641.3
9	Aranayake	80.47	7.18	1970-2000	2164.4	1975-2005	1967.87

ARF- Average annual rainfall

The mean annual precipitation (MAP) can be found in Table 3.5. R-factor estimation was performed using the following (Equation 3.8), as proposed by Wickramasinghe and Premalal in 1988 (Wijesekera et al., 2013) for the Sri Lankan condition:

$$R = (972.75 + 9.95 \times P)/100 \qquad (3.8)$$

where, R is the annual rainfall erosivity (MJ mm ha^{-1} h^{-1} yr^{-1}), and P is the mean annual precipitation (mm). The calculated R factor for each station was converted to a raster surface with a 30 m grid cell using interpolation techniques (IWD) for the spatial analysis in ArcGIS. Dissanayake et al. (2019).employed a similar method. The R-factor ranges from 152.5 to 399 MJ mm ha^{-1} $h^{-1}yr^{-1}$. The higher value indicates a high capability of rainfall to cause soil erosion, while the lower value shows a low capability of rainfall to cause soil erosion (Uddin et al., 2018).

The soil erodibility (K-factor) indicates the soil susceptibility to erosion, which is dependent on soil type and properties of the soil, such as texture, organic matter, and permeability (Pradhan, 2011). The most prominent soil type in the Central Highlands is

the red-yellow Podzolic soil with steeply dissected hilly and rolling terrain characteristics. The K-factors of the different types of local soil are given in Table 3.6 were generated from the previous studies of Fayas et al., (2019) and Dissanayake et al. (2019). The values of these factors were used to generate the K-factor map of the Central Highlands. The soil erosion susceptibility increases with higher K-factor values (Adornado et al., 2009). The K-factor values range from 1 to 0.27 t ha h $MJ^{-1}mm^{-1}$.

Table 3. 6. Details of the soil erodibility values (t ha h $MJ^{-1}mm^{-1}$)

Soil Type	K-Factor Value
Reddish-Brown Latasolic	0.2
Reddish-Brown Earth	0.3
Alluvial soils	0.3
Red-Yellow Latasol	0.3
Non-Calsic Brown	0.4
Immature brown loams	0.3
Red Yellow Podzolic	0.2

The LS factors that represent topographic factors length (L) and steepness (S) of a slope provide the terrain characteristics of a given site. The digital elevation model (DEM), which can be used to identify the terrain characteristics, was generated using the digital contour map (1:50,000) from the Survey Department of Sri Lanka. Equation 3.9, adopted from Moore and Burch (Moore and Burch, 1986), was used to compute LS-factor. The LS-factor values range between 0 and 293.5. The higher LS-factor value means a higher impact on soil loss, while a lower value means a lower impact on soil loss (Pradhan, 2011).

$$LS = (m + 1) \times \left[\frac{A}{L_0}\right]^m \times [\sin b/S_0]^n \quad (3.9)$$

where: A (m) is the upslope contributing area per unit of width as a proxy for discharge; β is the slope angle (degree); L_0 is the length (72.6 ft., equal to 22.13 m) and S_0 is the angle of the standard terrain parcel (9%, equal to 5.16 degree slope) of USLE/RUSLE. Finally, m and n are exponent parameters depending on the specific prevailing type of erosion (sheet erosion m- 0.4 to 0.6, rill n-1.0 to 1.3).

The crop management (C-factor) corresponds to ground cover management, such as the effect of soil disturbance due to changes in land-use patterns. The C-factor values can be

measured in the field and a satellite-derived normalized differenced vegetation index-NDVI. However, field survey is time-consuming, and labor is required to process them (Durigon et al., 2014). Remote sensing and GIS integrated method is an efficient and accurate method for C-factor estimation (Durigon et al., 2014). The remote sensing method can be repeated frequently by reasons of vegetation dynamic regularly observation needed to reduce the soil erosion process. The C-factor is dimensionless, and its values vary between 0 and 1. The C-factor value closer to zero means well-protected land cover, while this value reaches 1 for barren land (Ganasri and Ramesh, 2016). The C-factor was derived from the normalized difference vegetation index (NDVI) (equation 3.10 and 3.11). Landsat satellite data were used for each year to generate the C-factor, and maps were developed.

$$NDVI = \frac{(NIR-RED)}{NIR+RED} \qquad (3.10)$$

van der Knijff et al.(2000) proposed this method for the vegetation cover in soil erosion modelling might increase the values for the tropical region. Durigon et al. (2014) have put forward C- factor can be calculated for tropical climate conditions using the following equation with more intense rainfall. The equation is as follows;

$$C = \frac{(-\mathrm{NDVI}+1)}{2} \qquad (3.11)$$

The method used in the present study was very useful in analysing erosion risk by estimating C-factor values from remote sensing images. It can also be applied for monitoring erosion risk in agricultural areas and natural vegetation. This is of great importance, especially for tropical forest regions, where high rainfall associated with human activity can promote soil loss, with consequent environmental degradation and quality loss. However, Almagro et al. (2017) and other researchers concluded that uncorrected atmospheric effects could impact up to 50% of the results of NDVI calculations. Alternative equations with different methods can be used to correct the atmospheric effect (Almagro et al., 2017). In the current study, Landsat images were less than 10% cloud cover, and the atmospheric correction was done using the dark-object subtraction (DOS) method (Wicaksono and Hafizt, 2018).

The conservation practice (P-factor) involves specific conservation practices, particularly soil loss due to tillage practices (Renard et al., 1997). P-factor is the conservation support-

practices factor which is also dimensionless (Yang et al., 2020). The values of the P-factor range from 0 to 1. This means the higher values indicate no conservation while lower values indicate sufficient conservation practices. In this study, the P factor was attributed to past studies. Table 3.7 provides the details of P-factor values for each land-use class (Dissanayake et al. 2019).".

Table 3. 7. P-factor and C-factor values for land-use classes.

No	Land-use types	P Factor Value
1	Dense forest	1
2	Less dense forest/ Open forest	0.5
3	Cropping area/ agriculture area	0.35
4	Urban area/Built up area	0.8
5	Streams	0.3
6	Water bodies	1

The R, K, LS, C, and P factor layers were computed in 30m gridded raster format. The raster calculator tool in the spatial analysis was used to estimate the annual soil loss in the study area. The final soil erosion raster map was classified into five classes to identify the most vulnerable regions. The soil erosion hazards maps were generated for the years 2000, 2010 and 2019.

3.5.1.4 Soil erosion hazards in the Central Highlands

Landslides are a good indicator of soil erosion hazards (Pradhan et al., 2012). Landslides inventory (Figure 3.6) was prepared for the Central Highlands using the United Nations International Strategy for Disaster Reduction 'Desinventar' (UNISDR, 2021). Landslide frequency ratio (FR) for each farming system can be estimated using equation (3.12) (Lee and Talib, 2005; Meena et al., 2019).

$$FR_{(i)} = \frac{S_{(i)}/A_{(i)}}{\sum_1^n \left(S_{(i)}/A_{(i)}\right)}, \qquad (3.12)$$

where, S_i the number of pixels containing landslides in class (i), A_i is the total number of pixels in class (i).

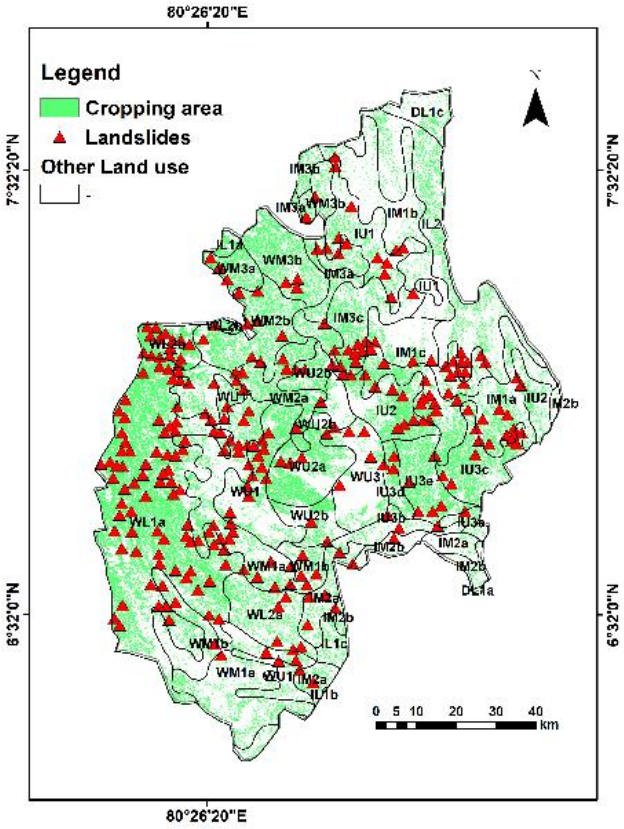

Figure 3. 5 Landslides inventory map of the Central Highlands of Sri Lanka.

The outcome of this analysis provided the most vulnerable areas for soil erosion hazards in the Central Highlands. A further analysis was carried out in a case study in the most vulnerable area for landslides, Sabaragamuwa province, for an in-depth understanding of soil erosion hazards.

3.5.1.5 Case study 1: Assessing soil erosion hazards using frequency ratio method in Sabaragamuwa province

3.5.1.5.1 Study site

Sabaragamuwa, which is one of the Provinces in the southwestern side of the Central Highlands in Sri Lanka, is a highly sensitive area for environmental deterioration and natural disasters (Ratnayake and Herath, 2005). The highest number of landslide incidents were observed in Sabaragamuwa Province. Its coverage is 4952 km^2, and it is located between the longitude of 80°12'03" E and 80°56'01" E and between the latitude of 7°22'28" N and 6°13'59" N. The altitude of the study area ranges from 0 to 2177 m above

mean sea level. The mean altitude is approximately 1085.5 m. Sabaragamuwa consists of two districts, namely, Ratnapura and Kegalle.

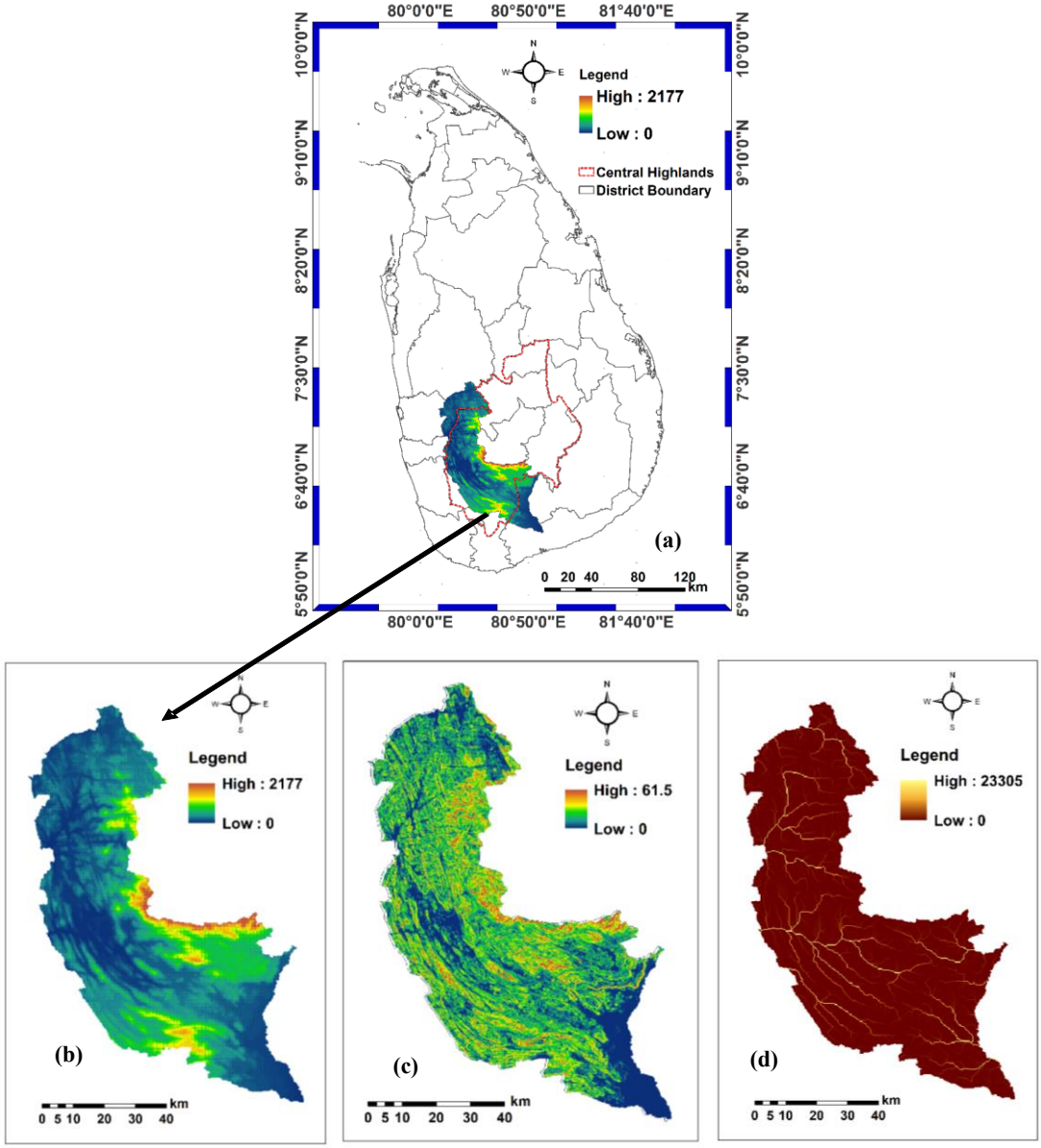

Figure 3. 6 (a) Location map of Sabaragamuwa Province in Sri Lanka; (b) digital elevation map; (c) slope angle map; (d) river distribution map.

The climate is characterised as humid with tropical monsoon weather. The annual average rainfall is greater than 3200 mm (Burt and Weerasinghe, 2014). Most of the rainfall (southwest monsoon and second inter-monsoon) occurs in May–August, October, and November. Tropical rain forests, such as parts of 'Sinharaja' and 'SriPada', are also

located in this province. Sabaragamuwa is drained by four major rivers, namely, the Kelani, Kalu, Gin, and Walawe rivers, located at the western and southern parts of the country. Kelani river, which is one of the major rivers, provides water supply to the capital city of Colombo and sourcing water for other purposes, including power generation (Fayas et al., 2019). The location map of Sabaragamuwa Province in Sri Lanka is shown in Figure 3.6a, a digital elevation map in Figure 3.6b, slope angle map in Figure 3.6c, and the river distribution map in Figure 3.6d. This case study conducted LULC and soil erosion assessments using the methodologies explained in sections 3.5.1.1 and 3.5.1.3 as above.

3.5.1.5.2 Landslide inventory map and frequency ratio calculation

Based on the severity of the damages (number of deaths and injuries from the landslide event) 163 landslide incidents were selected for the period from 2000 to 2019 to assess the relationship between the landslide incidents and soil erosion. The frequency ratio model is a probabilistic model with a reasonably high-prediction accuracy, and it is simple to use (Shinde et al., 2010). The landslide frequency ratio (LFR) was computed using equation 3.12 (Lee and Talib, 2005; Meena et al., 2019).

The frequency ratio method was also employed to evaluate the correlation between soil erosion hazard and land-use change of the study area. The frequency ratio was computed for each land-use class and soil erosion hazard class. The landslide incidents were overlaid on the erosion hazards map and land-use map to identify the correlation on landslide incidents. According to (Shahabi and Hashim, 2015) and (Meena et al., 2019) the average value of the landslide frequency ratio is 1 for the occurrence of landslide incidents in a particular area. A frequency ratio more than 1 (>1) refers to higher spatial correlation, and less than 1 (<1) refers to a lower spatial correlation regarding the occurrence of landslide incidents. Furthermore, the landscape vulnerability was assessed and ranked for soil conservation based on the frequency ratio, soil erosion rates, and land-use change. The ranking was applied for each river distribution zone (RDZ). This study considered the flowing area of respective rivers within the administrative boundary (Sabaragamuwa Province) as a river distribution zone. This case study considered RDZ as a significantly important hydrological unit for soil conservation. The DEM was used to extract RDZs of the study area as per the drainage characteristics (as shown in Figure 3.7b) and delineated into nine RDZs for prioritisation. These nine delineated RDZs are

coded as A-1 (Area-1), A-2 (Area-2), A-9 (Area-9). Moreover, this study explored the land-use change at RDZs level due to its importance for soil conservation. The number of landside incidents in each RDZ was used to compute the LFR. The soil erosion hazard classes and land-use change together with LFR were used to rank the RDZs. The overall methodology of this case study is illustrated in Figure 3.7.

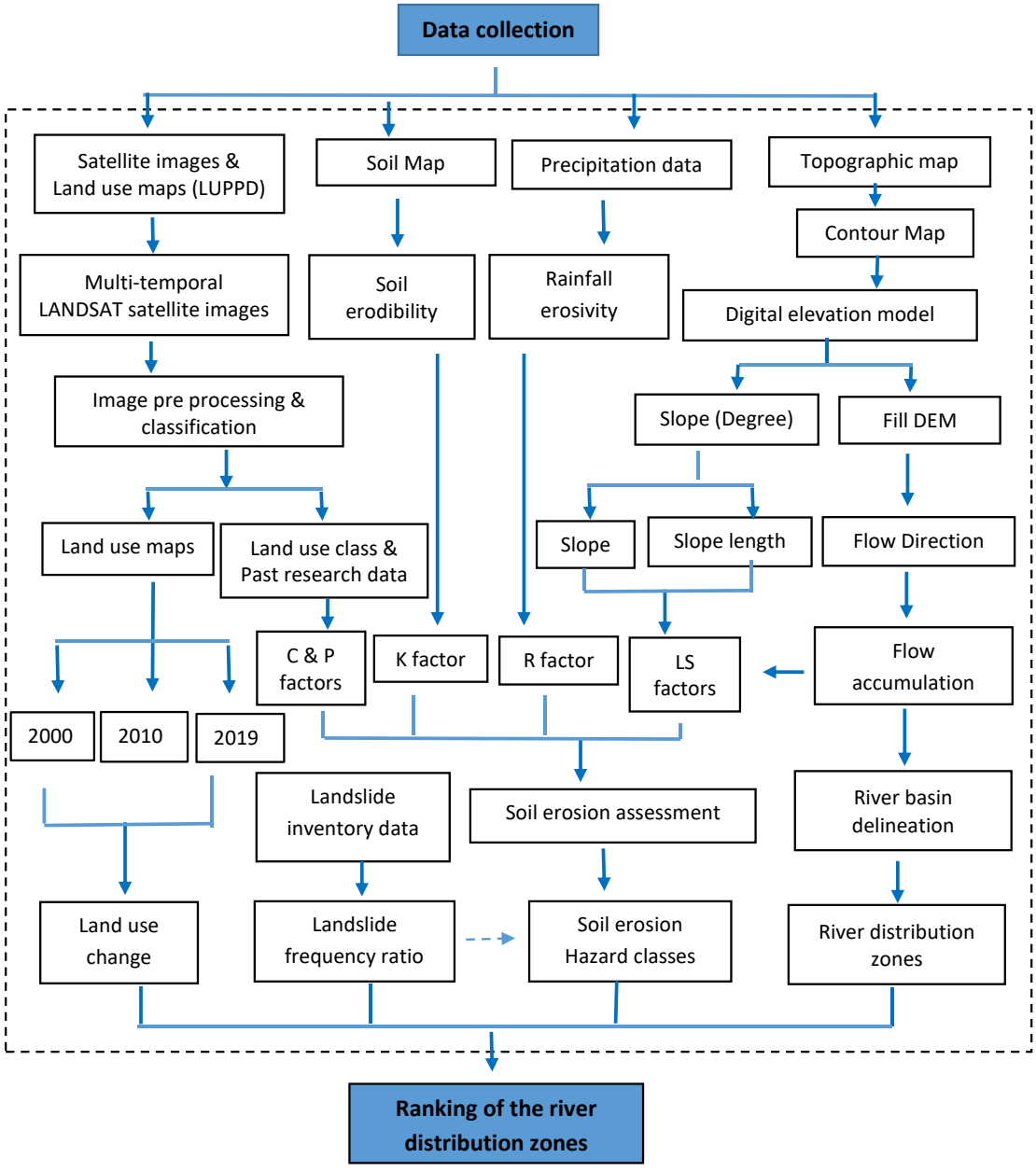

Figure 3. 7 The overall methodology of the study.

3.5.1.6 Crop diversity change analysis

Estimating plant diversity using remote sensing techniques has been conducted through direct and indirect methods (Turner et al., 2003; John et al., 2008). Direct methods are

used with spectral reflectance values and various spatial resolutions from different sensors (Warren et al., 2014). Indirect methods have been derived from environmental parameters or biophysical characteristics such as primary productivity or habitat structure which are estimated from remote sensing techniques (Turner et al., 2003; John et al., 2008).

Many researchers have studied plant diversity using vegetation indices, such as NDVI and EVI (Waring et al., 2006; Levin et al., 2007; Chitale et al., 2019). Several researchers have reported that there is a strong relationship between plant species diversity with vegetation indices such as NDVI (Levin et al., 2007; Pouteau et al., 2018) and the enhanced vegetation index (EVI) (Waring et al., 2006; Morisette et al., 2006). The difference between the EVI and NDVI of MODIS satellite products is an adjustment for the atmosphere and soil background (Huete et al., 2002). NDVI and EVI can be used for mapping and predicting patterns of species richness in large areas. These applications are relatively low cost (Levin et al., 2007; Nagendra et al., 2010). In addition, researchers commonly use the soil adjusted vegetation index (SAVI) to investigate land degradation. SAVI minimizes the spectral variation caused by the soil background (Huete, 1988). The vegetation indices and the respective equations can be found below (Eq 3.13 -3.15).

NDVI $$\text{NDVI} = \frac{(NIR - RED)}{NIR + RED} \quad (3.13)$$ (Rouse et al., 1974)

SAVI $$\text{SAVI} = \frac{(NIR - RED)(1 + L)}{NIR + RED + L} \quad (3.14)$$ (Huete, 1988)

Where L= correction factor between 0 and 1

EVI $$\text{EVI} = G\frac{(NIR - RED)}{(NIR + C1.RED - C2.B + L)} \quad (3.15)$$ (Huete et al., 2002)

G = 2.5; C1 = 6; C2 = 7.5; L = 1

This study uses multiple data sources to examine crop diversity change and soil erosion hazards using NDVI, EVI, and SAVI. Yang et al. (2020) highlighted that using various data sources complements the cross-validation of a study. Nagendra et al. (2010) claimed that Landsat imagery is more suitable for vegetation diversity assessment. They found medium-resolution Landsat ETM+ (30m) correlates stronger than high-resolution IKONOS imagery (4 m) with plant diversity in a dry tropical forest. Due to higher cloud cover around Sri Lanka throughout the year, trend analysis could not be carried out with

Landsat imageries only. Hence, MODIS -250m 16 days' products (MODIS-MOD13Q1) were used for time series analysis for 2001–2019 (LPDAAC, 2021). The MODIS-derived variables have also shown the ability to predict plant species richness at the regional level (John et al., 2008). In addition, MODIS productivity estimates (NDVI/EVI/GPP) are readily available online and provide global coverage (Huete et al., 2002). The MODIS vegetation index products are generated by compositing daily data every 16 days, resulting in 23 composites per year and avoiding cloud cover and other effects (Huete et al., 2002).

The Shannon diversity index is used to measure plant diversity (Nagendra, 2002). This diversity index produces an evaluation of landscape richness and evenness. It measures the number and the relative abundance or evenness of each species. A MODIS derived Shannon diversity index was used to evaluate the crop diversity during this period. The Shannon diversity index (SHDI) (Shannon, 1948) is given in equation (3.16).

$$\mathrm{SHDI} = 1 - \sum_{\mathrm{i}=1}^{\mathrm{N}} P_i \times \mathrm{In}P_i \qquad (3.16)$$

where, Pi is the proportional abundance of the i^{th} type and N is the number of land cover types. This index ranges in theory from 0 to infinity.

This study further assessed crop diversity changes using the case study approach. Three case studies (in 03 farming systems) were conducted covering the Central Highlands to identify the crop diversity changes at the farming system level. Figure 3.8 shows soil erosion hazard classes and landslide distribution in each AER. The most vulnerable two farming systems (WL1a, WM1a) and moderate vulnerable farming system (IU3e) for soil erosion were identified for the case studies. The following criteria were used to select farming systems for the case studies: (i) the percentage of land area under high and very high soil erosion hazard classes; (ii) the number of landslides occurrence in the past two decades; and (iii) the agricultural area's vulnerability to soil erosion.

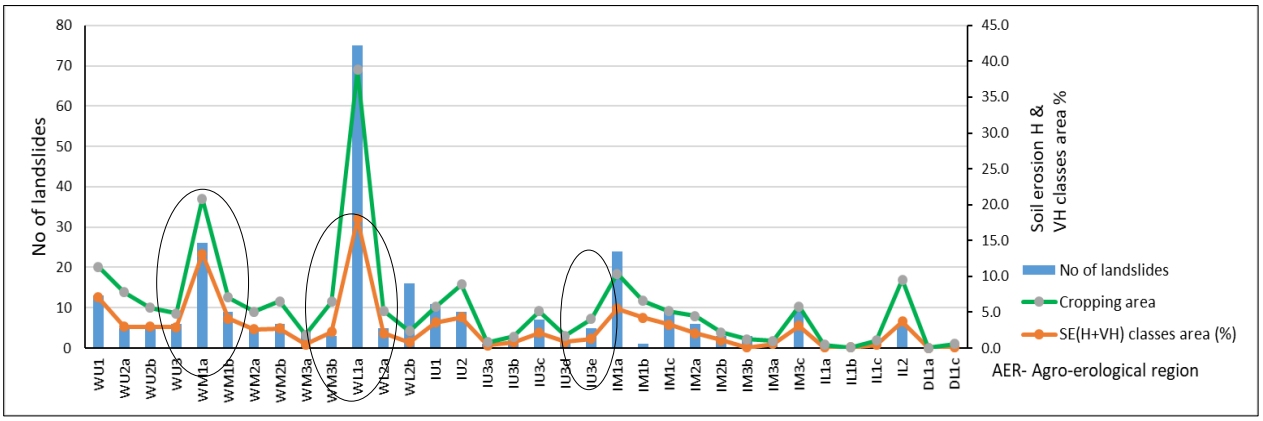

Figure 3. 8 Soil erosion hazard classes and landslide distribution in each AER.

Based on the classified land-use map, the cropping areas were extracted in the GIS environment. The agro-ecological regions (AER) map of the Central Highlands was overlaid on extracted cropping areas to demarcate the farming systems. Figure. 3.9 shows selected farming systems based on the above criteria.

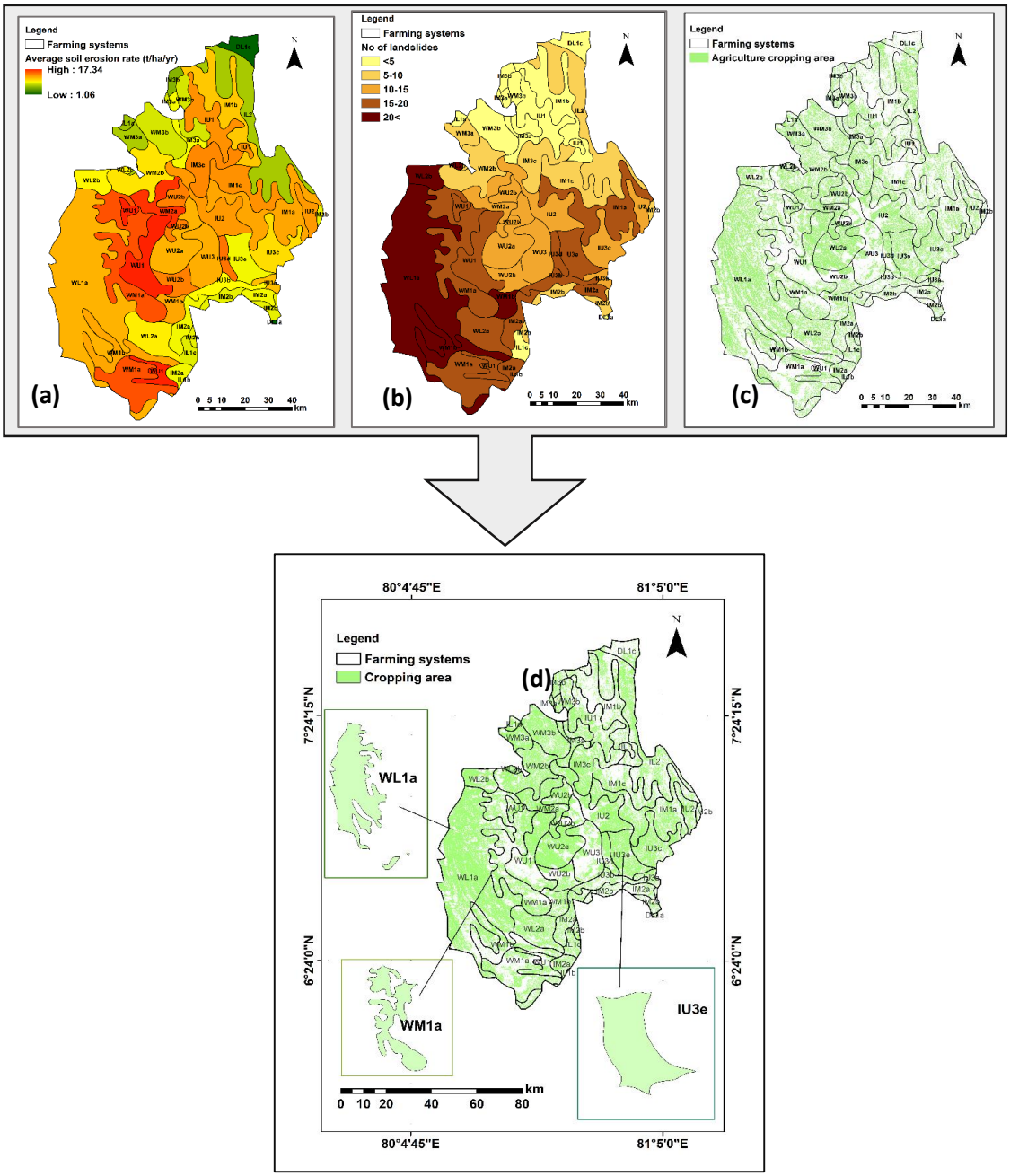

Figure 3. 9. (a) Average soil erosion rate, (b) the number of landslides occurred, (c) agricultural cropping area in the farming system, and (d) selected farming systems for three case studies.

The Pearson's correlation coefficients (r) were computed to explore the relationship between vegetation indices values, plant species richness and diversity of disturbance types (Warren et al., 2014). Pearson's correlation coefficient provides correlation statistically as a measure of the strength of the linear relationships. Values that are closer

to one (1) indicate a stronger relationship or correlation. Statistical models were developed using the linear regression technique.

3.5.1.7. Vegetation indices and rainfall

Researchers reveal vegetation indices are influenced by rainfall (Areola and Fasona, 2018). The MODIS data (MOD13Q1 - MODIS/Terra Vegetation Indices 16-Day) were downloaded (ORNL DAAC, 2018) from 2000 to 2019 and observed the relationship between NDVI and ground-based and satellite-based rainfall data. Pearson's correlation coefficient was estimated between these two variables. Linear regression analysis was performed to estimate the coefficient of determination to identify respective trends of the NDVI. The coefficient of determination (R^2) was computed to find how much variability can be caused by its relationship to another related factor (Landmann and Dubovyk, 2014).

In addition, the latest modified Kling-Gupta efficiency (KGE) was used to test the goodness of fit. The results of the parameters were found to be consistent with Pearson's correlation coefficient (r), bias (beta), and variability ratio (gamma) (Gupta et al., 2009; Kling et al., 2012).

Modified Kling-Gupta efficiency (KGE) was calculated as follows:

$$\mathrm{KGE} = 1 - \sqrt{(r-1)^2 + (\beta-1)^2 + (\gamma-1)^2} \qquad (3.17)$$

$$\beta = \frac{\mu_o}{\mu_s} \qquad and \quad \gamma = \left(\frac{\sigma_s}{\mu_s}\right) / \left(\frac{\sigma_o}{\mu_0}\right)$$

where μ is the mean and σ is the standard deviation. The s and o indicate the simulated and observed values. The two factors range from ($-\infty$) with an optimal value of (1) (Abd Elhamid et al., 2020; Santos et al., 2018).

3.5.1.8 Vegetation indices and soil erosion

Many researchers have used vegetation indices to differentiate soil erosion/land degradation from climate change and anthropogenic activities. The Rain-use efficiency (RUE) and residual trend (RESTREND) indices are derived from vegetation indices (NDVI and EVI) to study land degradation (Wessels et al., 2012; Cunha et al., 2020). RUE and RESTREND analyses have been popularized for assessing the long-term changes in vegetation over the last few decades (Kundu et al., 2017). The following rule of thumb is applied: where vegetation dynamics are strongly driven by rainfall, declining RUE is correlated with land degradation. In humid areas, where vegetation is not as strongly driven by rainfall variation, the NDVI is strongly correlated with vegetation dynamics and may be taken as a proxy for land degradation (Yengoh et al., 2014).

3.5.1.8.1 Rain-use efficiency

Rain-use efficiency (RUE) can be used to normalize the effects of rainfall in vegetation productivity (Fensholt et al., 2013; Liu et al., 2015). The RUE is the ratio between the annual sum of vegetation productivity and annual rainfall (Wessels et al., 2012). The temporal change of RUE has been used to detect land degradation (Liu et al., 2015). Prince et al. (1998) highlighted that decreased RUE referred to land degradation by reduced vegetation coverage and increased run-off. The declining RUE is correlated with land degradation (Yengoh et al., 2014). RUE may vary with species distribution (Fensholt et al., 2013). However, some researchers still argue whether RUE is an effective indicator of land degradation (Wessels et al., 2007). The RUE can be derived from equation 3.18,

$$\mathrm{RUE} = \frac{\sum \mathrm{NDVI}}{\text{Average annual rainfall}} \qquad (3.18)$$

where, ∑NDVI is the average annual sum of NDVI.

3.5.1.8.2 Residual trend analysis

Residual trend analysis (RESTREND) was proposed by Evans and Geerken (2004). Predicted NDVI indicates the climatic impact on NDVI, whereas observed NDVI is the result of both climate and anthropogenic factors. A negative RESTREND indicates human-induced degradation of vegetation, and a positive RESTREND indicates the improvement of vegetation conditions (Kundu et al., 2017). RESTREND is obtained from

the differences between the observed ∑NDVI and the ∑NDVI predicted by the rainfall using regressions calculated for each pixel. The equation for RESTREND is in equation 3.19 (Wessels et al., 2008; Wessels et al., 2012).

$$\text{RESTREND} = \text{observed} \sum\text{NDVI} \; - \; \text{predicted} \sum\text{NDVI} \quad (3.19)$$

In this study, the RUE and RESTREND were employed using NDVI and EVI indices of MODIS data to find the impact of climate and human-induced soil erosion/land degradation. The time-series analyses of NDVI and EVI indices from 2000 to 2019 were used to derive RUE and RESTREND.

3.5.2 Objective 2

This study aims to investigate the relationship between soil erosion hazards and rainfall variation in the Central Highlands of Sri Lanka. The impact of extreme climate events on agricultural ecosystems was observed with changing precipitation amounts and seasonality. The rainfall variation was analysed using extreme rainfall indices, rainfall anomaly index, SPI index and trend analysis. Trend analysis was carried out using gauged rainfall and satellite-based rainfall datasets. The overall methodology of objective 2 is shown in Figure 3.10.

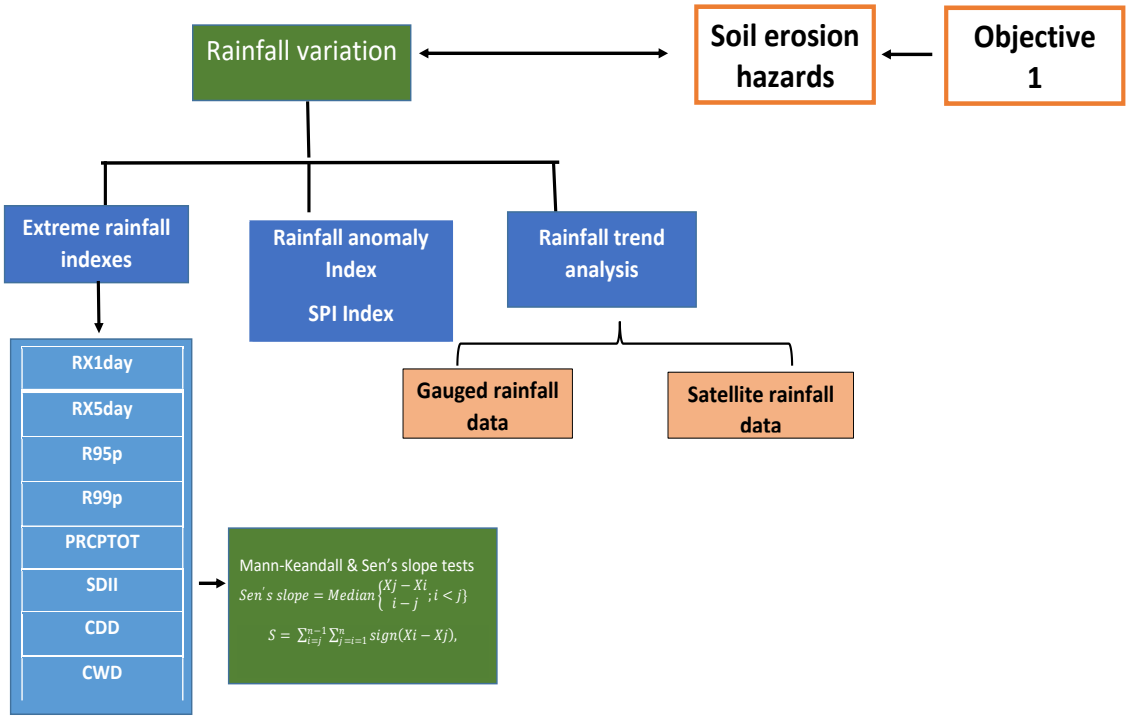

Figure 3. 10 The flowchart of the methodology used for objective 2 of this study.

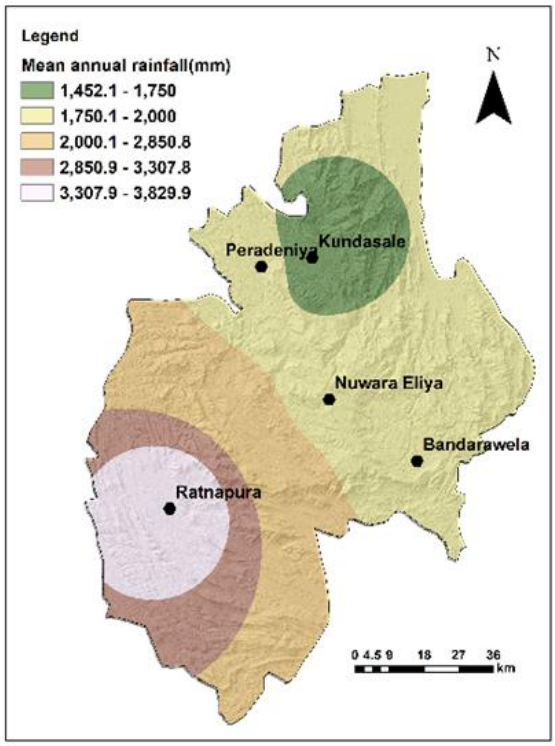

Figure 3. 11 Selected five agro-meteorological stations at the Central Highlands.

Five agro-meteorological stations were selected over the highlands, illustrated in Figure 3.11. The details of the five stations are given in Table 3.8.

Table 3. 8. Details of selected five agro-meteorological stations at the Central Highlands.

Agro met stations	Latitude	Longitude	Elevation (m.s.l)	Average annual rainfall	Max RF	Min RF	CV	SD
Ratnapura	80.4738	6.3656	51	3834.25	4968.2	3280.8	13.49	517.6
Peradeniya	80.3617	7.2162	479	1941.81	2841.9	1272.6	13.8	381.5
Nuwara Eliya	80.7734	6.9780	1933	1923.94	2826.9	1102.6	19.82	381.1
Bandarawella	80.5952	6.4937	1255	1753.20	2171.4	920.8	17.68	310.0
Kundasale	80.4145	7.1629	513	1452.7	1961	489.3	23.67	344.0

3.5.2.1 Extreme weather events

Five agro-meteorological stations (for gauge rainfall data) were selected: Ratnapura, Peradeniya, and Nuwara Eliya (Wet Zone), Bandarawella and Kundasale (Intermediate Zone). The rainfall erosivity, extreme rainfall indices, rainfall anomaly and trend analysis, were conducted. The indices from the World Meteorological Organization's (WMO's) were used and given in Table 3.9. Extreme indices such as SDII, R99p, Wet and Dry days and rainfall erosivity, were employed for datasets obtained from these five agro-met stations. Modified Mann-Kendall trend test and Sens' slope test were executed on extreme indexes and annual average rainfall at five stations to examine the significant levels. A geo-statistical tool called interpolation techniques with radial basis functions was used to map the spatial distribution of extreme indices and average annual rainfall in the Central Highlands.

Table 3. 9. Details of extreme indices

Class	Index	Indicator name	Definition	Units
Quantity indices	RX1day	Max 1 day precipitation amount	Monthly maximum 1 day precipitation	mm
	RX5day	Max 5 day precipitation amount	Monthly maximum consecutive 5 day precipitation	mm
	R95p	Very wet days	Annual total PRCP when RR > 95th percentile	mm
	R99p	Extremely wet days	Annual total PRCP when RR > 99th percentile	mm
	PRCPTOT	Annual total wet day precipitation	Annual total PRCP in wet days (RR ≥ 1 mm)	mm
Time indices	R10	Number of heavy precipitation days	Annual count of days when PRCP ≥ 10 mm	days
	CDD	Consecutive dry days	Maximum number of consecutive days with RR < 1 mm	days
	CWD	Consecutive wet days	Maximum number of consecutive days with RR ≥ 1 mm	days
Intensity index	SDII	Simple daily intensity index	Annual total precipitation divided by the number of wet days (defined as PRCP ≥ 1.0 mm) in the year	mm/day

3.5.2.2 Standard precipitation index

Standard Precipitation Index **(**SPI) represents the difference of precipitation from the mean divided by the standard deviation. The SPI helps in computation to represent abnormal wetness and dryness. The SPI, often called the Z score, vary from +3 to -3 high positive values correspond to wet sequences, and high negative values correspond to drought periods (Table 3.10). SPI values apply to any month (n) where *n*, the number of months of accumulation, is the time scale. SPI can be calculated for different time intervals such as 3, 6, 9, 12, and 24 months. The 3-month SPI value provides a comparison of accumulated precipitation over that specific 3-month period with the mean precipitation total for the same annual period as calculated over the full study period. For

drought evaluation (negative SPI), short time scales on the order of 3 months may be important for agricultural applications, whereas long time scales of up to many years are interested in water-supply management (Guenang and Kamga, 2014). R software was employed to calculate SPI for 3, 6, 9, and 12- month periods. The study provides useful information to better understand the historical variability of drought events and their relative intensity.

Table 3. 10. Wet and dry classification based on the *Z* index and SPI value.

Class	Type *Z* value	SPI value
1 Severely wet	$Z > 1.96$	SPI > 2.0
2 Moderately wet	$1.44 < Z \leq 1.96$	$1.5 <$ SPI ≤ 2.0
3 Abnormally wet	$0.84 < Z \leq 1.44$	$1.0 <$ SPI ≤ 1.5
4 Normal	$-0.84 \leq Z \leq 0.84$	$-1.0 \leq$ SPI ≤ 1.0
5 Abnormally dry	$-1.44 \leq Z < -0.84$	$-1.5 \leq$ SPI < -1.0
6 Moderately dry	$-1.96 \leq Z < -1.44$	$-2.0 \leq$ SPI < -1.5
7 Severely dry	$Z < -1.96$	SPI < -2.0

3.5.2.3. Trend analysis of average annual rainfall

Rainfall anomaly was observed by rainfall distribution over the period (2000-2019) in the five agro-met stations. Average yearly rainfall was derived from daily rainfall data. Thirty years of average rainfall data were used to detect the rainfall anomaly for the above period.

3.5.2.4 Innovative trend analysis

The study employed both gauge rainfall data (collected for 05 agro-met stations) and satellite rainfall data for this analysis. The satellite rainfall dataset (PERSIANN-CDR) was downloaded from the Center for Hydrometeorology and Remote Sensing (CHRS). This product is available at a high spatial resolution (0.25m x 0.25m) and temporal (monthly) resolution. A recent innovative trend analysis test (ITA) developed by Şen (2012) was also employed to evaluate the rainfall trends further (Şen, 2017). Satellite-based PERSIANN-CDR products matched well with the gauge-based precipitation in tropical regions (Sun et al., 2018). Many researchers used the CHRS data due to its capability to assess rainfall trends (Baez-Villanueva et al., 2018; Sadeghi et al., 2021).

The time-series average annual rainfall (satellite and gauge data) was divided into two sub-series, and two groups were sorted into ascending order. A scatter plot diagram was

plotted on the first and second sub-series on the x- and y-axis, respectively. The presence of a trend indicated, based on two data sequences with respect to the 1:1 line (having a slope of 45°). If data under investigation fall above or below the 1:1 line, then there exists an upward or a downward trend in the time series, respectively (Şen, 2017).

3.5.2.5 Modified Mann-Kendall and Sen's slope tests

Modified Mann-Kendall and Sen's slope tests were employed to detect significant trends in precipitation indices using the R software for statistical analysis (McLeod and McLeod, 2014). Modified Mann–Kendall test was applied to serially independent series of data toward trend detection, and Sen's slope test was applied to calculate trend magnitude. Nonparametric Mann–Kendall test is widely used in the literature for trend detection in time series data in the case of serially independent data. Serial correlation affects the power of trend, resulting in misinterpretation of the trend analysis (Patakamuri et al., 2020). A Trend-free pre-whitening (TFPW) test is used to improve the results from serial correlation. Pre data analysis was conducted to check for autocorrelation. Following Figure 3.12 illustrates correlation up to 10^{th} lag (with 5% significance). There was no evidence for autocorrelation.

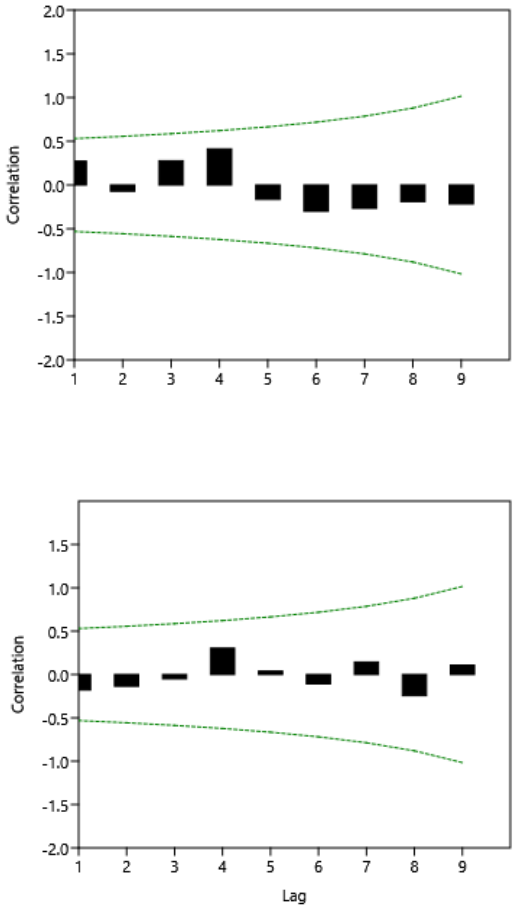

Figure 3. 12 The autocorrelation results of a) rain gauge data and b) satellite rainfall data.

Modified Mann-Kendall and Sen's slope tests were performed using equations 3.20 to 3.24.

$$S = \sum_{i=1}^{n=1} \sum_{j=i=1}^{n} sign(X_j - X_i) \qquad (3.20)$$

where, n is the number of data points, Xi and Xj are the annual values in years i and j, j > i, respectively, and sign $(X_j - X_i)$ is the sign function as

$$\text{sign}\,(X_j - X_i) = \begin{cases} \text{-1 if } (X_j - X_i) < 0; \\ 0 \text{ for } (X_j - X_i) = 0, \\ 1 \text{ for } (X_j - X_i) > 0. \end{cases} \qquad (3.21)$$

Statistics S is normally distributed with parameters E(S) and variance $V(S)$ as given below:

$$\text{E(S)} = 0$$

$$\text{V(S)} = \frac{n(n-1)(2n+5) - \sum_{k=1}^{m} t_k(k)(k-1)(2k+5)}{18} \qquad (3.22)$$

where n is the number of data points, m is the number of tied groups, and t_k denotes the number of ties of extent k. Standardized test statistic Z is calculated using the formula below.

The Z score of S is calculated from $Z = S \Big/ \sqrt{var(s)}$. (3.23)

$$\text{Z} = \begin{cases} S - 1 \Big/ \sqrt{var(s)} & \text{if S} > 0 \\ 0 & \text{if S} > 0 \\ S + 1 \Big/ \sqrt{var(s)} & \text{if S} < 0 \end{cases} \qquad (3.23)$$

Sen's Slope Estimator

$$T_i = \frac{X_j - X_k}{j - k} \qquad (3.24)$$

where, for i= 1,2,3….n, j>k Ti is the slope and X_j and X_k are the values at time j and k, respectively. The median of the n values of Ti is symbolized as Sen's slope estimator (Qi) and given in $Qi = T_{(n+1)/2}$, when n is odd value, $Qi = \frac{1}{2}(T_{n/2} + T_{n+2/2})$ when n is even value.

3.5.2.6. The rainfall variation and soil erosion hazards

The relationship between rainfall variation and soil erosion hazards was assessed using the landslides frequency ratio in each farming system. Pearsons' correlation and Modified Kling–Gupta efficiency index (equation 3.17) were used to establish the correlation between soil erosion and rainfall variation.

3.5.3 Objective 3

This study aims to assess the ecologically viable and economically sound farming systems in the Central Highlands of Sri Lanka to achieve the third objective. The present study was conducted on farming systems-based evaluation in terms of ecological and economic perspectives concerning soil erosion hazards. Many studies have been conducted evaluations on farming systems using geo-informatics technology such as agricultural land-use change and soil erosion assessments (Bakker et al., 2005; Leh et al., 2013; Borrelli et al., 2017). However, none of these studies identified the farming systems by delineating the agricultural areas under agro-ecological regions using geo-informatics technology.

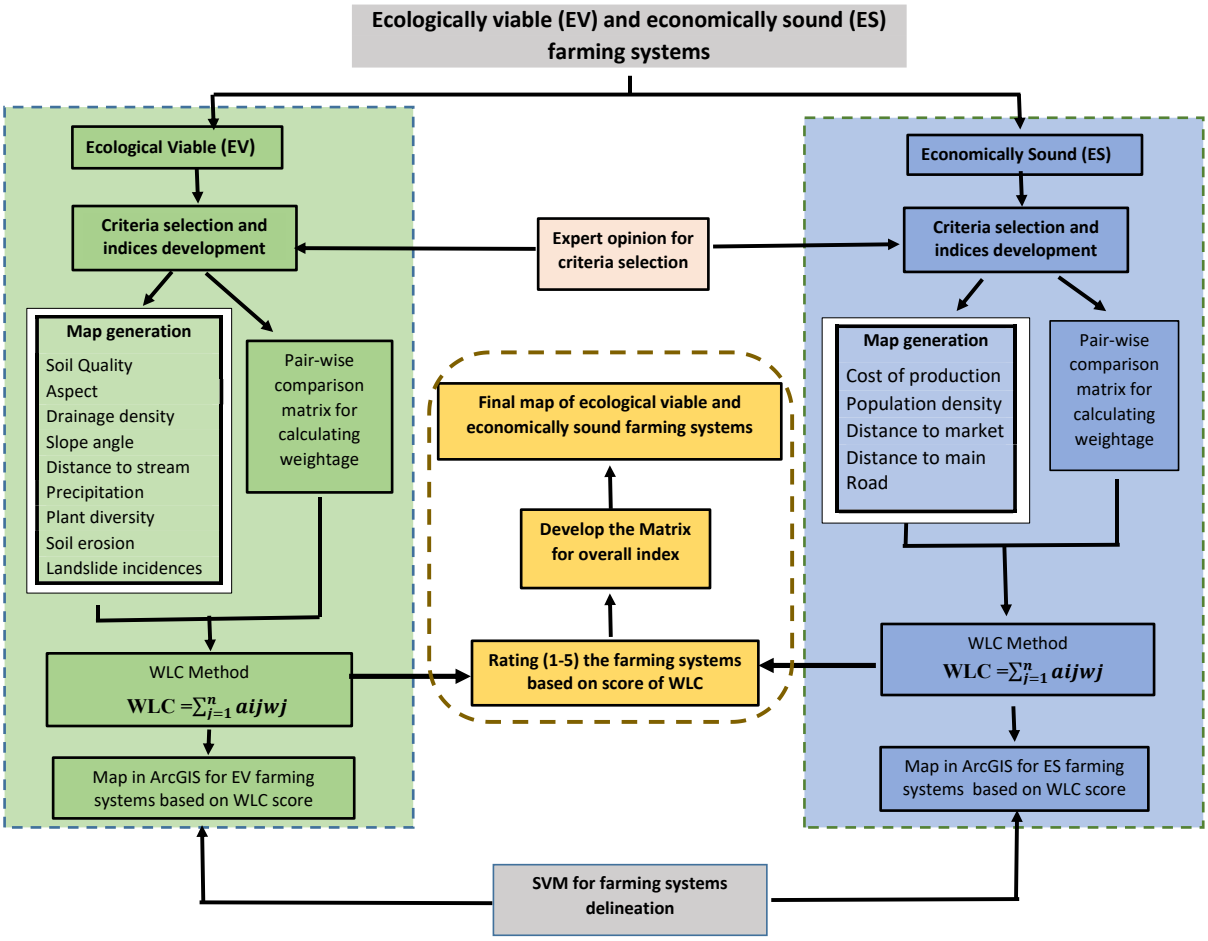

Figure 3. 13 Overall methodology used for identifying ecologically viable and economically sound farming systems in the study area.

Furthermore, this study attempts to introduce a new approach on the matrix based AHP and the weighted linear combination method concerning soil erosion hazards with present climate conditions to identify and evaluate the ecologically viable and economically sound farming systems. The overall methodology of objective 3 illustrates in Figure 3.13.

3.5.3.1 The matrix-based analytic hierarchy process

The analytic hierarchy process (AHP) of multi-criteria decision-making describes a simplified method for pair-wise comparison of homogenous elements (Saaty and Vargas, 2013). The AHP method was proposed by Thomas L Saaty in 1980 based on the criteria evaluation procedure to determine the weights of the factors through a matrix that compared all the identified attributes against one another. The main advantage of the AHP method is its ability to work with available data and limited resources. This method has

been applied in various fields such as urban land use planning (Mosadeghi et al., 2015), earthquake risk assessments (Jena et al., 2020), landslide susceptibility mapping (Shruthi et al., 2015), landfill suitability mapping (Karimi et al., 2019), crop suitability mapping (Jayasinghe et al., 2019) and flood assessment (Abenayake et al., 2018).

The AHP method was employed for criteria selection and pair-wise comparison. Researchers identified that the criteria selection was imperative to solve complex problems. Furthermore, the criteria were selected with relevance to the specific problem and the geographical location (ul Haq and Boz, 2020). The weight of each indicator was obtained from the pair-wise comparison matrix. The criteria indicators were arranged in a hierarchical order and assigned values based on the scale of relative importance in the pair-wise comparison. In this study, the criteria indicators were elected from the literature to evaluate the soil erosion hazard status.

3.5.3.2 Criteria indicators for ecologically viable farming systems

The selection of appropriate criteria and indicators is very important, especially in data-scarce regions. However, there are no defined guidelines for criteria selection in the multi-criteria method (Alilou et al., 2019). Therefore, based on literature evidence from past research, factors relevant to the study area and expert opinions were used to select the criteria indicators (Li et al., 2012; Zabihi et al., 2019). The indicators were selected based on soil erosion related factors, and maps were generated based on the available geo-spatial data gathered from various sources. Nine indicator maps were developed to evaluate ecologically viable farming systems, and four indicator maps were developed to assess economically sound farming systems.

The following environmental indicators were selected to detect ecologically viable farming systems: the soil quality, percentage of highly vulnerable areas for soil erosion, drainage density, slope angle, aspect, vegetation cover, precipitation, distance to stream and the number of landslides that occurred in the last 20 years. These criteria have been widely applied in environmental assessments (Jain and Goel, 2002; Khoi and Murayama, 2010).

3.5.3.2.1 Soil quality

The soil characteristics such as physical, chemical and biological properties: structure and texture, organic matter and moisture content, density (compactness), shear strength

influence on the infiltration capacity and detach, disperse and transportation of the soil particles (Jain and Goel, 2002). If soil quality is high, it provides adequate nutrients and water for better plant growth. Healthy vegetation cover helps to reduce surface runoff and soil erosion (Liu et al., 2020). Hence, the level of soil quality is an excellent indicator to detect soil erosion. The characteristics of soil such as soil texture, clay percentage, organic matter percentage, permeability and pH were obtained from secondary data sources (Moorman and Panabokke, 1961) and are given in Table 3.11.

Table 3. 11. Soil characteristics in the Central Highlands of Sri Lanka.

Soil classification of the study area	Texture	% Clay	% Organic matter	Permeability	pH
Red-Yellow Podzolic soils; steeply dissected, hilly and slow rolling terrain	Loam	0.14	9%	Somewhat to very slow	4.6
Red-Yellow Podzolic soils with soft or hard laterite; rolling and undulating terrain	Loam	0.14	9%	Somewhat slow to very slow	4.6
Red-Yellow Podzolic soils with strongly mottled subsoil & Low Humic Gley soils; rolling and undulating terrain	Loam	0.14	9%	Somewhat slow	4.8
Bog and Half-Bog soils; flat terrain	Moderate clay	0.05–0.2	2.5–3.0%	Moderate	4
Regosols on recent beach sands; flat terrain	Sandy loam	0.15–0.2	1%	Rapid	4
Regosols on recent beach and dune sands; flat terrain	Moderately fine silty sand	0.15–0.2	2%	Somewhat fast to rapid	4
Latosols and Regosols on old red and yellow sands; flat terrain	Sandy with fine clay	0.1–0.13	0.40%	Moderate	5.7
Alluvial	Sandy clay	0.3–0.4	3%	Somewhat slow to very slow	6.1
Immature Brown Loams; steeply dissected, hilly and rolling terrain	Sandy loam or loam	0.15–0.2	1%	Rapid	5.7
Reddish Brown Earths & Immature Brown Looms; rolling, hilly and steep terrain	Sandy loam	0.15–0.2	1.20%	Somewhat fast	6.1
Reddish Brown Earths & Low Humic Gley soils; undulating terrain	Sandy loam	0.15–0.25	1.20%	Somewhat fast	6.1
Reddish Brown Earths with high amount of gravel in subsoil & Low Humic Gley soils; undulating terrain	Sandy loam	0.15–0.25	1.20%	Somewhat fast	6.1

Reddish Brown Latosolic soils; steeply dissected, hilly and rolling terrain	Clay Loam	0.3-0.4	4%	Moderate	5.5
Reddish Brown Latosolic soils; steeply dissected, hilly and rolling terrain	Clay Loam	0.3-0.4	4%	Moderate	4

Farming systems were categorised by soil quality into five classes (from 1 very- poor to 5 very-good) based on the soil types and their characteristics (Table 3.12). This study used a 1-5 scale, which is more appropriate for this classification (Jayasinghe et al., 2019).

Table 3. 12. Soil quality indicators.

Scale	Texture	Clay percentage	Organic matter percentage	Permeability	pH
Very-poor (1)	Sand, gravel	0–0.05	1-2	Very rapid	3.0-3.5
Poor (2)	Loamy sandy and sandy loam	0.1–0.15	2-4	Somewhat fast	3.5-4.0
Moderate (3)	Loam, moderately loam	0.2–0.25	4-6	Moderate	4.0-4.5
Good (4)	Heavy clay with gravel	0.35–0.4	6-8	Somewhat slow	4.5-5.0
Very-good (5)	Silty clay, clay,	0.4–0.45	>-8	Very slow	5.0-5.5

3.5.3.2.2 Aspect

Aspect is the direction of maximum slope on the terrain surface (Ranasinghe et al., 2019). The slope aspect is responsible for receiving a significant amount of wind-driven rainfall (monsoonal rainfall), which ultimately impacts the magnitude of soil erosion. The western slope of the Central Highlands gets the highest amount of rainfall from the south-west monsoon, and eastern slopes receive rainfall from the north-east monsoon (Burt and Weerasinghe, 2014). Therefore, this study assumes that more precipitation is received if the slope direction faces a windward direction and positively contributes to soil erosion. It is assumed that the slope direction facing leeward direction may receive comparatively less precipitation (Foulds and Warburton, 2007). Hence, a lower score was given for windward direction slopes. Thus, the slopes which face the south-west in the Central Highlands receive more precipitation and have more potential to soil erosion during the south-west monsoon. The slopes facing north-east also have high soil erosion trends (during the north-east monsoon) compared to other slope directions. Hence, the lowest

scores (1) for south and south-west, (2) north and north-east slopes, then (3) west and north-west, (4) east and south-east and finally highest (5) for flat areas were employed.

3.5.3.2.3 Distance to stream

Distance from the stream has a significant impact on soil erosion. Gayen and Saha (2017) specified that distance to stream is an important parameter for soil erosion due to slope stability and degree of saturation of soil in the slope. Hence, the distance to the stream is considered as one of the indicators for this study. When the distance from the stream to the farming system; is less, high runoff and soil erosion could be observed. Hence, these farming systems were classified as very-poor (1). When the farming systems were far from the river (long distance), low runoff and lower potential for soil erosion were observed and ranked as very-good (5).

3.5.3.2.4 Precipitation

Many researchers identified rainfall amount and rainfall intensity correlate with soil erosion (Jain and Goel, 2002; Nearing et al., 2005; Ratnayake and Herath, 2005; Pradhan et al., 2012; Dang et al., 2019). When the rainfall amount and intensity are high, the surface runoff is also increased and leads to a high rate of soil erosion. If rainfall is low, soil erosion is also low. Hence, when the soil erosion is low, that can be categorised as very-good (5), and when the soil erosion is high due to high intensity of rainfall, that can be categorised as very-poor (1).

3.5.3.2.5 Soil erosion

Soil erosion assessment was conducted using the revised universal soil loss equation (RUSLE), an empirical soil erosion model, and the soil erosion map was generated for the Central Highlands of Sri Lanka.. Areas vulnerable to soil erosion were categorised into five classes based on the soil erosion rate: very high, high and moderate soil erosion areas were identified in the Central Highlands. We tabulated the area as a percentage of moderate to very high classes in each farming system and made the classification. The percentage of moderate to very high classes was above 4% is considered very poor and less than 1%, considered very-good. The farming systems of the Central Highland were

classified accordingly from very-poor (1) to very- good (5) based on the above soil erosion classes.

3.5.3.2.6 Slope

The slope angle of the Central Highlands varies between 0 to 80 degrees. Literature shows that soil erosion increases with rising slopes linearly or greater than linearly (Cerdà et al., 2018; Wischmeier and Smith, 1978; Alilou et al., 2019). Therefore, this study assumed that if the slope is high, the potential soil erosion is also high. If the slope is low, the potential soil erosion is reduced. Thus, the area was classified over a 35-degree slope as a high slopping area (very-poor) and less than 5 degrees as a low slopping area (very-good 5).

3.5.3.2.7 Vegetation cover

Vegetation cover is important to control water runoff and prevent soil erosion (Nearing et al., 2005; Hou et al., 2016). Additionally, plant diversity improves the vegetation cover and physical and chemical characteristics of soil properties (Levin et al., 2007). Plant diversity helps control soil erosion by reducing runoff (Hou et al., 2016; Liu et al., 2018; Berendse et al., 2015). Therefore, this study argues that when plant cover is high, soil erosion is low. When plant cover is low, there is a high potential for soil erosion. Vegetation cover can be obtained from NDVI (D'Arrigo et al., 2000; Levin et al., 2007). The high NDVI value indicates a higher plant density. The map of NDVI values is obtained using equation (2) on Landsat images. This study rated high NDVI value as very-good (5) and low NDVI value as very-poor (1).

3.5.3.2.8 Number of landslides

Landslides significantly contribute the soil erosion (Hewawasam, 2010). The Central Highlands of Sri Lanka are highly vulnerable to landslides, and previous research observed that most of these landslides were initiated in agricultural lands (Hewawasam, 2010; Ratnayake and Herath, 2005; Dang et al., 2019). Hence, the number of landslides that occurred in the past 20 years was used as an indicator for this study. As mentioned above (objective 1), the number of landslides in the past 20 years was obtained from the UNISDR, and a landslides inventory map was developed. The number of landslides that had occurred in each farming system was calculated in ArcGIS. Farming systems were

rated based on the incidence of landslides. When the number of landslides is less than 1, it was rated as very-good (5), and if the number of landslides is greater than 10, the rating is very-poor (1) in farming systems.

3.5.3.2.9 Drainage density

Researchers have identified that drainage density is positively correlated with the soil erosion rate (Tarboton et al., 1992; Jain and Goel, 2002; Moeini et al., 2015; Clubb et al., 2016; Das et al., 2020). According to Jain and Goel (2002), drainage density is the cumulative length of the streams to the total drainage area expressed as length per unit area. Higher drainage density represents higher soil erosion (Jain and Goel, 2002). Hence, this study assumed when the drainage density is high, vulnerability to soil erosion is also high. Thus, higher drainage density was rated as very-poor (1) and lower drainage density as very-good (5) for agricultural activities.

The ecological indicators were classified into five classes considering their capability to induce soil erosion hazards from 1(very-poor) to 5 (very-good). The summary of criteria indicators and respective classifications to evaluate the ecologically viable farming systems can be found in Table 3.13.

Table 3. 13. Summary of ecological indicators and classification

Soil Quality	Very-good (5)	Good (4)	Moderate (3)	Poor (2)	Very-poor (1)
Aspect	Flat areas	East and South-east	North and North-west	North and North- east	South and South- east
Distance to stream (m)	0-500	501-1000	1001-1500	1501-2000	2000<
Precipitation (mm)	<2500	2500-3000	3001-3500	3501-4000	4000<
Soil erosion (Moderate to High class area %)	<1%	1-2%	2.1-3%	3.1-4%	4%<
Slope (degrees)	0-5	6-10	11-20	21-35	35<
Vegetation cover (NDVI value)	-0.2-0.15	0.16-0.25	0.26-0.35	0.36-0.45	0.45<
Number of landslides	<1	1-2	3-4	5-10	10<
Drainage density (km^2 per unit area)	0-1000	1001-2000	2001-3000	3001-4000	4000<

3.5.3.3 Criteria indicators for economically sound farming systems

The following criteria indicators were used to assess the economically sound farming systems: cost of production, population density, distance to market, and distance to the main road. Other researchers also used these economic criteria for farm evaluation (Montgomery et al., 2016; Tiwari et al., 2000; ul Haq and Boz, 2020). These indicators reflect the economic cost for crop management and land rehabilitation, transportation and market demand, which are relevant to farm evaluation. The economic indicators were classified into five classes considering based on the relative cost and access to the market from 1 (very-poor) to 5 (very- good).

3.5.3.3.1 Cost of Production

Cost of production (COP) is an important factor to make farming decisions (Tiwari et al., 1999; Sousa et al., 2019). Three prominent crops in each AER were obtained from "Crop suitability database" in the DOA (http://nrmc.lk/NRMC/). The COP per kg of each crop at the farm-gate was gathered from secondary data (Cental Bank of Sri Lanka, 2019). The average price of these three crops was calculated for each AER and categorised into 5 classes. The average price was greater than LKR 300/kg rated as 1 (very high price), and less than LKR 50/kg was rated as 5 (very low price) in 1-5 scale respectively (Table 3.14).

3.5.3.3.2 Population Density

Population density is a socio-economic indicator (Rahman et al., 2015; Xue et al., 2019). However, the population density can be considered as an indicator of the customer base in the market, customer demand for crops, and agriculture labour availability. The population densities of main districts were obtained from secondary 2019 sources (Cental Bank of Sri Lanka, 2019). When the population density is high, demands for the crops in the market and agriculture labour availability are high. Population density was ranked 1-5 scale from low population density (1 very- poor) to high population density as very-good (5).

3.5.3.3.3 Distance to Market

Four major markets were selected. Distance to market place was obtained using the ArcGIS tool called Euclidean distance. This study considered the distance to market as an indicator for the cost of transportation of crop production. If the distance to the marketplace is low, the cost of transport is also low. If the distance to market was low it

was rated as very-good (5) and distance to market was ranked as very-poor (1) if the distance was high.

3.5.3.3.4 Distance to the main road

Distance to main roads was considered an indicator of efficient access to logistics and supply (Montgomery et al., 2016; Khoi and Murayama, 2010). Having easy access to the main road allows efficiently transporting of the harvest and receiving inputs such as equipment, seeds and fertilizer. If the distance to the main road was low, it was rated as very-good (5). If the distance to the main road was high, then it was rated as very-poor (1).

The summary of criteria indicators and respective classifications to evaluate the economical sound farming systems is presented in Table 3.14.

Table 3. 14. Summary of economic indicators and classification

	Very-good (5)	**Good (4)**	**Moderate (3)**	**Poor (2)**	**Very-poor (1)**
Cost of Production LKR/kg	< 50	50-100	101-200	201-300	300 <
Population Density (Persons per Sq.km)	665<	566-665	466-565	366-465	<365
Distance to Market (km)	<10	10-20	21-30	31-40	40<
Distance to main road(m)	0-500	501-1000	1001-1500	1501-2000	2000<

3.5.3.4 Constructing a pair-wise comparison matrix

Determining the weights of criteria indicators is an important step in multi-criteria analysis (Saaty and Vargas, 2013). The weights of criteria indicators were determined using pair-wise comparison analysis. The research presented here used the following steps to complete the pair-wise comparison analysis: (a) construction of pair-wise comparison matrix, (b) the consistency ratio generation (CR) evaluation CR value: equal to or <0.1, and (c) validating pair-wise comparison matrix using expert opinion.

The pair-wise comparison is a useful tool for investigating the relative importance of factors to each other and is used to generate the weights. However, weights may depend on the knowledge of the decision-maker (Penadés-Plà et al., 2016). The AHP uses a scale of 1 to 9 to express individual preferences (Wind and Saaty, 1980). The matrix values for pair-wise comparisons were obtained from the table of relative importance (Table 3.15). The value of 1 expresses "equal importance", and the value of 9 is given for factors that have "extreme importance".

Table 3. 15. The scale of relative importance (Wind and Saaty, 1980).

Comparative importance	**Numerical expression**
Equal importance	1
Moderate importance	3
Strong importance	5
Very strong importance	7
Extreme importance	9
Intermediate values between the two adjacent judgements	2,4,6,8
Values for inverse comparison	1/3,1/5,1/7,1/9

(Note: 1 is the highest importance, and 9 is the least importance).

In pair-wise comparison, if the alternatives were denoted by (A_1, A_2, ... A_n) n is the number of compared alternative, and the current weight of each alternative can be denoted by (W_1, W_2 …..W_n). The matrix of all ratios is denoted by weighted as the equation (3.25).

$$W = \left[{}^{w_i}/_{w_j}\right] = \begin{bmatrix} {}^{w_1}/_{w_1} & {}^{w_1}/_{w_2} \cdots & {}^{w_1}/_{w_n} \\ {}^{w_2}/_{w_1} & {}^{w_2}/_{w_2} & {}^{w_2}/_{w_n} \\ \cdot & \cdot & \cdot \\ \cdot & \cdot & \cdot \\ \cdot & \cdot & \cdot \\ {}^{w_n}/_{w_1} & {}^{w_n}/_{w_2} & {}^{w_n}/_{w_2} \end{bmatrix} \qquad (3.25)$$

The matrix of pair-wise comparison matrix A= [a_{ij}] represents the intensity of expert's preferences between individual pairs of alternative.

$$A = [a_{ij}] \qquad (3.26)$$

where i,j = 1,2,3……n and a_{ij} =1for i=j , $a_{ij} = \frac{1}{aij}$ for $i \neq j$

Equation 3.26 indicates a matrix of n × n dimensions where n is the number of elements being compared. This equation is an expression of the principle of preference, in which two identical elements compared to each other are not differentiated by preference and the difference in preferences is expressed by the number 1, hence all values of the elements on the diagonal of the matrix are equal to 1.

3.5.3.5 Consistency ratio and random index table

The eigenvalues (λ) was calculated for each row using equation (Eq.) 3.27, n is the number of elements in the row.

$$l_i = \sqrt[n]{a_{11} \times a_{12} \times a_{13} \dots a_{1n}} \qquad (3.27)$$

The weights of each criterion were normalised by matrix values to 1. The maximum eigenvalues (λmax) of the normalised matrix were computed based on the following equation (Eq. 3.28).

$$\lambda_{max} = \sum_{j=1}^{n} (W_j \times \sum_{i=1}^{m} a_{ij}) \qquad (3.28)$$

Where W_j is the value of assigned weights of each criterion and a_{ij} is the sum of criteria in each column.

The consistency of the matrix (consistency ratio) was computed using following equation (Eq. 3.29).

$$\mathrm{CR} = \mathrm{CI}/\mathrm{RCI} \qquad (3.29)$$

The consistency index (CI) was estimated using equation (3.29). The random consistency index (RCI) in Table 3.16 was used to determine the degree of consistency or consistency ratio (CR) according to equation 5. If the CR value is less than or equal to 0.1, it is acceptable. If not, the pair-wise comparison may need to revise. n is the number of criteria, in this case, Saaty defined the consistency index (CI) as follows:

$$CI = {(\lambda_{max} - n)}/{(n-1)} \qquad (3.30)$$

Table 3. 16 Average random inconsistency indicators (RCI).

n	1	2	3	4	5	6	7	8	9	10	11	12	13	14	15
RCI	0	0	0.58	0.90	1.12	1.24	1.32	1.41	1.45	1.49	1.51	1.48	1.56	1.57	1.59

3.5.3.6 Expert opinion

Expert knowledge and experience are very important to select and validate relevant criteria. The expert opinion provides study area-specific information to enhance the research outcome based on their expertise and accumulated knowledge (Malczewski, 1999). Therefore, expert opinion is a robust decision rule (Malczewski, 1999; Rinot et al., 2019). Hence, scholars have widely used expert opinion for validation (Alilou et al., 2019; Abenayake et al., 2018; ul Haq and Boz, 2020). The expert opinions were obtained from 15 local experts (soil scientists, agronomists, hydrologists, economists, and field agricultural officers) from the Department of Agriculture, Sri Lanka. These expert opinions were used first to review criteria indicators and then to validate the results of the pair-wise comparison.

3.5.3.7 Weighted linear combination method

In the weighted linear combination **(**WLC) method, the criteria indicators and their corresponding weights were combined to obtain the final score for map generation (Khoi and Murayama, 2010). Therefore, the WLC was executed to combine the indicators with their corresponding weights and scores to generate the maps. In this research, WLC scores have been used to evaluate the influence of each criterion for analysing and classifying the farming systems in the Central Highlands. Economic and ecological criteria indicators were separately analysed. The equation of WLC can be presented as:

$$WLC = \sum_{j=1}^{n} C_{ij} W_j \qquad (3.31)$$

where C_{ij} is i^{th} rank of j attribute, W_j is the weightage of j attribute.

These WLC scores were rated in 1-5 scale to generate an ecologically viable index and economical sound index. These indices were separately obtained using a matrix. The WLC scores were used to generate a separate map of ecologically viable farming systems and economically sound farming systems in the ArcGIS environment.

3.5.3.8 Mapping ecologically viable and economically sound farming systems

Both ecological and economic indices were considered in developing an overall index. The average cumulative value of ecological and economic indices was computed as the overall index (equation 3.32). The scale for the overall index was adapted from previous research (Gray et al., 2015). The overall index map was generated to identify ecologically viable and economically sound farming systems in the Central Highlands.

$$Overall\ index = (Ecologically\ viable\ index\ +\ Economically\ sound\ index)/2 \quad (3.32)$$

3.5.4 Objective 4

Investigating the impacts of climate variation on soil erosion hazards and predicting soil erosion vulnerability is important to introduce mitigating measures and protect precious natural resources. Identifying vulnerable hotspots is also necessary to advise conservation strategies and direct policy implementations. Thereby, modelling the future potential rate of soil erosion is crucial to minimize the adverse impacts of climate variation, particularly rainfall. However, there is limited knowledge regarding soil erosion predictions over the Representative Concentrative Pathway (RCP) climate scenarios in the Central Highlands of Sri Lanka.

In objective 4, this study aims to develop a spatiotemporal process to predict soil erosion vulnerability using future climate scenarios. This research employed a combined methodology: empirical soil erosion models, statistical, machine learning and hybrid methods and techniques for modelling and predicting soil erosion under two different RCP climate scenarios. The overall methodology of objective 4 is illustrated in Figure 3.14.

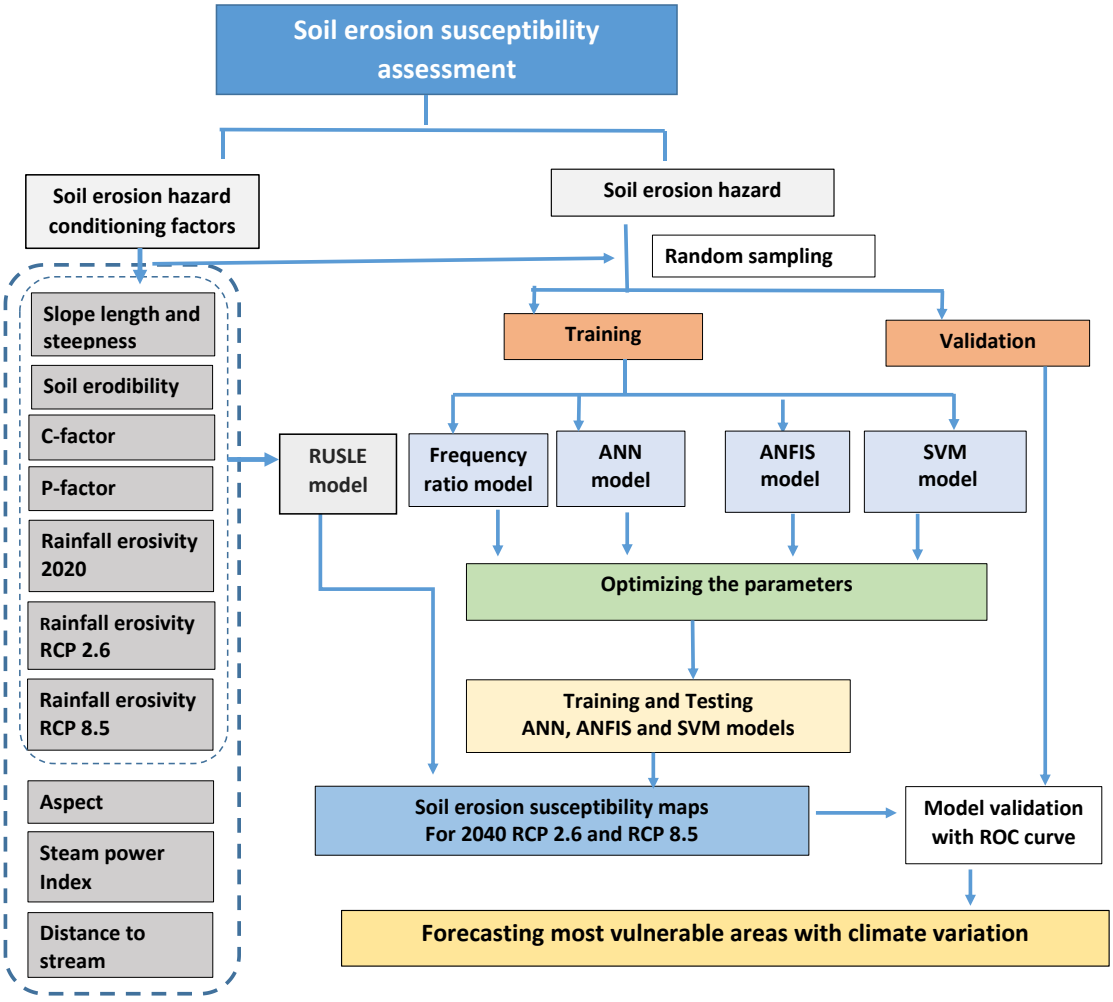

Figure 3. 14 The overall flowchart of the process for objective 4 of this study.

3.5.4.1 Climate change scenarios

A quantitative assessment of soil erosion is important to identify and minimize the impact of climate change risk (Chen et al., 2020). The IPCC has produced four future warming scenarios, which examined different possible future greenhouse gas (GHG) emissions under Coupled Model Inter-comparison Project Phase 5- CMIP5 (IPCC, 2015). The RCP scenarios visualize temperature and precipitation changes throughout the 21st century due to increasing GHG emission levels over time, leading to high GHG concentration levels. The RCP scenarios: RCP 2.6, 4.5, 6.0, and 8.5 (watts per meter squared), specifically the earth system, will change a little or aggressively change with no mitigation actions. In this study, soil erosion was predicted to 2040 using RCP 2.6 for the best scenario (low level of greenhouse gas emissions) and the worst scenario (RCP8.5), a high level of greenhouse gas emissions. Under these two scenarios, the anticipated emission of GHG

and air pollutants will substantially reduce with RCP2.5 and worsen under RCP8.5. This research utilised precipitation projections data under RCP 2.5 and RCP 8.5 scenarios. The statistically downscaled Community Climate System Model (CCSM) projections' precipitation dataset were downloaded from National Centre for Atmospheric Research (NCAR) in GIS formats at a global 1-degree grid cell area (Hoar and Nychka, 2008).

3.5.4.2 Soil erosion susceptibility using frequency ratio

The frequency ratio (FR) model is a statistical-based bivariate approach which can be utilised to identify the spatial relationship between independent and dependent variables (Rahmati et al., 2017). This method has been employed to analyse the probability of the occurrence of an event from probability mapping by Bonham-Carter (1994). Many researchers have frequently used this method for flood susceptibility and landslide susceptibility mapping (Jebur et al., 2014; Gayen and Saha, 2017). FR can be computed using equation 3.12 (As mentioned in objective 1). This research attempts to predict soil erosion for the year 2040 based on two climate scenarios using a frequency ratio method with eight conditioning factors. Following soil erosion, conditioning factors were used: slope length and steepness, aspect, land use, distance to stream, steam power index, soil erodibility, and rainfall erosivity (2020, RCP2.6 and RCP8.5). The soil erosion susceptibility maps were developed using natural breaks. Maps were developed using ArcGIS software.

3.5.4.2.1 Soil erosion hotspots

A large amount of soil is delivered to streams due to the occurrence of landslides (Gunatilaka, 2007). The amount of sediments delivered to the reservoirs and tributaries has considerably increased in recent years. Researchers highlighted this sediment occurrence from landslides might be much larger than the flows of sediments supplied by other erosion processes. Landslide inventory helps identify the mutual relationship between landslides occurrence and their drivers, which are important to predict future landslides. Researchers have obtained more reliable soil erosion susceptibility prediction results by introducing landslide incidents. The soil erosion conditioning factor can be used in landslide susceptibility prediction (Huang et al., 2020). Researchers found a correlation between soil erosion and landslide occurrences in several locations (Rozos et al., 2013; Pradhan et al., 2012). Although rainfall plays the main role in landslide

susceptibility in Sri Lanka, researchers found soil erosion may also contribute as one of the reasons for these incidences (Dang et al. 2019). Therefore, past landslides incidence was used as training and testing datasets. The total number of 279 landslide locations during 2000–2019 in this study area was recorded from the United Nations International Strategy for Disaster Reduction (UNISDR, 2021).

3.5.4.2.2 Soil erosion conditioning factors

The selection of suitable soil erosion conditioning factors is one of the prerequisites for soil erosion susceptibility assessment and mapping. In the present study, the selection of the most suitable conditioning factors was drawn heavily based on extensive literature reviews and expert advice. Soil erosion susceptibility was analysed using eight conditioning factors, including rainfall erosivity under two climate scenarios RCP 2.6 for the best and RCP 8.5 for the worst situation. Following soil erosion conditioning factors were used; soil erodibility, slope length and steepness, rainfall erosivity, land cover, aspect, distance to stream and steam power Index. Natural beaks were used to distinguish the classes in each condition factor. Raster maps were developed in the ArcGIS environment, and detailed explanations are given in the following sections.

3.5.4.2.2.1 Soil erodibility

Soil erodibility is an important factor for delineating soil erosion vulnerability. The soil susceptibility to water is called soil erodibility (Rosa et al. 1999). The most significant soil parameters are erodibility, which includes soil texture, soil structure, organic matter, soil permeability and infiltration, and soil mineralogy. Data were gathered from past research (Dissanayake et al. 2019).

3.5.4.2.2.2 Slope length and steepness

Slope length and steepness represent the effect of slope length (L) and gradient (S), which resulted in soil erosion due to rainwater runoff. Slope length (L) is defined as the distance from the point of origin of soil particles moving with water flow to the point where it results in a deposition. The soil erosion increases with the increasing slope length and steepness (Renard et al., 1997). The digital elevation map was used to find the elevation

in the area. Slope length and steepness were estimated with the following equation (Moore and Wilson, 1992; Moore and Burch, 1986):

3.5.4.2.2.3 Land cover - Crop factor (C) and conservation practices (P)

Vegetation cover is important to control surface runoff and prevent soil erosion (Nearing et al. 2005; Hou et al., 2016). The major land-use types of this study area are water bodies, dense forests, built-up areas, agricultural land, and open forest. The land cover map is generated based on support vector machine (SVM) classification using Landsat 8 satellite data set. Crop factor (C) generation was explained in section 2.5.1.3. The P - values were developed based on the study of Dissanayake et al. (2019).

3.5.4.2.2.4 Rainfall erosivity

Rainfall erosivity represents the driving force of soil particles from one place to another, and it is the central feature for creating sheet and rill erosion (Wischmeier and Smith, 1978). The intensity, total rainfall and seasonal distribution of the rain are more important for soil erosion (Wischmeier and Smith, 1978). In the present study, 30 years of daily rainfall data from 1990 to 2019 were considered for 2020, and grid rainfall data layers of RCP were obtained to develop a rainfall erosivity map. The rainfall erosivity was calculated using equation 3.8 (As mentioned in objective 1).

3.5.4.2.2.5 Aspect

Aspect has been defined as the direction of the maximum slope on the terrain surface (Ranasinghe et al., 2019). The slope aspect is responsible for receiving a significant amount of wind-driven rainfall (monsoonal rainfall), which ultimately affects the magnitude of soil erosion. The western slope of the Central Highlands gets the highest amount of rainfall from the southwest monsoon, and the eastern slopes receive rainfall from the northeast monsoon (Burt and Weerasinghe 2014). The aspect was generated from the digital elevation model (DEM) in the ArcGIS environment.

3.5.4.2.2.6 Distance to stream

Distance from the stream has a significant impact on soil erosion. Gayen and Saha (2017) specified that distance to stream is an important parameter for soil erosion due to slope stability and degree of saturation of soil in the hillslope. Hence, the distance to stream is considered as one of the indicators for this study.

3.5.4.2.2.7 Stream power index

The stream power index (SPI) is an important attribute for calculating the erosive power of running water (Moore and Wilson, 1992). The amount of water discharge is proportional to a catchment area. This indicator is useful for predicting net erosion and deposition based on profile curvature (convexity and concavity). The SPI map is derived from the following formula:

$$SPI = A_s \times Tan\beta \qquad (3.30)$$

where, A_s and β denote the specific area of a basin (m^2/m) and slope degree, respectively.

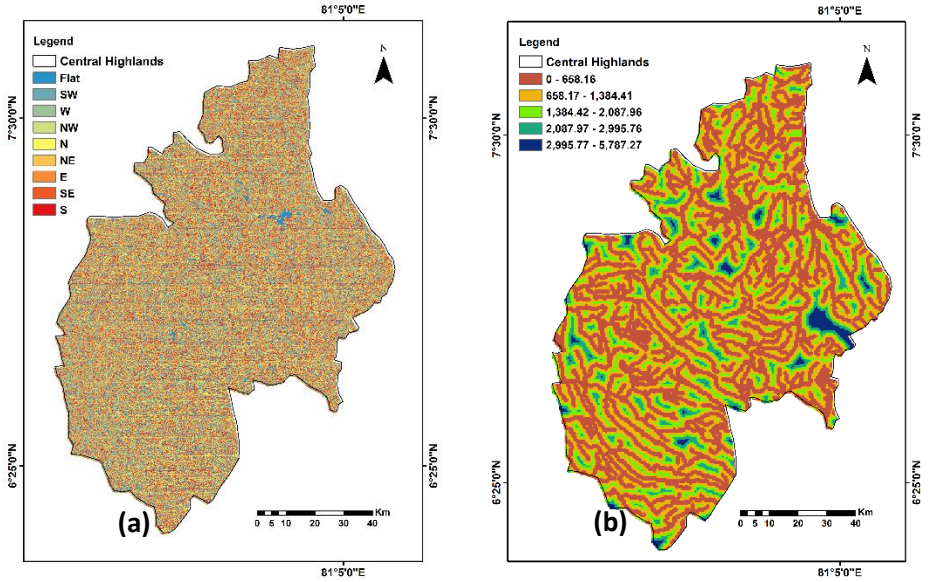

Figure 3. 15 Condition factor maps (a) aspect, (b) distance to stream,

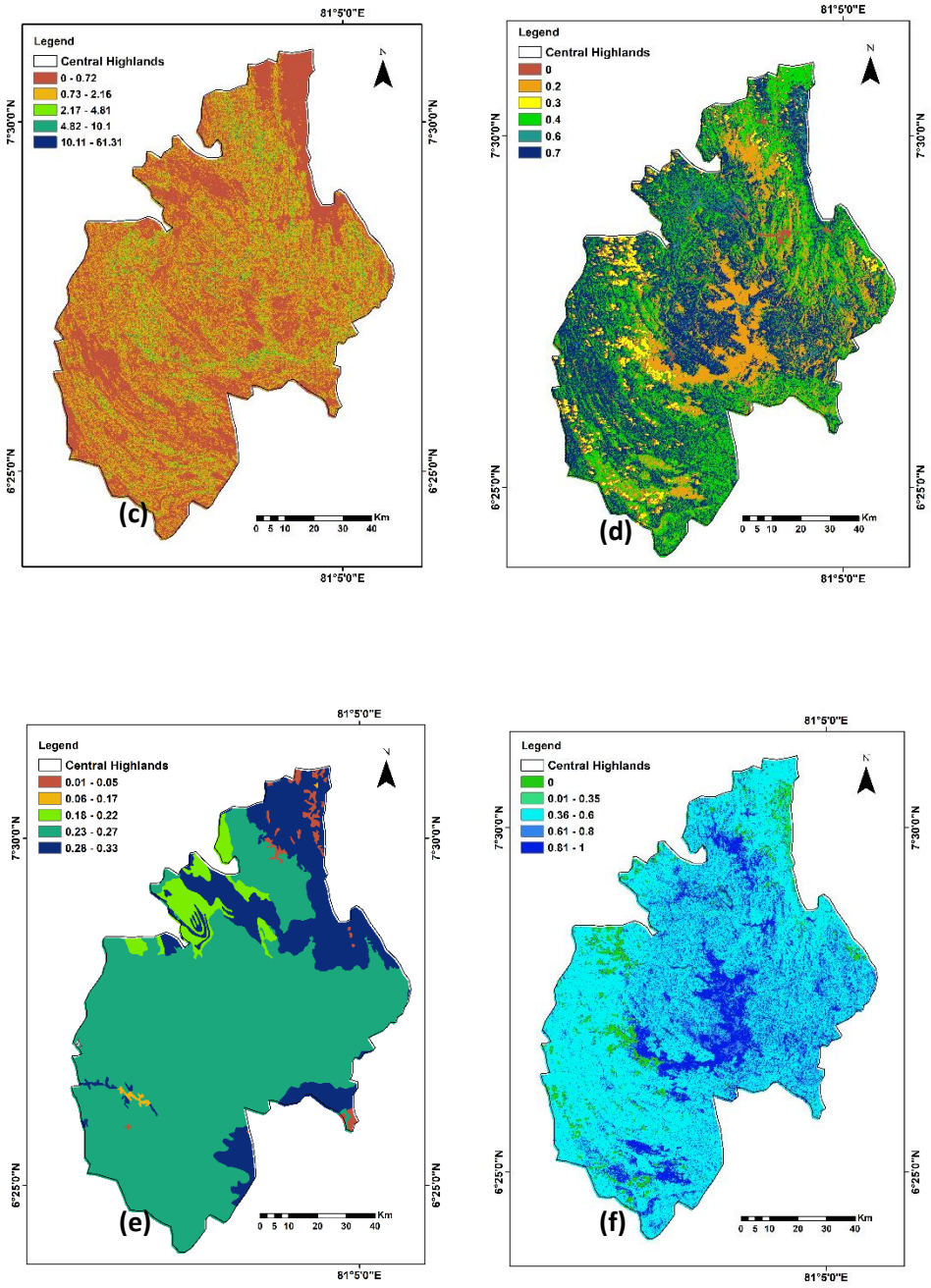

Figure 3. 16 (Continue)**.** Condition factor maps (c) slope length and steepness, (d) P factor (e) soil erodibility, (f) C factor.

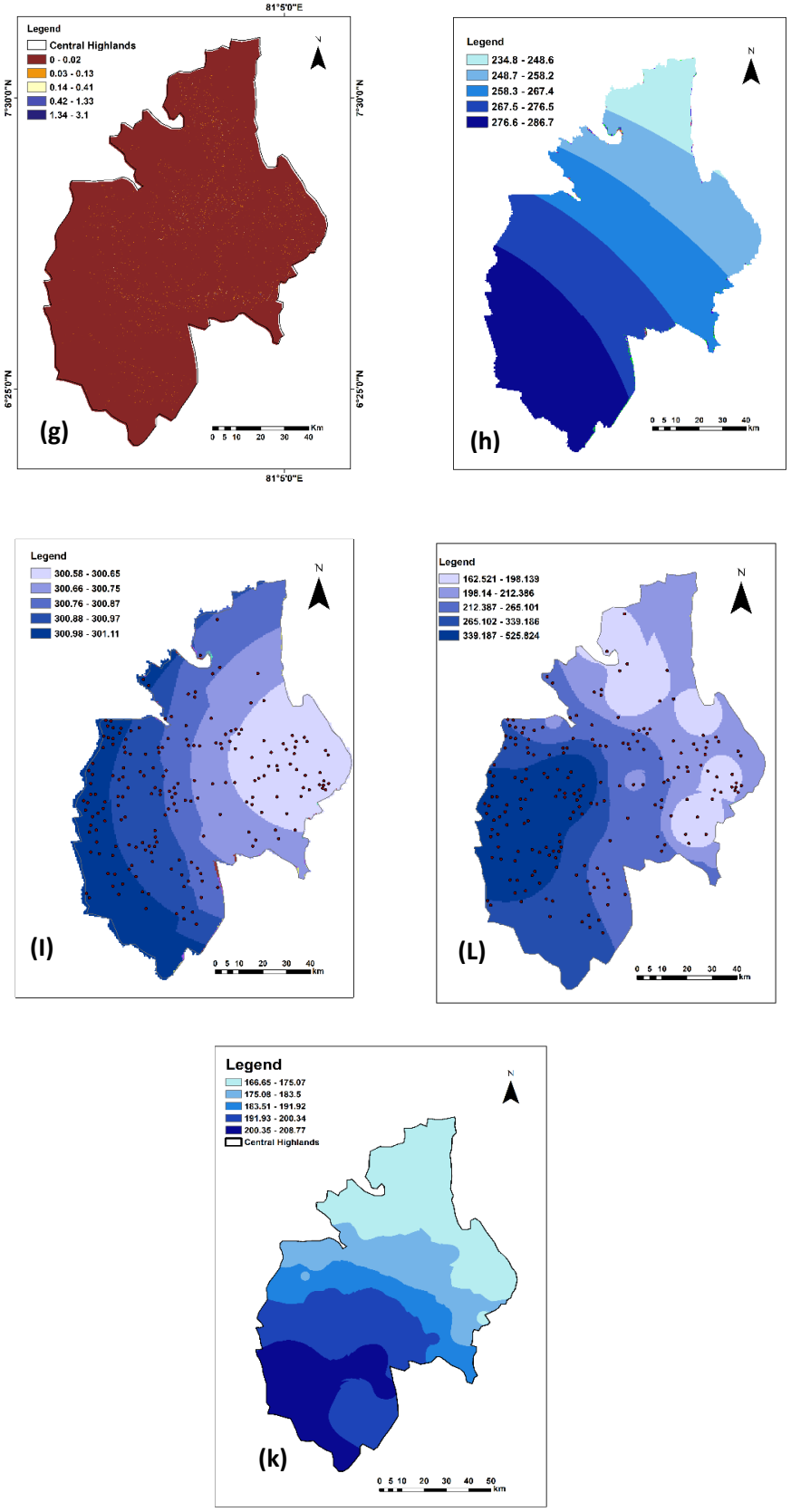

Figure 3. 17 (Continue) Condition factor maps (g) steam power Index (h) rainfall erosivity RCP 8.5, (I) rainfall erosivity RCP 2.6 (j) rainfall gauge erosivity (k) satellite-based rainfall erosivity.

3.5.4.3 Artificial neural network methods

Artificial neural network (ANN) has been applied for nonlinear complex environmental applications. The ANN is a machine learning model which can be used to construct soil erosion causative factors as inputs, and soil erosion can observe using output (Chakrabortty et al., 2020). The most popularized ANN model for prediction is a multilayered perceptron (MLP) with a feed-forward and back-error propagation type of learning algorithm (Pradhan and Lee, 2010b). MLP with a three-layered interconnected neural network was performed using soil erosion causative factors as input nodes in Figure 3. 16. The weightage computations of the input data were used for hidden layer activation, and identity function was used for output layer activation. The weight component act as a coefficient to the inputs. The hidden layer (sum of the weighted inputs) computed network output through a non-linear activation function. The trial and error method was used to determine the number of neurons for hidden layer. The poor or excessive number of neurons in the hidden layer most likely causes the problems of bad generalization and overfitting (Orhan et al., 2011).

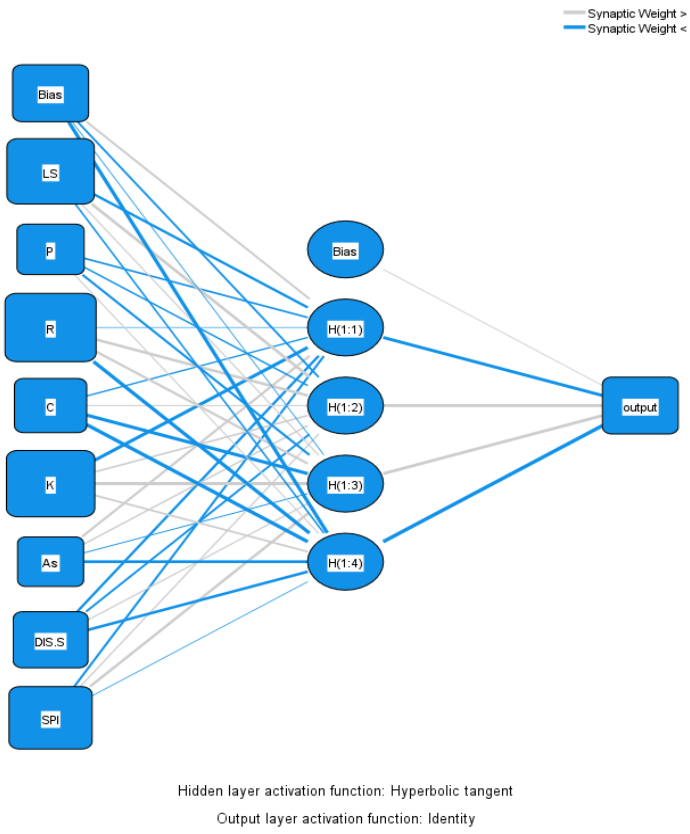

Figure 3. 18 Multilayered perceptron (MLP) with feed-forward network.

There are two stages involved in neural networks for multi-sourced classification: the training stage where the internal weights are adjusted and the classifying stage.

Each neuron j in the hidden layer sums its input x_i (soil erosion causative factors) after multiplying them by their respective connection weights w_{ji}. The output of each neuron is described as follows:

$$y_i = f\left(\sum w_{ji}\, x_i\right) \qquad (3.31)$$

where f is an activation function using the weighted summation of the inputs. The activation function can be a simple threshold, sigmoid, or hyperbolic tangent function

The sum of squared differences between the desired and actual values of the output neurons E (soil erosion) is defined as follows (Orhan et al., 2011).

$$E = \frac{1}{2}\sum_j (y_{dj} - y_i)^2 \qquad (3.32)$$

Where y_{dj} is the desired value of output neuron j and y_j is the actual output of that neuron. Each w_{ji} weight is adjusted to minimize the value E depending on the training algorithm adopted.

Eights inputs (soil erosion causative factors) were given to the model at the training stage. Ten hidden layers were used. One output (actual soil erosion rates) was also given to the model as in Figure 3.18. Inputs were multiplied with the weights in the hidden layers. The value of output neurons was also multiplied with each weight, and finally, one output (soil erosion rates) was obtained as explained in equations 3.31 and 3.32.

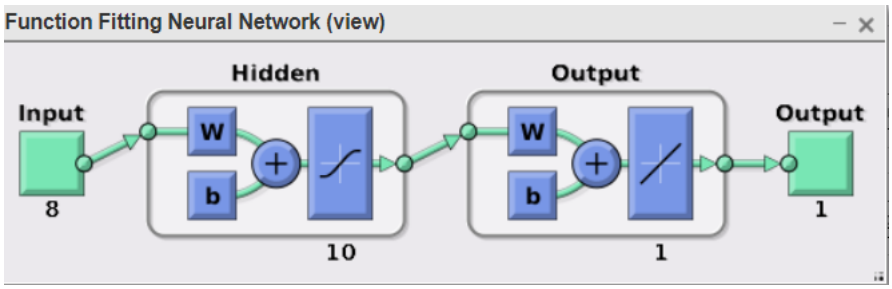

Figure 3. 19 The structure of the multilayer ANN method from MATLAB.

3.5.4.4 The adaptive neuro-fuzzy inference system

The adaptive neuro-fuzzy inference system (ANFIS) uses as a hybrid-learning algorithm by a combination of gradient descent and the least square method. This method was developed by Jang (1993) using the Takagi–Sugeno rule format, which is the combination of an optimized premise membership function (gradient descent) with an optimized consequent equation (linear least squares estimator). ANFIS is a process of both fuzzy logic and artificial neural network methods and uses for driving the fuzzy If-then rules into the artificial neural network with high computational power (Tien Bui et al., 2012). Fuzzy rules and suitable membership functions of training paired are executed and further lead to an interface (Islam et al., 2018). There are several membership functions (Table 3.17). This model has been applied in many environmental hazard applications such as floods, landslides and soil erosion assessment. Figure 3.19 shows the ANFIS architecture.

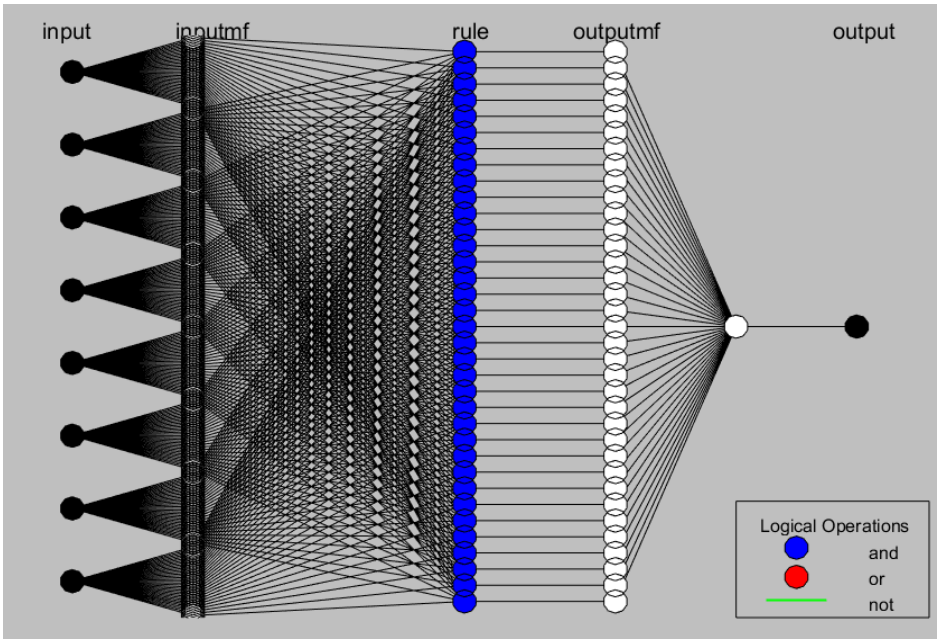

Figure 3. 20 The architecture of the ANFIS model.

The first layer of the ANFIS accepts as inputs and converts them to memberships.

$$Q_{1,i} = \mu A_i(x) \qquad (3.33)$$

$$Q_{1,i} = \mu B_i(y) \qquad (3.34)$$

where, x and y are the input neurons, A and B are the linguistic variables, and μAi(x) and μBi(y) and μ is the weight obtained relating the fuzzy membership function for that node.

The second layer employs the neurons, which corresponds to a rule. Thus, number of the neuron in level 2 is equal to the number of rules. There are two rules.

Rule 1IF (*x* is *A1*) and (*y* is *B1*) THEN,

$$f_1 = p_1 x + q_1 y + r_1 \quad (3.35)$$

Rule 2 IF (*x* is *A2*) and (*y* is *B2*) THEN

$$f_2 = p_2 x + q_2 y + r_2 \quad (3.36)$$

where f_i are the outputs for the inputs *x* and *y* in the fuzzy extent generated by the fuzzy rules, A_i and B_i are the fuzzy sets, and p_i q_i and r_i are the shape parameters determined in the training period.

Layer 2 contains fixed neurons and is denoted as $\prod$. The output of each neuron is the product of all input signals to that neuron

$$Q_{2,i} = \omega_i \ = \ \mu A_i(x) \mu B_i(y), \quad i = 1,2 \quad (3.37)$$

where, W_i is the output for each neuron.

The third layer is responsible for the normalization of values coming from layer 2. Layer 3 includes the fixed neurons, which are denoted as N. Thus, the output of this layer can be called as normalized firing strengths.

$$Q_{3,i} = \grave{}\omega_1 = \frac{\omega_i}{\omega_1 + \omega_2}, i = 1,2 \quad (3.38)$$

The fourth layer serves as a defuzzifier, and the fifth layer includes only a single neuron for the summation of all defuzzified outputs.

$$Q_{4,i} = \grave{}\omega_1 f_i = \grave{}\omega_1 (p_1 x + q_1 y + r_1) \quad (3.39)$$

where, $\grave{}\omega_1$ is the normalised fire strength of layer 3 and p_1, q_1, and r_1 is neuron parameters. The parameters of this layer can be interpreted as the result parameters.

Layer 5 contains a single neuron denoted as Σ which is all input signals summed up of all defuzzified outputs and produces the single output of the ANFIS (Tien Bui et al. 2012; Termeh et al. 2018):

$$Q_{5,i} = \sum \grave{}\omega_1 f_i = \frac{\omega_i f_i}{\sum \omega_i}, \quad i = 1,2 \quad (3.40)$$

Table 3. 17. The membership functions.

No	Membership functions	Type of MF Descriptions
1	Gaussmf	Gaussian curve membership function
2	Gauss2mf	Two-sided Gaussian membership function
3	Gbellmf	Generalized bell curve membership function
4	Sigmf	Sigmoid curve membership function
5	Dsigmf	Difference of two sigmoid membership functions
6	Psigmf	Product of two sigmoidal membership functions

3.5.4.5. Support vector machine algorithm

Support vector machine (SVM) is one of the most popular machine learning algorithms and is considered as a high-performing technique. The SVM is a non-parametric supervised machine learning technique. SVM algorithm is a supervised pattern classification (Cortes and Vapnik, 1995). SVM is founded on the theory of structural risk minimization. The primary basis of SVM method is to find the optimal separation hyper-plane from the dataset (Lee, Hong, and Jung 2017) and the training points that are closer to hyper-plane called support vectors. When considering the training data set (X_i, Y_i), corresponding influencing factor if $X_i \in R^n$, and $Y_i \in \{+1,-1\}$, i= 1……m the optimal separating hyperplane which can separate two classes, i.e. eroded areas and non-eroded areas can be determined as in equation 3.41.

$$Y = (W \times X_i + \mathrm{b}) \geq 1 - \zeta_i \qquad (3.41)$$

where *W* is a coefficient vector that determines the orientation of the hyperplane in the pace of the feature, b is the offset of the hyperplane from the origin, *Xi* is the positives lack variables (Cortes and Vapnik, 1995).

3.5.4.6 Long short -term memory (LSTM)

LSTM was introduced by Hochreiter and Schmidhuber in 1997 (Kratzert et al., 2018) and used for time series prediction in different applications such as drought. The LSTM is a kind of RNN; nevertheless, it minimizes these drawbacks of RNN. The architecture of the LSTM neural network is shown in Figure 3.20.

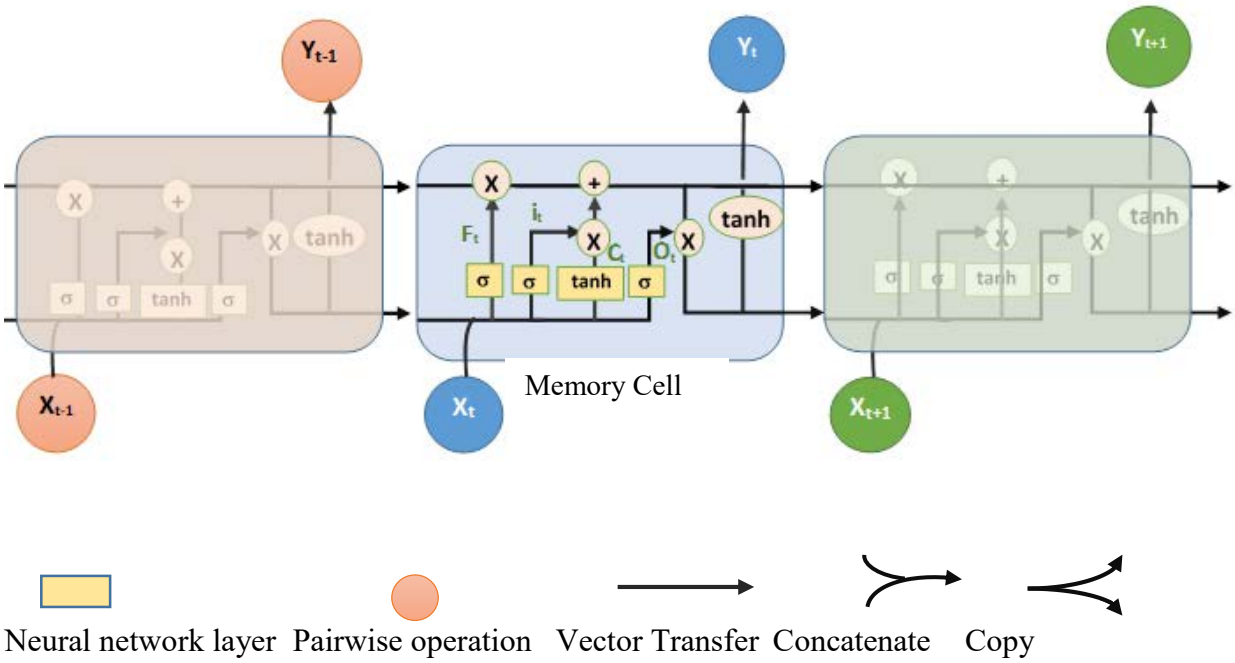

Figure 3. 21 The architecture of repeating module in the LSTM neural network.

In a LSTM cell (Figure 3.18) $\boldsymbol{x}$ is the input layer and $\boldsymbol{y}$ is the output layer. $\boldsymbol{t}$ represents a certain time step. $\boldsymbol{i_t}$, $\boldsymbol{f_t}$ and $\boldsymbol{o_t}$ are the input gate, forget gate and output gate, respectively. $\tilde{\boldsymbol{c}}_t$ is the current input memory state and $\boldsymbol{c_t}$ and is $\boldsymbol{c_{t-1}}$ cell state vectors at time t and t-1.

The LSTM network consists of three layers: an input layer, a hidden layer and an output layer. The LSTM structure is similar to RNN. The only difference is the memory blocks which is called cells. The data can be added to or removed from the cell state via sigmoid gates. A gate is similar to a layer or a series of matrix operations, which can contain different weights and biases of each gate. The structure of the LSTM is designed to avoid the long-term dependency problem using gates to control the memorizing process (Le et al., 2019).

The x is sequential input (x_1,x_2,…..x_n) y is sequential output (y_1,y_2,…y_n.), and the forget gate is the key state to that helps to determine the current information should forget or remembrance. It can be determined for a certain time period t by the following equation,

$$f_t = \sigma(W_f x_i + R_i h_{t-1} + b_f) \qquad (3.42)$$

where $W_f x_t$ and $W_f h_{t-1}$ are the forget weight matrix and the forget-hidden weight matrix, respectively, b_f is the bias of the forget gate, and σ is the activation function similar to sigmoid or ReLU. The input gate *it* determines the information updating and $\tilde{c}_t$ memorises the new information, and they are defined as follows:

$$i_t = \sigma(W_i x_i + R_i h_{t-1} + b_i) \quad (3.43)$$

$$\tilde{c_t} = \tanh(W_{ch} x_i + R_i h_{t-1} + b_c) \quad (3.44)$$

where W_{ix} and W_{ch} denote the weight matrix, b_i and b_c are the bias vectors of the input gate and the updating cell state, respectively. The new memory cell state c_t can update as follows:

$$c_t = f_t \odot c_{t-1} + i_t \odot c_t \quad (3.45)$$

$$h_t = o_t \odot \tanh(c_t) \quad (3.46)$$

where c_{t-1} is the previous memory cell state and $\odot$ represents the element-wise product. Finally, the output gate controls the output activations. The hidden layer sent to the next time step is defined as follows:

$$O_t = \sigma(W_{ox} x_i + W_{oh} h_{t-1} + b_o) \quad (3.47)$$

where W_{ox} is the output weight matrix, W_{oh} is the output-hidden weight matrix, and b_o is the bias of the output gate. I_t, C_t and O_t are the outputs of three sigmoid functions, σ, and their values range from 0 to 1.

The rainfall erosivity was estimated from predicted rainfall data by the LSTM model at five agro-meteorological stations. The rainfall erosivity values were estimated from Equation 3.8, which was proposed for the Sri Lankan condition by Wickramasinghe and Premalal in 1988 (Wijesekera et al., 2013). The erosivity map layer was employed to RUSLE (equation 3.7) to assess the soil erosion susceptibility in 2024. All the factor layers were computed into raster format with a 30m grid cell. The annual soil loss was estimated using the raster calculator tool in the spatial analysis. The soil erosion map was classified into five classes to detect the most vulnerable areas in the Central Highlands.

3.5.4.7. The model validation using a statistical method

To optimize the system performance, proposed models were evaluated using root mean square error (RMSE), mean absolute error (MAE), and the area under the receiver operating characteristic curve (AUROC). Validation of soil erosion maps was done using ROC/AUC analysis. The AUC value is equal to 1 indicates the perfect prediction. The ROC curve was obtained using SPSS software for the validation of soil erosion susceptibility maps. The ROC curve was developed based on the false positive rate (1-specificity) regarding the true positive rate (sensitivity) with the various cut-off thresholds;

$$\text{RMSE} = \sqrt{\frac{\sum_{i=1}^{N}[\bar{X} - X]^2}{N}} \qquad (3.48)$$

$$\text{MAE} = \frac{1}{N}\sum_{i=1}^{N}[\bar{X} - X] \qquad (3.49)$$

where N is the sample size, $\bar{X}$ is means predicted values, and X means observed values. Means absolute error is the sum of the deviation between the predicted values of a variable and the real observed values. RMSE optimal value is zero (0), which indicates a higher model performance and prediction rate. However, the optimal value is close to zero is relative. Hence, previous studies revealed that RMSE with standard deviation (SD) of the observation values is appropriate for evaluating the acceptable model performance. It is known that RMSE values less than half the SD of the measured data may be considered low and acceptable for model evaluation (Singh et al., 2005; Moriasi et al., 2007; Kastridis et al., 2020)."

R^2 value is used to represent the extent of association between the observed and forecasted values. This value varies between 0 and 1, where 1 indicates exact matching and 0 indicates no association.

$$R^2 = \frac{\sum_{i=1}^{N}(\hat{Y}_i - \overline{Y_i})}{\sum_{i=1}^{N}(Y_i - \overline{Y_i})^2} \qquad (3.50)$$

where, the mean value represent by $\overline{Y_i}$, observed and forecasted values are represented by Y_i and $\widehat{Y_i}$, N is the number of data points.

$$\bar{Y} = \frac{1}{N}\sum_{i=1}^{N} Y_i \qquad (3.51)$$

The area under the ROC curve (AUC) is a quantitative measure of the quality of a model, which can be categorised as poor (0.5–0.6), average (0.6–0.7), good (0.7–0.8), very good (0.8–0.9), and excellent (0.9– 1) (Chen et al., 2017c; Yesilnacar, 2005). A higher AUC value indicates a better model, and an AUC value of 1 indicates a perfect model (Youssef et al., 2015).

3.6 Summary

The followings are the summary of the materials and methodology:

- The Central Highlands of Sri Lanka was selected for this study. According to the global climate hazard index, Sri Lanka was ranked second (2019) and third (2018). Every year Sri Lanka experiences a number of hazardous events. Sri Lanka is highly vulnerable to climate hazards, particularly floods, droughts, and landslides. Soil erosion is a significant problem in the Central Highlands.
- This research focused on crop diversity change in farming systems with soil erosion hazards and rainfall variation. The study employed time series analysis of soil erosion hazards, rainfall variation and plant diversity change using remote sensing data and GIS software environment. No major study has been conducted on farming systems in relation to soil erosion hazards in this area.
- Land-use change assessment was proposed using SVM, RF and Interactive supervised classification methods and soil erosion assessment was conducted using the RUSLE model combined with geo-informatics technology.
- A novel methodology was proposed to delineate the farming systems using cropping areas and agro-ecological zones.
- Soil erosion hazard was assessed using RUSLE and Geo-informatics technology and the frequency ratio method.
- A case study was planned to further assess the soil erosion hazard vulnerability in Sabaragamuwa Province, which has the most vulnerable farming systems in the Central Highlands. Every year Sabaragamuwa Province experiences the highest number of landslides and flood events than other provinces in the Central Highlands of Sri Lanka.
- The use of MODIS derived vegetation indices and the Shannon diversity index were proposed to evaluate the crop diversity change during this period.

- Rain-use efficiency (RUE) and residual trend analysis (RESTREND) combined with a regression approach were proposed to partition the soil erosion due to human and climate-induced land degradation.
- Rainfall variation in the Central Highlands was examined using rainfall anomaly, SPI and extreme rainfall indices, such as maximum 1-day precipitation, 95p, 99p (very and extremely wet days), the simple daily intensity index (SDII) and annual total wet day precipitation (PRCPTOT). Modified Mann-Kendall and Sen's slope tests were proposed to test the significance of the rainfall variation. Innovative trend analyses with satellite-based and rain gauged rainfall data were proposed for trend analysis. Pearson correlation and modified Kling-Gupta were proposed to find the correlation with the relationship between rainfall variation and soil erosion hazards.
- A matrix-based geo-informatics approach was proposed to identify the ecologically viable and economically sound farming systems. The proposed framework has been developed using the analytic hierarchy process (AHP) and weighted linear combination method combined with geo-informatics tools. Indices and matrices were developed with the perspective of economically sound and ecologically viable farming systems against soil erosion hazards.
- The combined approach of RUSLE, FR, and ANN methods with geo-spatial technology were used to predict soil erosion in farming systems under RCP 2.6 and 8.5 climate scenarios. The potential of soil erosion susceptibility was predicted using vulnerability maps for 2040 under climate change scenarios; RCP 2.6 and RCP 8.5. Eight geo-environmental factors were selected as inputs to model the soil erosion susceptibility. Five models: revised universal soil loss (RUSLE), frequency ratio (FR), artificial neural networks (ANN), support vector machine (SVM), adaptive network-based fuzzy inference system (ANFIS) and LSTM were selected as widely applied methods for many applications.
- Soil erosion hazard vulnerability was explored to produce soil erosion hazard susceptibility maps. Calibration and validation of produced soil erosion hazard vulnerability maps and susceptibility maps were done by RMSE, MEA and ROC, respectively.

CHAPTER 4

RESULTS AND DISCUSSION

4.1 Overview

This chapter presents the results of the analyses employed to answer the four research questions: First, what is the impact of soil erosion hazards and crop diversity changes in different farming systems during the last 20 years (2000 – 2019)? Secondly, what is the relationship between soil erosion hazards and rainfall variation in the Central Highlands? Thirdly, how can the status of erosion hazards be used to identify ecologically viable and economically sound farming systems? And finally, how to develop a predictive model based on soil erosion hazards to identify the vulnerability of farming systems? The chapter is structured as follows: The results describe the impact of soil erosion hazards with crop diversity changes in different farming systems using geo-informatics. Then, the results of the analyses are discussed in the context of the relationship between soil erosion hazards and rainfall variation in the Central Highlands. This is followed by a description of the results of the evaluation of ecologically viable and economically sound farming systems using a matrix-based geo-informatics approach. Finally, the results are presented within the framework of the spatiotemporal modelling process (using statistical and machine learning techniques) to predict the vulnerability in different farming systems for soil erosion hazard, based on representative concentrative pathways (RCP) climate scenarios.

4.2 Objective 1

For objective 1, this study conducted the assessment of the land-use change, soil erosion hazards and crop diversity changes in different farming systems in the Central Highlands. Land-use change was assessed using three classification methods. Soil erosion hazards were assessed using the RUSLE method. Vegetation indices and the Shannon index examined crop diversity change.

4.2.1 Land-use and land-cover change in the Central Highlands

Land-use and land-cover (LULC) change analysis was carried out using Landsat imagery for 2000, 2010 and 2019 by employing the interactive supervised classification, SVM, and RF methods. Figure 4.1 shows the resulting classification maps using SVM for 2000, 2010 and 2019. Table 4.1 shows the respective findings of the analysis. The results indicate that dense forests and open forests have decreased during this period by 14.5%

and 5.8%, respectively, while agricultural areas and built-up areas have increased by 15.4% and 2.35%. All six classes of each classifier were examined. The accuracy assessments of SVM indicate the Kappa coefficients: 0.83 in 2000, 0.81 in 2010 and 0.83 in 2019 (Table 4.2). The summary results of the accuracy assessment are given in Table 4.2.

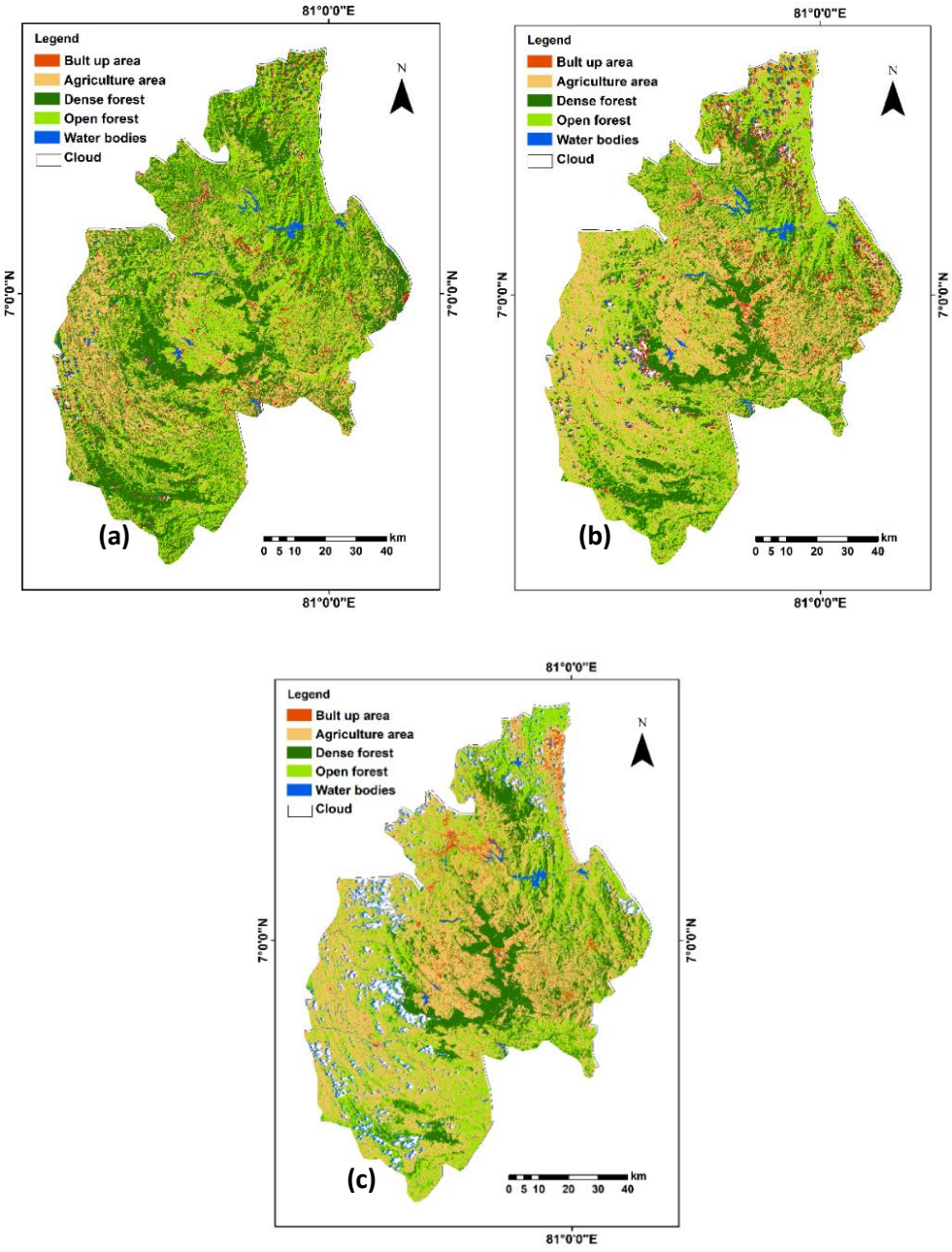

Figure 4. 1. LULC maps in the Central Highlands: (a) 2000, (b) 2010, and (c) 2019.

Table 4. 1. LULC change from 2000 to 2019.

	Land area (km^2)						
Classes	**2000**	%	**2010**	**%**	**2019**	**%**	**Change**
Dense Forest	3452.9	32.9	2491.9	23.7	1927.5	18.4	-1525.4
Open forest	3761.4	35.8	3391.6	32.3	3150.9	30.0	-610.6
Agriculture area	2718.3	25.9	3881.4	37.0	4333.2	41.3	1614.9
Built-up area	299.5	2.85	373.6	3.6	546.0	5.2	246.5
Water bodies	137.4	1.31	59.9	0.6	137.3	1.3	-0.1
Other (Cloud)	130.4	1.24	383.6	3.7	404.6	3.9	274.2
	10500.0	100.0	10500.0	100.0	10500.0	100.0	

The results of LULC evaluation indicate forest and open forest areas have decreased while agricultural and built-up areas have increased during the study period. This research highlighted the large-scale deforestation which has taken place due to agricultural activities, expansion of home gardens and construction of household settlements. Other studies also indicated similar findings (Jayawardena et al., 2018). According to another recent study, forest areas are decreasing in Sri Lanka (Mondal et al., 2020). Ranasinghe et al. (2019) also confirmed some of these findings, such as decreasing the forest cover and increasing home gardens and agricultural areas in the Badulla district of the Central Highlands during the period 1990 to 2018. These findings clearly show the anthropogenic impact on natural ecosystems during the past few decades.

4.2.2 Demarcation of farming systems

The farming systems were extracted in terms of the land area using cropping areas in each agro-ecological region (AER). The cropping areas were extracted from the classified land-use map (Figure 4.1c) using ArcGIS extraction tool, and approximately 4320.4 km^2 of cropping areas could be identified. Accuracy assessment of the LULC classifications was done using the confusion matrix. The resulted Kappa coefficients are given in Table 4.2.

Table 4. 2. Results of three LULC accuracy assessments using a confusion matrix.

Classifiers	Year	Accuracy	Dense Forest	Open forest	Agricult-ural area	Built up area	Water bodies	Other (Clouds)	Overall coefficient	Kappa coeffici-ent
SVM	2000	User's	97.98	85.45	84.28	57.1	100	99.85	87.6	0.83
		Producer's	68.27	97.08	56.41	95.55	99.97	99.85		
	2010	User's	89.39	69.73	62.68	80.58	99.46	99.1	87.4	0.81
		Producer's	91.67	28.74	87.96	93.99	99.68	100		
	2019	User's	99.72	59.72	63.93	81.45	100	100	86.9	0.83
		Producer's	93.36	67.56	52.48	99.44	97.76	99.77		
ISC	2000	User's	57.1	61.8	75.0	97.9	64.9	92.9	90.25	0.9
		Producer's	100.0	72.4	63.6	97.2	89.2	81.5		
	2010	User's	89.4	88.2	50.0	75.0	82.2	67.7	78.5	0.78
		Producer's	98.9	37.5	25.0	75.0	96.6	86.8		
	2019	User's	94.03	60.00	86.67	97.44	90.88	83.89	85.71	0.78
		Producer's	88.73	66.67	68.42	100.00	96.00	91.67		
RF	2000	User's	97.4	93.9	100.0	94.0	86.7	78.9	90.49	0.90
		Producer's	100.0	95.8	75.0	88.7	68.4	100.0		
	2010	User's	97.4	93.9	100.0	94.0	86.7	78.9	80.06	0.80
		Producer's	100.0	100.0	75.0	93.0	68.4	100.0		
	2019	User's	100.00	20.69	82.86	100.00	100.00	100.00	84.68	0.84
		Producer's	93.67	66.67	93.55	100.00	70.00	100.00		

The classified farming systems in the Central Highlands of Sri Lanka are shown in Figure 4.2. The farming systems were labelled according to AER and delineated 34 farming systems in the Central Highlands (Table 4.3).

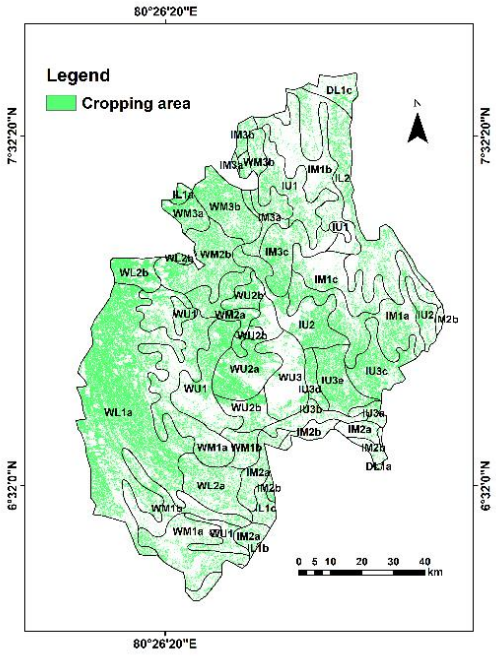

Figure 4. 2 Farming systems of the Central Highlands of Sri Lanka.

Table 4. 3. Details of farming systems in the Central Highlands.

No	Farming system Name	Name of agro-ecological region	Area(km²)
1	DL1c	Dry zone Low country 1c	120.771
2	IM1b	Intermediate zone Mid country 1b	447.183
3	IL2	Intermediate zone Low country 2	679.433
4	IM3b	Intermediate zone Mid country 3b	47.795
5	WM3b	Wet zone Mid country 3b	426.866
6	IL1a	Intermediate zone Low country 1a	27.647
7	IU1	Intermediate zone Up country 1	315.616
8	IM3a	Intermediate zone Mid country 3a	108.538
9	WM3a	Wet zone Mid country 3a	109.749
10	WL2b	Wet zone Low country 2b	145.173
11	WM2b	Wet zone Mid country 2b	349.910
12	IM3c	Intermediate zone Mid country 3c	264.277
13	IM1c	Intermediate zone Mid country 1c	287.464
14	IU2	Intermediate zone Up country 2	420.539
15	IM1a	Intermediate zone Mid country 1a	539.011
16	WM2a	Wet zone Mid country 2a	194.632
17	WU2b	Wet zone Up country 2b	263.516
18	WL1a	Wet zone Low country 1a	1718.975
19	WM1a	Wet zone Mid country 1a	1010.926
20	WU2a	Wet zone Up country 2a	356.282
21	WU1	Wet zone Up country 1	496.741
22	IM2b	Intermediate zone Mid country2b	159.600
23	IU3c	Intermediate zone Up country 3c	249.752
24	WU3	Wet zone Up country 3	293.012
25	IU3e	Intermediate zone Up country 3e	222.224
26	IU3d	Intermediate zone Up country 3d	73.292
27	DL1a	Dry zone Low country1a	3.472
28	IU3b	Intermediate zone Up country 3b	124.353
29	IU3a	Intermediate zone Up country 3a	48.157
30	IM2a	Intermediate zone Mid country 2a	281.186
31	WM1b	Wet zone Mid country 1b	371.184
32	WL2a	Wet zone Low country 2a	274.513
33	IL1c	Intermediate zone Low country 1c	67.381
34	IL1b	Intermediate zone Low country 1b	0.893

4.2.3 Soil erosion in the Central Highlands

The generated RUSLE factors maps for soil erosion assessment are shown in Figures 4.3 and 4.4. The soil erosion maps are illustrated in Figure 4.5. The details of soil erosion class distribution from 2000 to 2019 are given in Table 4.4. According to the results of the study, soil erosion rates are increasing. The mean annual soil erosion rate was 9.08

Mg/ha/yr in 2000, and it increased to 10.17 Mg/ha/yr in 2010 and 11.08 Mg/ha/yr in 2019 (Table 4.5). The land areas under high and very high soil erosion classes increased by 286.1km^2 and 166.3 km^2, respectively. The average soil erosion rate and landslide frequency ratio in each farming system were also assessed. The results are given in Table 4.4. The highest soil erosion rates can be observed in farming systems in the wet zone. This increasing soil erosion trend may be a result of anthropogenic impact of LULC change or climate variation.

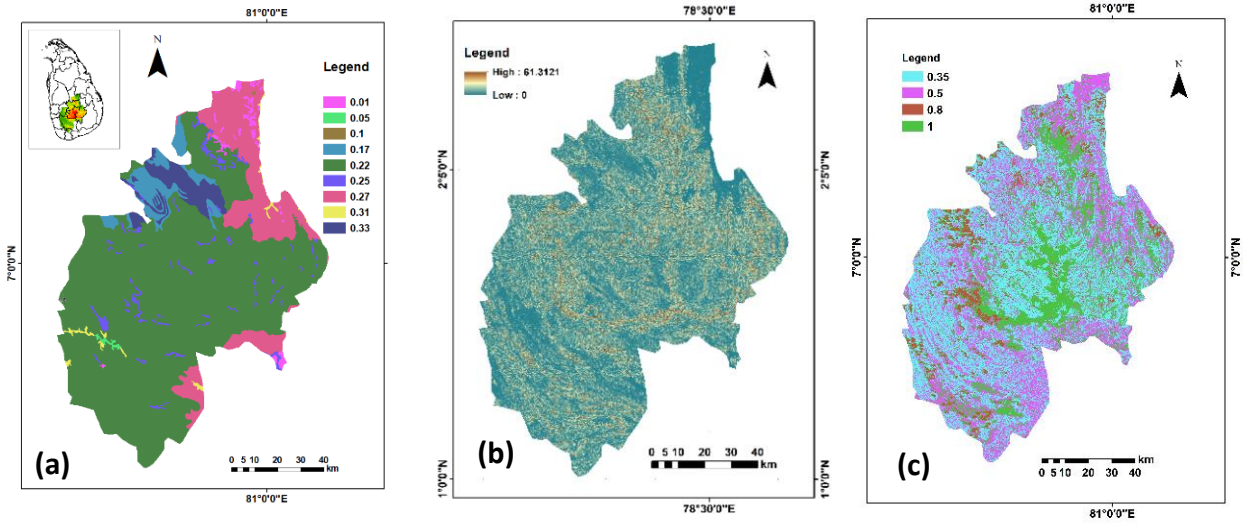

Figure 4. 3. Factor maps (a) K- factor, (b) LS factor, (c)P- factor, (d) R- factor 2000, (e) R- factor 2010, and (f) R- factor 2019.

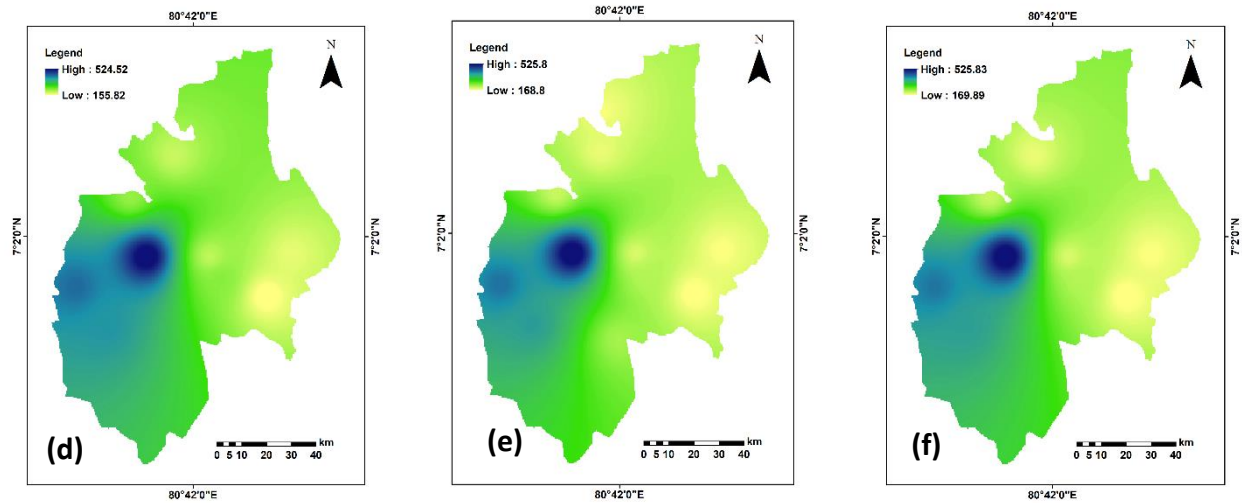

Figure 4. 3. Factor maps (a) K- factor, (b) LS factor, (c) P- factor, (d) R- factor 2000, (e) R- factor 2010, and (f) R- factor 2019.

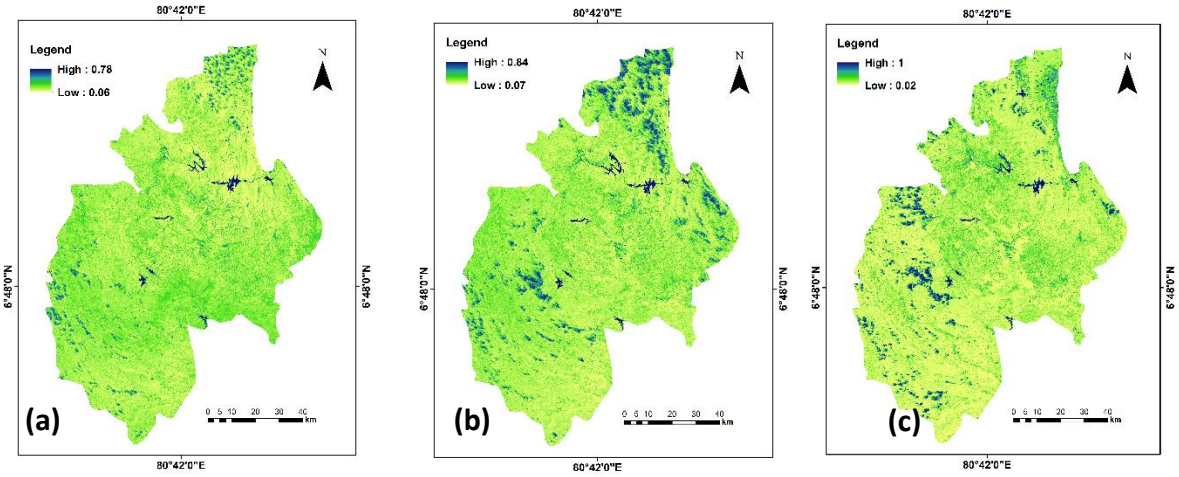

Figure 4. 4 C-Factor maps (a) 2000, (b) 2010, and (c) 2019.

Table 4. 4. The details of soil erosion classes, rates, and area distribution in the Central Highlands

Class	Soil erosion rate	Area (km^2)			Change
		2000	2010	2019	2000 -2019
Very low	<5	5494.7	5345.6	5140.3	-354.4
Low	5-10	1733.3	1569.5	1555.3	-178.1
Moderate	10-20	1831.1	1847.4	1911.2	80.2
High	20-50	1221.2	1404.3	1507.3	286.1
Very high	50<	219.7	333.2	385.9	166.3
Total land		10500.0	10500.0	10500.0	
Average annual soil erosion (t/ha/yr)		9.08	10.17	11.08	

According to the RUSLE analysis, the majority of the land areas of the Central Highlands have been subjected to soil erosion over the past two decades in the sense of ecological and economical. The analysis revealed high and very-high soil erosion classes, representing 18.04% of the total land area. The global investigation of modelling and mapping studies (GIMMS) in 1981–2003 has indicated 32.09% of the land area was under degradation in Sri Lanka (Bai et al., 2012). The higher rate of soil erosion was evident from the amount of silt piling up behind the dams across the Mahaweli River, which drains through the greater part of the Central Highlands (Khaniya et al., 2019). The soil erosion maps are illustrated in Figure 4.5.

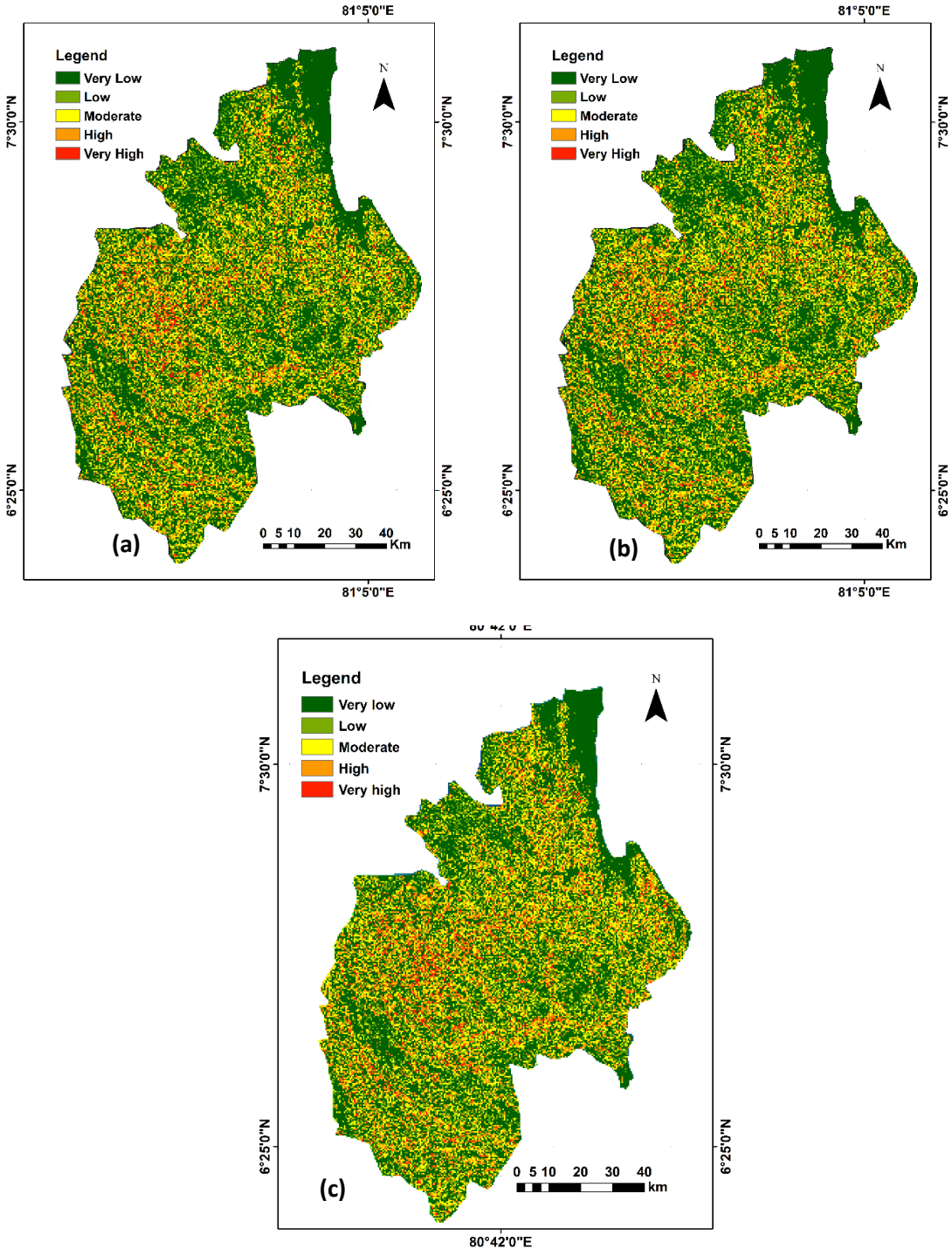

Figure 4. 5 Soil erosion map for (a) 2000, (b) 2010, and (c) 2019.

4.2.4 Soil erosion hazards in the Central Highlands

The results of the landslides frequency ratio (LFR) were utilised to evaluate soil erosion hazards in the farming systems. Table 4.5 indicates the average soil erosion rates, and soil erosion hazards levels) in each farming systems. The highest LFR values were observed

in WL2b, WL1a and IM1a. The farming systems WL2b and WL1a are situated in the Subragamuwa province of the Central Highlands. That indicates farming systems WL2b and WL1a are the most vulnerable areas for soil erosion hazards. Further analysis was carried out through a case study in Suberagamuwa province.

Table 4. 5. Details of the farming systems

No	Farming system name	Area (km2)	Average soil erosion (t/ha/yr)			Landslide frequency ratio (LFR)	Past Landslides incidence	Average RF
			2000	2010	2019			mm
1	DL1c	120.77	0.67	0.90	1.06	0	0	2032.90
2	IM1b	447.18	8.84	9.71	11.49	0.1	1	1948.17
3	IL2	679.43	5.08	5.72	6.59	0.4	6	2000.92
4	IM3b	47.80	3.62	3.51	5.49	0	3	1815.18
5	WM3b	426.87	5.88	6.62	7.97	0.5	3	1874.33
6	IL1a	27.65	5.01	6.21	6.30	0	0	2061.35
7	IU1	315.62	11.48	12.31	13.62	1.3	11	1880.55
8	IM3a	108.54	6.28	7.25	8.55	0.7	2	1760.13
9	WM3a	109.75	5.79	6.71	6.83	1	4	2068.22
10	WL2b	145.17	8.81	10.35	9.40	4.1	16	2457.09
11	WM2b	349.91	8.67	9.82	10.19	0.8	6	2213.59
12	IM3c	264.28	10.55	12.71	13.93	1.3	9	1920.65
13	IM1c	287.46	10.70	13.22	13.45	1	9	2017.28
14	IU2	420.54	10.52	11.38	13.17	0.7	9	2048.08
15	IM1a	539.01	10.29	11.36	12.72	1.7	24	1962.30
16	WM2a	194.63	13.66	15.50	17.12	1.2	5	2857.69
17	WU2b	263.52	12.51	13.82	14.16	0.9	5	2493.94
18	WL1a	1718.98	9.87	11.90	12.27	1.6	75	3516.38
19	WM1a	1010.93	13.40	15.07	15.94	0.9	26	3295.94
20	WU2a	356.28	9.11	10.12	12.22	0.4	5	2570.99
21	WU1	496.74	14.98	16.61	17.32	1.2	13	3340.70
22	IM2b	159.60	7.03	7.98	8.40	0.7	3	2141.30
23	IU3c	249.75	8.22	9.46	10.64	1.1	7	1847.07
24	WU3	293.01	10.54	11.45	12.37	0.8	6	2151.26
25	IU3e	222.22	6.93	8.19	8.85	0.8	5	1858.53
26	IU3d	73.29	11.75	12.44	15.11	1	2	2048.44
27	DL1a	3.47	1.31	1.42	1.35	0	0	2159.37
28	IU3b	124.35	7.41	8.61	9.21	0.6	2	2104.57
29	IU3a	48.16	8.79	10.35	11.75	0.8	1	1890.69
30	IM2a	281.19	7.14	8.57	8.91	0.7	6	2303.81
31	WM1b	371.18	10.91	12.51	12.80	0.9	9	2841.95
32	WL2a	274.51	7.95	9.52	9.91	0.7	5	2734.34
33	IL1c	67.38	6.50	8.22	8.38	0	0	2452.71
34	IL1b	0.89	3.35	4.36	6.68	0	0	2554.79

4.2.5. The case study on assessing soil erosion hazards in Sabaragamuwa Province

4.2.5.1. LULC change

The confusion matrix was employed to assess the overall accuracy of the image classification. The overall accuracy is 86.89% for 2000, 96.70% for 2010, and 84.4% for 2019, with Kappa coefficients of 0.84, 0.92, and 0.82, respectively. The confusion matrix between ground truth data and land-use classes for 2019 is given in Table 4.6, and respective values of commission, omission, producer accuracy and user's accuracy are given in Table 4.7.

Table 4. 6. Confusion matrix between ground truths and land-use classes.

Land-use Dataset		**Ground Truth Data**							
		A	B	C	D	E	F	G	**Total**
A	Water bodies	29		2				1	32
B	Dense forest		40				1	6	47
C	Streams	3		20					23
D	Paddy			1	29	1	1	1	33
E	Urban area			1	2	30	1		34
F	Cropping area	1	1		4	2	50	9	67
G	Less dense forest				1		6	46	53
	Total	33	41	24	36	33	59	63	289

Table 4. 7. Respective values of commission, omission, producer accuracy, and user's accuracy for classified land-use classes for 2019.

(b)	**Commission**	**Omission**	**Producer Accuracy**	**User's Accuracy**
Water bodies	9.4	12.1	87.9	90.6
Dense forest	14.9	2.4	97.6	85.1
Streams	13.0	16.7	83.3	87.0
Paddy	12.1	19.4	80.6	87.9
Urban area	11.8	9.1	90.9	88.2
Cropping area	25.4	15.3	84.7	74.6
Less dense forest	13.2	27.0	73.0	86.8

The land-use classes were categorised according to the land-use classes level-II of the Anderson classification scheme (Anderson et al., 1976), namely dense forest, less dense forest, waterbody, stream, paddy, cropping area, and urban area. Tea and rubber plantations and home gardens, as per LUPPD classification, cannot be clearly distinguished in the images; hence, they were considered as cropping areas. The processed LULC maps for 2000, 2010, and 2019 are given in Figure 4.6a–c. The respective findings from the analysis are given in Table 4.8.

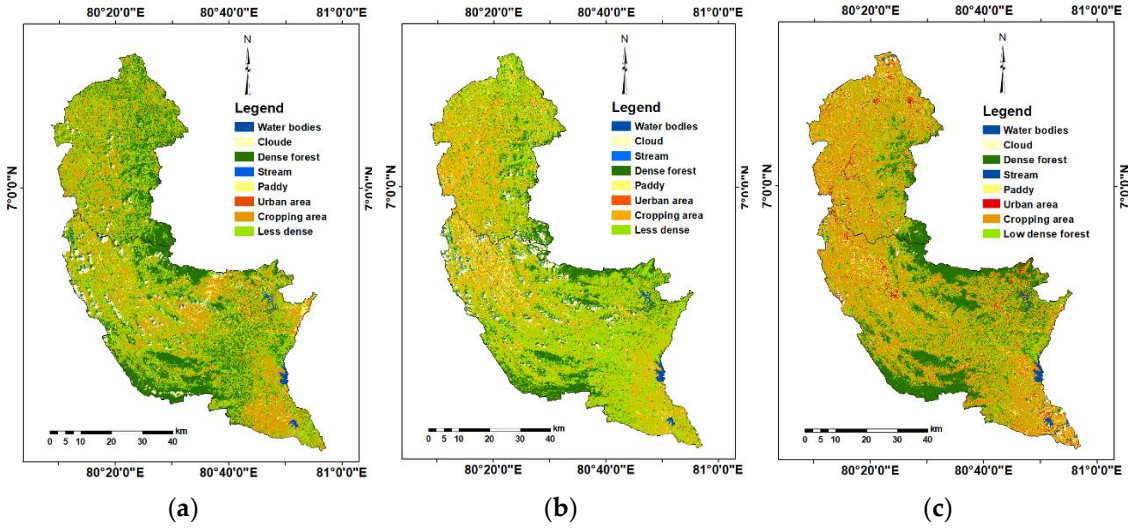

(a) (b) (c)

Figure 4. 6 Land-use land-cover (LULC) maps: (a) 2000; (b) 2010; (c) 2019.

Table 4. 8. Land-use change between 2000 and 2019.

Land use classes	2019		2010		2000		2019-2000	
	Area (km^2)	%	Area (km^2)	%	Area (km^2)	%	Area (km^2)	%
Dense forest	971.84	19.63	1064.54	21.51	1292.09	26.09	−320.25	−6.46
Less dense forest	1124.87	22.72	1930.24	39.00	1827.00	36.90	−702.13	−14.18
Cropping area	2379.23	48.05	1483.97	29.98	1490.20	30.09	889.03	17.96
Paddy	230.11	4.65	284.5	5.75	155.13	3.13	74.98	1.52
Urban area	154.9	3.13	96.21	1.94	3.21	0.06	151.69	3.07
Water bodies	24.22	0.49	26.84	0.5	23.86	0.48	0.36	0.01
Streams	34.25	0.69	45.78	0.92	59.20	1.20	−24.95	−0.51
Other (due to cloud cover)	32.42	0.65	19.5	0.39	101.15	2.04		
	4951.83	100	4951.58	100	4951.84	100		

The overall LULC change is deduced by comparison. The cropping areas and the urban areas in Sabaragamuwa Province have increased by 17.96% and 3.07%, respectively. Simultaneously, the less dense forest and the dense forest in the Province have decreased by 14.18% and 6.46%, from 2000 to 2019, respectively. Anthropogenic activities, such as the expansion of agriculture activities, urban and infrastructure development, deforestation, and abandonment of agricultural lands due to low productivity, are the likely reasons of LULC change in this period. For instance, the extent of tea plantations in Sabaragamuwa Province has increased by 58.71 km^2 from 2008 to 2015, according to the land-use statistics of LUPPD.

4.2.5.2 Soil erosion hazards in Sabaragamuwa Province

The generated slope length and steepness factor (LS-factor) map is shown in Figure 4.7a. The rainfall erosivity (R-factor) map is shown in Figure 4.7b. The soil erodibility (K-factor) map is shown in Figure 4.7c. The crop management (C-factor) map and the conservation practice (P-factor) map are shown in Figure 4.7d and Figure 4.7e, respectively. The generated soil erosion hazard map for the year 2019 can be found in Figure 4.7f.

The soil erosion hazard map of Sabaragamuwa Province (Figure 4.7f) shows 9.5% of the area in the high-erosion hazard category and 3.4% in the very-high category. This finding indicates that approximately 13% of the total land area of the Sabaragamuwa Province is highly vulnerable to soil erosion. In addition, approximately 22% of the total land area is moderately vulnerable to soil erosion. Findings further reveal the average annual soil erosion is 14.56 t ha^{-1} in the year 2000, and it has increased to 15.53 t ha^{-1} in the year 2019 (Table 4.9).

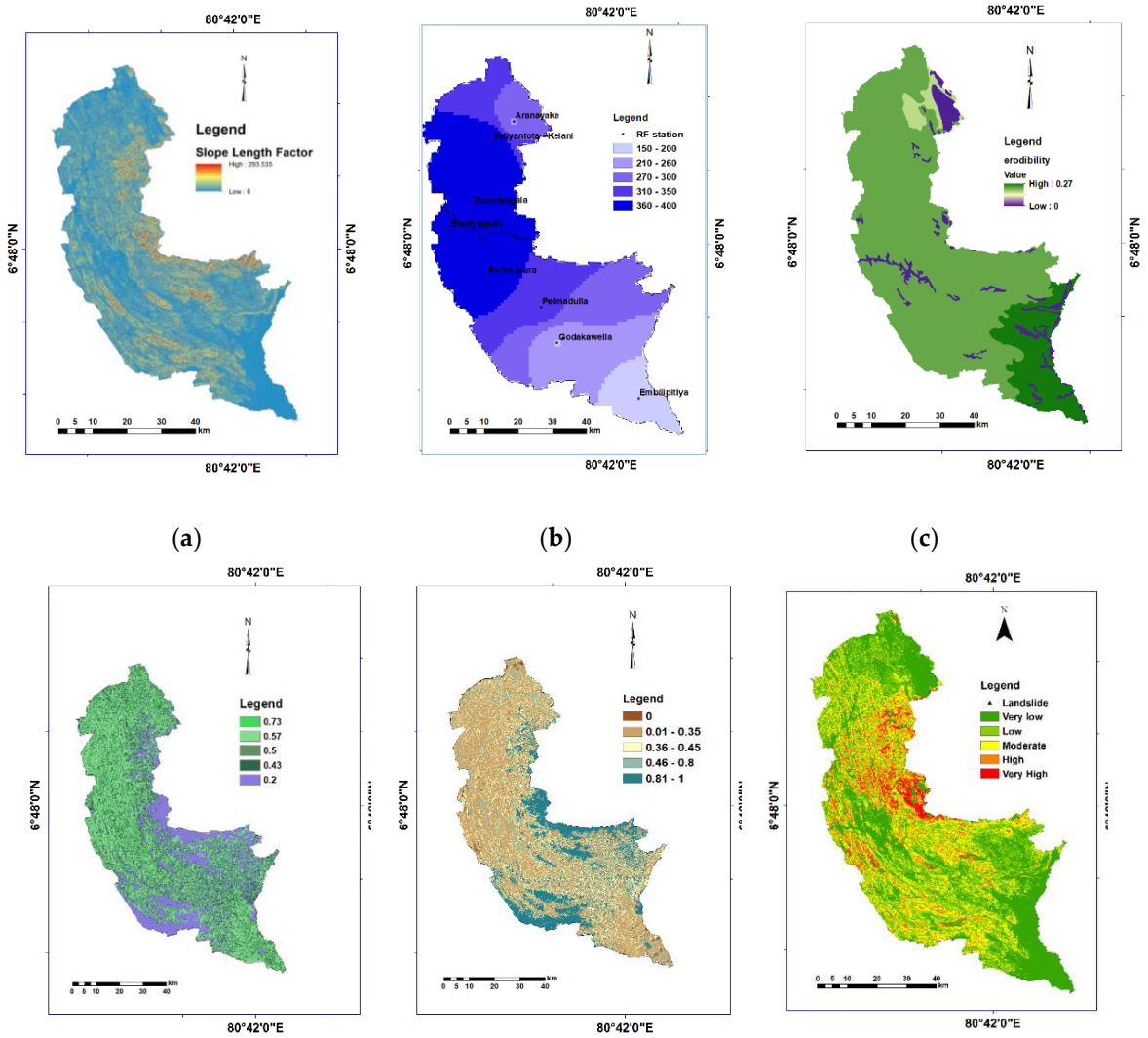

Figure 4. 7 Factor maps of Sabaragamuwa Province: (a) slope length and steepness (LS)-factor; (b) rainfall erosivity (R)-factor; (c) soil erodibility (K)-factor; (d,e) crop management (C) -factor and conservation practice (P)-factor; (f) soil erosion hazard map.

Literature shows the average soil erosion rate for a tropical region is often less than 10 t $ha^{-1}year^{-1}$ (FAO, 2019). However, findings indicate higher soil erosion rates than the average of a tropical region. The details of soil erosion category, rate, and respective land area are given in Table 4.9. Jayasinghe et al. (2017) reported that landslides frequently occur in cultivated agricultural lands with Red-Yellow Podzolic soil types and steeply dissected, hilly, and rolling terrains.

Table 4. 9. The details of soil erosion category, rates, and land area.

Category	2000			2019	
	Erosion rate	Area km^2	%	Area km^2	%
Very low	0–5	1871.69	37.797	1761.24	35.566
Low	5–10'	1479.29	29.873	1452.28	29.327
Moderate	10–20	1055.59	21.316	1095.86	22.130
High	20–50	442.47	8.935	472.12	9.534
Very high	>50	102.96	2.079	170.5	3.443
		4952.00	100.00	4952.00	100.00
Average annual soil erosion		14.56 tons/ha/year		15.53 tons/ha/year	

4.2.5.3. Land-use change and its correlation with landslides

This study estimated the LFR for each land-use class in 2019. The LFR of each land-use class is provided in Table 4.10. The higher LFR (>1) was observed in a less dense forest area, cropping area, streams, and urban areas. The findings indicate a higher correlation between these land-use classes and landslide incidents (Shahabi and Hashim, 2015; Meena et al., 2019).

Table 4. 10. The landslide frequency ratio for each land-use type.

Land-Use Class	Area (Km^2)	Percentage	No of Landslides	Percentage	LFR
Dense forest area	971.84	19.63	14	11.02	0.56
Water bodies	24.22	0.49	0	0.00	0.00
Streams	34.25	0.69	1	0.79	1.14
Cropping area	2379.23	48.05	71	55.91	1.16
Less dense forest	1124.87	22.72	34	26.77	1.18
Urban area	154.90	3.13	4	3.15	1.01
Paddy area	230.11	4.65	2	1.57	0.34

The current study considered RDZ as an important hydrological unit for soil conservation. Hence, this case study investigated the land-use change at RDZ level. The prominent land-use change in each RDZ was calculated to find out the correlation between land-use change and landslide incidents. The land-use change in each RDZ is provided in Table 4.11.

Table 4. 11. The major land-use change in each zone.

River distribution zone	Dense Forest	Water bodies	Stream	Cropping area	Less Dense	Urban Area	Paddy	Sign of land-use change
A-1	-144.23	-0.11	2.97	165.79	-103.17	29.41	46.84	Cropping area, Dense forest
A-2	-12.14	-0.01	-0.88	29.66	-23.21	2.55	6.22	Cropping area, Less dense forest
A-3	-67.15	-1.22	-1.13	112.81	-65.10	18.69	12.97	Cropping area, Dense forest
A-4	21.04	-0.59	-22.63	212.38	-181.00	33.55	-10.79	Cropping area, Less dense
A-5	79.96	-0.29	-4.42	-15.31	-39.32	14.17	-32.94	Dense forest, Less dense
A-6	-74.95	2.37	0.06	109.10	-65.63	15.19	11.12	Cropping area, Dense forest
A-7	-20.14	0.14	3.76	20.85	-40.48	13.02	15.86	Less dense forest, Cropping area,
A-8	0.46	0.02	-1.81	63.15	-54.43	4.14	-1.59	Cropping area, Less dense forest
A-9	-101.96	-0.03	-1.02	184.88	-122.93	19.07	27.19	Cropping area, Less dense forest

The most prominent land-use changes of RDZs are observed in cropping areas and less dense forest classes. As revealed in Table 4.10, LFR is greater than 1 in cropping area (LFR=1.16) and less dense forest classes (LFR=1.18). The LFR is greater than 1, indicating a higher correlation between land-use change and landslide incidents (Pradhan and Lee, 2010a; Meena et al., 2019). Furthermore, Figure 4.8 shows the percentage of land-use change and LFR over each RDZ. The following RDZs, A-2, A-3, A-4, and A-9, show that the LFR is greater than 1. Overall, these results indicate that increasing cropping area may contribute to inducing the landslide occurrence at RDZs (Figure 4.8).

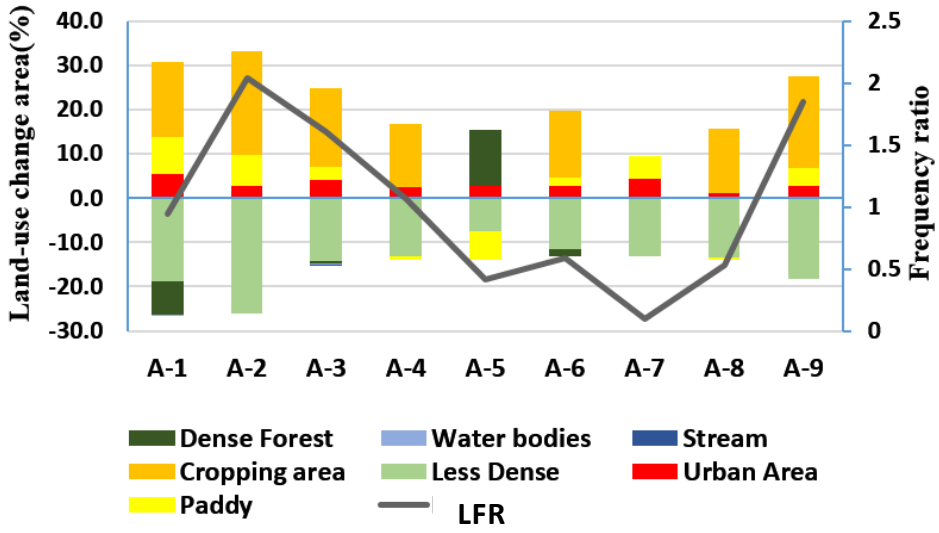

Figure 4. 8 The percentage of land-use change and landslide frequency ratio over the river distribution zones (RDZs).

4.2.5.4. Soil erosion hazard and its correlation with landslides

Areas highly susceptible to soil erosion need to be identified and prioritized for the implementation of soil conservation practices. A map of the RDZs is presented in Figure 4.9a. A landslide inventory map was also developed (Figure 4.9b). The soil erosion hazard map was overlaid with the landslide inventory and RDZ map, as shown in Figure 4.9c. Then, from Figure 4.9c, the areas under the different classes of erosion hazard were computed for each RDZ to obtain the corresponding landslide frequency ratio.

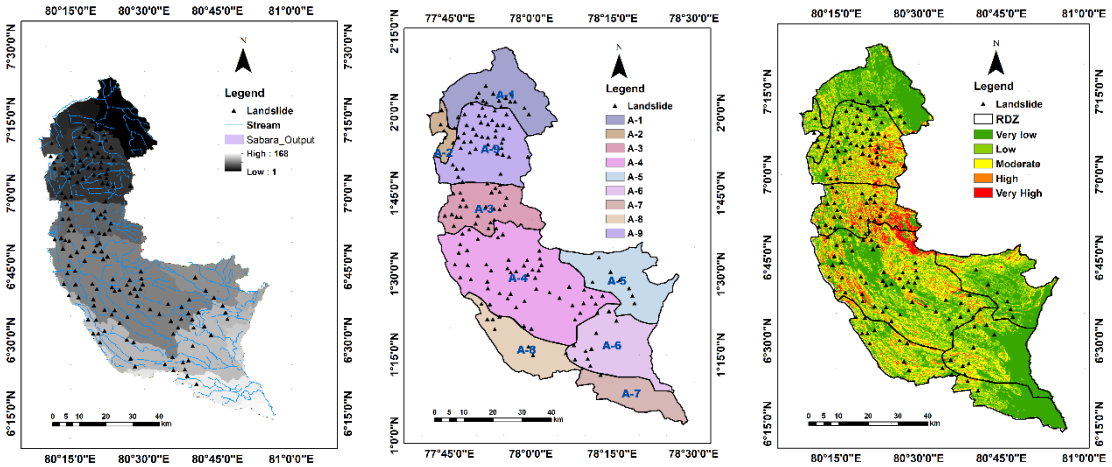

(a) (b) (c)

Figure 4. 9 (a) River distribution zones map; (b) landslide inventory map; (c) soil erosion hazard map with landslide locations.

The soil erosion hazard class of each RDZ is correlated with the LFR as a method of statistical analysis. The utilization of the frequency ratio is based on the observed relationships between the distribution of landslides and soil erosion hazard classes to reveal the correlation between these two related phenomena in the study area (Das et al., 2020). The LFR was calculated from the analysis of the land extent of the RDZ and the number of landslide incidents. The LFRs of RDZs are given in Table 4.12.

Table 4. 12. Landslide frequency ratios of the RDZ.

ID	RDZ Code	Name of the RDZ	Extent (km^2)	Extent % (a)	No of Landslides	Landslide Occurrence % (b)	Frequency Ratio (b/a)
1	A-1	Maha Oya	549.02	11.09	17	10.43	0.94
2	A-2	Athtanagalu Oya	89.19	1.80	6	3.68	2.04
3	A-3	Kalani River-south	453.80	9.16	24	14.72	1.61
4	A-4	Kalu River	1388.01	28.03	49	30.06	1.07
5	A-5	Weli Oya	522.79	10.56	7	4.29	0.41
6	A-6	Welawe River-north	565.69	11.42	11	6.75	0.59
7	A-7	Welawe River-south	306.18	6.18	1	0.61	0.10
8	A-8	Kuda Oya	405.04	8.18	7	4.29	0.53
9	A-9	Kalani River-north	672.44	13.58	41	25.15	1.85
	Total		4952.16	100.00	163		

The LFR in each of the RDZ was plotted to examine their relationships. Figure 4.10a shows the distribution of the LFRs amongst the RDZs. The extent of the soil erosion hazard classes was computed for each RDZ. The soil erosion hazard classes were plotted against the extent of each RDZ in percentages based on the computed values. The plot output is given in Figure 4.10b.

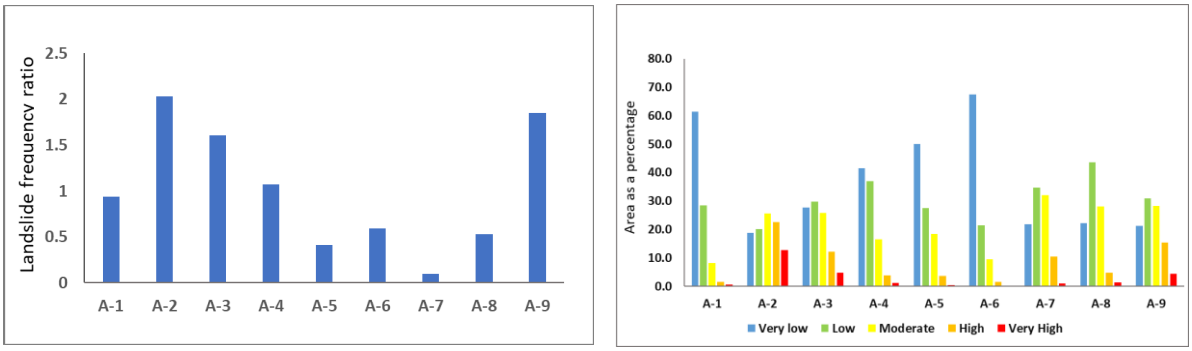

(a) (b)

Figure 4. 10 (a) Landslide frequency ratio of each RDZ; (b) the area covered by soil erosion hazard classes of each RDZ.

As shown in Figure 4.10a, the highest landslide frequency ratios, with values near 2, are for A-2, A-9, and A-3. The land-use class of these RDZs is prominently a cropping area (Table 4.10). The highest percentage extent of 'high' and 'very-high' soil erosion categories fall within A-2, A-3, and A-9 RDZs (Figure 4.10b). Pradhan et al. (2012) reported a rise in LFR for areas in the 'high' and 'very-high' soil erosion classes; the current study is in line with the previous study. They also revealed that if the landslide frequency ratio is greater than 2, more landslides are likely to occur.

Other studies have shown that a few of the critical areas are responsible for the heavy-load sediment yields in the watersheds (Hewawasam and Illangasinghe, 2015). Hence, priority should be given to RDZs with high categories of soil erosion hazards for conservation, as these RDZs can significantly reduce the total sediment yield. The priority rankings of the RDZs were based on LFR, average soil erosion rate, and area of land-use change. As shown in Figures 4.8 and 4.10a,b and Table 4.13, land-use change, the values of LFR, and soil erosion rate is ranging from high to very high for RDZs of A-3 (Kelani River-south), A-2 (Attenagalu Oya), and A-9 (Kelani River-north). Hence, A-2, A-3, and A-9 are the priority RDZs for soil conservation. The list of prioritized RDZs in Sabaragamuwa Province for soil conservation is shown in Table 4.13.

Table 4. 13. Prioritization of RDZ in Sabaragamuwa Province.

RDZ Code	Name of RDZ	Maximum Elevation (m)	Landslide Frequency Ratio	Sign of Land-Use Change	Average Erosion Rate (t/ha/yr.)	Priority
A-1	Maha Oya	1023.64	0.94	Cropping area, less dense forest	7.7	5
A-2	Athtanagalu Oya	395.64	2.04	Cropping area, less dense forest	27.5	1
A-3	Kelani River- south	1906.15	1.61	Cropping area, dense forest	18.9	2
A-4	Kalu River	2057.9	1.07	Cropping area, less dense	11.9	3
A-5	Weli Oya	2177.38	0.41	Dense forest, less dense	10.6	5
A-6	Welawe River- north	1341.45	0.59	Cropping area, dense forest	6.6	6
A-7	Welawe River- south	1320	0.1	Less dense forest, cropping area	17.8	5
A-8	Kuda Oya	1354.13	0.53	Cropping area, urban area	15.9	4
A-9	Kelani River- north	1299.02	1.85	Cropping area, paddy area	20.6	1

This study, evaluated LULC change, soil erosion hazard, and their associated dynamics of Sabaragamuwa Province using the RUSLE model combined with a GIS environment. The study employed a new approach by combining the landslide frequency ratio method, soil erosion severity, and land-use change assessments. Results reveal that nearly 13% of the total land area of the province is highly vulnerable to soil erosion and around 22% of the total land area is moderately vulnerable to soil erosion. Findings further indicate the average soil erosion rates in years 2000 and 2019 are higher than the average of tropical countries (<10t $ha^{-1}year^{-1}$) (Dissanayake et al., 2019). The assessment of LULC change shows a higher correlation between land-use classes and landslide incidents. In addition, RDZs of A-2, A-3, and A-9 reported the highest landslide frequency ratios. Overall, these results are in line with previous studies (Perera et al., 2018; Fayas et al., 2019). Landslides frequently occur in Sri Lanka. Approximately 30.7% of its total land area is highly susceptible to landslides (Hewawasam, 2010). The Sabaragamuwa Province has been declared as one of the landslide-prone areas in the country (Perera et al., 2019). Hewawasam (2010) and earlier researches reported that 35%, 20%, 10%, 13%, and 8% of the landslides occurred in tea, rubber, coconut, paddy, and vegetable cultivated lands,

respectively, by analysing 200 landslides in the Central Highlands. The present study shows a change in land-use particularly the increase in cropping areas, including tea and rubber plantations, while decreasing the dense and less dense forest cover in Sabaragamuwa Province from 2000 to 2019. Hence, increasing cropping area may contribute to inducing landslide occurrence at RDZs. This rapid change of land-use in sloping land areas may affect erosion hazard levels and landslide vulnerability.

The soil may be permanently damaged due to inappropriate land levelling, causing a decrease in soil quality during extensive agricultural activities. In most cases, land levelling results in increased surface and subsurface soil erosion, due to the soil erodibility of newly exposed subsoil. In addition, land levelling may increase the landslide susceptibility of sloping lands (Poesen, 2018). Hence, implementing soil conservation strategies with appropriate land-use planning practices is important to reduce erosion hazards. Dissanayake et al. (2019) have also claimed a similar result and recommend soil conservation on agricultural lands to reduce soil erosion for food security. Thereby, priority should be given to RDZs of A-2, A-3, and A-9 (these RDZs are in WL1a and WL2b farming systems) for soil conservation. This case study considered RDZ a significantly important hydrological unit for soil conservation. In addition, socio-economic factors, such as land ownership problems and the high cost of land preparation, affect farmers who seldom use soil conservation practices in hilly areas. Therefore, a sustainable land-use management system should consider soft engineering conservation and management practices, such as ecological farming practices, planning, and prioritizing areas for soil conservation to reduce soil erosion while reducing the risk of landslide vulnerability. Proper identification of land-use systems, appropriate soil conservation practices and techniques can help to minimize soil erosion. Furthermore, high-intensity tropical rainfall within a short duration due to the effect of climate variation is also another influential factor of soil erosion hazards. Assessments on soil erosion hazards under the impact of rainfall variation in the Central Highlands are recommended to study further.

4.2.6 Crop diversity change in the farming systems

Vegetation indices (NDVI, EVI and SAVI) were derived from Landsat and MODIS data to examine the crop diversity change in the farming systems. Based on the results of vegetation indices, the NDVI, EVI and SAVI show an overall increasing trend over the years in the Central Highlands. Figure 4.11 shows vegetation indices (VI) distribution over the period and respective images (Figure 4.12 - 4.14) derived from Landsat imagery for the NDVI, EVI and SAVI.

4.2.6.1 Landsat data analysis

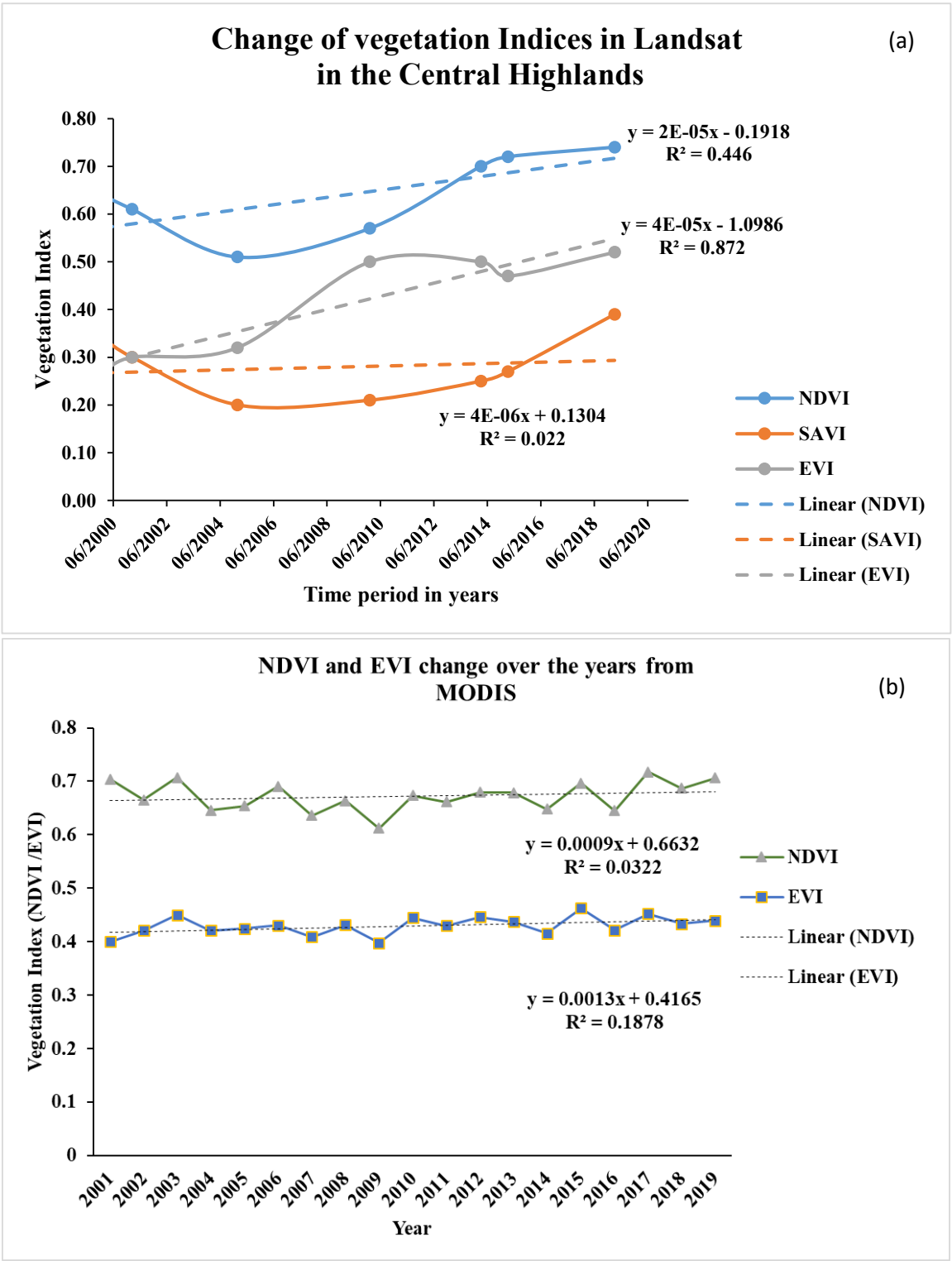

Figure 4. 11 (a) NDVI, EVI and SAVI distribution (b) MODIS derived over the period in the Central Highlands

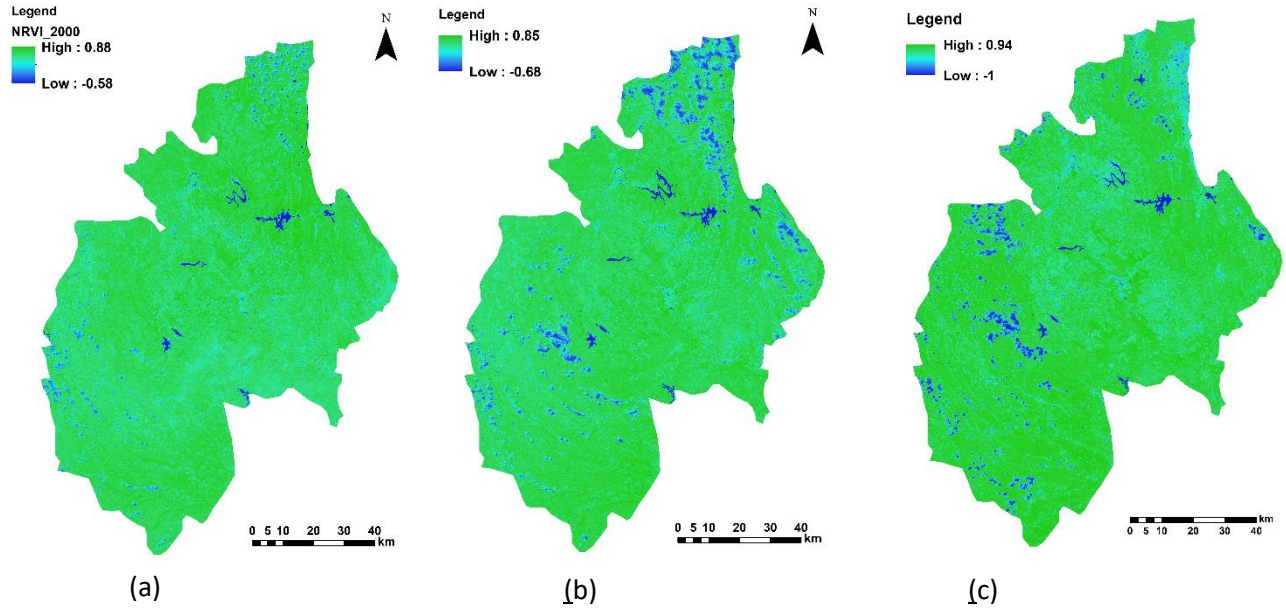

(a) (b) (c)

Figure 4. 12 NDVI maps in the Central Highlands for (a) 2000 (b) 2010 and (c) 2019.

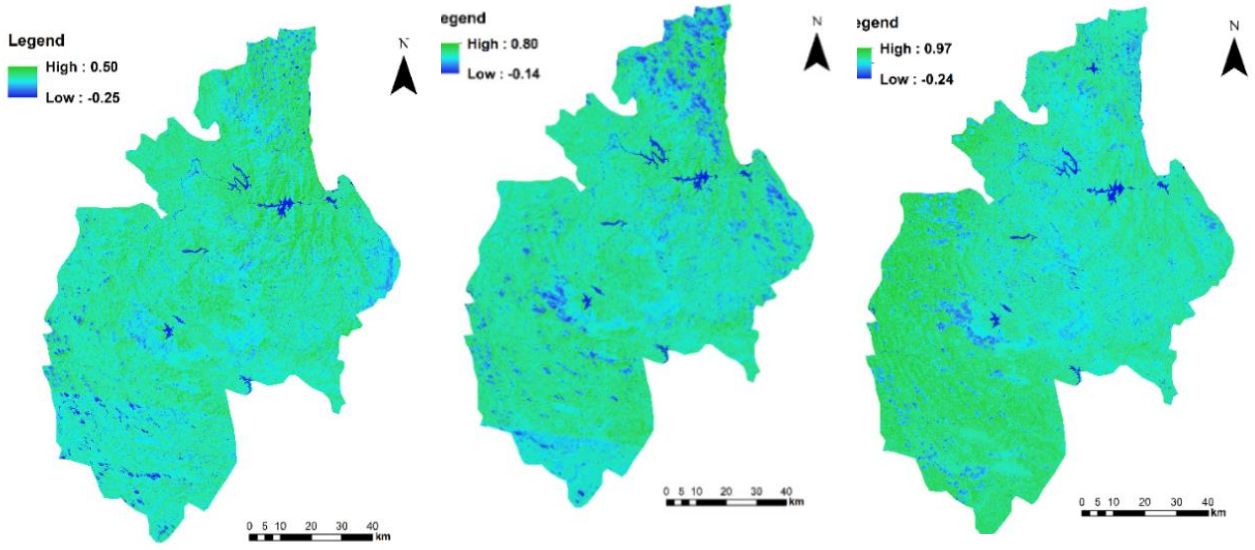

(a) (b) (c)

Figure 4. 13 EVI maps for the Central Highlands (a) 2000 (b) 2010 and (c) 2019.

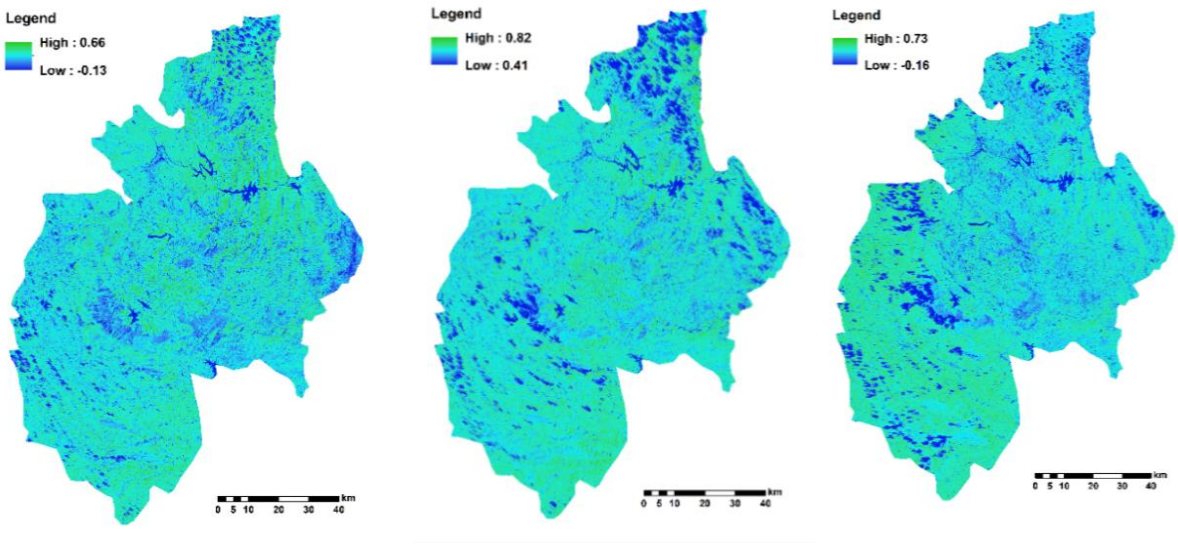

(a) (b) (c)

Figure 4. 14 SAVI maps for the Central Highlands (a) 2000 (b) 2010 and (c) 2019.

In this study, Landsat data provide the NDVI, EVI and SAVI values that demonstrate the combined effect of land-uses in the Central Highlands: dense forest, open forest, agriculture, water bodies and urban/built-up areas. Although Landsat is generally adequate for crop diversity analysis (Nagendra et al., 2010), cloud cover is one of the major limiting factors for the study area (Nay et al., 2018), especially to obtain several images throughout the year. Seasonal variation from the VI could not be observed from fewer satellite images.

Nagendra et al. (2010) claimed that Landsat imagery is more suitable for vegetation diversity assessment. They found medium-resolution Landsat ETM+ (30m) correlates stronger with high-resolution IKONOS imagery (4 m) with plant diversity in a dry tropical forest. The MODIS-derived variables have also shown the ability to predict plant species richness at the regional level (John et al., 2008). In addition, MODIS productivity estimates (NDVI/EVI/GPP) are readily available online and provide global coverage (Huete et al., 2002). The MODIS vegetation index products are generated by compiling daily data every 16 days, resulting in 23 composites per year and avoiding cloud cover and other effects (Huete et al., 2002). Hence, atmospherically corrected, Landsat and Moderate Resolution Imaging Spectroradiometer (MODIS) -250m 16 days' products (MODIS-MOD13Q1) were used for time series analysis of crop diversity from the years

2001–2019 (LPDAAC, 2021). However, spatial resolution may affect on crop diversity change.

4.2.6.2 MODIS data analysis

Vegetation indices (NDVI and EVI) were derived from MODIS data shown in Figure 4.15. Based on the results of vegetation indices, the NDVI and EVI show an overall increasing trend over the years. Figure 4.16 shows the vegetation indices (VI) distribution over the period derived from MODIS imagery and distribution over the year in three farming systems of the NDVI and EVI (Figure 4.17- 4.19).

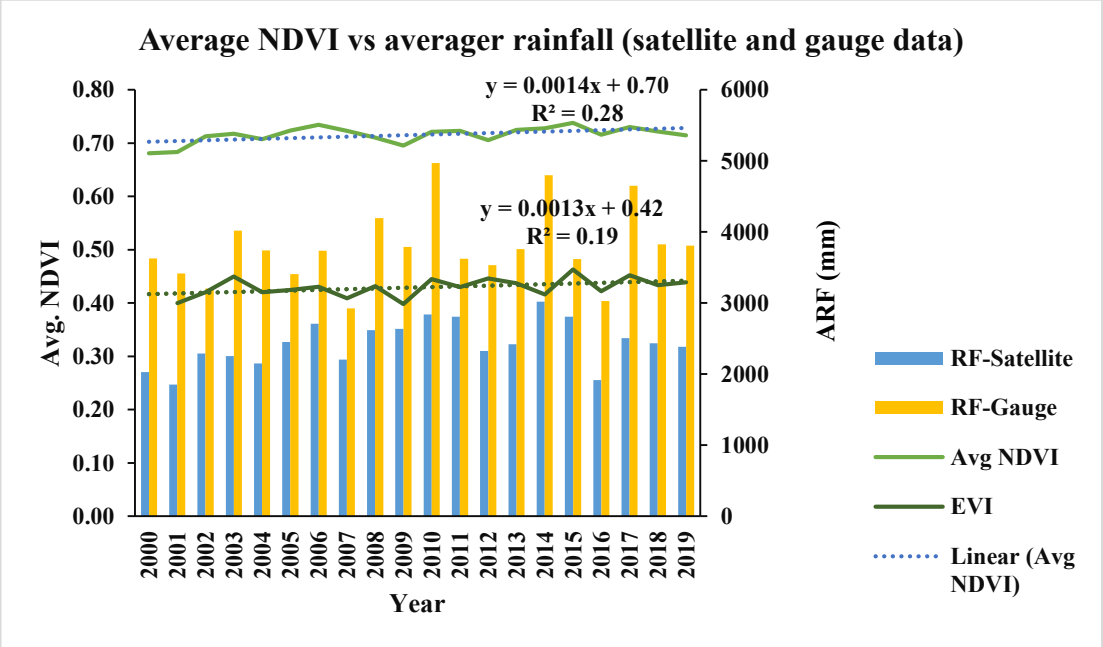

Figure 4. 15 MODIS-derived: NDVI and EVI distribution over the period with annual average rainfall (ARF- satellite and gauge) in Ratnapura area (WL1a).

For further analysis of crop diversity in farming systems, three case studies (in 03 farming systems) were conducted. From the analysis of three case studies, a similar pattern of NDVI and EVI variation could be observed over the years (Figure 4.17-4.19). Further to this, the increasing trend of NDVI and EVI was greater than SAVI. Researchers also observed similar trends in other regions (Sarmah et al., 2018; Liu et al., 2018).

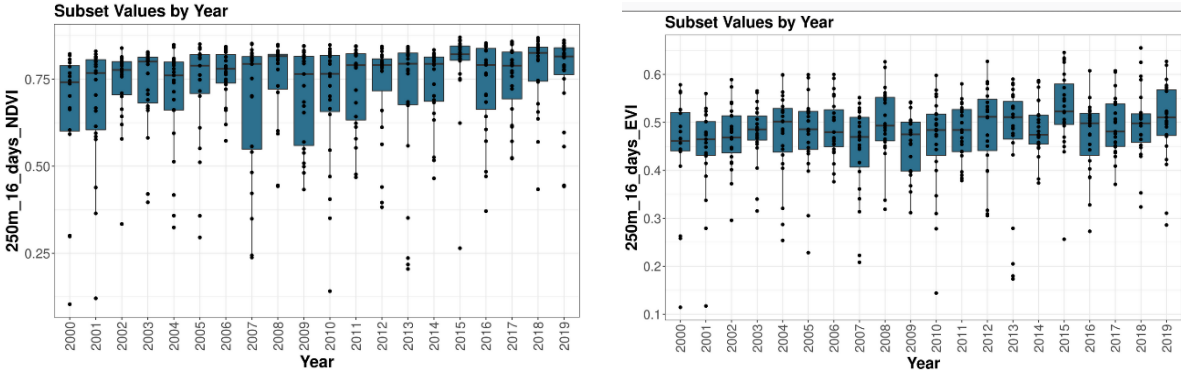

Figure 4. 16 MODIS (a) NDVI (b) EVI indices distribution from 2000 to 2019.

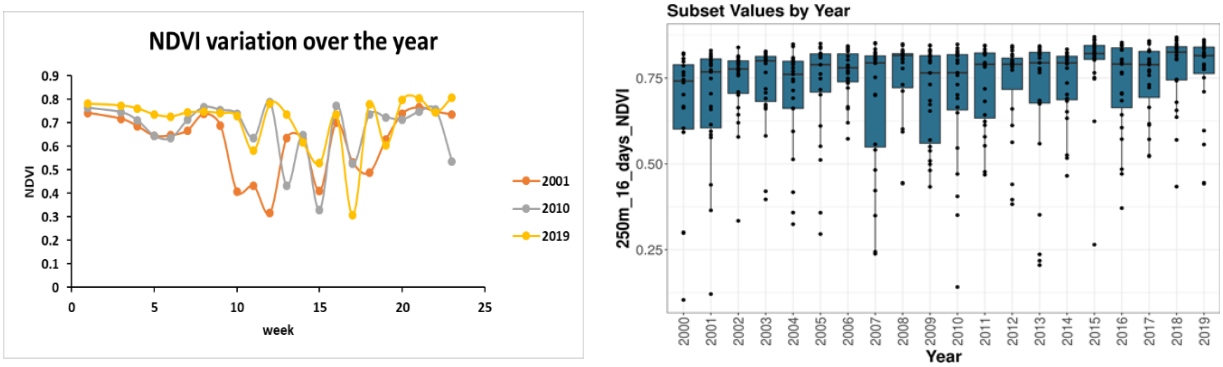

Figure 4. 17 NDVI values (within the year and over the years) for WM1a farming system.

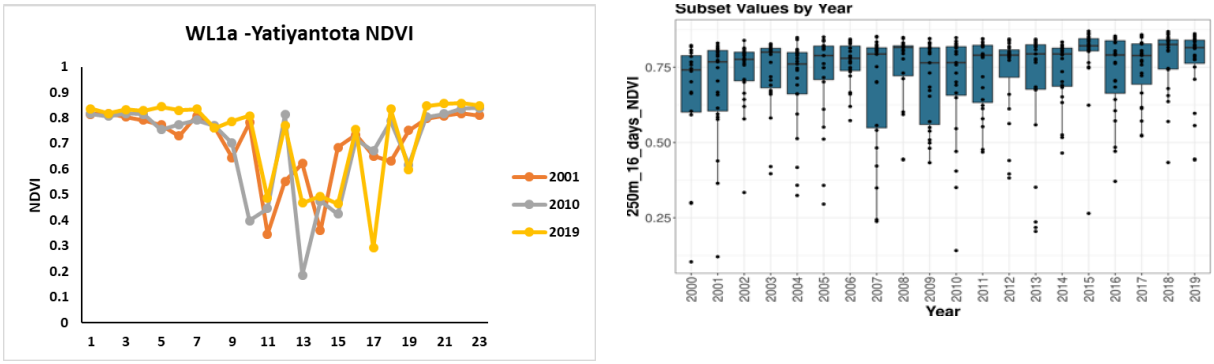

Figure 4. 18 NDVI values (within the year and over the years) for WL1a farming system.

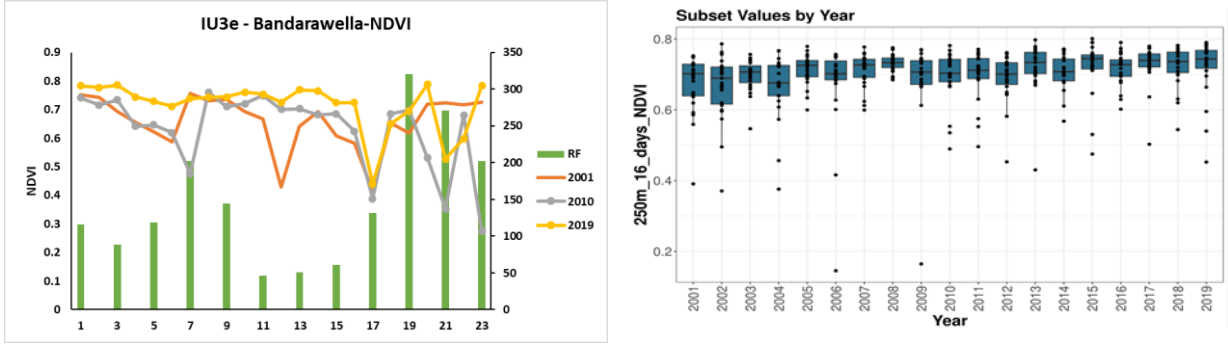

Figure 4. 19 NDVI values (within the year and over the years) for IU3e farming system.

NDVI is closely related to net and gross primary productivity. NDVI strongly correlates with plant biomass and net primary productivity (NPP), which is the difference between carbon fixed by photosynthesis and carbon lost to autotrophic respiration (Evans and Geerken, 2004). The MODIS-derived GPP and EVI provide reasonable estimates of productivity in the forest and grassland biomes (Waring et al., 2006). The MODIS derived NDVI and EVI values are positively correlated with NPP (0.76 and 0.53). Earlier research has revealed a positive relationship between species richness and productivity (Fensholt et al., 2013), although the relationship may differ among ecosystems and be dependent on spatial scales. Therefore, increasing trends in vegetation indices may indicate increasing heterogeneity or species diversity. Hence, this study further analysed crop diversity and evenness using the Shannon diversity index derived from MODIS data.

The Shannon diversity index of these three case studies shows some change over the period (Table 4.14). However, the most prominent change was observed in the farming system of WL1a. The richness and evenness have decreased in WL1a from 2000 to 2019. The evenness values have changed on WM1a in this period. Nagendra (2002) described landscape diversity as evaluating richness and evenness in the context of measuring diversity. Richness refers to the number of different species (land cover types) in the landscape, and evenness refers to the relative percentage of land distributed amongst these different cover types. The reasons for these changes would be land fragmentation, land degradation, land-use change, and landslides during this period.

Table 4. 14. Details of Shannon index- richness and evenness during the period.

Year	Case study 1-WL1a (6° 65', 80° 39')		Case study 2- WM1a (7° 06', 80° 48')		Case study 3- IU3a (6° 79', 80° 96')	
	Richness	**Evenness**	**Richness**	**Evenness**	**Richness**	**Evenness**
2000	5	0.45	2	0.69	4	0.83
2001	5	0.45	2	0.65	4	0.83
2002	3	0.41	2	0.59	4	0.83
2003	3	0.41	2	0.59	4	0.83
2004	3	0.41	2	0.66	4	0.83
2005	3	0.40	2	0.59	4	0.83
2006	3	0.40	2	0.59	4	0.83
2007	3	0.40	2	0.63	4	0.83
2008	3	0.40	2	0.63	4	0.83
2009	3	0.41	2	0.63	4	0.83
2010	3	0.41	2	0.63	4	0.83
2011	3	0.41	2	0.63	4	0.83
2012	3	0.41	2	0.63	4	0.83
2013	3	0.41	2	0.65	4	0.83
2014	3	0.41	2	0.65	4	0.83
2015	3	0.41	2	0.63	4	0.83
2016	3	0.41	2	0.63	4	0.83
2017	3	0.41	2	0.61	4	0.83
2018	3	0.41	2	0.65	4	0.83
2019	3	0.41	2	0.69	4	0.83

4.2.6.3 Vegetation indices and rainfall

NDVI and EVI relationships between rainfalls were also observed. It is somewhat surprising to note a weak correlation between NDVI and rainfall (r = 0.22). However, there is a moderate positive correlation between EVI and rainfall (r = 0.45) (Table 4.15) and KGE index in Table 4.16. The correlation between NDVI and EVI was observed (r = 0.36). Pau et al. (2012) indicated that precipitation and structural complexity strongly affected the correlation between the NDVI and plant species. Precipitation has a consistent direct effect on the NDVI and species richness. However, structural complexity has strong direct and indirect effects on the NDVI. The increase in rainfall would enhance the growth of weeds and crop growth in farming systems. These may be reasons for the increase in NDVI value in the study. The effect of rainfall can be normalized by employing rain use efficiency (RUE). Researchers previously highlighted that the RUE

index identifies land degradation that is independent of rainfall (Wessels et al., 2008; Prince et al., 1998).

Table 4. 15. The Pearson's correlation matrix.

	Mean soil erosion	**Mean NDVI**	**Mean EVI**	**Mean erosivity**	**Landslide frequency ratio**
Mean Soil erosion	1	0.158	-0.211	.395*	.416*
Mean NDVI	0.158	1	.368*	0.221	0.031
Mean EVI	-0.211	.368*	1	.454**	0.252
Mean erosivity	.395*	0.221	.454**	1	.219
Landslides Frequency Ratio	.416*	0.031	0.252	.219	1

*. Correlation is significant at the 0.05 level (2-tailed).
**. Correlation is significant at the 0.01 level (2-tailed).

Table 4. 16. The KGE index for NDVI and rainfall.

	r	**β**	**γ**	**KGE**
NDVI vales and satellite based rainfall	0.611855	0.000294	0.162494	-0.24639
NDVI vales and ground-based rainfall	0.154223	0.002259	0.00225862	-0.64611

Santos et al. (2018) and (Pour et al., 2020) found KGE values range between $-\infty$ and 1. When the value of KGE reaches 1 indicates a perfect correlation.

This study estimated the ratio between VI and rainfall in the farming systems of the three case studies. The time series analysis was executed from 2000 to 2019 to normalize the VI for the influence of rainfall. This is known as rain-use efficiency (RUE). The temporal change of RUE is a good indicator to detect land degradation. This study examined the correlation between RUE and rainfall. The ratio between RUE and rainfall can be found in (Table 4.17).

Table 4. 17. The vegetation indices and rainfall in three farming systems.

Farming system	Variables	Slope	Intercept	R^2
WL1a	NDVI- RF	0.00009	8.20	0.023
	EVI- RF	183.43	2749.1	0.005
WM1a	NDVI- RF	0.0002	8.11	0.028
	EVI- RF	224.6	2499.3	0.005
IU3e	NDVI- RF	0.0002	8.1145	0.028
	EVI- RF	495.56	1080.9	0.238

There is a strong negative correlation between RUE and rainfall (r = -0.94, standard deviation = 0.001). Further to this, the coefficient of determination (R^2) was estimated to find the relationship between RUE and rainfall. The results show there is a strong negative relationship between RUE and rainfall in three case studies: WL1a (R^2 =0.88), WM1a (R^2 =0.78), and IU3e (R^2 =0.86) (Figure 4.20).

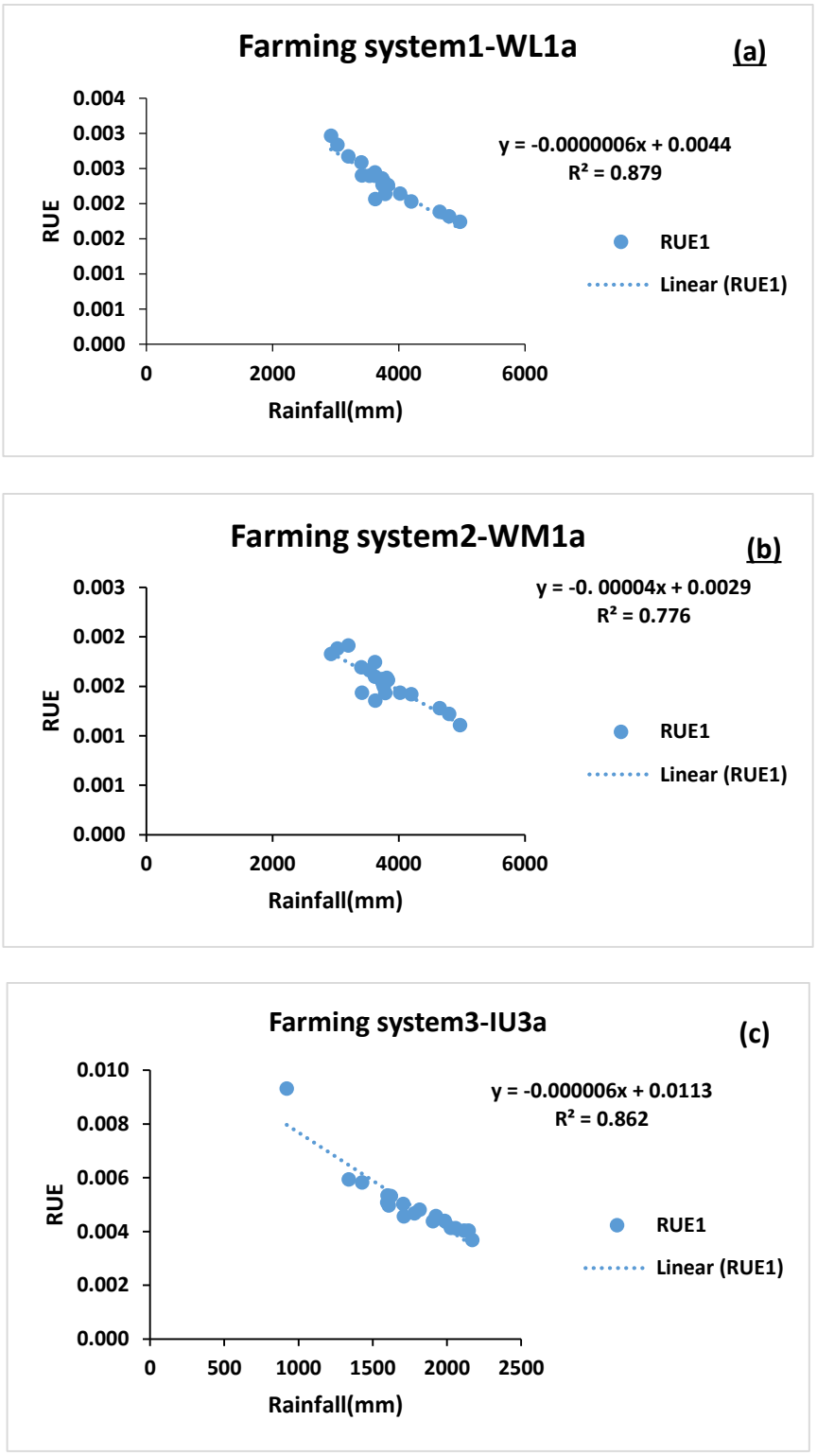

Figure 4. 20 RUE variation with rainfall (a) WL1a (b) WM1a and (c) IU3e farming systems.

4.2.6.4 Crop diversity change and soil erosion hazards

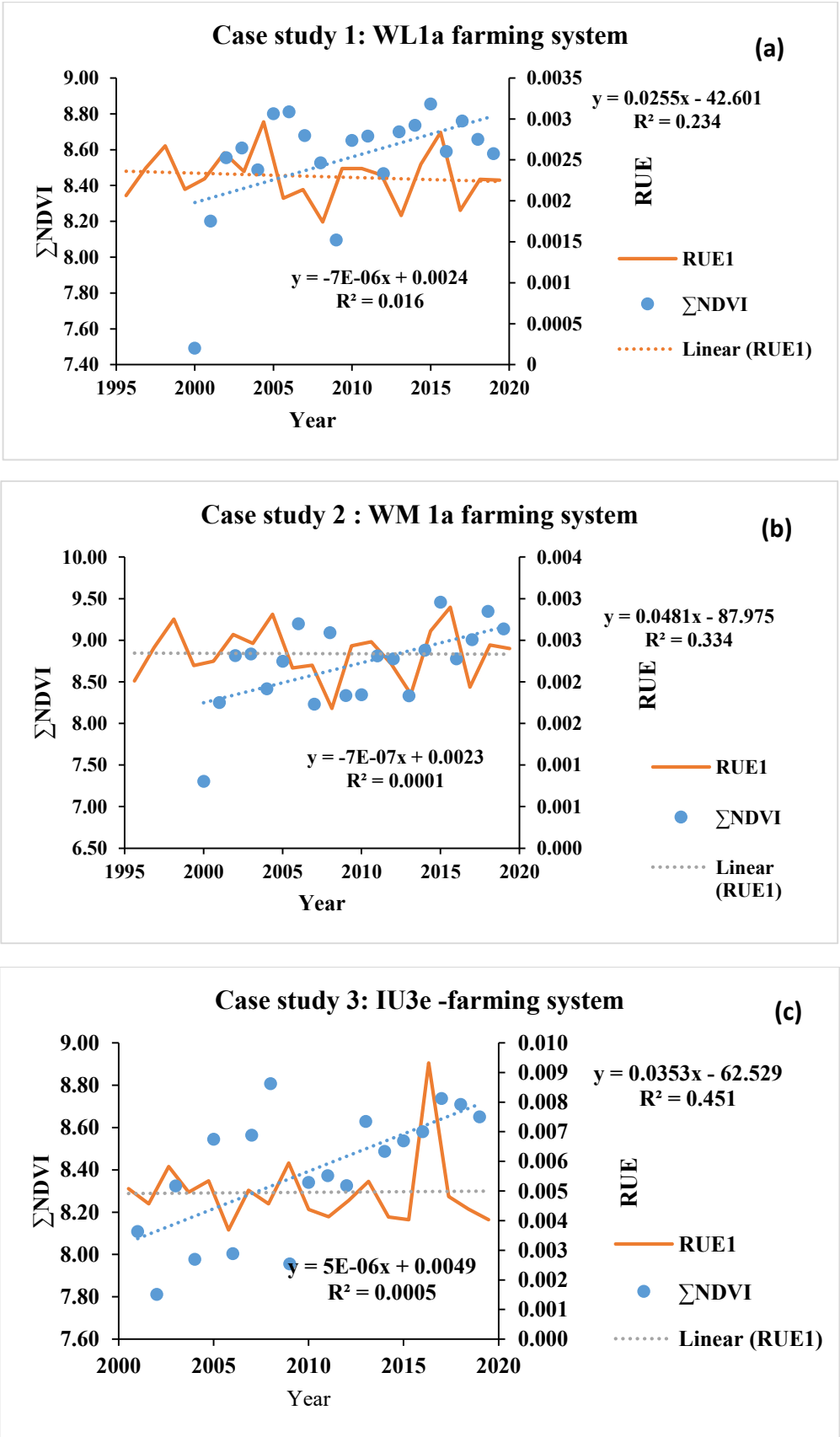

Figur 4. 21 The trend of RUE in three farming systems: (a) WL1a, (b) WM1a, and (c) IU3e farming systems.

Figure 4.21 shows the ΣNDVI and RUE variations for the three case studies. The farming systems WL1a and WM1a showed a negative trend of the RUE index, while IU3e showed a positive trend over the years. A similar trend of EVI based RUE (ΣEVI/rainfall) was also observed in farming systems WL1a and WM1a (Table 4.18). The areas with a negative trend of RUE indicated land degradation. It is also noteworthy that these farming systems receive the highest rainfall compared to the IU3e. The positive trend of RUE in the IU3e farming system indicates the changes in increasing land cover or land conditions during the study period. The negative trend may occur due to land-use changes, which reduce NDVI values. Landmann and Dubovyk (2014) have observed a negative NDVI trend that indicates a gradual decline of vegetation cover or sudden land transformations such as deforestation.

RESTREND index can be used to partition the soil erosion due to human and climate-induced land degradation. The time-series analysis of MODIS VI was employed to obtain the RESTREND. The RESTREND of the three farming systems has shown a positive slope over the years. The farming system WL1a showed a slightly positive trend of RESTREND (R^2=0.23). However, the farming systems WM1a and IU3e reported a stronger positive trend of RESTREND R^2=0.33 and R^2=0.45, respectively. A similar trend of the EVI based RESTREND was also found in the same farming systems (Table 4.18).

Table 4. 18. Details of R^2 of EVI and NDVI for RUE and RESTREND values.

Farming system	Index	Slope	Intercept	R^2
WL1a	RUE (NDVI)	-0.000007	0.0024	0.01
	RUE (EVI)	-0.000006	0.0016	0.03
	RESTREND (NDVI)	0.0255	51.101	0.23
	RESTREND (EVI)	0.009	18.498	0.06
WM1a	RUE (NDVI)	-0.0000007	0.0023	0.0001
	RUE (EVI)	-0.0000002	0.0015	0.00002
	RESTREND (NDVI)	0.0481	96.675	0.33
	RESTREND (EVI)	0.0328	65.862	0.28
IU3e	RUE (NDVI)	0.000005	0.0049	0.0005
	RUE (EVI)	0.000006	0.0033	0.002
	RESTREND (NDVI)	0.0353	70.919	0.45
	RESTREND (EVI)	0.0324	65.027	0.39

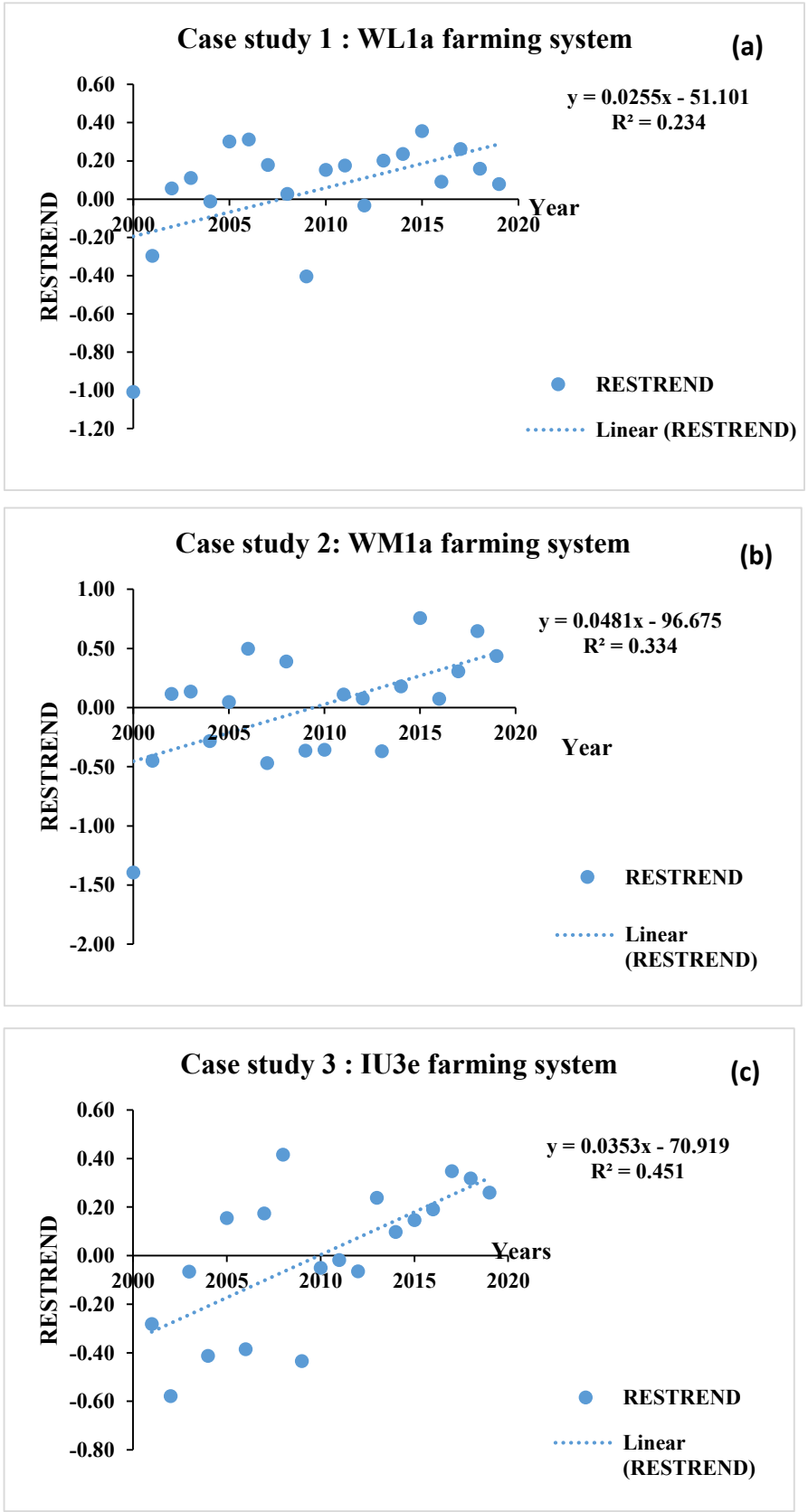

Figure 4. 22 RESTREND over the years: (a) WM1a, (b) WL1a, and (c) IU3e farming systems

The NDVI, EVI and standard deviations of GPP across the highlands were used as surrogated measures of vegetation heterogeneity. Ecosystem productivity has shown a good correlation with species diversity, as it is the integrative expression of factors such as topography, land use, disturbance, and soil nutrients (Evans and Geerken, 2004; John et al., 2008). As a measure of plant diversity, plant species richness is often considered a measure of ecosystem health and resilience (Symstad and Jonas, 2011). Pohl et al. (2009) indicated that plant species richness significantly increased the topsoil aggregate stability on slopes.

In the crop diversity assessment of this study, NDVI was normalized by rainfall (RUE index). Findings show a decreasing trend of RUE in WL1a and WM1a farming systems. Further to this, soil erosion of these two farming systems is also high. Previous research emphasizes that a decreasing trend of RUE indicates land degradation that is independent of rainfall (Wessels et al., 2008; Prince et al., 1998). Thus, the findings of this study confirmed the land degradation in WL1a and WM1a farming systems. Levin et al. (2007) found that a decreasing trend of vegetation indices would be an indication of decreasing heterogeneity or species diversity. The Shannon index (plant richness and evenness) in the WL1a and WM1a farming systems (western part of the Central Highlands) also decreases. Hence, the present study provides evidence for the decreasing of crop diversity. Besides, crop diversity in farmland can vary due to various reasons, such as socio-economic factors. Farmers would shift from one crop to another crop due to changes in market prices (Maitima et al., 2009), environmental influences or socio-economic factors in farming systems (Shrestha et al., 2010). Therefore, further assessment and ground-based validation are needed to generalize the correlation between soil erosion and plant diversity change.

The study further investigated land degradation using RESTREND analysis to distinguish human-induced land degradation. To interpret the NDVI trends in terms of land degradation or improvement, researchers have to eliminate the impact of climatic variability from the residual sum of NDVI to detect human influence (Wessels et al., 2007; Kundu et al., 2017). A negative trend of RESTREND indicates human-induced land degradation, while a positive trend of RESTREND indicates human influences on the improvement of vegetation (Kundu et al.,2017; Evans, 2004). The present study

demonstrates an increasing trend of RESTREND, which means an improvement of vegetation cover in the farming systems (Figure 4.22). Findings provide evidence to prove the effect of human interference on the improvement of vegetation in three case studies. However, the RUE index indicates land degradation in farming systems WL1a and WM1a. Hence, the above findings suggest climate-induced soil erosion may be responsible for land degradation in these farming systems.

The increasing farming areas, improved farming techniques, and land reclamation may be the reasons for improving vegetation cover. Similarly, Burrell et al. (2017) found that certain farming practices, such as fertilizer applications, irrigation, hybrid varieties of seasonal crops, etc., significantly increase the NDVI values. Fensholt et al. (2013) described trends of vegetation productivity as dependent on climatic factors and non-climatic factors such as land management, cropping practices, and nutrient status. Climatic factors are precipitation, atmospheric temperature, global sea surface temperature, and soil moisture (Fensholt et al., 2013; Ibrahim et al., 2015). Burrell et al. (2017) and other researchers argued that increasing trends of vegetation cover are due to the long-term increasing trend of rainfall or CO_2 fertilization due to anthropogenic greenhouse gas emission (Sarmah et al., 2018; Anyamba and Tucker, 2005).

4.3 Objective 2

The rainfall variation and soil erosion hazards were examined in objective 2 of this study. Extreme rainfall events, rainfall anomalies and rainfall trends were used to evaluate the rainfall variation. The relationship between soil erosion hazards and rainfall variation was analysed. The significance of rainfall variation was tested by modified Mann-Kendall, Sen's slope tests and modified Kling-Gupta index.

4.3.1 The extreme rainfall analysis

The spatio-temporal variations of the core extreme precipitation indices were observed, and results indicated scientific evidence of regional climate variation in the last two decades. The highest simple daily intensity index (SDII) was found in Nuwara Eliya station (Figure 4.23b). According to modified Mann-Kendall and Sen's slope tests, there was a statistically significant increasing rainfall intensity in this area (Table 4.19). The map of Figure 4.23d illustrates that Ratnapura's Consecutive wet days (CWD) were increasing and had the highest extremely wet days (R95 and R99). Consecutive dry days

(CDD) were increasing in Bandarawella and Peradeniya. The annual total wet day precipitation (PRCPTOT) in Bandarawella indicated a statistically significant increasing trend (Table 4.19). This shows there is an increasing rainfall intensity in Bandarawella. However, it is not significant yet.

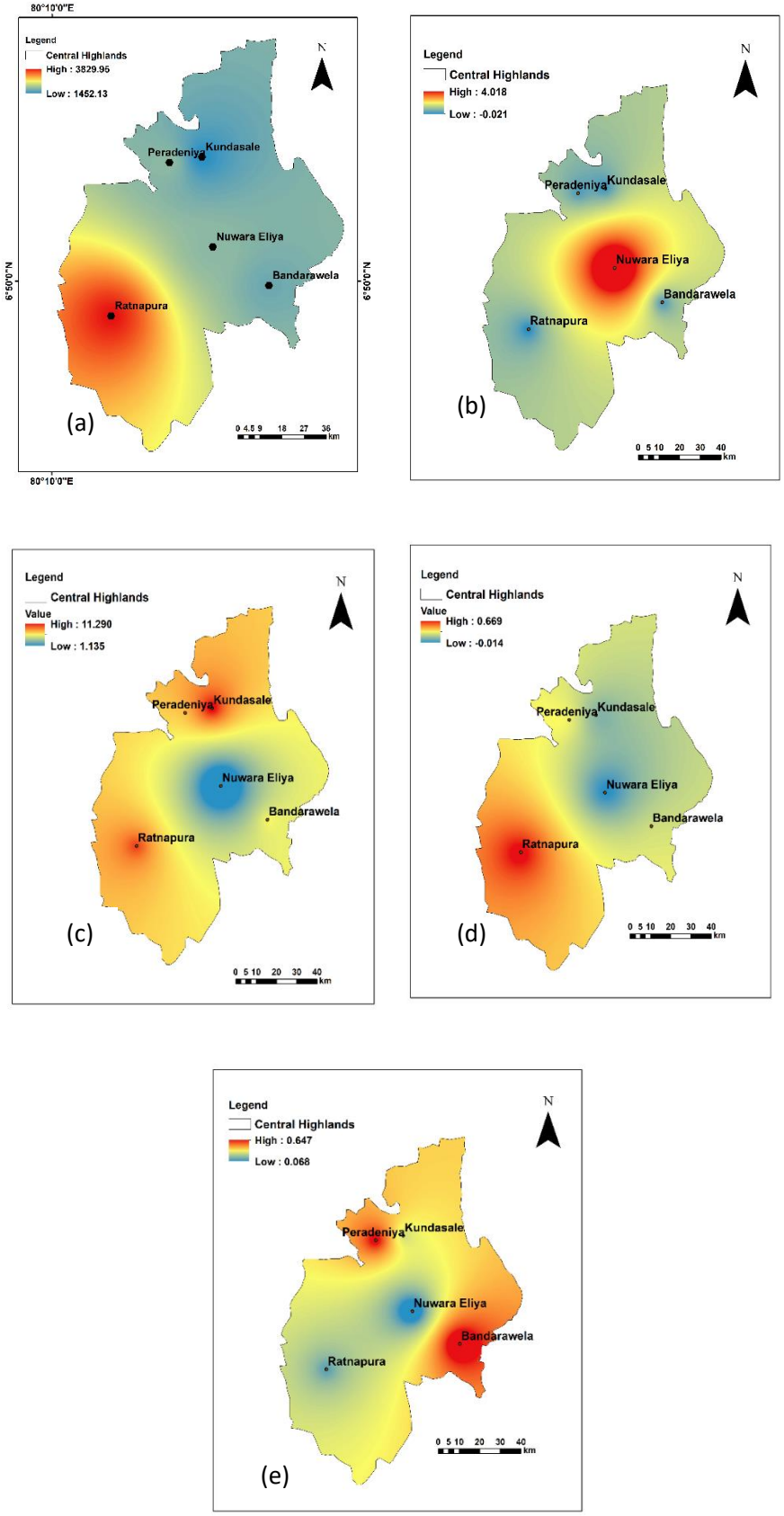

Figure 4. 23 Extreme rainfall events in the Central Highlands (a). ARF (b) SDII (c) R99 (d) CWD and (e) CDD.

Table 4. 19. Results of Mann-Kendall and Sen's slope tests for extreme rainfall indices.

	Index	ARF	RX1day	R95p	R99p	PRCPTOT	SDII
Rathnapura	MK	0	1.27	**2.01**	**2.06**	0.36	-0.42
	SS	-0.56	0.75	**7.02**	**12.57**	7.45	-0.29
Peradeniya	MK	1.01	0.75	1.2	1.14	1.01	1.56
	SS	20.717	0.41	6.08	11.36	20.717	0.1
Nuwara Eliya	MK	1.57	-0.49	1.91	0.62	1.57	**1.98**
	SS	15.77	-0.198	4.21	1.37	15.77	**3.88**
Bandarawella	MK	1.78	-0.36	1.88	1.91	**2.17**	1.96
	SS	18.05	-0.16	6.31	8.06	**22.14**	0.19
Kundasale	MK	0.36	-0.71	-0.85	**2.5**	0.36	1.01
	SS	4.6	-0.52	0	**10.05**	4.61	0.086

SS = Sens' slope MK= Mann-Kendell test

Significance levels of 0.05 and 0.01 were used in this study.

At the 5% significance level, the null hypothesis of no trend is rejected if > 1.96, and it is rejected if > 2.33 at the 1% significance level.

4.3.2 Standard precipitation index

The dry-wet variation was derived using the standard precipitation (SPI) index into different sub-periods 3, 6, 9 and 12 months periods. The standard precipitation (12 months) of five stations are illustrated in figure 4.24. When the SPI value reaches -2 indicates a severely dry period. If the SPI value is greater than 2, it indicates a severe wet period. The SPI values of Bandarawella and Nuwara Eliya indicate sever dry periods (drought) for 2009 and 2017. During the 2012 to 2013 period, the SPI index for Kundasale agro-met station indicated severe drought conditions. The SPI time series analysis in Kundasale, Bandarawella and Nuwara Eliya maps shows increasing severity trends.

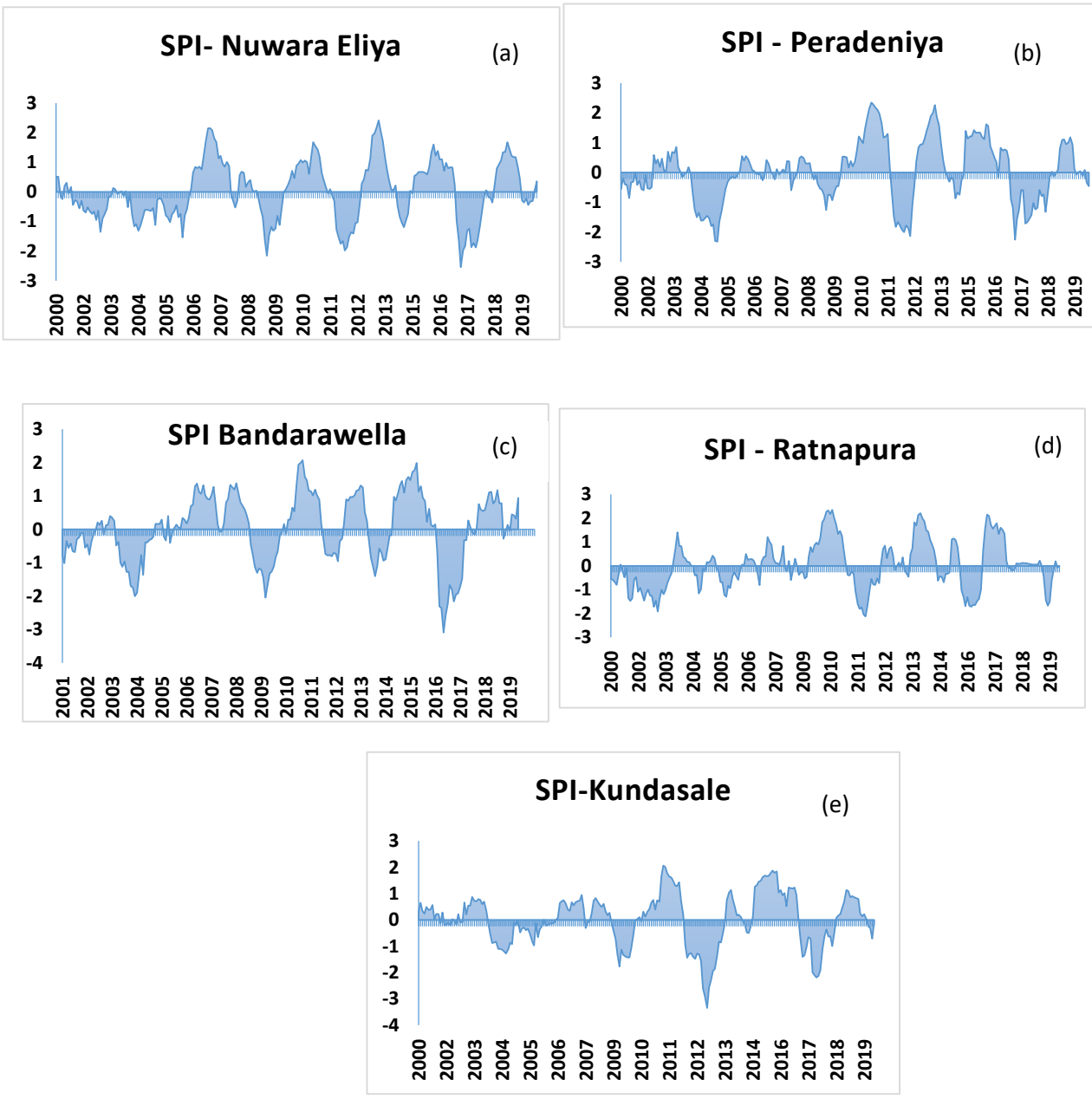

Figure 4. 24 The rainfall variation over the period in five stations.

4.5.3 Rainfall anomaly index

The rainfall anomaly index (RAI) illustrates the amount of rainfall deviation with respect to the period of 1970 - 2010. Findings indicate an increasing rainfall tends from 2000 to 2019 in four agro-met stations. However, Nuwara Eliya agro-met station shows a decreasing rainfall trend from 2000 to 2019 (Figure 4.25 c). This finding is in line with the study of de Silva and Sonnadara (2016). They found decreasing rainfall trend in the Nuwara Eliya area in south-west monsoon (SWM). Wickramagamage (2016) also

observed a consistently declining trend, particularly during the SWM rainfall data assessment over the last 100 years at Nuwara Eliya.

Figure 4. 25 Annual average rainfall and rainfall anomaly in five agro-met stations.

4.5.4 Innovative trend analysis

The innovative trend analysis is applied to detect rainfall trends under the context of climate change. Satellite rainfall and gauged rainfall were assessed by innovative trend analysis. According to Table 4.20, satellite-based rainfall data show a significantly

increasing trend in all the stations. Similarly, ground-based rainfall data also indicate significantly increasing rainfall except in Nuwara Eliya and Kundasale stations (Table 4.20). Figure 4.26 illustrates the results of innovative trend analysis based on satellite rainfall data. Due to low resolution, there were two stations in the same grid: Nuwara Eliya and Bandarawella, Peradeniya and Kundasale in satellite data. Figure 4.26 illustrates the results of the innovative trend analysis from satellite-based rainfall data and Figure 4.27 illustrates the results of ground-based rainfall data.

Table 4. 20. Results for innovative trend test of annual rainfall in the Central Highlands.

Station	Slope (s)	Trend indicate(r)	Standard deviation (σ)	Slope standard deviation (σs)	Level 90% Sig.	Level 95% Sig.	Level 99% Sig.	Type of trend
Satellite rainfall data								
Ratnapura	22.66**	0.98	317.45	1.61	±2.64	±3.14	±8.17	Increasing
Peradeniya	21.53**	1.18	281.64	2.48	±4.08	±4.86	±6.39	Increasing
Nuwaea Eliya	21.30**	1.03	300.21	2.68	±4.4	±5.24	±5.29	Increasing
Bandarawella	21.30**	1.03	300.21	2.68	±4.40	±5.24	±6.89	Increasing
Kundasale	21.53**	1.18	281.64	2.48	±4.08	±4.86	±6.39	Increasing
Ground-based rainfall data								
Ratnapura	35.53**	0.99	536.89	4.90	±8.60	±9.06	±12.62	Increasing
Peradeniya	22.90**	1.20	381.54	2.71	±4.46	±5.31	±6.99	Increasing
Nuwaea Eliya	3.40	0.20	381.89	3.99	±6.57	±7.83	±10.29	Increasing
Bandarawella	16.97**	1.02	310.07	4.77	±7.84	±9.35	±12.28	Increasing
Kundasale	5.20	0.36	343.97	3.17	±5.22	±6.22	±8.17	Increasing

* and ** represent 95% and 99% significance levels, respectively

The rainfall trends in both methods were compared and found a similar increasing trend. The results of modified Kling–Gupta efficiency values (Table 4.21) indicate the satellite and rain-gauge datasets are positively correlated (KGE= 0.6 to 0.29). However, the satellite rainfall data shows low rainfall compared to the rain gauge data. Researchers have reported the increasing trend of average annual precipitation in Sri Lanka. Nearly 75% of meteorological stations have shown a significantly increasing trend (Jayawardena et al., 2018).

Table 4. 21. KGE index for rain gauge measured rainfall in five stations.

Station	Bandarawela	Nuwara Eliya	Ratnapura	Peradeniya	Kundasale
r	0.7644	0.4114	0.6219	0.5463	0.4670
b	1.2134	1.0603	0.5584	1.0012	1.1567
g	0.7699	0.6143	0.9197	0.7715	0.6052
KGE	0.6076	0.2937	0.4132	0.4920	0.3184
R^2	0.5900	0.0030	0.3800	0.3000	0.2100

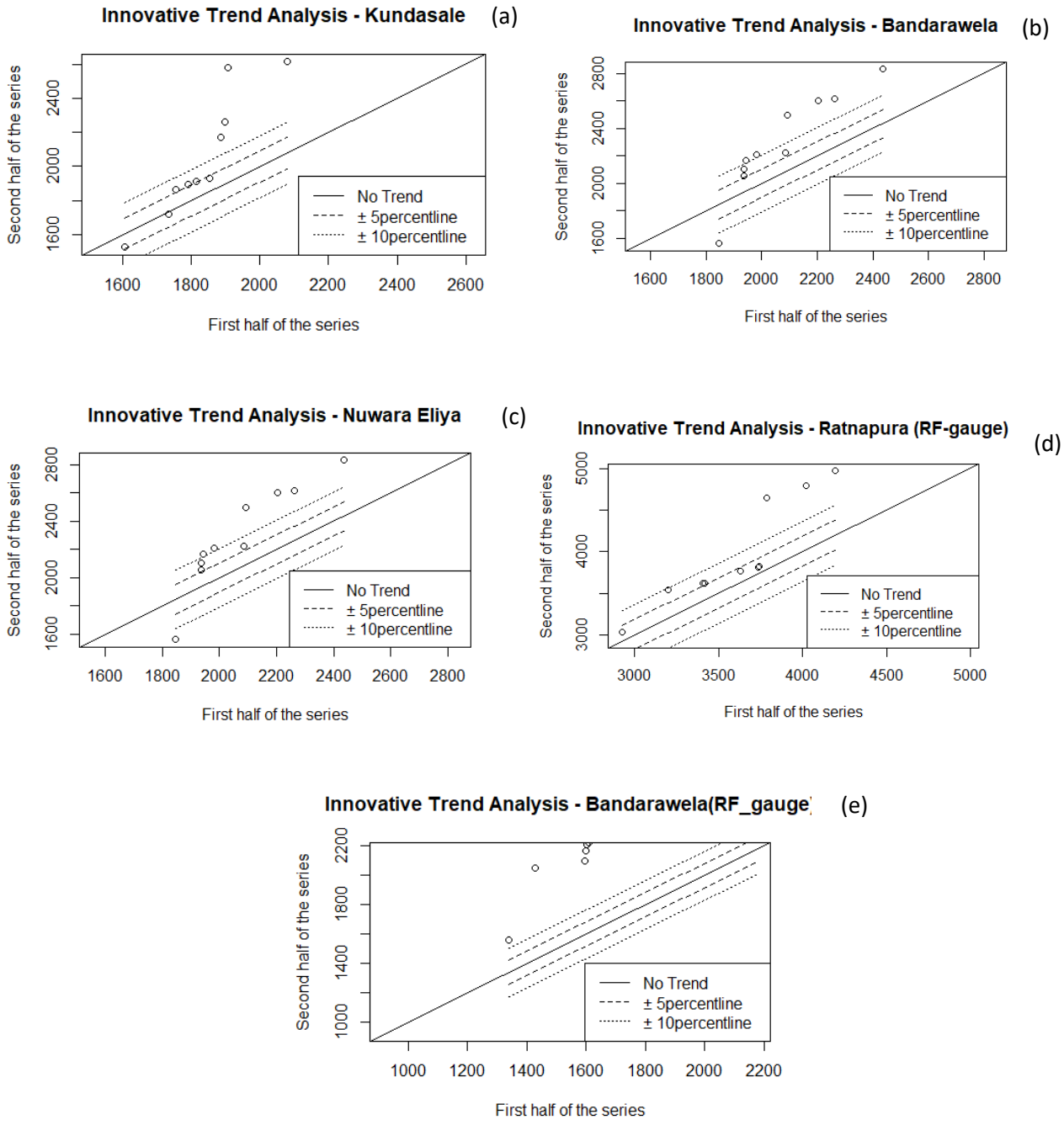

Figure 4. 26 Results of the innovative trend analysis from satellite-based rainfall data.

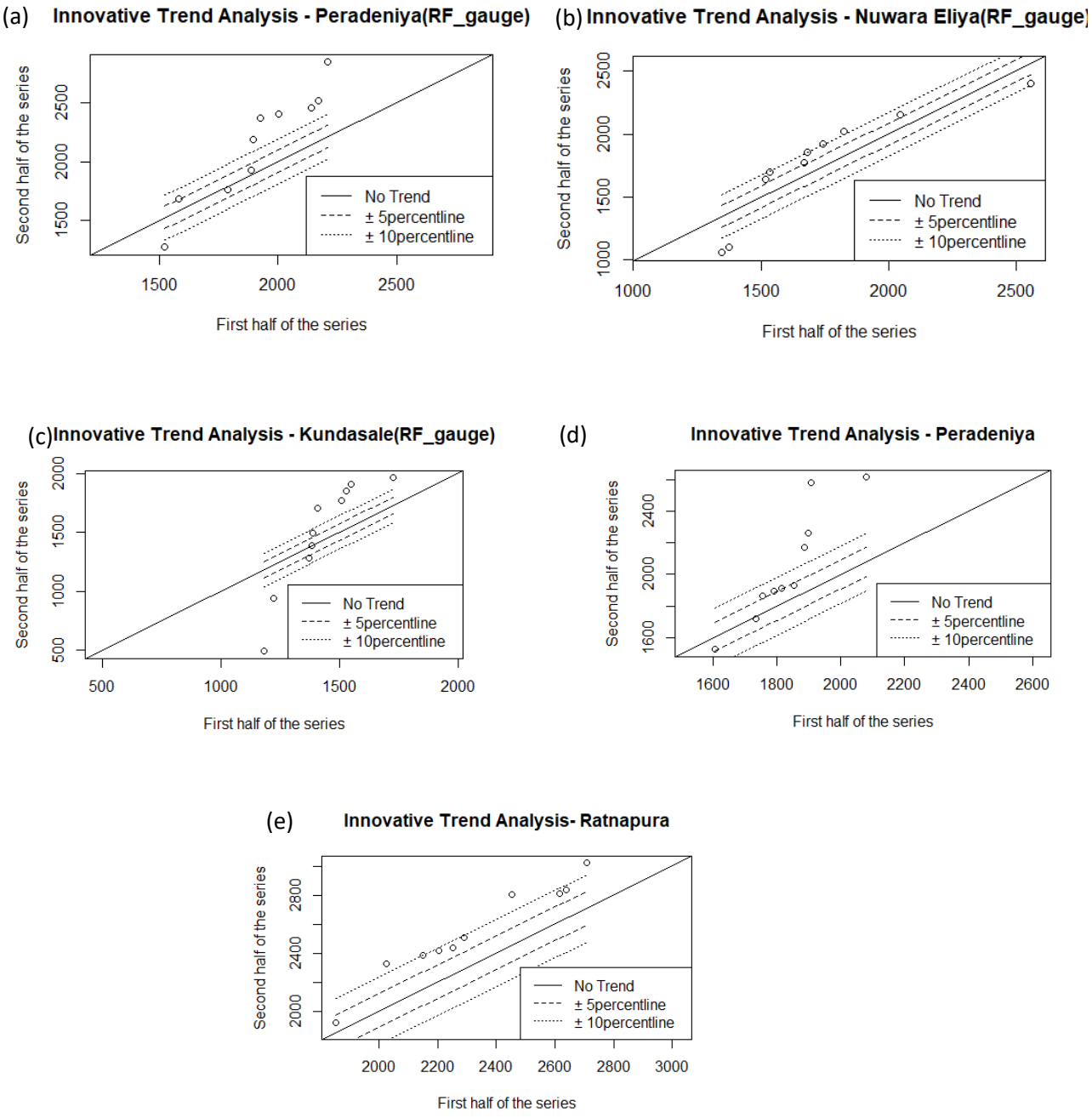

Figure 4. 27 Results of the innovative trend analysis from gauged rainfall data in five stations.

This study analysed the temporal variation of different rainfall features in the Central Highlands to identify the regional variation of rainfall. According to (Liang, 2019), understanding the variation of rainfall trends and precipitation indices is extremely important to identify changes in the hydrological cycle, which provides water resources for agricultural activities and the key control factor for the environment ecological

restoration. Increasing precipitation and its extreme changes impact the local hydrological process, and understandings it helps disaster prevention. The SPI helps to understand all types of effects of droughts, namely, the meteorological, hydrological, agricultural, and socio-economic effects as well as for future prediction. According to (Attogouinon et al., 2017) and other researchers, the analysis of extreme rainfall helps to develop strategies and concepts to mitigate the effects of climate change and helps to understand previous evolution, current and future trends. Researchers found that the intensification of extreme precipitation events and changes in rainfall trends might be a result of global warming (Westra et al., 2013).

4.5.5 The relationship between rainfall variation and soil erosion hazards

Findings indicate that there are positive correlations between average annual rainfall and soil erosion rates $r = 0.395$ ($p<0.05$), landslides frequency ratio and average soil erosion rate $r = 0.416$ ($p<0.05$). The regression model in Figure 4.28 shows the relationships between soil erosion rate and average annual rainfall, average soil erosion rate and landslide frequency ratio in each farming system. Modified Kling–Gupta efficiency values are shown in Table 4.22.

Table 4. 22. KGE index: soil erosion, rainfall erosivity and landslides frequency ratio.

	r	β	γ	KGE
Average soil erosion and average rainfall	0.395	0.009	0.005	-0.530
Average soil erosion and landslide frequency ratio	0.416	0.189	0.081	-0.358
Landslide frequency ratio and rainfall erosivity	0.219	0.016	0.004	-0.604

The finding of this study indicates that rainfall erosivity increases soil erosion and triggers the incidence of landslides in the Central Highlands. Ranasinghe et al. (2019) also highlighted that heavy and prolonged rainfalls are the main triggering factors for landslides in Sri Lanka. Rozos et al. (2013) argued that soil erosion could trigger landslide manifestation. The results of this study indicate that rainfall erosivity and soil erosion triggers the incidence of landslides in the Central Highlands.

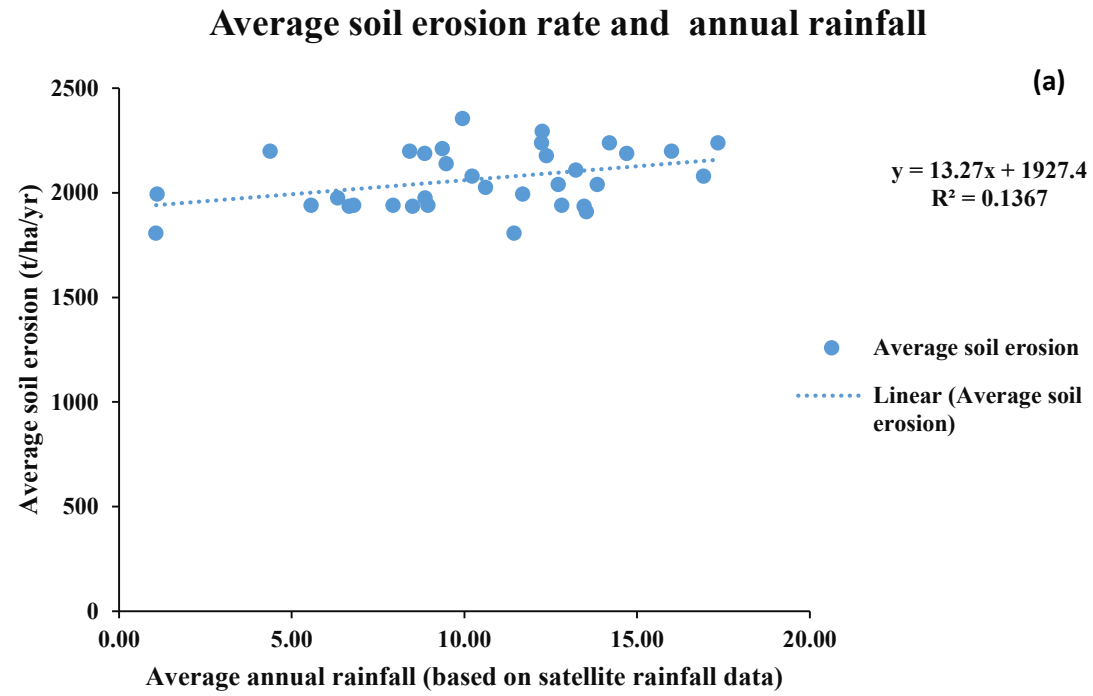

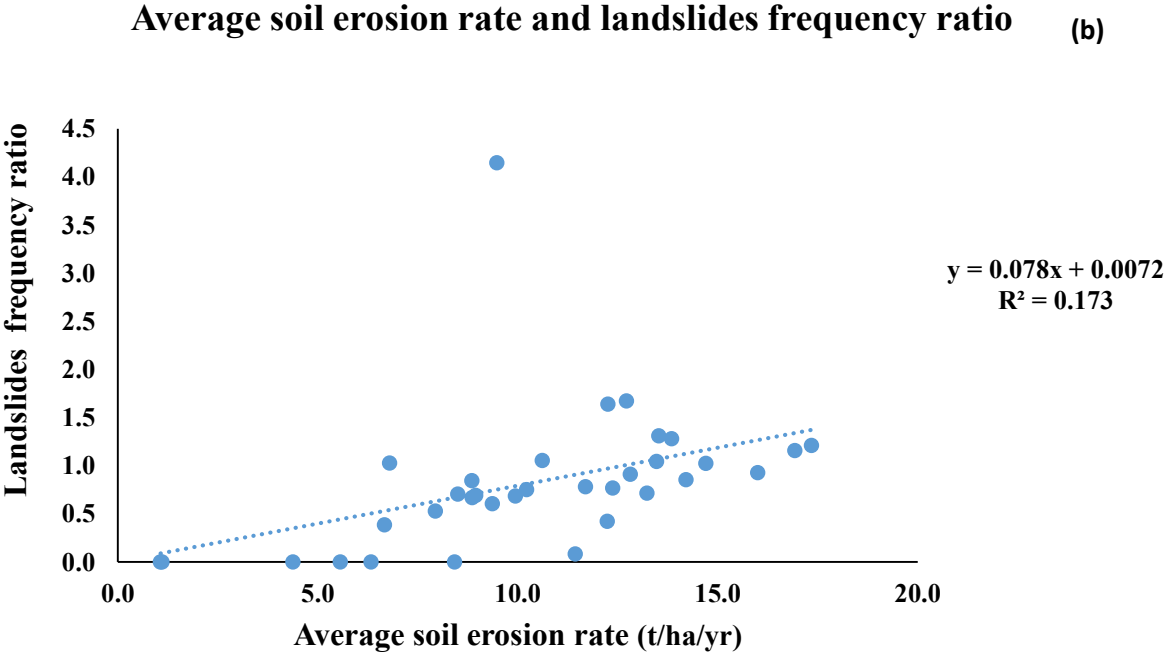

Figure 4. 28 The details of the relationship between (a) Average soil erosion and average annual rainfall and b) average annual soil erosion rate and landslide frequency.

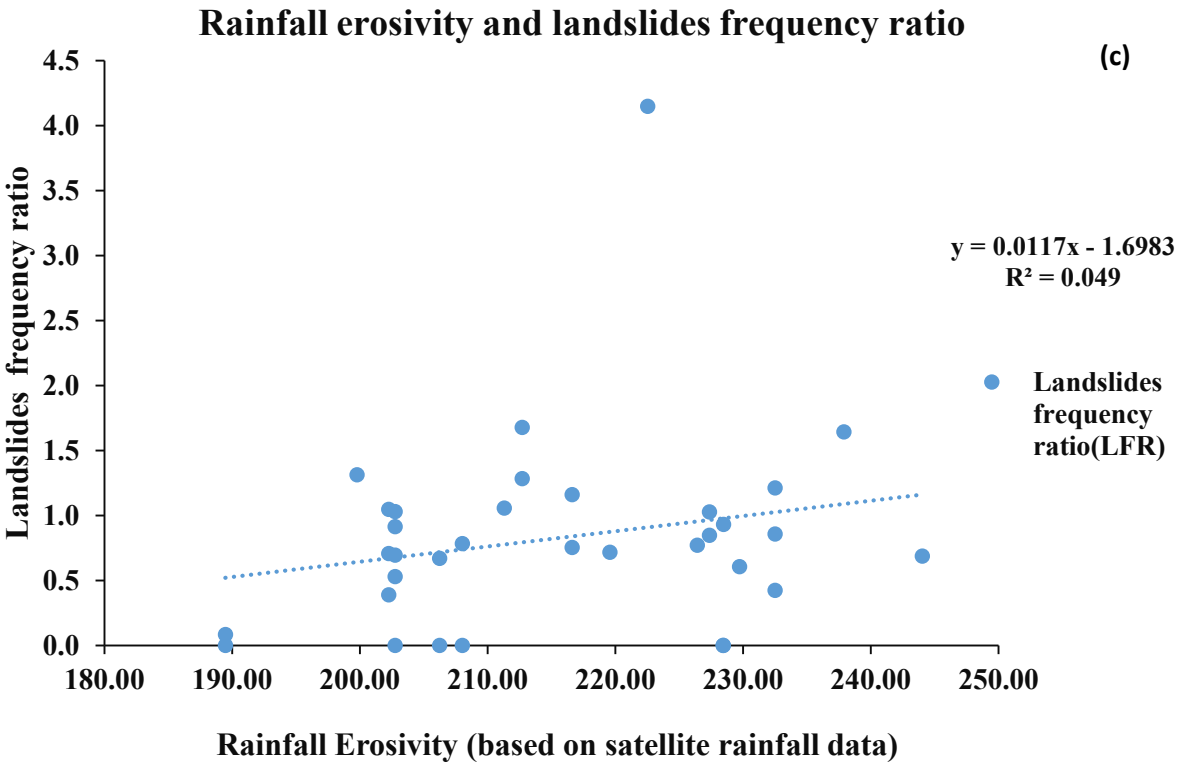

Figure 4. 29 (countinue) The details of the relationship between (c) Average rainfall erosivity and landslides frequency ratio in each farming system.

Studies show that the onset of the two-monsoon pattern (southwest and northeast) in Sri Lanka has also been altered, and the increase of rainfall intensity could be observed in the recent past (Jayawardena et al., 2018; Burt and Weerasinghe, 2014). The changes of the onset of monsoons have affected farming activities in the Central Highlands. Smallholdings and rain-fed agriculture dominate the Central Highlands. Borrelli et al. (2017) also highlighted that small-holder farmers in developing countries would mostly feel severe impacts of global climate change.

4.6 Objective 3

In objective 3, this study assesses the ecologically viable and economically sound farming systems using a matrix-based geo-informatics approach. Criteria indicators, a weighted linear combination score, and an AHP approach were used to determine the ecologically viable and economically sound farming systems in the Central Highlands.

4.6.1 Determination of criteria indicators

This research identified the relevant conditional factors on soil erosion in the Central Highlands from the literature as criteria indicators. However, expert opinion was used to review and validate these indicators. The resultant maps for ecological and economic indicators are shown in Figure 4.30 and Figure 4.31, respectively.

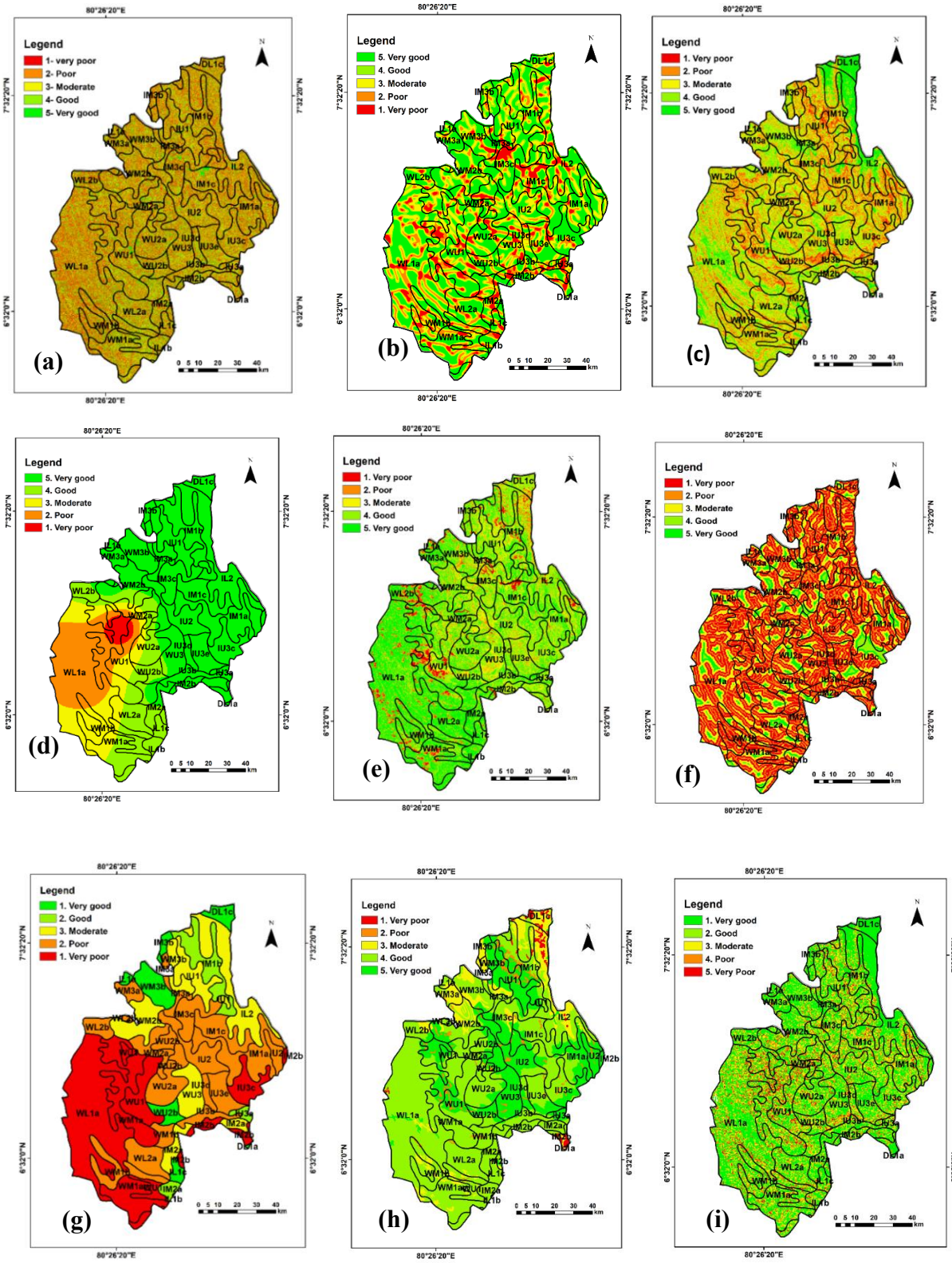

Figure 4. 30 Maps of ecological indicators**:** (a) Aspect, (b) Drainage density, (c) Slope, (d) Precipitation, (e) Vegetation cover, (f) Distance to stream, (g) Landslides, (h) Soil quality, and (i) Soil erosion classes.

Precipitation and landslide vulnerability are high in the western part of the Central Highlands, which can be seen in Figure 4.30. In addition, the distance to the main road and the cost of production are high, and the population density is low in the same area, according to Figure 4.31. Therefore, in overall, these results of indicators reveal very-poor status of soil erosion in the western part of the Central Highlands. However, according to this classification, the vegetation cover of ecological indicators and distance to market of economic indicators show a comparatively very-good status in the western part of the Central Highlands.

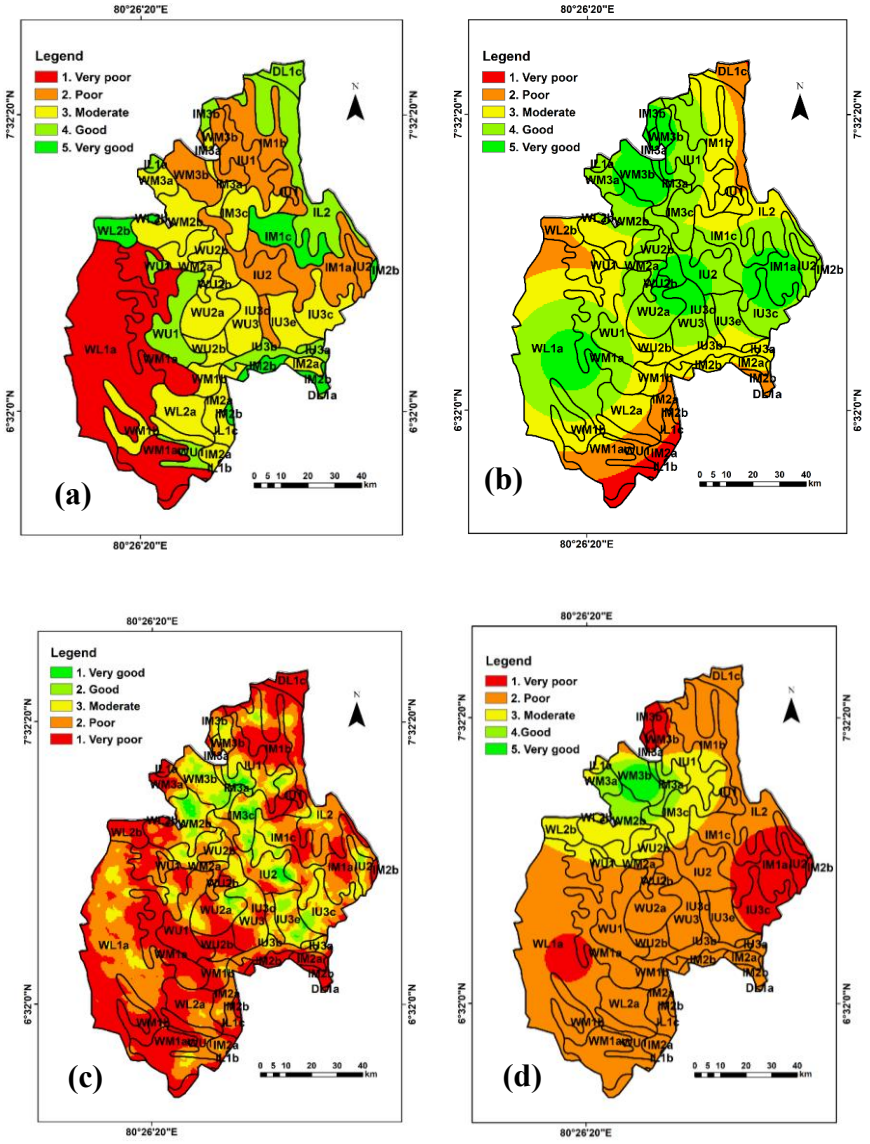

Figure 4. 31 Maps of economic indicators**:** (a) Cost of production, (b) Distance to market, (c) Distance to the main road, and (e) Population density.

4.6.2 Determination of weights for criteria indicators

The ecological and economic indicators were assessed using a pair-wise comparison method to obtain the relative weights. Eigenvalues were used to designate the relative importance. The CR value was computed for the normalisation of the weights. An acceptable CR value is less than 0.1 (Wind and Saaty 1980; Saaty 2002). The CR value results were within the acceptable level (0.1> 0.013 and 0.04). The relative weights for ecological and economic criteria indicators can be found in Tables 4.23 and 4.24, respectively. Among the ecological indicators, soil quality received the highest weight. The cost of production shows the highest weight among economic indicators.

Table 4. 23. Pair-wise comparison for ecological indicators.

Matrix										**Normalization**			
Indicators	(a)	(b)	(c)	(d)	(e)	(f)	(g)	(h)	A1	Weight	λ	RCI	CR
(a) Aspect	1.00	0.50	0.33	0.20	0.20	0.16	0.16	0.14	0.14	0.02	0.02	1.49	0.013
(b) Distance to stream	2.00	1.00	0.50	0.33	0.25	0.20	0.20	0.16	0.14	0.03			
(c) Number of landslides	3.00	2.00	1.00	0.50	0.33	0.25	0.25	0.20	0.16	0.04			
(d) Drainage density	5.00	3.00	2.00	1.00	0.50	0.33	0.33	0.25	0.20	0.06			
(e) Plant cover	5.00	4.00	3.00	2.00	1.00	0.50	0.50	0.33	0.25	0.09			
(f) Slope length	6.00	5.00	4.00	3.00	2.00	1.00	0.50	0.33	0.33	0.12			
(f) Soil erosion	6.00	5.00	4.00	3.00	2.00	2.00	1.00	0.50	0.33	0.15			
(g) Precipitation	7.00	6.00	5.00	4.00	3.00	3.00	2.00	1.00	0.50	0.21			
(h) Soil Quality	7.00	7.00	6.00	5.00	4.00	3.00	3.00	2.00	1.00	0.29			

Table 4. 24. Pair-wise comparison for economic indicators.

Matrix						**Normalization**				
	COP	PD	DM	DMR	A1	Weight	λ	CI	RCI	CR
Cost of production (COP)	1.00	5.00	3.00	7.00	3.20	0.56	4.12	0.04	0.90	0.04
Population density (PD)	0.20	1.00	0.33	3.00	0.67	0.12				
Distance to market (DM)	0.33	3.00	1.00	5.00	1.50	0.26				
Distance to main road (DMR)	0.14	0.33	0.20	1.00	0.31	0.05				
	1.68	9.33	4.53	16.00	5.68	1.00				

4.6.3 Assessing ecologically viable farming systems

The ecological indicators and respective weights of the indicators were multiplied, and a cumulative value was obtained for the weighted linear combination (WLC) score using equation 3.28. This WLC score was classified on a 1-5 scale as the ecologically viable index (EV index). Scores of less than 3.6 were classified as 1 (very-poor), 3.6 to3.9 as 2 (poor), 4.0 to 4.2 as 3 (moderate), 4.3 to 4.5 as 4 (good) and 4.6 to 4.8 as 5(very-good).

Table 4.25 shows the WLC score and EV index for ecologically viable farming systems. The maps were developed based on WLC scores for agro-ecological regions (Figure 4.32) and farming systems (Figure 4.32) to visualize the ecological viability.

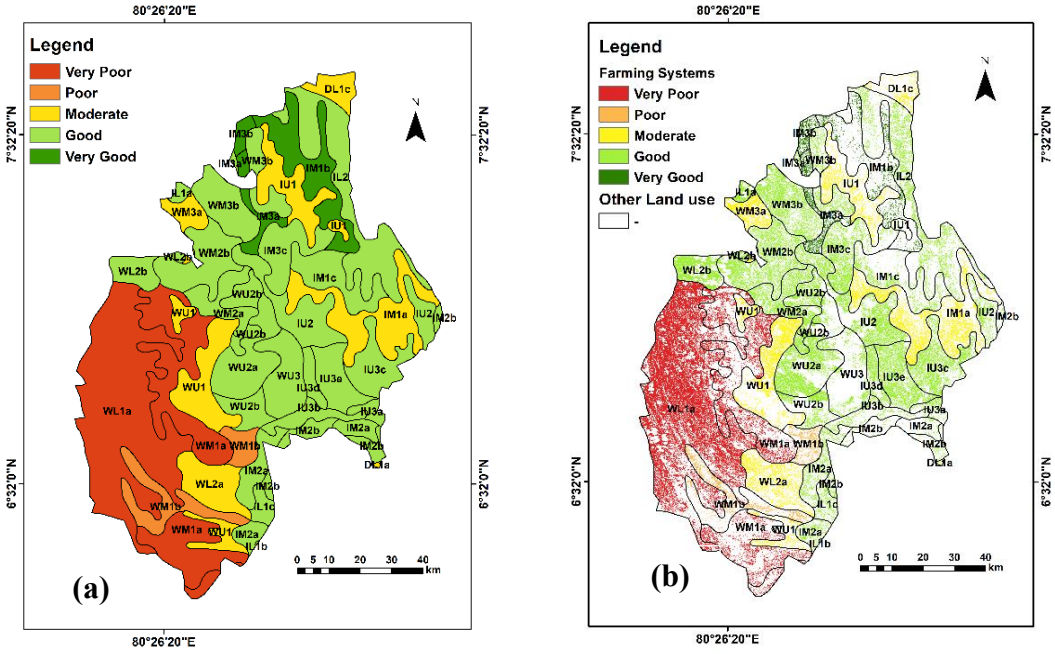

Figure 4. 32 Ecological viability maps for (a) AERs, and (b) farming systems.

Figure 4.32 shows the farming systems of the following AERs: IM1b, IM3a and IM3b. These are ecologically very-good statuses from the viewpoint of soil erosion for agricultural activities. According to ecological criteria indicators, these farming systems show low soil erosion, high soil quality, good precipitation, and less landslide vulnerability. However, the rest of the farming systems show some degree of unhealthy condition from soil erosion. Farming systems in AERs: WL1a and WM1a indicate very-poor status of ecological viability. The precipitation and landslide vulnerability are very-

high in these two farming systems. Thus, these farming systems are highly vulnerable to soil erosion. These findings align with the work of Fayas et al., (2019). Poor agricultural crop production activities would further exacerbate the present status of ecologically viability in these farming systems.

Table 4. 25. Total score and final ratings for ecologically viable farming systems.

	Farming Systems	Landslide	Aspect	Drainage density	Distance to stream	Vegetation cover	Slope	Soil Erosion	Soil Quality	Preci-pitation	WLC Score	EV index
1	DL1a	0.2	0.02	0.3	0.03	0.35	0.6	0.73	0.86	1.07	4.1	4
2	DL1c	0.2	0.08	0.3	0.03	0.35	0.6	0.73	0.86	1.07	4.2	3
3	IL1a	0.2	0.02	0.3	0.03	0.44	0.6	0.73	1.15	1.07	4.5	4
4	IL1b	0.2	0.02	0.3	0.08	0.44	0.6	0.73	1.15	0.86	4.4	4
5	IL1c	0.2	0.02	0.3	0.03	0.44	0.6	0.73	1.15	1.07	4.5	4
6	IL2	0.08	0.04	0.3	0.03	0.44	0.6	0.58	1.15	1.07	4.3	4
7	IM1a	0.04	0.04	0.18	0.03	0.44	0.36	0.44	1.43	1.07	4	3
8	IM1b	0.16	0.04	0.3	0.03	0.44	0.6	0.58	1.43	1.07	4.6	5
9	IM1c	0.08	0.02	0.24	0.03	0.44	0.6	0.58	1.43	1.07	4.5	4
10	IM2a	0.08	0.08	0.24	0.03	0.44	0.6	0.73	1.15	1.07	4.4	4
11	IM2b	0.12	0.08	0.24	0.03	0.44	0.6	0.73	1.15	1.07	4.4	4
12	IM3a	0.16	0.02	0.24	0.03	0.44	0.6	0.73	1.43	1.07	4.7	5
13	IM3b	0.2	0.02	0.24	0.03	0.44	0.6	0.73	1.43	1.07	4.8	5
14	IM3c	0.08	0.02	0.24	0.03	0.44	0.6	0.58	1.43	1.07	4.5	4
15	IU1	0.04	0.02	0.18	0.03	0.44	0.24	0.58	1.43	1.07	4	3
16	IU2	0.08	0.04	0.12	0.03	0.44	0.6	0.58	1.43	1.07	4.4	4
17	IU3a	0.16	0.02	0.24	0.03	0.44	0.36	0.73	1.43	1.07	4.5	4
18	IU3b	0.16	0.04	0.24	0.03	0.44	0.6	0.73	1.15	1.07	4.4	4
19	IU3c	0.08	0.04	0.12	0.03	0.44	0.6	0.73	1.43	1.07	4.5	4
20	IU3d	0.16	0.08	0.12	0.03	0.44	0.36	0.73	1.43	1.07	4.4	3
21	IU3e	0.08	0.04	0.12	0.03	0.44	0.6	0.73	1.43	1.07	4.5	4
22	WL1a	0.04	0.02	0.3	0.03	0.44	0.6	0.15	1.15	0.43	3.1	1
23	WL2a	0.08	0.02	0.3	0.03	0.44	0.6	0.73	1.15	0.86	4.2	3
24	WL2b	0.04	0.02	0.3	0.03	0.44	0.6	0.73	1.15	1.07	4.4	4
25	WM1a	0.04	0.02	0.24	0.03	0.44	0.6	0.15	1.15	0.86	3.5	1
26	WM1b	0.08	0.02	0.24	0.03	0.44	0.6	0.58	1.15	0.64	3.8	2
27	WM2a	0.08	0.02	0.18	0.03	0.44	0.6	0.73	1.43	0.86	4.4	4
28	WM2b	0.08	0.02	0.24	0.03	0.44	0.6	0.58	1.43	1.07	4.5	4
29	WM3a	0.12	0.02	0.24	0.08	0.44	0.6	0.73	0.86	1.07	4.2	3
30	WM3b	0.08	0.02	0.24	0.03	0.44	0.6	0.58	1.43	1.07	4.5	4
31	WU1	0.04	0.08	0.12	0.03	0.44	0.6	0.44	1.43	0.86	4	3
32	WU2a	0.12	0.02	0.12	0.03	0.44	0.6	0.58	1.43	1.07	4.4	4
33	WU2b	0.08	0.08	0.12	0.03	0.44	0.6	0.58	1.43	1.07	4.4	4
34	WU3	0.08	0.08	0.06	0.03	0.35	0.6	0.58	1.43	1.07	4.3	4

4.6.4 Assessing economically sound farming systems

The WLC scores were obtained and rated 1-5 scale as the economical soundness index (ES index). Scores less than 2.3 were classified as 1 (very-poor), 2.3 to 2.8 as 2 (poor), 2.9 to 3.3 as 3 (moderate), 3.4 to 3.8 as 4 (good) and greater than 3.8 as 5 (very-good). Table 4.26 shows WLC scores and ES index for economically sound farming systems. The maps were generated based on WLC scores to identify the economically sound agro-ecological regions (Figure 4.33 a) and farming systems (Figure 4.33b).

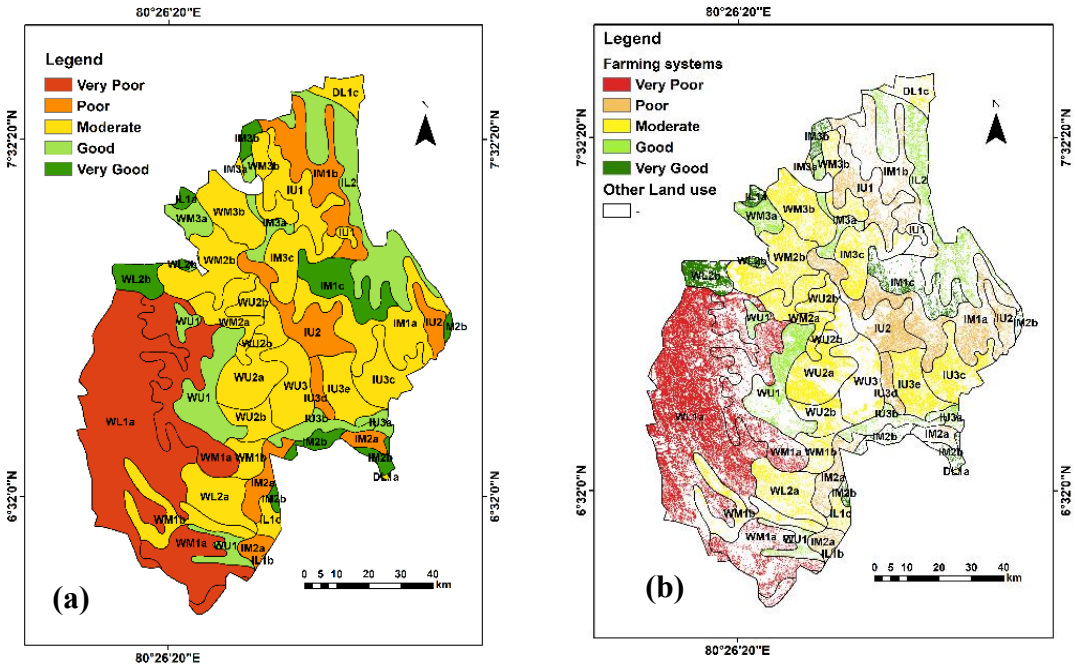

Figure 4. 33 Maps showing economically sound WLC for (a) AER, and (b) farming systems.

The AERs: IL1a, IM1c, IM2b, IM3b and WL2b are very good in terms of the economic soundness status for agricultural activities. However, farming systems in AERs WM 1a and WL1a show the status of economically unsound farming systems. In these farming systems, the cost of production (COP) and distance to the main road are very-high, and population density was very-low. Plantation and other agricultural cropping systems dominate these farming systems (Seo et al., 2005; Jacob and Alles, 1987). The prominent crops in WL1a are rubber, tea, cinnamon and in WM1a tea, pepper, and cloves. These cropping systems show very high COP compare to other cropping systems in the Central Highlands. The COP may vary with environmental conditions, level of soil fertility, and status of land degradation in farming systems (Jayasinghe et al., 2019). In addition, the

population density of the western part is low compared to other parts of the Central Highlands. The distance to access major markets is also high for these farming systems.

Table 4. 26. Total score and final ratings for economically sound farming systems.

No	Farming systems	Cost of production	Population density	Distance to market	Distance to the main road	WLC Score	ES index
1	DL1a	2.3	0.2	0.5	0.3	3.3	3
2	DL1c	2.3	0.2	0.5	0.3	3.3	3
3	IL1a	2.3	0.4	1.1	0.2	3.9	5
4	IL1b	2.3	0.2	0.3	0.3	3.0	3
5	IL1c	1.7	0.2	1.1	0.3	3.3	3
6	IL2	2.3	0.2	0.8	0.3	3.6	4
7	IM1a	1.1	0.1	1.3	0.2	2.8	2
8	IM1b	1.1	0.2	0.8	0.3	2.4	2
9	IM1c	2.8	0.2	1.1	0.2	4.3	5
10	IM2a	1.7	0.2	0.5	0.2	2.7	2
11	IM2b	2.8	0.2	0.8	0.2	4.1	5
12	IM3a	1.7	0.5	1.3	0.2	3.6	4
13	IM3b	2.3	0.1	1.3	0.2	3.9	5
14	IM3c	1.7	0.4	1.1	0.2	3.3	3
15	IU1	1.1	0.4	1.1	0.2	2.8	2
16	IU2	1.1	0.2	1.1	0.2	2.6	2
17	IU3a	2.3	0.2	0.8	0.2	3.4	4
18	IU3b	2.3	0.2	0.8	0.2	3.5	4
19	IU3c	1.7	0.1	1.1	0.2	3.0	3
20	IU3d	1.1	0.2	1.1	0.2	2.6	2
21	IU3e	1.7	0.2	1.1	0.2	3.1	3
22	WL1a	0.6	0.2	1.1	0.2	2.0	1
23	WL2a	1.7	0.2	0.8	0.3	3.0	3
24	WL2b	2.8	0.4	0.5	0.2	3.9	5
25	WM1a	0.6	0.2	0.8	0.2	1.8	1
26	WM1b	1.7	0.2	0.8	0.3	3.0	3
27	WM2a	1.7	0.4	1.1	0.2	3.3	3
28	WM2b	1.7	0.4	1.1	0.2	3.3	3
29	WM3a	1.7	0.5	1.1	0.2	3.4	4
30	WM3b	1.1	0.6	1.3	0.2	3.2	3
31	WU1	2.3	0.2	1.1	0.2	3.8	4
32	WU2a	1.7	0.2	1.1	0.2	3.1	3
33	WU2b	1.7	0.2	1.1	0.2	3.2	3
34	WU3	1.7	0.2	1.1	0.2	3.1	3

4.6.5 Classification of ecologically viable and economically sound farming systems

The average cumulative value of ecological and economic indices was computed as the overall index. The scale of the overall index was adapted from the land management within the capability (LMWC) scheme of New-South Wales, Australia (Gray et al., 2015). This scheme provided an appropriate scale for the overall index. The values of five defined classes are given in Table 4.27. The final matrix with the overall index can be found in Table 4.28. The maps were generated using the overall index for ecologically viable and economically sound AERs (Figure 4.34 a) and farming systems (Figure 4.34 b).

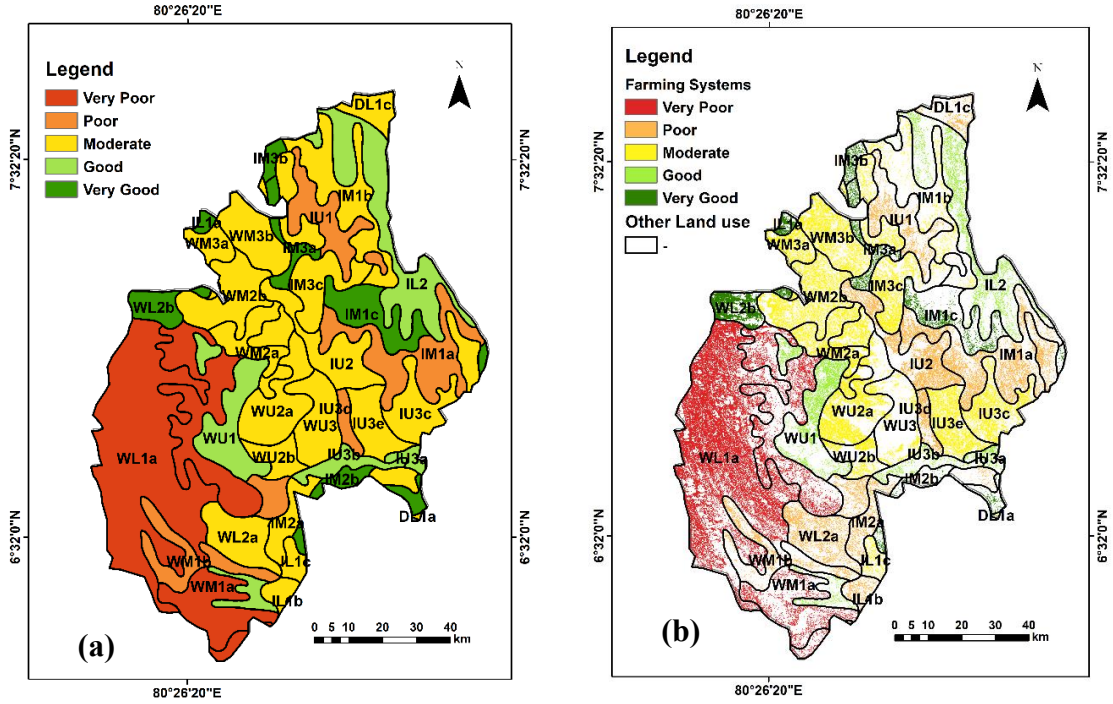

Figure 4. 34 Map of ecologically viable and economically sound (a) AERs, and (b) farming systems.

Figures 4.34 (a) and (b) show the final map of ecologically viable and economically sound AERs and farming systems in the Central Highlands. The farming systems in AERs: IM1c, IM2b, IM3a, IL1a, WL2b, and WM3b can be identified as very-good, and the farming systems: IL2, IU3a, IU3b and IU1 illustrated a good status as per the overall index, for agricultural activities in terms of the ecological and economic aspects regarding in this study. Furthermore, these farming systems are enriched with plantation crops (e.g. tea, coconut, coffee and sugarcane), horticulture crops (e.g. mango, tomato and

Table 4. 27. Classes of the overall index.

Color code	Value range	Status
	1.0 - 1.9	Very poor
	2.0 - 2.9	Poor
	3.0 -3.9	Moderate
	4.0 - 4.4	Good
	4.5 - 5.0	Very good

Table 4. 28. Final matrix with the overall index.

No	Farming systems	Ecologically viable index	Economical sound index	Overall index
1	DL1a	4	3	3.5
2	DL1c	3	3	3.0
3	IL1a	4	5	4.5
4	IL1b	4	3	3.5
5	IL1c	4	3	3.5
6	IL2	4	4	4.0
7	IM1a	3	2	2.5
8	IM1b	5	2	3.5
9	IM1c	4	5	4.5
10	IM2a	4	2	3.0
11	IM2b	4	5	4.5
12	IM3a	5	4	4.5
13	IM3b	5	5	5.0
14	IM3c	4	3	3.5
15	IU1	3	2	2.5
16	IU2	4	2	3.0
17	IU3a	4	4	4.0
18	IU3b	4	4	4.0
19	IU3c	4	3	3.5
20	IU3d	3	2	2.5
21	IU3e	4	3	3.5
22	WL1a	1	1	1.0
23	WL2a	3	3	3.0
24	WL2b	4	5	4.5
25	WM1a	1	1	1.0
26	WM1b	2	3	2.5
27	WM2a	4	3	3.5
28	WM2b	4	3	3.5
29	WM3a	3	4	3.5
30	WM3b	4	3	3.5
31	WU1	4	4	4.0
32	WU2a	4	3	3.5
33	WU2b	4	3	3.5
34	WU3	4	3	3.5

capsicum), mixed homegarden crops (e.g. banana, cocoa and black pepper), paddy and agro-forestry (NRMC, 2015; Punyawardena et al., 2003).

Results revealed that more than 50% of farming systems demonstrated moderate status in terms of both ecological and economic aspects. Those farming systems were dominated by similar cropping systems with different crops such as plantation crops (e.g. Tea, and Coconut), horticulture crops (e.g. Banana, Mango, Tomato, Capsicum, Cabbage and Carrot), Kandyan home garden crops (e.g. Nutmeg, Black Pepper, Cloves, Coffee, Avocado and Cassava), paddy and agro-forestry. Studies show soil erosion in this area has increased to some degree due to land-use changes and other anthropogenic activities over the past period (Hewawasam, 2010) and the impact of climate variation (Ratnayake and Herath, 2005; Gunathilaka et al., 2018). Further to this, farming systems in AERs: WM 1a and WL1a show very-poor status in terms of the ecological and economic aspects. Studies confirmed that increasing rainfalls, landslide vulnerability, high soil erosion rates, as well as significant land-use changes were featured in the area covered under these farming systems (Fayas et al., 2019).

The cropping pattern in these farming systems is mainly dominated by plantation crops (e.g. rubber, coconut and tea) and minor export crops (e.g. Cinnamon, Clove and Cocoa), mixed homegarden crops (Rambutan, Banana, Coffee and Mango) and paddies. Researchers indicated that the COP might run very high with plantation crops, and it varies from place to place (Jayasinghe et al., 2019; Gunathilaka et al., 2018). For example COP of Tea crop has increased due to increased fertilizer and herbicide applications (Jayasinghe et al., 2019; Gunathilaka et al., 2018). Studies show that prolonged dry periods, intensive rainfall, crop-weed competition and soil losses have been experienced in the Central Highlands (Gunathilaka et al., 2018). This situation caused a decrease in soil fertility in the cropping fields. However, intensifying fertiliser application to maintain soil fertility and adopting soil conservation measures may significantly increase the cost of production. Figure 4.35 shows the ground situation in some eroded areas of the WL1a farming systems.

Figure 4. 35 Field photographs showing some eroded areas in WL1a farming system (rubber plantation converted to pineapple cultivation)

The proposed approach attempts to add a new dimension to the decision-making process relating to soil erosion hazards, one of the complex environmental issues with the present climate condition. The results demonstrated the simplicity and flexibility of a matrix-based AHP method that can be applied to obtain a reasonable outcome in developing countries lacking financial means and resources. Mosadeghi et al. (2015) stated that the selection of more sophisticated techniques might not necessarily generate a more precise outcome; a simplified method may be sufficient to get the outcome. Especially in developing countries where resources are scarce and there is a lack of sufficient information on environmental and economic aspects, this decision-making technique and process could help generate meaningful results (Tiwari et al., 2000). The method presented here allows breaking the assessment into two significant perspectives: ecologically viability from the viewpoint of soil erosion and economic perspectives. Criteria indicators take into account ecological factors relating to soil erosion and certain economic factors relating to crop production and market access. The findings indicate that the AHP approach can effectively capture the complex effects in farming systems and analyse ecologically viable and economically sound status to cope with future challenges for sustainable farming system management.

In Sri Lanka, increasing agricultural areas could be observed during the past two decades due to the increasing demand for foods caused by population growth. In this study, the overall index in Table 4.28 indicates the status of farming systems from the viewpoint of ecological viability and economic perspective. Results show that farming systems (WM 1a and WL1a) need an immediate restoration plan. Criteria indicators of these farming systems highlight the status and the severity of the degradation. Therefore, these farming

systems need more soil conservation measures to prevent further deterioration. A priority-based restoration plan can be utilised with resource constraints in terms of policy implications. The current study enables development practitioners to recognize the most critical farming systems for priority restoration planning.

Several studies (Hewawasam and Illangasinghe, 2015) proved that soil erosion is a considerable problem in Sri Lanka. Researchers used various methods such as field plot experiments or fallout radionuclides (Hewawasam et al., 2003; Hewawasam and Illangasinghe, 2015) and a review of past research outcomes to verify and confirm this problem of soil erosion (Hewawasam, 2010). Udayakumara et al. (2010) identified the average annual soil erosion rate in the Samanalawawe watershed (AERs: IM2a and IU3b) in the Central Highlands as approximately 4.3 t/ha/yr. In 2013, Hewawasam and his colleagues conducted a plot scale experiment with fallout radionuclides in a rain forest area. They found background soil erosion was about 3 t /ha/ yr in the rain forest area (Hewawasam et al., 2013). Another study of an agriculture plot experiment (Perawella of upper Oma Oya catchment) in the Central Highlands (AER: IU3d), demonstrated the net sheet erosion rates were about 20 t/ha/yr (Hewawasam and Illangasinghe, 2015). This agricultural plot experiment's study area is adjoined to the study area of previous work by Hewawasam and his colleagues in 2013. In this agriculture plot experiment, Hewawasam and Illangasinghe (2015) concluded that the soil erosion has increased due to deforestation and agricultural activities. In addition, Udayakumara and his colleagues conducted a farm level household survey and recognized inappropriate soil, and crop management practices were major causes of soil erosion in agricultural lands (Udayakumara et al., 2010).

Bandara et al. (2001) found that soil erosion imposes substantial economic costs in Sri Lanka. Poverty and inadequate labour requirement were indirectly affected by soil erosion. Appropriate site-specific conservation strategies reduce the cost of production. Udayakumara et al. (2012) and Diyabalanage et al. (2017) found soil conservation measures successfully contributed to controlling soil erosion in critical areas of the Central Highlands. Hewawasam and Illangasinghe (2015) have also pointed out that soil erosion can be reduced by 99% by implementing soil conservation strategies and improving vegetation cover in the tropical region.

Further to this, strategies to improve soil organic carbon storage are also important for tropical and subtropical infertile farmlands (Lal, 2004; Montanarella et al., 2015). Arabameri et al. (2018) indicated soil erosion could significantly decrease with implementing proper soil conservation and management measures in hilly areas such as contour planting, cover cropping, crop rotating, changing land-use pattern, and construction of check dams and stone bunds. In addition, they also highlight the importance of flood control measures, as well as controlling animal grazing in sloping lands. In contrast, the use of improper soil conservation activities may exaggerate the problem. Inappropriate assessment and conservation measures would result in an increase of soil erosion hazards such as landslide vulnerability (Tarolli et al., 2014). Ranasinghe et al. (2019) identified rapid land-use changes, lack of proper land-use systems (abandoned tea plantations) and the neglected drainage system maintenance as the main reasons for recent landslides in the Central Highlands of Sri Lanka.

4.7 Objective 4

This study employed a spatiotemporal modelling process (using statistical and machine learning techniques) to predict the vulnerability in different farming systems for soil erosion hazards based on RCP climate scenarios to achieve objective 4. Soil erosion susceptibility was analysed in projected RCP 2.6 and RCP 8.5 climate scenarios. Five predictive models: RUSLE, FR, ANN, SVM, and ANFIS were employed to quantify and demarcate the spatial vulnerability of soil erosion in 2040 at the Central Highlands of Sri Lanka. LSTM deep learning model was also deployed to predict soil erosion susceptibility.

4.7.1 Soil erosion susceptibility mapping and model performance in RUSLE method

Predictions show average soil erosion rates will increase to 10.5 t/ha/yr under the RCP 2.6 and 12.4 t/ha/yr under the RCP 8.5 climate scenario in 2040. The results of RUSLE indicate the soil erosion rate in 2020 is 10.18 t/ha/yr with the satellite rainfall data. However, the ground-based gauge rainfall data indicate that soil erosion rates are a little higher than the results of satellite rainfall data (11.8 t/ha/yr). The rainfall erosivity derived from gauged and satellite data is illustrated in Figure 4.36.

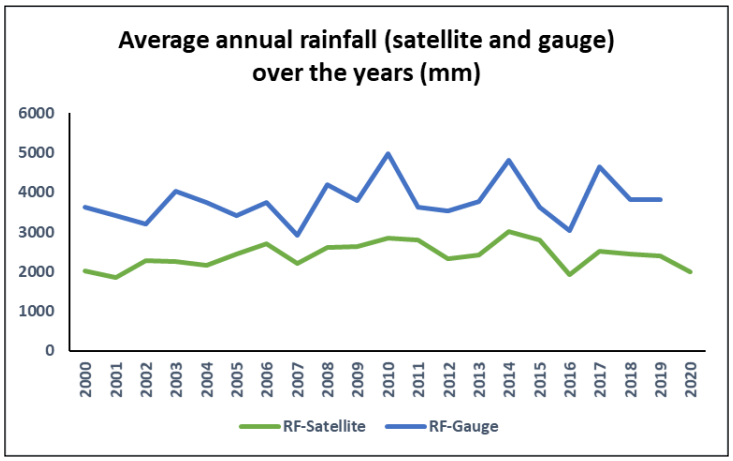

Figure 4. 36 Average annual rainfall in Rathnapura area

The soil erosion susceptibility, generated from gauge and satellite data shows very little difference according to Table 4.29. The areas covered by soil erosion hazards high and very-high categories are predicted to increase by 2040 as projected by the RCP 8.5 scenario. The risk of soil erosion vulnerability in RCP 8.5 is much greater than RCP 2.6. The respective soil erosion susceptibility maps and the area covered by each soil erosion category are illustrated in Figure 4.37 and Table 4.29.

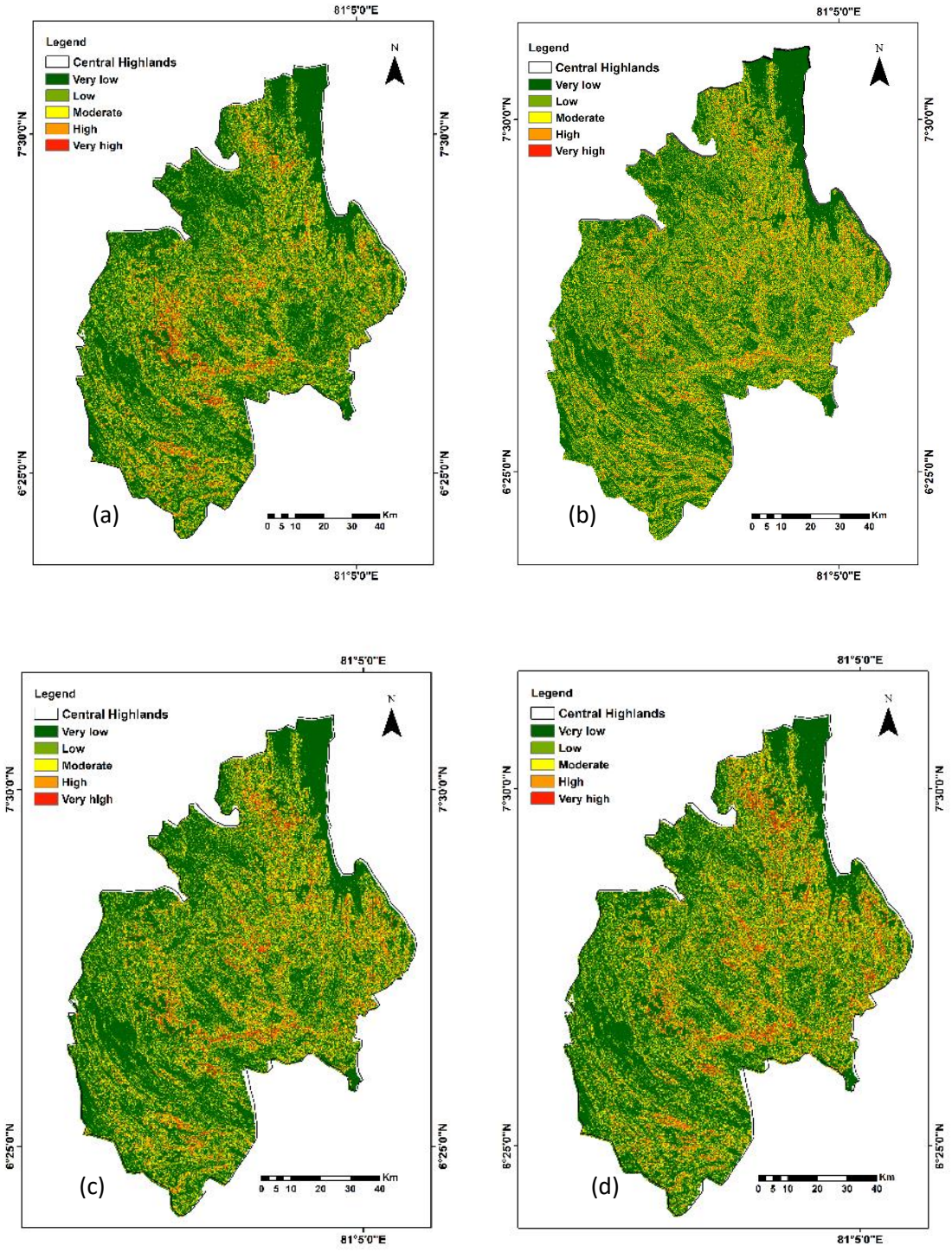

Figure 4. 37 Soil erosion susceptibility maps (a) 2020 based on gauged rainfall data, (b) 2020 based on satellite rainfall data (c) RCP 2.6, and (d) RCP 8.5 in 2040 respectively.

Table 4. 29. Area covered by the soil erosion category from the RUSLE model.

Class		2020		2040	
		Gauge rainfall	Satellite rainfall	RCP2.6	RCP 8.5
Very Low	<5	5147.04	5228.71	5176.9	4845.05
Low	5-'10	1594.27	1630.48	1604.85	1396.54
Moderate	10 -' 20	1913.96	1927.82	1928.87	1961.01
High	20-50	1463.26	1383.80	1436.95	1765.93
Very High	50<	381.47	329.19	352.42	531.46
Total area		10500.00	10500.00	10500.00	10500.00

4.7.2 Frequency ratio method

Soil erosion susceptibility was analysed with eight conditioning factors using the FR method. The results of the FR analysis and weights for each factor are given in Table 4.30. The soil erodibility, stream power index and slope length and steepness are obtained by using the highest weights. The susceptibility maps of the frequency ratio method indicate the western side of the Central Highlands is more vulnerable with the projected RCP 8.5 scenario.

Table 4. 30. Frequency ratios analysis and weight for each factor.

Factor	No	Class	Area	%	LS	%	FR	Weight
Aspect	1	Flat	1149.1	10.9	18	9.23	0.84	1.04
	2	N	1161.5	11.1	33	16.92	1.53	
	3	NE	1179.3	11.2	21	10.77	0.96	
	4	E	1197.9	11.4	20	10.26	0.90	
	5	SE	1168.9	11.1	17	8.72	0.78	
	6	S	1179.7	11.2	23	11.79	1.05	
	7	SW	1158.0	11.0	23	11.79	1.07	
	8	W	1159.8	11.0	19	9.74	0.88	
	9	NW	1150.4	11.0	21	10.77	0.98	
			10504.6		195		9.00	
Slope length	1	0 - 0.72	5230.67	49.8	120	61.54	1.24	3.7
	2	0.72 - 2.16	4405.10	42.0	50	25.64	0.61	
	3	2.16 - 4.8	636.80	6.1	20	10.26	1.69	
	4	4.8 - 10.09	208.10	2.0	4	2.05	1.03	
	5	10.1 - 61.3	19.33	0.2	1	0.51	2.79	
			10500.00		195		7.36	
Soil erodibility	1	0.01 - 0.04	547.2709	5.21	1	0.512821	0.10	6
	2	0.05 - 0.179	22.07296	0.21	1	0.512821	2.44	

	3	0.17 - 0.21	464.7765	4.43	7	3.589744	0.81	
	4	0.22 - 0.27	7922.812	75.46	178	91.28205	1.21	
	5	0.27 - 0.33	1543.068	14.70	8	4.102564	0.28	
			10500	100.00	195.00		4.84	
Land-use - C & P factor	1	Dense Forest	1702.00	16.21	29	14.87	0.92	1.43
	2	Less dense forest	3185.71	30.34	54	27.69	0.91	
	3	Cropping area	4320.40	41.15	97	49.74	1.21	
	4	Cloud	401.88	3.83	0	0.00	0.00	
	5	Bult up area	348.84	3.32	7	3.59	1.08	
	6	Water	541.18	5.15	8	4.10	0.92	
			10500.00		195	100.00	0.91	
Distance to stream	1	0 - 453.90	2080.40	19.81	39	20.00	1.01	1.81
	2	453.90 - 1,043.97	4657.82	44.36	65	33.33	0.75	
	3	1,043.97 - 1,974.48	2915.62	27.77	66	33.85	1.22	
	4	1,974.48 - 2,995.76	695.87	6.63	21	10.77	1.62	
	5	2,995.76 - 5,787.27	150.29	1.43	4	2.05	1.43	
			10500.00	10500.00		195	6.04	
Stream power Index	1	0 - 0.0488	10327.26	98.0000	192	98.46	1.01	4.80
	2	0.0489 - 0.329	88.00	0.8300	2	1.03	1.22	
	3	0.33 - 3.1	84.74	0.5300	1	0.51	0.95	
			10500.00					
Rainfall erosivity-2019-2	1	162.52 - 198.14	1750.07	16.67	23	12	0.71	2.94
	2	198.15 - 212.39	2481.30	23.63	29	15	0.63	
	3	212.4 - 265.1	2183.80	20.80	41	21	1.01	
	4	265.11 - 337.76	2034.39	19.38	33	17	0.87	
	5	337.77 - 525.82	2050.43	19.53	69	35	1.81	
			10500.00		195		5.03	
Rainfall erosivity-2040RCP2.6	1	231.48 - 241.5	2097.80	19.98	9.00	4.615	0.23	3.00
	2	241.51 - 245.67	2096.25	19.96	54.00	27.692	1.39	
	3	245.68 - 249.61	2092.58	19.93	47.00	24.103	1.21	
	4	249.62 - 254.68	2108.84	20.08	56.00	28.718	1.43	
	5	254.69 - 260.2	2104.53	20.04	29.00	14.872	0.74	
			10500.00		195		5.00	
Rainfall erosivity-2040RCP8.5	1	300.58 - 300.65	2094.20	19.94	44	22.56	1.13	1.84
	2	300.66 - 300.75	2135.13	20.33	23	11.79	0.58	
	3	300.76 - 300.87	2088.21	19.89	31	15.90	0.80	
	4	300.88 - 300.97	2084.48	19.85	51	26.15	1.32	
	5	300.98 - 301.11	2098.23	19.98	46	23.59	1.18	
			10500.00		195		5.01	

4.7.3 Artificial neural network method

Figure 4.38 shows the results of the best validation process and performance curve. The results show that the best validation performance was achieved from seven epochs, the MSE = 1.31 and R values for training = 0.95, testing 0.84, validation = 0.85 and overall = 0.91.

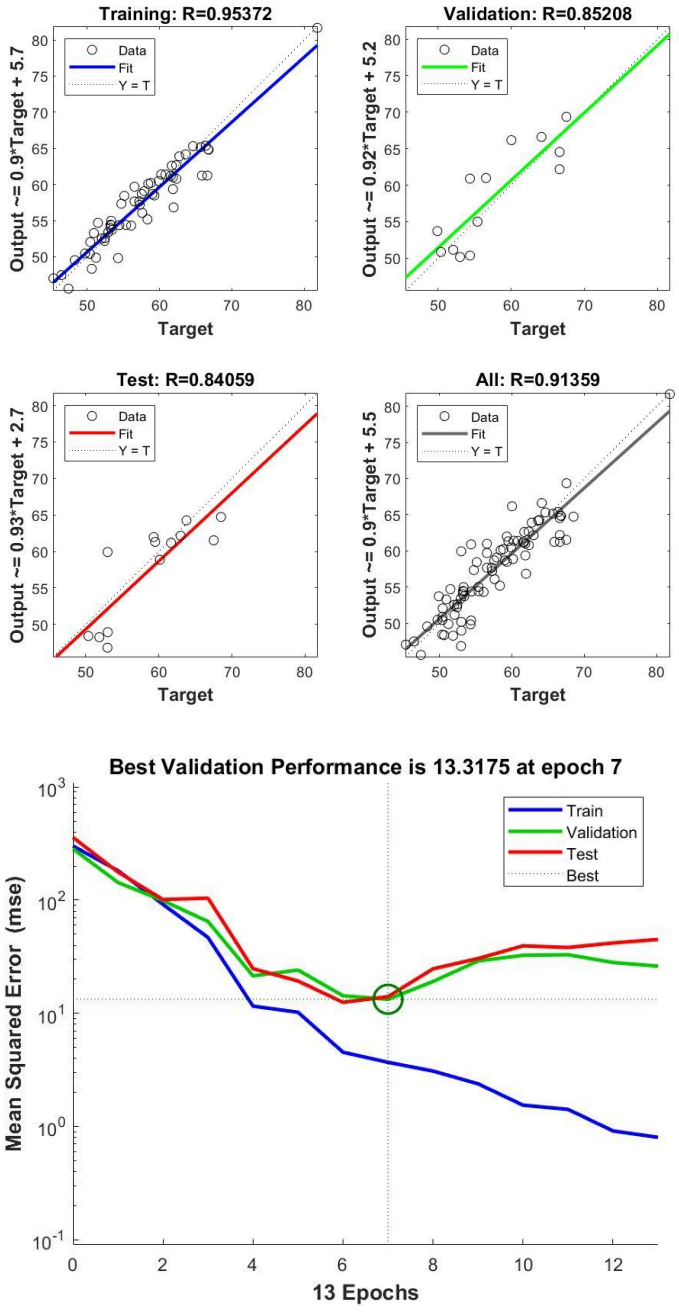

Figure 4. 38 (a) The best validation process and (b) performance curve of the ANN method.

4.7.4 Support vector machine learning method

This research applied SVM with eight predictors using the Gaussian kernel function with optimization. The best performance of SVM is found in the RMSE = 2.292 and R^2= 0.70. The AUC indicates soil erosion susceptibility was performed well with SVM and performed better than the ANN model (Figure 4.39). Figure 4.38a illustrates the prediction vs actual relationship and results of a comparison between target and SVM output (Figure 4.38a).

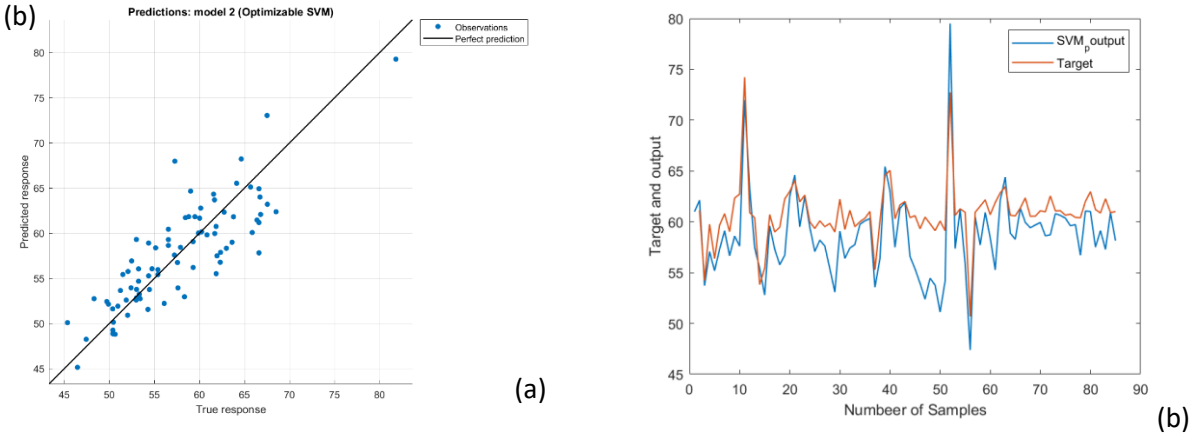

Figure 4. 39 (a) Predicted vs actual (b) Comparison between target and SVM output.

4.7.5 Adaptive neuro-fuzzy inference system method

The ANFIS model was applied in a trial-and-error method to obtain the best outputs in the training process. The best validation performance of the ANFIS model was obtained in RMSE = 0.001 from 2 epochs and R^2 = 0.73. The AUC results (Table 4.32) show ANFIS model performs better than the ANN model. The respective soil erosion susceptibility maps and the area covered by each soil erosion categories are shown in Figure 4.40 and Table 4.31.

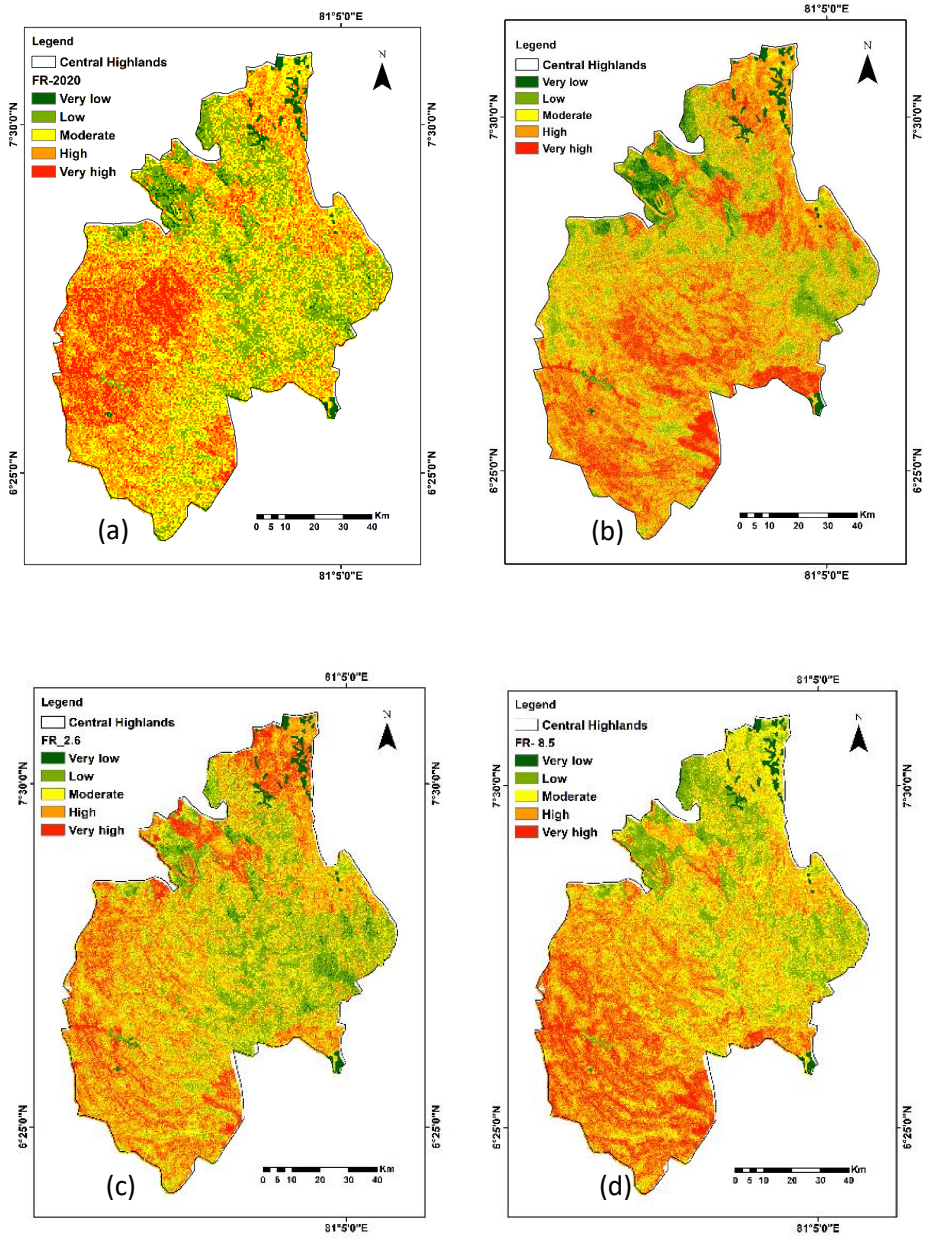

Figure 4. 40 Soil erosion susceptibility map for (a) 2020 based on gauged rainfall data, (b) 2020 based on satellite rainfall data (c) RCP 2.6 and (d) RCP 8.5 in 2040 respectively.

Table 4. 31. Area covered by the soil erosion category from the ANFIS model.

	2020		2040	
Soil erosion Class	**Gauge RF Area (km2)**	**Satellite RF Area (km2)**	**RCP 2.6 Area (km2)**	**RCP-8.5 Area (km2)**
Very Low	282.76	44.65	527.06	45.8
Low	1572.75	1835.24	1671.09	1658.6
Moderate	2719.98	1724.49	1605.08	1560.0
High	4116.70	3870.92	3772.82	3744.5
Very High	1807.81	3024.70	2923.95	3491.1
	10 500.00	10 500.00	10 500.00	10 500.00

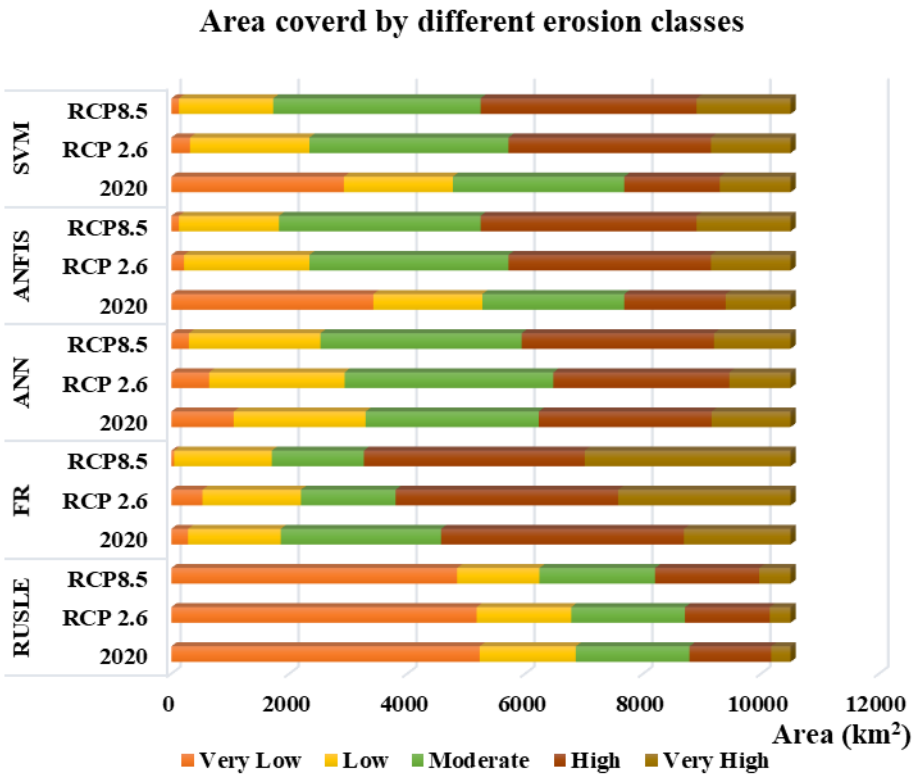

Figure 4. 41 The areas vulnerable to soil erosion by different erosion models.

Figure 4.41 indicates the comparison of different models' predictions for soil erosion vulnerable classes. Although the areas covered by different soil erosion susceptibility classes are varied, one thing is prominent. The areas covered by very high and high susceptibility classes under projected RCP 8.5 are increasing in 2040 with all the models.

4.7.6 Validation of susceptibility maps

Figure 4.42 and Table 4.32 indicate the model efficiency obtained from ROC and AUC analysis. Findings of the analyses revealed all five models employed in this study met the requirement of a threshold value of the ROC curve. The highest AUC values were

obtained for ANFIS and SVM models. The SVM works better than both ANFIS and ANN in terms of AUC values as well as standard error (Table 4.32). The ANN and FR methods received the lowest accuracy levels. A summary of the models AUC values is shown in Table 4.32.

Table 4. 32. The model performance using AUC

Test Result Variable(s)	Area under the curve	Std. Error[a]	Asymptotic Sig.[b]	Asymptotic 95% Confidence Interval	
				Lower Bound	Upper Bound
ANFIS_2020	.891	.089	.194	.716	1.000
ANFIS_RCP2.6	.957	.049	.129	.860	1.000
ANFIS_RCP8.5	.891	.102	.219	.670	1.000
SVM-SE2020	.891	.089	.194	.716	1.000
SVM-RCP2.6	.891	.089	.194	.716	1.000
SVM-RCP8.5	.891	.089	.194	.716	1.000
ANN_2020	.826	.126	.279	.579	1.000
ANN_RCP2.6	.870	.102	.219	.670	1.000
ANN_RCP8.5	.891	.089	.194	.716	1.000
FR_2020	.870	.089	.194	.716	1.000
FR_RCP2.6	.783	.150	.348	.489	1.000
FR_RCP8.5	.783	.150	.348	.489	1.000

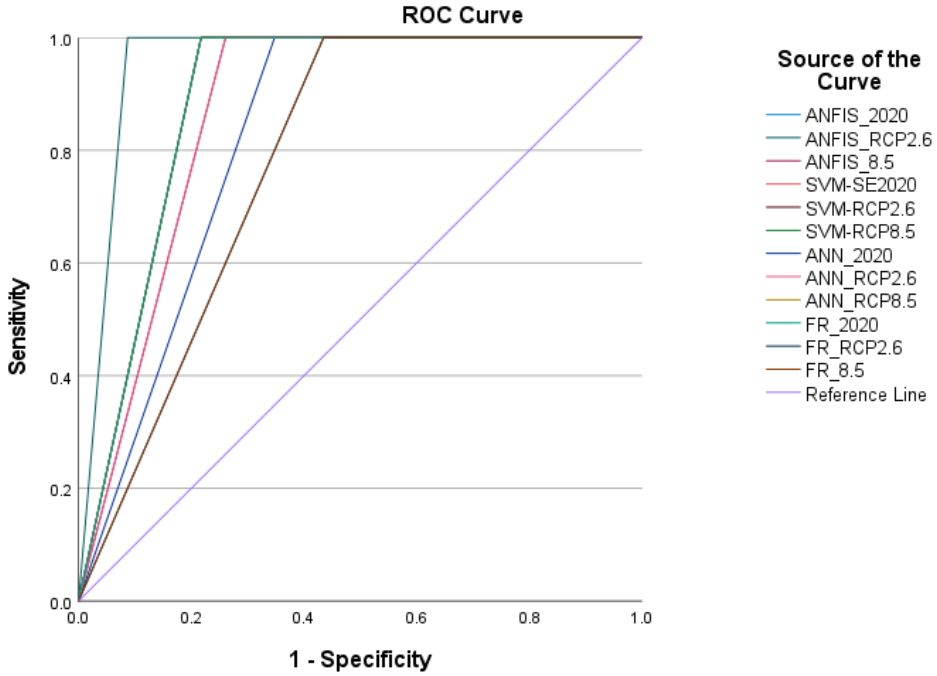

Figure 4. 42 Model validation from ROC curve.

4.7.7 Relative importance of the soil erosion conditioning factors

The results of calculation on variable importance indicate that rainfall, soil erodibility, slope length, and steepness are the most responsible factors for soil erosion susceptibility in this study area. Figure 4.43 illustrates the relative importance of soil erosion conditioning factors.

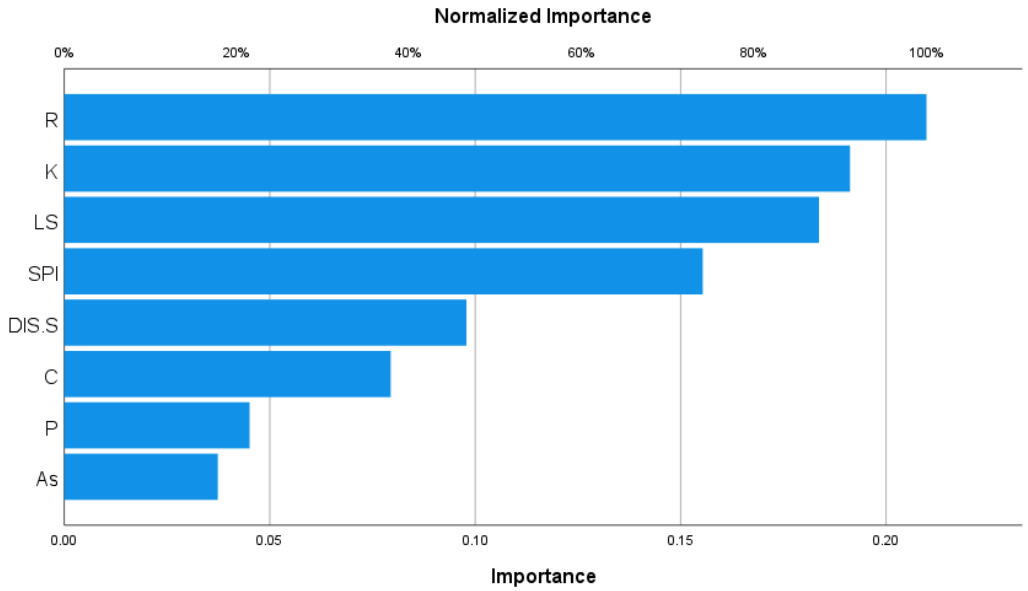

Figure 4. 43 The relative importance of soil erosion conditioning factors.

This study identified rainfall and soil erodibility as the most important conditioning factors for soil erosion hazards in this study area. This study found that increasing rainfalls influence the soil erosion runoff in the western slopes of the Central Highlands. They have observed rainfall variation in terms of increasing rainfall intensity and average rainfall. Burt and Weerasinghe (2014) had investigated the main drivers of changes in daily precipitation in Sri Lanka. They found sea surface temperature of the Pacific and Indian Ocean drives the atmospheric changes of regional climate change. Researchers observed that an increase of one degree Celsius in the global mean temperature increases water holding capacity in the atmosphere by 7%, resulting in intense rainfall and a vigorous hydrological cycle (Mullan et al., 2012). Hence, the areas with steep slopes and higher altitudes are more vulnerable to climate variability. Specifically, the western part of the Central Highlands will be more susceptible to soil erosion in future. Therefore, considerable attention should go to strengthening soil conservation measures over the highlands continuously. The potential risk of soil erosion and changing rainfall patterns should be further studied.

Soil erodibility mainly depends on the chemical and physical structure of the soil (De Rouw and Rajot, 2004). The Central Highlands are covered by 73% of Red-Yellow Podzolic soils which have relatively high soil erodibility values. Increasingly, lands are exposed to poor agricultural practices resulting in poor soil organic matter content. That implies a loss of soil structure (chemical and physical) and subsequently less stable aggregates (De Rouw and Rajot, 2004). This study found the agricultural land areas were increasing significantly from 2000 to 2019 in the Central Highlands with increasing soil erosion rates. This indicates more attention should go to improving the soil condition using appropriate measures, such as increasing the organic matter content, especially in highly vulnerable areas for soil erosion. In addition, this research proposes to conduct research on soil erodibility assessment under different land uses. The results will indicate the critical soil organic matter content values in different land uses.

The present study contributes by addressing a knowledge gap in a methodological approach for the spatiotemporal process to predict soil erosion susceptibility in the Central Highlands of Sri Lanka under different climate scenarios. This research gives a novel approach of assessing five different soil erosion hazards models and climate change scenarios with geoinformatics tools. Many researchers have combined a two or more models. However, none of them has employed these five models together for the projection of the soil erosion hazards with climate change scenarios using geoinformatics techniques and evaluating the best model performance for the projection. This study introduces a methodological improvement by combining projected rainfall erosivity under RCP scenarios as conditioning factors for empirical equation, statistical, machine learning and hybrid machine learning techniques to predict soil erosion. In addition, this research investigated the variation of satellite data and real ground situations. Results of this study provide scientific insights indicating a higher degree of vulnerability than the model prediction, which badly affects sustainable land and farming system management. These insights are critical in developing food security and sustainable land management strategies. In other words, food security and sustainable land management are two paramount aspects in achieving sustainable development goals (SGDs) and 2030 agenda: particularly in achieving goals 2 and 15 (Zero hunger and Life on land). Hence, this research contributes to developing strategies in achieving SGDs of the United Nations.

This study identified that soil erosion rates will increase from 4% to 22% in 2040, compared to 2020, under these predicted climate scenarios. The results revealed the current soil erosion rate is 11.8 t/ha/yr (2020) in the Central Highlands. The satellite-based rainfall erosivity shows a relatively low value than gauged rainfall erosivity. Hence, the ground-based soil erosion rate is higher than the value of satellite-based measurement. This is primarily due to the low spatial resolution of the satellite images. However, satellite and gauge rainfall data have a better correlation (r=0.62, KEGs =0.41). Researchers have identified that tolerable soil erosion loss is around 1-2 t/ha/yr in the Central Highlands of Sri Lanka (Somasiri et al., 2021). According to the projected RCP 8.5 scenario, all models employed in this study indicates soil erosion susceptibility and vulnerability are increasing by 2040. In other words, the risk of soil erosion will be high in the Central Highlands by 2040.

Increasing temperature and CO_2 are correspond to the RCP pathway. These RCP pathways show the most significant climatic variability with the highest greenhouse gas emissions. These model results imply the importance of reducing carbon emissions with international collaborative efforts. The above findings are in line with the study of Zheng et al. (2018). These estimated future climate and runoff projections across South Asia, including Sri Lanka, use a consistent method by 42 General circulation models (GCMs) in CMIP5. The modelling results indicate that projected runoff will increase throughout the region. The change in runoff is mainly driven due to the change in precipitation. The median projection indicates mean annual runoff increases by 20–30% in the Indian sub-continent for 2046–2075 relative to 1976–2005.

It is important to understand the climate change risk of soil erosion in terms of physical, transitional, and human risk and their possible consequences for better preparedness. A recent study found that high intensive rainfall caused sudden and long-travelling landslides in the Central Highlands of Sri Lanka (Dang et al., 2019). The above area received 446.5 mm of heavy rainfall within the days from May 14 to 17 in 2017. This soil mass movement caused more significant damage in Aranayake area by killing 127 people and demolishing 75 houses. In addition, almost all the houses in this area are still at risk of future landslides. Perera et al. (2018) have observed that 52% of household incomes were generated from agricultural activities from homegarden and plantation agriculture. Due to this massive landslide, the social and economic systems were badly impacted both

on a household level as well as the country's economy. This implies the possible risk of soil erosion hazards, which will enhance landslide incidences and damage to agricultural activities and livelihoods. It will also threaten the lives of peoples and may give rise to the migration of peoples to other areas. Hence, the potential risk of future environmental problems is important by assessing the impact of extent, frequency, and magnitude of soil erosion hazards to reduce the negative consequences.

Socio-economic factors were not incorporated into this analysis. However, these factors may influence soil erosion over the next century. These projections could be achieved when the mitigation targets of RCPs are combined with the Shared Socio-economic Pathways (SSPs) in the Coupled in Model Intercomparison Project Phase 6 (CMIP6). Almazroui et al. (2020) researched the latest CMIP6 dataset to examine the projected changes in temperature and precipitation over six South Asian countries. The average annual precipitation is projected to increase by 25.1 % in Sri Lanka under the SSP5-8.5 scenario by the end of the twenty-first century. The projected temperature shows to increase by 1.2 (0.7–2.1) °C, 2.1 (1.5–3.3) °C, and 4.3 (3.2–6.6) °C under the SSP1-2.6, SSP2-4.5, and SSP5-8.5 scenarios, respectively over South Asia.

4.7.8. LSTM model

This further analysis was executed to predict the rainfall using the LSTM model, a deep learning method. In order to obtain an optimum number of training samples, several attempts were made by the trial-and-error approach. The number of data sets were changed from 0.5 to 1 to reduce the impact of the number of training data sets on forecasting results. The optimum partition for the training and test dataset was obtained as 9:1 (Figure 4.44). The first 90% of the sequence data were used to train and test the last 10% dataset. The outputs were given for 36 months (3 years) forecast for five agro-meteorological stations.

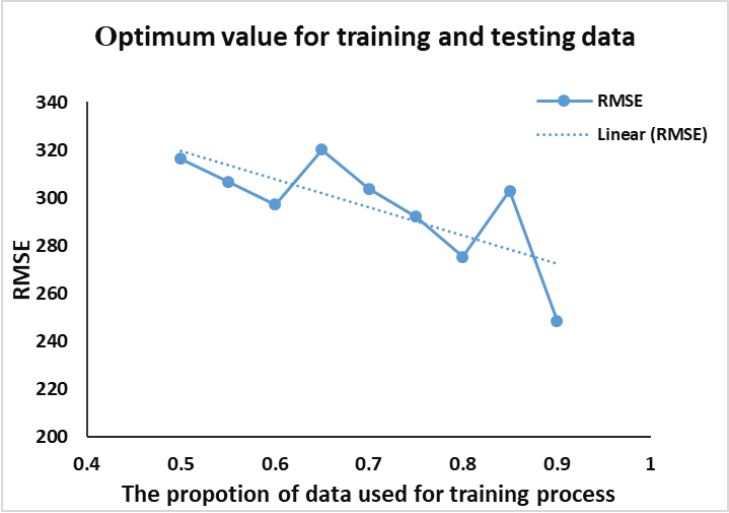

Figure 4. 44 The root means squire error (RMSE) values of LSTM different training datasets.

4.7.8.1. LSTM forecasting results of five rainfall stations

The results of LSTM rainfall forecasting outputs for five stations are depicted in Figure 4.45 and Figure 4.46. The number of hidden layers and maximum epochs were conducted to obtain the optimum output values. The forecasting results indicate LSTM was able to predict rainfall using time-series data over 36 months. The RMSE values for model outputs in five agro-meteorological stations are shown in Table 4.33. The minimum value of RMSE was obtained for the Kundasale agro-meteorology station. These results show the LSTM model is capable of adequately forecasting rainfall for a short period of time.

Bandarawella (a)

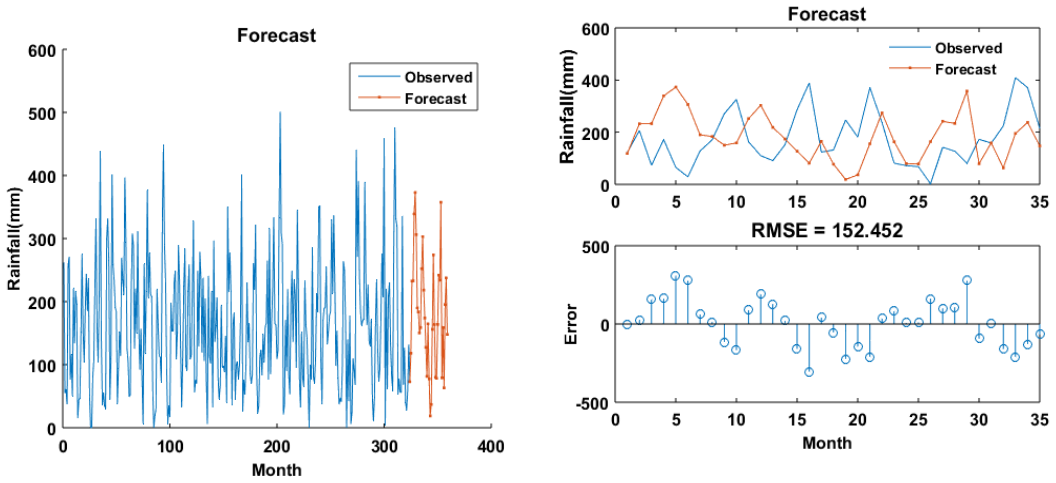

Nuwara Eliya (b)

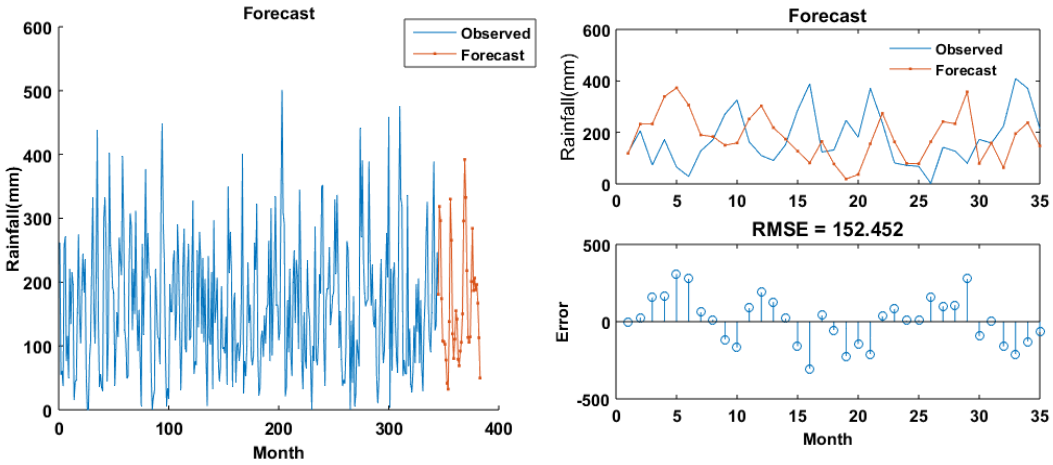

Kundasale

(c)

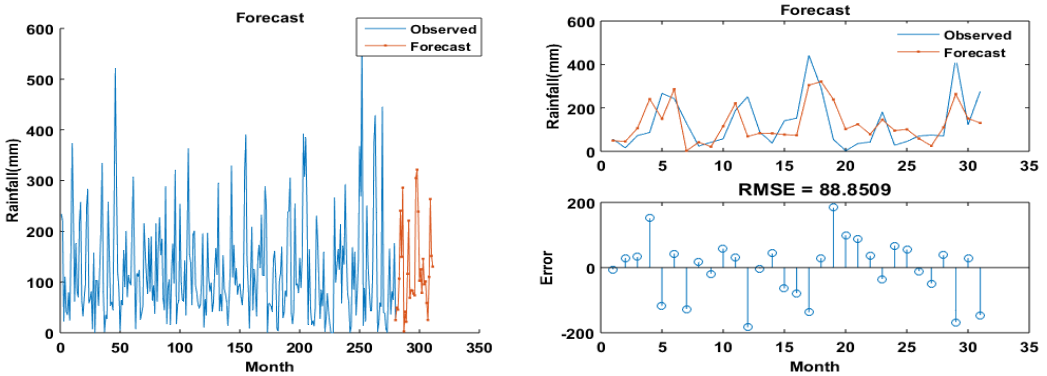

Figure 4. 45 Observed and LSTM predicted rainfall at five gauge stations (a) Bandarawela (b) Nuwara Eliya (c) Kundasale.

Peradeniya (d)

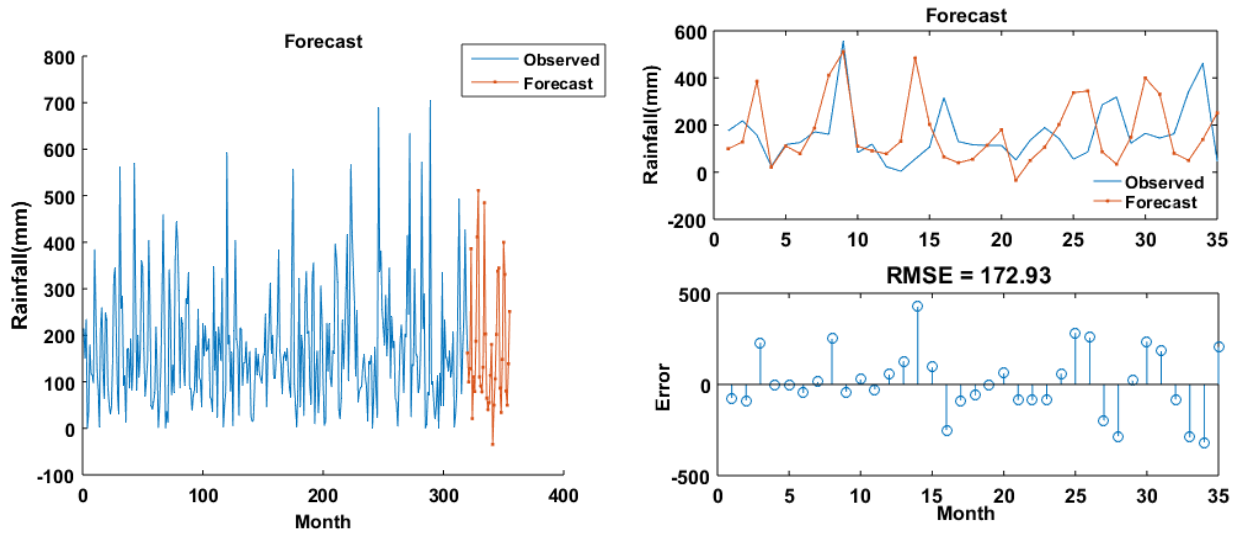

Ratnapura (e)

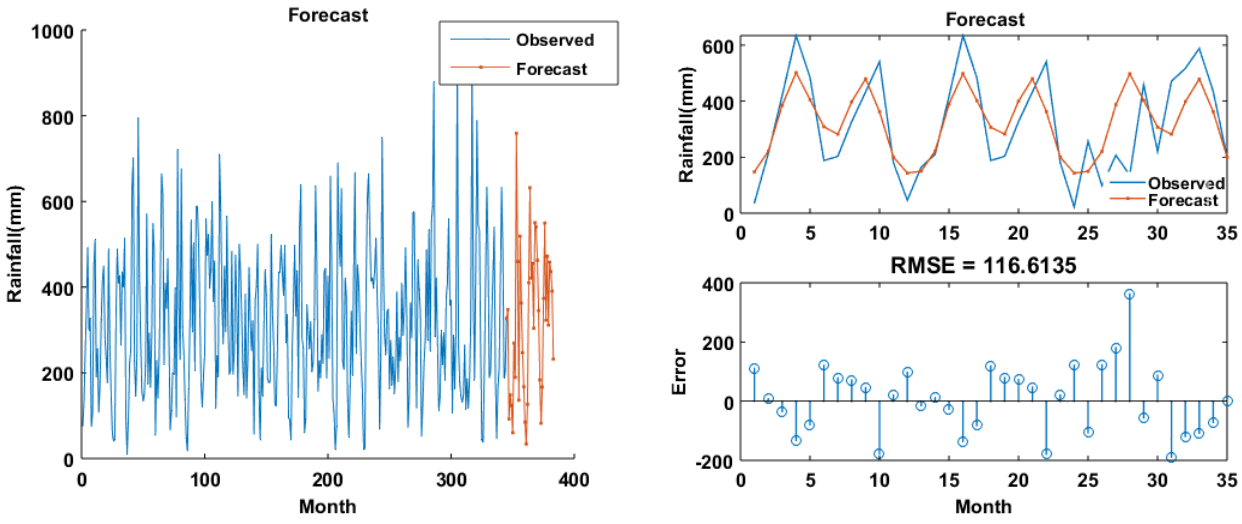

Figure 4. 46 (continue**)** Observed and LSTM predicted rainfall at five gauge stations (d) Peradeniya and (e) Ratnapura.

Table 4. 33. LSTM summary results of five agro metrological stations.

Agro-met. station	No of the Hidden layers	Max Epochs	Training: Testing	RAMSE	Model output annual rainfall		
					2022	2023	2024
Bandarawela	200	300	9:1	153.2	1589.7	1486.7	1582.9
Nuwara Eliya	200	300	9:1	124.1	2338.3	908.3	1402.3
Kundasale	200	350	9:1	88.85	1431.7	1457.1	1433.8
Peradeniya	250	350	9:1	172.9	2301.5	1878.3	3199.7
Ratnapura	250	350	9:1	116.6	3217.3	2912.9	4594.2

4.7.8.2 Rainfall erosivity map

The rainfall erosivity was estimated using equation 3.8 using predicted rainfall data from the LSTM model. The rainfall erosivity map was developed for the Central Highlands of Sri Lanka. The resulting rainfall erosivity map indicates the highest rainfall will be received in Ratnapura station in the next few years, which is located in the western part of the Central Highlands of Sri Lanka. Figure 4.47 indicates the average annual rainfall and rainfall erosivity map for 2024.

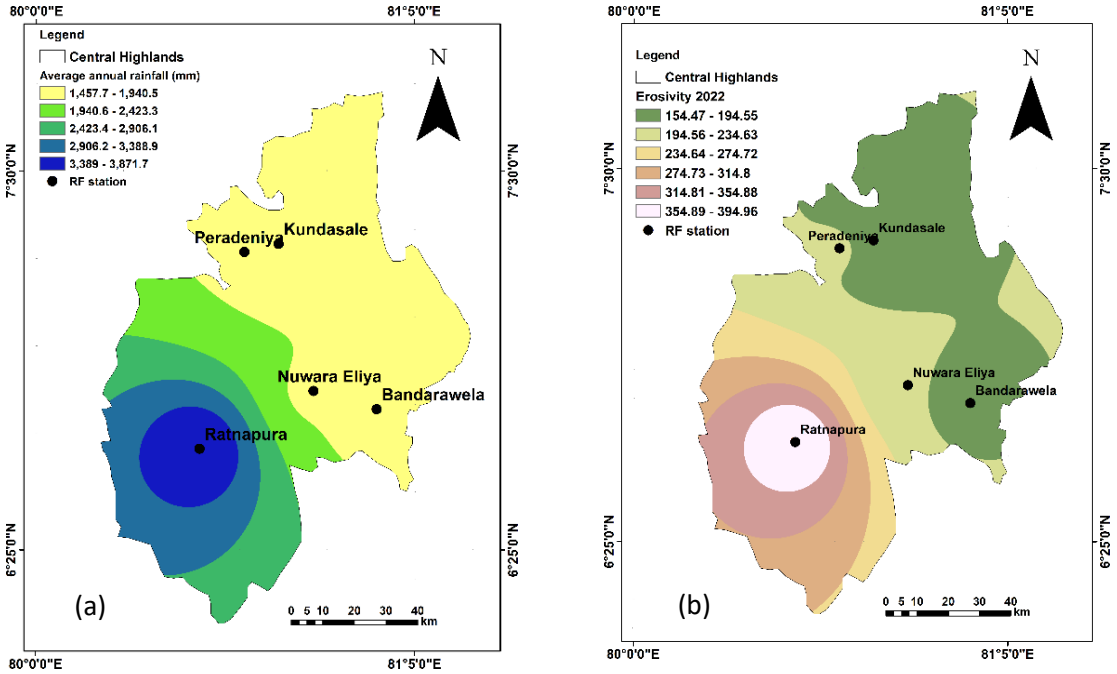

Figure 4. 47 The spatial distribution of (a) observed mean annual rainfall and (b) corresponding predicted rainfall erosivity map for 2024 using the LSTM dataset.

4.7.8.3 Soil erosion susceptibility map for 2024

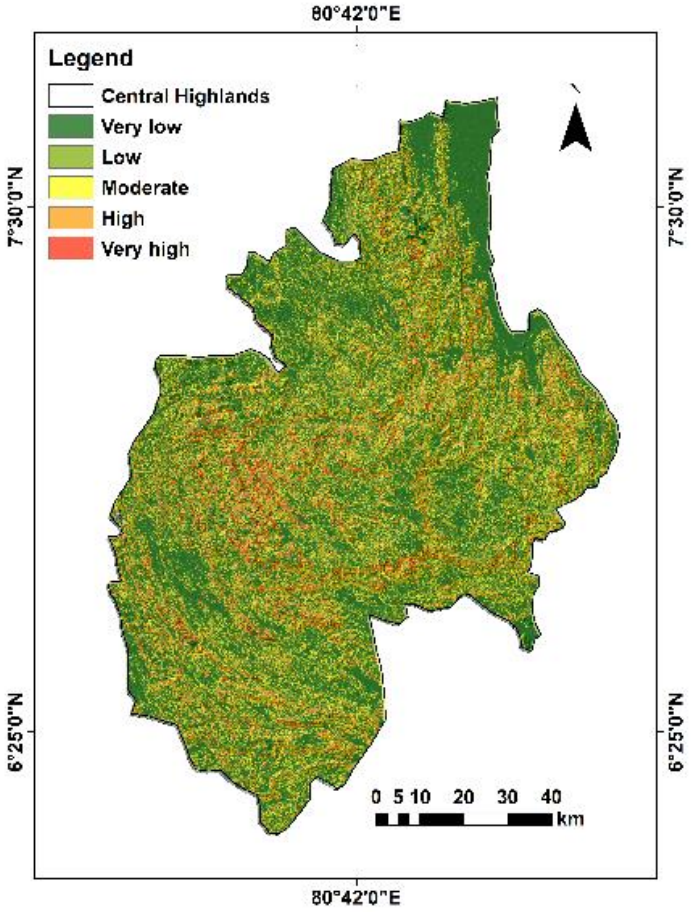

Figure 4. 48 Spatial distribution of soil erosion susceptibility map in 2024.

The rainfall erosivity map was employed to obtain the spatial distribution of soil erosion susceptibility, and Figure 4.48 indicates the soil erosion susceptibility map in 2024. The average annual soil erosion rate for 2024 has been predicted as 11.92 t/ha/yr for the Central Highlands of Sri Lanka. The area under moderate to very high soil erosion susceptibility classes is around 3,503.17 km^2 (33%). However, researchers identified the tolerable soil erosion loss is around 10.0 t/ha/yr (Borrelli et al., 2017). Table 4.34 indicates the soil erosion susceptibility classes and their distribution.

Table 4. 34. The details of soil erosion hazard classes, rates, and area distribution in 2024.

Class	Soil erosion rate	Area(km^2)	The total land area as a percentage
Very Low	<5	5300.38	50.48
Low	5-10	1695.42	16.15
Moderate	10-20	1900.17	18.10
High	20-50	1312.95	12.50
Very High	50<	291.08	2.77
Total land		10500.0	100
Average annual soil erosion (t/ha/yr)		**11.92**	

In this research, C and P factors were derived based on the land-use and land-cover map developed for 2019. The land cover change may also affect soil erosion. The susceptibility map of the Central Highlands indicates that the north-western part of the highlands will be more vulnerable compared to other areas. This study found the north-western side of the Central Highland is more vulnerable to soil erosion and landslides. More than 48.05% of this land area is covered by cropping area, and most of the landslides occurred in these cropping areas from 2000 to 2019. Perera et al. (2019) have researched and found soil erosion risk can be minimized by adopting proper land cover in respective vulnerable areas. The area under high and very high soil erosion classes should be prioritized to grow more perennial crops to minimize soil erosion. In addition, government authorities should encourage the farmers to initiate appropriate soil and water conservation measures to reduce soil erosion hazards, such as the construction of contour and leader drains to remove excess water from the lands, construction of stone bunds, contour plantings etc.

4.7.8.4 Model performance and model sensitivity analysis

Accurate models are vital for soil erosion susceptibility prediction, hazard impact assessment, and to assess the potential effects of climate change on soil and water resources. Most of soil erosion modelling presents a challenge. In recent years, soil erosion susceptibility studies have been increasingly conducted using machine learning techniques, especially in gully erosion susceptibility studies (Arabameri et al., 2020). Some researchers found the performance of the models can be improved with an increase in the number of input parameters (Ouma et al., 2021). Hence, more input data such as humidity, cloud cover, temperature, wind and pressure can be included in the future assessment for better performance. In Sri Lanka, machine learning techniques were used

for forecasting rainfall data on several occasions, such as artificial neural networks (ANN) (Kumarasiri and Sonnadara, 2008). However, the ANN model was able to predict one year ahead with a success rate of 80%. Compared to this model, the LSTM was able to predict 36 months (3 years) with an accuracy of 93%. Figure 4.49 shows the AUC of the LSTM model.

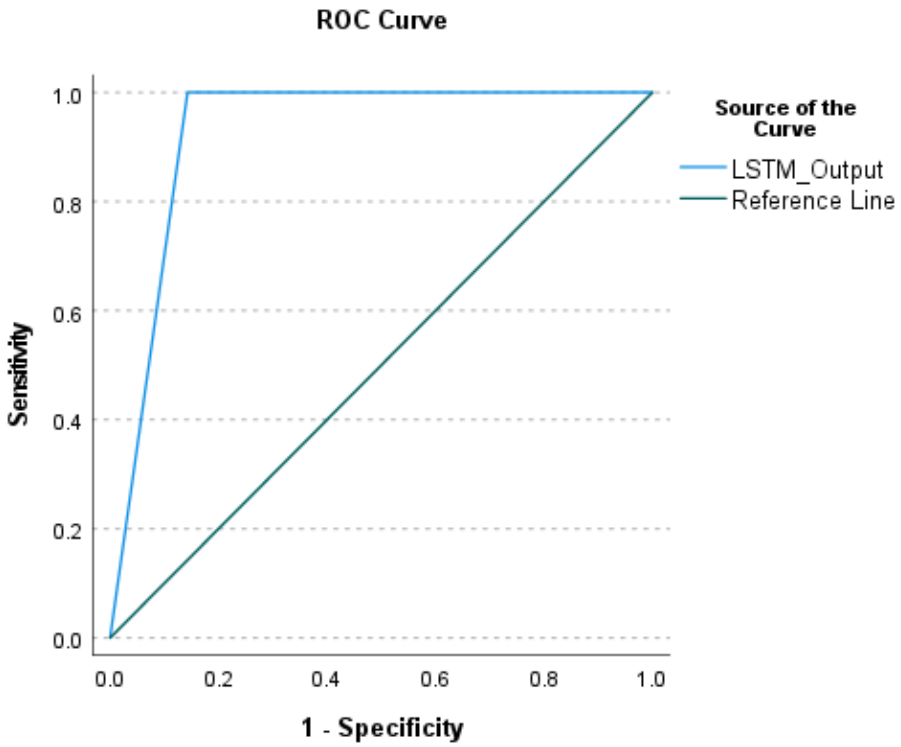

Figure 4. 49 The figure illustrates the area under the curve (AUC) of the Soil erosion susceptibility map for the year 2024.

The LSTM has been used for time series forecasting for many other applications; however, it has rarely been used for soil erosion or gully erosion assessment. The present study predicted the rainfall data for three years using the LSTM model and incorporated the resulting erosivity value into the RUSLE model. The LSTM model is as an appropriate tool for short term forecasting of soil erosion. The results of the research can be used to identify the highly vulnerable areas for soil erosion and plan priority actions for soil erosion mitigation purposes. Different model outputs can be tested to enhance the predictability capabilities further. In addition, rainfall is one of the major causes of landslide vulnerability in the Cantal Highlands of Sri Lanka. Therefore, accurate rainfall prediction may help reduce the damage and prevent landslide vulnerability.

4.9 Summary

In objective 1, first, the results of LULC classifications were presented, identified the cropping land area from the other land uses and then described the results of the LULC change. The support vector classification model provided the best performance for LULC classification. The results of the LULC indicate changes in increasing agricultural and built-up areas while decreasing dense forest and less dense forest from 2000 to 2019.

The LULC classification was employed to demarcate the farming systems. This study proposed a novel method to delineate farming systems using agro-ecological regions. The cropping area under each agro-ecological region is considered as a farming system. There are 34 farming systems identified from this methodology. These farming systems were used to identify soil erosion hazards and vulnerability.

The RUSLE integrated geo-informatics tools were used to analyse the soil erosion hazards in this study. Findings indicate that average annual soil erosion has increased by 9.08 to 11.08 t/ha/year from 2000 to 2019, respectively. Very low and low soil erosion hazard classes have been reduced by 354 km^2 and 178 $km^{2,}$ while moderate, high, and very high soil erosion hazard classes have been increased by 80 km^2, 286 km^2 and 166 $km^{2,}$ respectively. The soil erosion hazards, such as landslide incidence also increased during this period.

The findings of the case study in the Sabaragamuwa Province indicate the relationship between the soil erosion hazards and land-use classes. The assessment of LULC change shows a higher correlation between land-use change and landslide incidents. This case study considered RDZ a significantly important hydrological unit for soil conservation.

Vegetation index: NDVI, EVI and SAVI were used to carry out the time series analyses to observe the relationship of crop diversity change and soil erosion. The vegetation index values show an increasing trend over the period from 2000 to 2019 in the Central Highlands. Crop diversity was measured using the Shannon diversity index. Remote sensing derived, NDVI and EVI indices provide the best solution for monitoring vegetation cover and plant diversity change. RUE and RESTREND combined with a regression approach were applied to partition the soil erosion from human and climate-induced land degradation. The RUE and RESTREND analyses revealed that climate-induced soil erosion is more responsible for land degradation in these farming systems

and is a threat to sustainable food production in the farming systems of the Central Highlands.

In objective 2, the findings of innovative trend analysis, modified Mann Kandel and Sens' slope tests imply an increase in the average annual rainfall except in Nuwara Eliya station. However, a significant increase in rainfall intensity could be observed in Nuwara Eliya. The increasing rainfall erosivity can influence the soil erosion hazard. The average annual rainfall has increased in the western part of the Central Highlands. However, crop diversity has been decreasing in farming systems, namely wet zone low country (WL1a) and wet zone mid-country (WM1a), in the western part of the Central Highlands. This indicates WL1a and WL1a farming systems are becoming more vulnerable to soil erosion from 2000 to 2019.

The rainfall variation revealed a significant increasing trend. This study found a positive correlation between average annual rainfall and soil erosion. Further to this, a significant correlation was observed between soil erosion and rainfall, soil erosion and landslide frequency ratio, as well as landslide frequency ratio and rainfall erosivity. Most of the extreme indices such as increasing wet and dry days, R99p percentile and SDII show rainfall variation with the present climate in the Central Highlands of Sri Lanka. Hence, these findings revealed the vulnerability of farming systems is increasing in the Central Highlands.

In order to achieve objective 3, this study proposed an efficient framework to evaluate ecologically viable and economically sound farming systems using a matrix-based analytic hierarchy process (APH) and weighted linear combination method with geo-informatics tools. Results reveal that more than 50% of farming systems demonstrated moderate status in terms of ecological and economic aspects. However, two vulnerable farming systems on the western slopes of the Central Highlands, named WL1a and WM1a, were identified as very poor status. These farming systems should be a top priority for restoration planning and soil conservation to prevent further deterioration. The findings indicate that a combination of the ecologically viable (nine indicators) and economically sound (four indicators) criteria are a practical method to scrutinize farming systems and decision making on soil conservation and sustainable land management.

To achieve objective 4, this study employed six predictive models: RUSLE, FR, ANN, SVM, ANFIS and LSTM to quantify and demarcate the spatial vulnerability of soil

erosion in the Central Highlands of Sri Lanka. Soil erosion susceptibility was analysed using eight conditioning factors to observe the soil erosion vulnerability for the present situation and 2040 under projected RCP 2.6 and RCP 8.5 climate scenarios. The results indicate rainfall and soil erodibility are the most important factors for vulnerability assessment. The frequency ratio method is the least accurate model for predicting soil erosion vulnerability for 2040. The probability maps of the ANFIS and SVM methods provide accuracy with 89% model predictions. The results of these models' outputs indicate farming systems in the Central Highlands will be more vulnerable to soil erosion under climate scenarios RCP 8.5 in 2040. The prediction of soil erosion rate in 2040 suggests 12.4 t/ha/y under RCP 8.5, which increases the recommended threshold in tropical areas or tolerable soil loss value globally. In addition, the combined approach of the LSTM and RUSLE model based soil erosion probability map provides a satisfactory outcome for soil erosion susceptibility with the highest accuracy value of 93% (AUC = 0.93) in the Central Highlands of Sri Lanka. Findings suggest more soil conservation with short and long-term strategies to achieve the SGDs in the 2030 UN agenda.

Finally, the findings of this research indicate the farming systems in the western part of the Central Highlands are more ecologically and economically degraded and highly vulnerable to future climate hazards. Therefore, considerable attention needs to improve the present condition and reduce future vulnerability.

CHAPTER 5

CONCLUSION AND RECOMMENDATIONS

5.1 Overview

The research presented in this thesis investigated the impact of soil erosion hazards and crop diversity changes with rainfall variation in farming systems of the Central Highlands. The study area is located in one of the most vulnerable for climate hazards countries: Sri Lanka. This study employed remotely sensed data in a geo-informatics environment to assess and identify the vulnerability of soil erosion hazards by employing modelling, simulating, and predicting approaches. The present situation of soil erosion in the farming systems was evaluated against economic and ecological aspects by employing a matrix-based approach. Time series analyses were used to observe the soil erosion rate, soil erosion hazards, plant diversity change and rainfall variation. The correlation of each variable (soil erosion, soil erosion hazards, plant diversity and rainfall) was measured with the Pearson coefficient. The vulnerability of the farming system was assessed using several models (statistical, empirical and machine learning methods) with eight conditioning factors, including rainfall erosivity in future climate scenarios. The model simulation was evaluated to optimise the system performance. Finally, the comparison was made between present and future projected situations in the year 2040 in terms of soil erosion hazards. The resilience development actions were also proposed to achieve the SDGs.

This research addressed the research gaps in the literature, selecting the most appropriate methods to identify soil erosion at farming system levels using geo-informatics tools. Research on the spatial and temporal pattern of soil erosion and crop diversity changes against the present rainfall variation was a research need. This research need was addressed by developing new techniques and strategies for landscape evaluation to enhance productivity in a sustainable manner. Further, there were no satisfactory real-time data mining techniques using geo-informatics for effective analysis to solve prevailing issues on soil erosion and forecast soil erosion hazards for improving the environmental condition sustainably. The present study introduces a novel geo-informatics delineation approach to identify farming systems in a region. In addition, it introduces a combined approach of integrating LULC, soil erosion hazards, and crop

diversity change with rainfall variation in time series analysis for soil erosion hazard detection in the farming systems using geo-informatics tools. The ecological and economic aspects of farming systems were evaluated with a matrix-based AHP, and weighted linear combination method. A spatio-temporal process (using statistical and machine learning techniques) was proposed as a soil erosion hazard prediction for two RCP future climate scenarios. Furthermore, this research addressed the gap in knowledge by applying the LSTM deep-learning model on soil erosion susceptibility to state-of-the-art research.

There are several important areas in this study that make an original contribution to the body of knowledge; extraction of farming systems based on the agro-ecological regions, application of rain use efficiency and trend analysis for land degradation, and residual trend analysis to distinguish the climate-induced land degradation at a farming system level. This study provides a methodological contribution by introducing a novel approach to the delineation of farming systems by employing the cropping area under each agro-ecological region together with geo-informatics to identify farming systems. Thereafter, this research provides several theoretical contributions by integrating land-use and land-cover change, soil erosion hazards, and crop diversity change with rainfall variation in time series analysis for soil erosion assessment in farming systems. This combined spatiotemporal modelling approach further enables the partitioning between human and climate-induced land degradation. The study further employed a new approach by combining three methods: the landslide frequency ratio method, soil erosion severity, and land-use change assessments at the RDZ level for a deep investigation of soil erosion hazards. The RDZ is a significantly important hydrological unit for soil conservation.

This research proposed a matrix-based AHP and weighted linear combination method together with the geo-informatics approach to evaluate ecologically viable and economically sound farming systems, which is a practical method for data-scarce regions. Indices and matrices were developed with the perspective of economic and ecological measurement of farming systems against soil erosion hazards. Finally, several modelling approaches, such as RUSLE, FR, ANN, ANFIS and SVM models, were employed with geo-spatial technology to assess and predict soil erosion in farming systems under RCP 2.6 and 8.5 climate scenarios. In addition, the LSTM method was implemented and used to simulate early detection and prediction of soil erosion hazards.

Moreover, this study provides comprehensive scientific insights into sustainable land and farming system management. These insights are critical in developing strategies to ensure food security and sustainable land management. In other words, food security and sustainable land management are the two paramount aspects of achieving sustainable development goals (SDGs) in the 2030 agenda: particularly for achieving goals 2 and 15 (Zero hunger and Life on land). Hence, this research contributes to developing strategies for achieving SGDs of the United Nations.

The significance of this study implies a better comprehension of soil erosion hazards brought on by rainfall variation and crop diversity changes through remote sensing applications, along with the formulation of strategies and mitigating actions for climate risk for better management of farming systems and risk reduction. The main conclusion of this research indicates that soil erosion hazards are increase with increasing rainfall and decreasing crop diversity. A few farming systems, particularly WL1a and WM1b farming systems (covering a substantial land area in the Central Highlands), are in the very-poor status from an ecological and economic perspective and are predicted to be more vulnerable in 2040 under predicted future climates and will worsen under the climate scenarios RCP 8.5.

The conclusion of each objective is given in the following sub-sections.

5.2 Conclusion of objective 1

The first objective was to assess of soil erosion hazards and crop diversity changes in different farming systems in the Central Highlands of Sri Lanka. This study employed the time-series segmentation of LULC change, soil erosion hazards, crop diversity change, and rainfall variation from 2000 to 2019. The results of the LULC analysis indicate agricultural lands (15.4%) and built-up areas (2.35%) have been increasing while reducing the dense forest (14.5%) and open forest cover (5.8%). Soil erosion has increased from 9.08 Mg/ha/yr to 11.08 Mg/ha/yr from 2000 to 2019. The stratified continuous monitoring of LULC and specific performance soil erosion changes over the period allowed for more specific early warning bulletins/adaptation strategies to be prepared.

A case study was conducted in the Subaragamuwa Province in the western part of the Central Highlands to further investigate the soil erosion hazards. The case study focused on assessing soil erosion hazards using the land-use change and landslide frequency ratio

method. The study found that freely available multi-temporal satellite data can be successfully employed for land-use mapping and change detection, subsequently providing data for soil erosion hazard modelling in a GIS environment. The proposed approach helped to effectively produce landscape vulnerability assessment and prioritise the area for soil conservation as part of the sustainable land-use management process. This study revealed substantial evidence of the correlation between land-use change and landslide incidents through the landslide frequency ratios. Furthermore, the highest landslides frequency ratios were found for A-2, A-3, and A-9 RDZs (WL1a, WM1a), indicating their immediate prioritization for soil conservation. The land-use class of these RDZs is prominently a 'cropping area', such as tea and rubber plantations. The change of forest lands into cultivation areas can be regarded as an important factor of landslide initiation.

The study on crop diversity change in the Central Highlands has indicated a decreasing trend of crop diversity in the WL1a (SHDI from o.45 to 0.41) and WM1a (SHDI from 0.69 to 0.65) farming systems. However, a positive trend of RESTREND was reported in WL1a, WM1a and IU3e farming systems. This evidence proves the effect of human interference on the improvement of vegetation in the WL1a, WM1a and IU3e farming systems. Hence, this research suggests climate-induced soil erosion may be responsible for land degradation in these farming systems. These findings imply the complex relationships among soil erosion, plant diversity change and climate variation. The combined spatial modelling approach provides a better understanding of the ground situation and can predict the situation with a meaningful outcome. Remote sensing derived, NDVI and EVI indices provide the best solution for monitoring vegetation cover and plant diversity change. Overall, these findings are evidence that human-induced LULC change and climate-induced land degradation create significant damage to farming systems that greatly threaten the food production of the Central Highlands of Sri Lanka.

5.3 Conclusion of objective 2

The second objective was achieved by executing the spatio-temporal analysis of rainfall anomaly, SPI and extreme indices such as maximum 1day precipitation, 95p, 99p (very and extremely wet days), SDII and PRCPTOT. Innovative trend analysis was also employed to detect the rainfall variation. Modified Mann-Kendall and Sen's slope tests were employed to detect significant trends in precipitation indices. The findings of this

study show more frequent extreme events, increased rainfall, and erosivity trends in the Central Highland of Sri Lanka. The average annual rainfall has increased in the western part of the Central Highlands, and soil erosion hazards such as landslide incidences also increased during this period.

The innovative trend analysis confirmed the statistically significant increasing rainfall trends except in Nuwara Eliya and Kundasale stations. However, a significant increase in rainfall intensity was found in the Nuwara Eliya area. Most extreme indices, such as increasing SDII, R99p percentile, and wet and dry days indicate rainfall variation with climate change happening in the Central Highlands. The increasing rainfall and erosivity is directly influenced by the soil erosion hazards and triggering landslides incidence. Hence, these findings revealed the increasing vulnerability to soil erosion hazards of farming systems in the Central Highlands.

5.4. Conclusion of objective 3

The work presented here proposes an efficient and simplified framework utilising a matrix-based approach, which couples with geo-informatics technology tools to evaluate ecological viability and economically sound farming systems. The proposed framework has been developed and tested in the Central Highlands of Sri Lanka. The current study considered nine ecological criteria (soil quality, percentage for highly vulnerable areas for soil erosion, drainage density, slope angle, aspect, vegetation cover, precipitation, distance to stream and number of landslides) and four economic criteria (cost of production, population density, distance to market, and distance to the main road). In addition, this study introduces a novel approach to delineate the farming systems based on agro-ecological regions and identifies 34 farming systems. Results revealed that most of the farming systems (more than 50%) demonstrated moderate status in terms of both ecological and economic aspects. However, two farming systems, namely WL1a and WM1a, are very-poor in terms of both ecological and economic aspects. The precipitation and landslide vulnerability are very-high in these two farming systems. Thus, these farming systems are highly vulnerable to soil erosion. Furthermore, the cost of production, distance to the main road, and distance to the major markets are very-high for these farming systems. The population density in the western part is also low compared to other parts of the Central Highlands. Hence, these indicators are critical in these two

farming systems. Therefore, these two farming systems need high priority for restoration plans and soil conservation to prevent further deterioration.

5.5. Conclusion of objective 4

Two assessments were conducted to achieve the objective four. Fist assessment was conducted by focusing on five models: RUSLE, FR, ANN, SVM, and ANFIS, to predict and quantify soil erosion vulnerability in the Central Highlands of Sri Lanka. Soil erosion susceptibility was analysed using eight conditioning factors to observe the soil erosion vulnerability for the present situation and 2040 under projected RCP 2.6 and RCP 8.5 climate scenarios. The results indicate that rainfall and soil erodibility are the most influential factors for hazards vulnerability. The frequency ratio method is the least accurate model for predicting soil erosion vulnerability. The probability maps of the ANFIS and SVM methods provide the highest accurate model predictions (accuracy 89%). The results of these models' outputs indicate farming systems in the western slopes of the Central Highlands will be more vulnerable to soil erosion under climate scenarios RCP 8.5 in 2040. The prediction of soil erosion rate in 2040 suggests 12.4 t/ha/y under RCP 8.5, which increases the recommended threshold in the country and tolerable soil loss value globally (10 t/ha/y).

The second assessment was on the combined approach of the LSTM and the RUSLE model for soil erosion prediction is a new approach. The gauged rainfall data for 32 years (1990-2021) in five agro-meteorological stations were used for the rainfall prediction. The LSTM model was able to predict time series rainfall values for the next 36 months. The predicted soil erosion rate is 11.92 t/ha/yr for 2024 in the Central Highlands. The LSTM predicted soil erosion probability map provides a satisfactory outcome for soil erosion susceptibility with the accuracy value of AUC = 0.93. Hence, this research suggests that the LSTM model has most accurate predictive capability of rainfall data and supports the understanding of the soil erosion susceptibility in the Central Highlands of Sri Lanka.

Finally, the findings of objective 3 indicate that the farming systems, specifically WL1a and WM1a in the western part of the Central Highlands, are very poor in terms of both ecological and economic aspects. The findings of objective 4 indicate these two farming systems are more vulnerable than other farming systems to future climate hazards.

Therefore, considerable attention is needed to improve the present condition of these two farming systems and reduce future vulnerability.

5.6 Implication of the study

The models developed by this study for assessing, evaluating and predicting soil erosion hazards in farming systems can be used for early detection and to reduce the potential adverse impact of climate change and future damages to farming systems. The RDZ is a significantly important hydrological unit for soil conservation. The soft engineering conservation and management practices, such as ecological farming practices, planning, and prioritizing areas for soil conservation to reduce the risk of landslide vulnerability, should have to be considered for a sustainable land-use management system. The proper identification of land-use systems, appropriate soil conservation practices and techniques can help to minimize soil erosion. However, socio-economic factors, such as land ownership problems and the high cost of land preparation, affect farmers who seldom use soil conservation practices in hilly areas. In these matters, the governments can get involved and provide incentives for agriculture and environmental protection.

The analysis of extreme rainfall helps to develop strategies and concepts to mitigate the effects of climate change and helps to understand previous evolution, current and future trends. The findings of this research can be used to develop management and mitigation strategies to build up the resilience in these farming systems to ensure food security in Sri Lanka.

A comprehensive environmental and economic dataset is required to evaluate detailed agricultural land capabilities for decision making in sustainable management. However, in developing countries where resources are scarce, there is a lack of sufficient environmental and economic data. The proposed framework of the matrix-based approach does not have such data requirements. The proposed matrix-based AHP, together with a weighted linear combination method and with the geo-informatics approach, was found to be a practical method to evaluate ecologically viable and economically sound farming systems. This framework and methodology are potentially very beneficial for low-income countries in tropical and sub-tropical regions. This framework could be implemented to generate meaningful results where resources are scarce in regions and countries. The current study highly recommends proper assessment, site-specific soil conservation measures, monitoring and maintenance activities for very

poor to moderate ecologically viable and economically sound farming systems in the Central Highlands. Moreover, the soil erosion hazard and risk maps help understand soil dynamics and predict the impacts to land-use planners, managers, and stakeholders for appropriate decision-making. Therefore, this study suggests that provisions of small grants or microfinance credit systems, education and capacity building programs are essential to improve farm practices and to adopt sustainable farming practices. In addition, appropriate regulations and pre/ post evaluation are essential to maintain the farming systems sustainably.

In addition, the proposed framework could be adapted to any region/ area with minimal modifications as per respective environmental and socio-economic conditions. In terms of policy implications, a priority-based restoration plan can be utilised with resource constraints. The current study enables the development practitioners to recognise the most critical farming systems for priority restoration planning.

The findings of objective 4 in this study provide direction for agricultural planning and management to resilience development and mitigate the potential impact of climate change. Soil erosion susceptibility maps with the vulnerability assessment can be useful for planners and policy-makers with respect to agricultural strategic planning and environmental protection. Quantifying the impacts of climate variability and its effects on soil erosion over the study area is important to assist the land managers in adopting new techniques and conservation strategies to protect and minimize further damages or prevent the occurrence of disasters such as landslides. This research proposes further education and awareness programs on soil erosion and conservation strategies, integrated agro-meteorological advisory services, adaptation measures for climate resilience agriculture, social networking and community-based adaptation as long term - strategies for resilience development on soil conservation. The projected increasing rainfall and subsequently influence increasing runoff and gully erosion. Hence, improving the drainage system to remove excess water from the land may need to protect the soil from runoff. In addition, the construction of rain-shelters such as protected agriculture technology/ poly-tunnel may need to protect crops from intense or erratic rainfall.

Lal et al. (2021) emphasized that sustainable soil management is key to achieving the SDGs. They have highlighted that achieving the SDGs: 2-zero hunger, 3-good health and well-being, 6- clean water and sanitation, 13- climate action, 15 - life on land and 17-

partnership have a direct connection with the soil activities. This research contributes to addressing some of the decision-making challenges to achieve the SDGs in the 2030 UN agenda, such as identifying appropriate method for risk assessment, understanding the location and magnitude of erosion, forecasting changes in soil erosion driven by water, land use, and climate change. These approaches provide a basis for a new direction for future research. Findings suggest implementing soil conservation activities with short and long-term strategies to achieve the SGDs in the 2030 UN agenda. The policy implication of this study provides a direction towards developing strategies for land management and resilience building, guiding future land-use planning for the soil and ecological conservation in areas under high and very high soil erosion categories to protect the farming systems sustainably. Healthy soils maintain the eco-service activities in the farming systems and improve food security in the country.

5.7. Research limitations

In this research, freely available satellite data were used for the analysis. However, cloud-free satellite data were limited for this study area (the Central Highlands). Abenayake et al. (2018) also highlighted that practitioners face challenges when conducting biophysical environmental data collection in regional geographies. Rodrigo-Comino et al. (2020) claimed one of the options for resource limitations is data sharing and more open data access.

The results indicate soil erosion and landslides have a strong relationship. However, this research did not consider some other factors such as the tectonic impact, temperature, and moisture regime changes for the analyses. It would be better to consider the tectonic impact, temperature and moisture regime changes in future studies for comprehensive understanding.

The relationship between plant and water availability is not a simple process, and a fraction of the rainfall becomes available for transpiration and evaporation. An increase in temperature and CO_2 changes may also influence on soil erosion. These parameters should be considered for future studies.

In the current study, satellite data were employed to investigate the plant diversity against soil erosion. However, location-specific crop diversity field data are helpful for validation. Due to COVID restrictions, it was not possible to collect field data.

This study observed that rainfall is a major factor in soil erosion and hazards. This study employed both satellite and ground-based rainfall (five agro-met stations) datasets to derive the results. However, satellite-based rainfall data had coarse resolution. Satellite-based rainfall data covers a larger area as one pixel. Hence, two agro-met stations were covered in one pixel in this study. Therefore, the regional rainfall variation may not be clearly observed. High-resolution rainfall satellite data will reduce this limitation.

This research proposed a matrix-based framework in terms of evaluating sustainable farming systems. From the sustainability perspective, social aspects should be considered together with economic and ecological factors. However, this study did not incorporate social-related data due to a lack of data availability. A socio-economic survey would be beneficial for respective social data and information.

The current study employed a spatiotemporal modelling approach to predict soil erosion hazards using RCP climate scenarios. The socio-economic factors can also include as they may influence soil erosion over the next century. These projections can be achieved when the mitigation targets of RCPs are combined with the Shared Socio-economic Pathways (SSPs) in the CMIP6. The SSP scenarios look at five different ways the world might evolve in the absence of climate policy or how different levels of climate change need mitigation. These projections include socio-economic factors such as population, economic growth, education, urbanization, and the rate of technological development.

5.8. Recommendation for future work

Future research could focus on investigating the pattern of the average soil erosion rate and total estimated soil erosion against LFR at RDZ level, using a statistical method to predict the effect of soil erosion rates on the occurrence of landslide incidents at the RDZ level. Future research could be focused on investigating the total estimated soil erosion against LFR at the RDZ level.

In addition, the factors on geological and tectonic details, such as distance to faults, lithology, and profile curvature, also need to be considered for future studies. Furthermore, high-intensity tropical rainfall has to be continuously investigated with soil erosion hazards. Assessments on soil erosion hazards under various rainfall intensities (i.e., rainfall amount and intensity) can be recommended for further study to observe and find various options to protect the soil from runoff.

Different statistical and machine learning methods can be implemented to predict the impacts of soil erosion hazards at the RDZ level. The model developed by this study can be used for the early detection of soil erosion hazards and to reduce the potential adverse impact of climate change on future damages to farming systems. This approach provides a basis for a new direction for future research such as, utilising remote sensing data for spatio-temporal change detection of soil erosion hazards at the RDZ level. The relationships among the variabilities can be used to implement strategies to reduce risk in future.

In future research, Light Detection and Ranging (LiDAR) data or unmanned aerial data (UAV) can be employed in this study area to conduct more detailed observation on the relationship between plant diversity and soil erosion.

The matrix-based farming system evaluation method proposed in the current research can be implemented in other areas to achieve more information on its efficiency and transferability of performance.

This study suggests future research on spatial distribution patterns and the estimation of soil erosion rates with more field data such as field-level socio-economic data collection to estimate the impacts in the Central Highlands. Further to this, it is important to conduct a more detailed study on the probability of soil erosion with future climate scenarios. The combined Representative Concentration Pathways (RCP) and Shared Socioeconomic Pathways (SSPs) of climate models developed by the IPCC can be employed to develop soil erosion susceptibility mapping in farming systems of the Central Highlands. These studies may help identify every possible way to detect and identify the future risk of soil erosion, develop and adopt mitigation strategies, and implement policy decisions to reduce and support resilience building.

References

Abd Elhamid, A.M.I., Eltahan, A.M.H., Mohamed, L.M.E., Hamouda, I.A., 2020. Assessment of the two satellite-based precipitation products TRMM and RFE rainfall records using ground based measurements. Alexandria Eng. J. 59, 1049–1058. https://doi.org/10.1016/j.aej.2020.03.035

Abdulkareem, J.H., Pradhan, B., Sulaiman, W.N.A., Jamil, N.R., 2019. Prediction of spatial soil loss impacted by long-term land-use/land-cover change in a tropical watershed. Geosci. Front. 10, 389–403. https://doi.org/10.1016/j.gsf.2017.10.010

Abedini, M., Ghasemian, B., Shirzadi, A., Shahabi, H., Chapi, K., Pham, B.T., Bin Ahmad, B., Tien Bui, D., 2019. A novel hybrid approach of Bayesian Logistic Regression and its ensembles for landslide susceptibility assessment. Geocarto Int. 34, 1427–1457. https://doi.org/10.1080/10106049.2018.1499820

Abedini, M., Tulabi, S., 2018. Assessing LNRF, FR, and AHP models in landslide susceptibility mapping index: a comparative study of Nojian watershed in Lorestan province, Iran. Environ. Earth Sci. 77, 405. https://doi.org/10.1007/s12665-018-7524-1

Abenayake, C.C., Mikami, Y., Matsuda, Y., Jayasinghe, A., 2018. Ecosystem services-based composite indicator for assessing community resilience to floods. Environ. Dev. 27, 34–46. https://doi.org/10.1016/j.envdev.2018.08.002

Adornado, H.A., Yoshida, M., Apolinares, H.A., 2009. Erosion Vulnerability Assessment in REINA, Quezon Province, Philippines with Raster-based Tool Built within GIS Environment. Agric. Inf. Res. 18, 24–31. https://doi.org/10.3173/air.18.24

Ahmad, M., Protasov, S., Khan, A.M., Hussain, R., Khattak, A.M., Khan, W.A., 2018. Fuzziness-based active learning framework to enhance hyperspectral image classification performance for discriminative and generative classifiers. PLoS One 13, e0188996. https://doi.org/10.1371/journal.pone.0188996

Alatorre, L.C., Beguería, S., 2009. Identification of eroded areas using remote sensing in a badlands landscape on marls in the central Spanish Pyrenees. Catena 76, 182–190. https://doi.org/10.1016/j.catena.2008.11.005

Alewell, C., Borrelli, P., Meusburger, K., Panagos, P., 2019. Using the USLE: Chances, challenges and limitations of soil erosion modelling. Int. Soil Water Conserv. Res. https://doi.org/10.1016/j.iswcr.2019.05.004

Alilou, H., Rahmati, O., Singh, V.P., Choubin, B., Pradhan, B., Keesstra, S., Ghiasi, S.S., Sadeghi, S.H., 2019. Evaluation of watershed health using Fuzzy-ANP approach considering geo-environmental and topo-hydrological criteria. J. Environ. Manage. 232, 22–36. https://doi.org/10.1016/j.jenvman.2018.11.019

Allen, D.E., Singh, B.P., Dalal, R.C., 2011. Soil Health Indicators Under Climate Change: A Review of Current Knowledge. Springer, Berlin, Heidelberg. https://doi.org/10.1007/978-3-642-20256-8_2

Almagro, A., Oliveira, P.T.S., Nearing, M.A., Hagemann, S., 2017. Projected climate change impacts in rainfall erosivity over Brazil. Sci. Rep. 7, 1–12. https://doi.org/10.1038/s41598-017-08298-y

Almazroui, M., Saeed, S., Saeed, F., Islam, M.N., Ismail, M., 2020. Projections of Precipitation and Temperature over the South Asian Countries in CMIP6. Earth Syst. Environ. 4, 297–320. https://doi.org/10.1007/s41748-020-00157-7

Althuwaynee, O.F., Pradhan, B., Park, H.J., Lee, J.H., 2014. A novel ensemble bivariate statistical evidential belief function with knowledge-based analytical hierarchy process and multivariate statistical logistic regression for landslide susceptibility mapping. Catena 114, 21–36. https://doi.org/10.1016/j.catena.2013.10.011

Ananda, J., Herath, G., 2003. Soil erosion in developing countries: A socio-economic appraisal. J. Environ. Manage. 68, 343–353. https://doi.org/10.1016/S0301-4797(03)00082-3

Anderson, J.R., Hardy, E.E., Roach, J.T., Witmer, R.E., 1976. Land use and land cover classification system for use with remote sensor data. U S Geol Surv, Prof Pap.

Anderson, K., Gaston, K.J., 2013. Lightweight unmanned aerial vehicles will revolutionize spatial ecology. Front. Ecol. Environ. https://doi.org/10.1890/120150

Angima, S.D., Stott, D.E., O'Neill, M.K., Ong, C.K., Weesies, G.A., 2003. Soil erosion prediction using RUSLE for central Kenyan highland conditions. Agric. Ecosyst. Environ. 97, 295–308. https://doi.org/10.1016/S0167-8809(03)00011-2

Anyamba, A., Tucker, C.J., 2005. Analysis of Sahelian vegetation dynamics using NOAA-AVHRR NDVI data from 1981-2003, in: Journal of Arid Environments. Academic Press, pp. 596–614. https://doi.org/10.1016/j.jaridenv.2005.03.007

Arabameri, A., Blaschke, T., Pradhan, B., Pourghasemi, H.R., Tiefenbacher, J.P., Bui, D.T., 2020. Evaluation of recent advanced soft computing techniques for gully erosion susceptibility mapping: A comparative study. Sensors (Switzerland) 20, 335. https://doi.org/10.3390/s20020335

Arabameri, A., Pradhan, B., Pourghasemi, H.R., Rezaei, K., 2018. Identification of erosion-prone areas using different multi-criteria decision-making techniques and gis. Geomatics, Nat. Hazards Risk 9, 1129–1155. https://doi.org/10.1080/19475705.2018.1513084

Arabameri, A., Pradhan, B., Rezaei, K., Lee, C.W., 2019a. Assessment of landslide susceptibility using statistical- and artificial intelligence-based FR-RF integrated model and multiresolution DEMs. Remote Sens. 11, 999. https://doi.org/10.3390/rs11090999

Arabameri, A., Pradhan, B., Rezaei, K., Sohrabi, M., Kalantari, Z., 2019b. GIS-based landslide susceptibility mapping using numerical risk factor bivariate model and its ensemble with linear multivariate regression and boosted regression tree algorithms. J. Mt. Sci. 16, 595–618. https://doi.org/10.1007/s11629-018-5168-y

Areola, M., Fasona, M., 2018. Sensitivity of vegetation to annual rainfall variations over Nigeria. Remote Sens. Appl. Soc. Environ. 10, 153–162. https://doi.org/10.1016/j.rsase.2018.03.006

Argent, R.M., 2005. A case study of environmental modelling and simulation using transplantable components. Environ. Model. Softw. 20, 1514–1523. https://doi.org/10.1016/j.envsoft.2004.08.016

Arshad, M.A., Mermut, A.R., 1988. Micromorphological and Physico-chemical Characteristics of Soil Crust Types in Northwestern Alberta, Canada. Soil Sci. Soc. Am. J. 52, 724–729. https://doi.org/10.2136/sssaj1988.03615995005200030024x

Aryal, J.P., Sapkota, T.B., Khurana, R., Khatri-Chhetri, A., Rahut, D.B., Jat, M.L., 2020. Climate change and agriculture in South Asia: adaptation options in smallholder production systems. Environ. Dev. Sustain. 22, 5045–5075. https://doi.org/10.1007/s10668-019-00414-4

Ashournejad, Q., Hosseini, A., Pradhan, B., Hosseini, S.J., 2019. Hazard zoning for spatial planning using GIS-based landslide susceptibility assessment: a new hybrid integrated data-driven and knowledge-based model. Arab. J. Geosci. 12. https://doi.org/10.1007/s12517-019-4236-0

Asner, G.P., Levick, S.R., Kennedy-Bowdoin, T., Knapp, D.E., Emerson, R., Jacobson,

J., Colgan, M.S., Martin, R.E., 2009. Large-scale impacts of herbivores on the structural diversity of african savannas. Proc. Natl. Acad. Sci. U. S. A. 106, 4947–4952. https://doi.org/10.1073/pnas.0810637106

Attogouinon, A., Lawin, A.E., M'Po, Y.N.T., Houngue, R., 2017. Extreme precipitation indices trend assessment over the Upper Oueme river valley-(Benin). Hydrology 4, 36. https://doi.org/10.3390/hydrology4030036

Ayanlade, A., Jegede, M.O., Borisade, P.B., 2014. Geoinformatics in Eco-Climatic Studies, in: Encyclopedia of Information Science and Technology, Third Edition. pp. 3136–3144. https://doi.org/10.4018/978-1-4666-5888-2.ch307

Azareh, A., Rahmati, O., Rafiei-Sardooi, E., Sankey, J.B., Lee, S., Shahabi, H., Ahmad, B. Bin, 2019. Modelling gully-erosion susceptibility in a semi-arid region, Iran: Investigation of applicability of certainty factor and maximum entropy models. Sci. Total Environ. 655, 684–696. https://doi.org/10.1016/j.scitotenv.2018.11.235

Baez-Villanueva, O.M., Zambrano-Bigiarini, M., Ribbe, L., Nauditt, A., Giraldo-Osorio, J.D., Thinh, N.X., 2018. Temporal and spatial evaluation of satellite rainfall estimates over different regions in Latin-America. Atmos. Res. 213, 34–50. https://doi.org/10.1016/j.atmosres.2018.05.011

Bai, Z.G., Conijn, J.G., Bindraban, P.S., Rutgers, B., 2012. Global changes of remotely sensed greenness and simulated biomass production since 1981: towards mapping global soil degradation. Rep. - ISRIC World Soil Inf. 33 pp.

Bakker, M.M., Govers, G., Kosmas, C., Vanacker, V., Oost, K. Van, Rounsevell, M., 2005. Soil erosion as a driver of land-use change. Agric. Ecosyst. Environ. 105, 467–481. https://doi.org/10.1016/j.agee.2004.07.009

Bandara, J.S., Chisholm, A., Ekanayake, A., Jayasuriya, S., 2001. Environmental cost of soil erosion in Sri Lanka: Tax/subsidy policy options. Environ. Model. Softw. 16, 497–508. https://doi.org/10.1016/S1364-8152(01)00019-6

Bardgett, R.D., Mommer, L., De Vries, F.T., 2014. Going underground: Root traits as drivers of ecosystem processes. Trends Ecol. Evol. https://doi.org/10.1016/j.tree.2014.10.006

Bartley, R., Croke, J., Bainbridge, Z.T., Austin, J.M., Kuhnert, P.M., 2015. Combining contemporary and long-term erosion rates to target erosion hot-spots in the Great Barrier Reef, Australia. Anthropocene 10, 1–12. https://doi.org/10.1016/j.ancene.2015.08.002

Becker, B.L., Lusch, D.P., Qi, J., 2005. Identifying optimal spectral bands from in situ measurements of Great Lakes coastal wetlands using second-derivative analysis. Remote Sens. Environ. 97, 238–248. https://doi.org/10.1016/j.rse.2005.04.020

Berendse, F., van Ruijven, J., Jongejans, E., Keesstra, S., 2015. Loss of plant species diversity reduces soil erosion resistance. Ecosystems 18, 881–888. https://doi.org/10.1007/s10021-015-9869-6

Bishop, Y.M., Holland, P.W., Fienberg, S.E., 2007. Discrete multivariate analysis theory and practice, Discrete Multivariate Analysis Theory and Practice. Springer New York. https://doi.org/10.1007/978-0-387-72806-3

Blaschke, P.M., Trustrum, N.A., Hicks, D.L., 2000. Impacts of mass movement erosion on land productivity: A review. Prog. Phys. Geogr.

https://doi.org/10.1191/030913300669154532

Bobrowsky, P., Couture, R., 2014. Landslide terminology, canadian technical guidelines and best practices related to landslides: a national initiative for loss reduction. Geol. Surv. Canada, Open File 7623, 68. https://doi.org/doi:10.4095/293940

Borrelli, P., Panagos, P., 2020. An indicator to reflect the mitigating effect of Common Agricultural Policy on soil erosion. Land use policy 92, 104467. https://doi.org/10.1016/j.landusepol.2020.104467

Borrelli, P., Robinson, D.A., Fleischer, L.R., Lugato, E., Ballabio, C., Alewell, C., Meusburger, K., Modugno, S., Schütt, B., Ferro, V., Bagarello, V., Oost, K. Van, Montanarella, L., Panagos, P., 2017. An assessment of the global impact of 21st century land use change on soil erosion. Nat. Commun. 8, 2017. https://doi.org/10.1038/s41467-017-02142-7

Borrelli, P., Robinson, D.A., Panagos, P., Lugato, E., Yang, J.E., Alewell, C., Wuepper, D., Montanarella, L., Ballabio, C., 2020. Land use and climate change impacts on global soil erosion by water (2015-2070). Proc. Natl. Acad. Sci. U. S. A. 117, 21994–22001. https://doi.org/10.1073/pnas.2001403117

Breiman, L., 2001. Random forests. Mach. Learn. 45, 5–32. https://doi.org/10.1023/A:1010933404324

Brits, A., Burke, M., Li, T., 2014. Improved modelling for urban sustainability assessment and strategic planning: local government planner and modeller perspectives on the key challenges. Aust. Plan. 51, 76–86. https://doi.org/10.1080/07293682.2013.808680

Brocca, L., Tullo, T., Melone, F., Moramarco, T., Morbidelli, R., 2012. Catchment scale soil moisture spatial-temporal variability. J. Hydrol. 422–423, 63–75. https://doi.org/10.1016/j.jhydrol.2011.12.039

Büchi, L., Wendling, M., Amossé, C., Necpalova, M., Charles, R., 2018. Importance of cover crops in alleviating negative effects of reduced soil tillage and promoting soil fertility in a winter wheat cropping system. Agric. Ecosyst. Environ. 256, 92–104. https://doi.org/10.1016/j.agee.2018.01.005

Bui, E.N., Hancock, G.J., Wilkinson, S.N., 2011. "Tolerable" hillslope soil erosion rates in Australia: Linking science and policy. Agric. Ecosyst. Environ. https://doi.org/10.1016/j.agee.2011.07.022

Burian, S.J., Brown, M.J., McPherson, T.N., 2002. Evaluation of land use/land cover datasets for urban watershed modeling, in: Water Science and Technology. IWA Publishing, pp. 269–276. https://doi.org/10.2166/wst.2002.0256

Burrell, A.L., Evans, J.P., Liu, Y., 2017. Detecting dryland degradation using Time Series Segmentation and Residual Trend analysis (TSS-RESTREND). Remote Sens. Environ. 197, 43–57. https://doi.org/10.1016/j.rse.2017.05.018

Burt, T.P., Weerasinghe, K.D.N., 2014. Rainfall distributions in Sri Lanka in time and space: An analysis based on daily rainfall data. Climate 2, 242–263. https://doi.org/10.3390/cli2040242

Buttafuoco, G., Conforti, M., Aucelli, P.P.C., Robustelli, G., Scarciglia, F., 2012. Assessing spatial uncertainty in mapping soil erodibility factor using geostatistical stochastic simulation. Environ. Earth Sci. 66, 1111–1125.

https://doi.org/10.1007/s12665-011-1317-0

Campbell, B.M., Vermeulen, S.J., Aggarwal, P.K., Corner-Dolloff, C., Girvetz, E., Loboguerrero, A.M., Ramirez-Villegas, J., Rosenstock, T., Sebastiang, L., Thorntonh, P.K., Wollenbergi, E., 2016. Reducing risks to food security from climate change. Glob. Food Sec. 11, 34–43. https://doi.org/10.1016/j.gfs.2016.06.002

Cental Bank of Sri Lanka, 2019. Central Bank of Sri Lanka, Annual Report 2019 [WWW Document]. URL https://www.cbsl.gov.lk/en/publications/economic-and-financial-reports/annual-reports/annual-report-2019 (accessed 12.26.20).

Cerdà, A., Rodrigo-Comino, J., Giménez-Morera, A., Keesstra, S.D., 2018. Hydrological and erosional impact and farmer's perception on catch crops and weeds in citrus organic farming in Canyoles river watershed, Eastern Spain. Agric. Ecosyst. Environ. 258, 49–58. https://doi.org/10.1016/j.agee.2018.02.015

Chakrabortty, R., Pal, S.C., Sahana, M., Mondal, A., Dou, J., Pham, B.T., Yunus, A.P., 2020. Soil erosion potential hotspot zone identification using machine learning and statistical approaches in eastern India. Nat. Hazards 104, 1259–1294. https://doi.org/10.1007/s11069-020-04213-3

Chander, G., Markham, B.L., Helder, D.L., 2009. Summary of current radiometric calibration coefficients for Landsat MSS, TM, ETM+, and EO-1 ALI sensors. Remote Sens. Environ. 113, 893–903. https://doi.org/10.1016/j.rse.2009.01.007

Chavez, P.S., 1996. Image-based atmospheric corrections - Revisited and improved. Photogramm. Eng. Remote Sensing 62, 1025–1036.

Chen, S.H., Su, H.B., Tian, J., Zhang, R.H., Xia, J., 2011. Estimating soil erosion using MODIS and TM images based on support vector machine and à trous wavelet. Int. J. Appl. Earth Obs. Geoinf. 13, 626–635. https://doi.org/10.1016/j.jag.2011.03.001

Chen, Y., Liu, A., Cheng, X., 2020. Quantifying economic impacts of climate change under nine future emission scenarios within CMIP6. Sci. Total Environ. 703, 134950. https://doi.org/10.1016/j.scitotenv.2019.134950

Chen, Z., Liang, S., Ke, Y., Yang, Z., Zhao, H., 2019. Landslide susceptibility assessment using evidential belief function, certainty factor and frequency ratio model at Baxie River basin, NW China. Geocarto Int. 34, 348–367. https://doi.org/10.1080/10106049.2017.1404143

Chitale, V.S., Behera, M.D., Roy, P.S., 2019. Deciphering plant richness using satellite remote sensing: a study from three biodiversity hotspots. Biodivers. Conserv. 28, 2183–2196. https://doi.org/10.1007/s10531-019-01761-4

Cohen, M.J., Shepherd, K.D., Walsh, M.G., 2005. Empirical reformulation of the universal soil loss equation for erosion risk assessment in a tropical watershed. Geoderma 124, 235–252. https://doi.org/10.1016/j.geoderma.2004.05.003

Conoscenti, C., Maggio, C., Rotigliano, E., 2008. Soil erosion susceptibility assessment and validation using a geostatistical multivariate approach: A test in Southern Sicily. Nat. Hazards 46, 287–305. https://doi.org/10.1007/s11069-007-9188-0

Corsini, A., Farina, P., Antonello, G., Barbieri, M., Casagli, N., Coren, F., Guerri, L., Ronchetti, F., Sterzai, P., Tarchi, D., 2006. Space-borne and ground-based SAR interferometry as tools for landslide hazard management in civil protection. Int. J.

Remote Sens. 27, 2351–2369. https://doi.org/10.1080/01431160600554405

Cortes, C., Vapnik, V., 1995. Support-vector networks. Mach. Learn. 20, 273–297. https://doi.org/10.1007/bf00994018

Cunha, J., Nóbrega, R.L.B., Rufino, I., Erasmi, S., Galvão, C., Valente, F., 2020. Surface albedo as a proxy for land-cover clearing in seasonally dry forests: Evidence from the Brazilian Caatinga. Remote Sens. Environ. 238, 111250. https://doi.org/10.1016/j.rse.2019.111250

Cutter, S.L., 1996. Vulnerability to environmental hazards. Prog. Hum. Geogr. 20, 529–539. https://doi.org/10.1177/030913259602000407

D'Arrigo, R.D., Jacoby, G.C., Bunker, D.E., Malmstrom, C.M., Los, S.O., 2000. Correlation between maximum latewood density of annual tree rings and NDVI based estimates of forest productivity. Int. J. Remote Sens. 21, 2329–2336. https://doi.org/10.1080/01431160050029611

d'Oleire-Oltmanns, S., Marzolff, I., Peter, K., Ries, J., 2012. Unmanned Aerial Vehicle (UAV) for Monitoring Soil Erosion in Morocco. Remote Sens. 4, 3390–3416. https://doi.org/10.3390/rs4113390

Dabi, N., Fikirie, K., Mulualem, T., 2017. Soil and Water Conservation Practices on Crop Productivity and its Economic Implications in Ethiopia: A Review. Asian J. Agric. Res. 11, 128–136. https://doi.org/10.3923/ajar.2017.128.136

Damaševičius, R., 2010. Optimization of SVM parameters for recognition of regulatory DNA sequences. TOP 18, 339–353. https://doi.org/10.1007/s11750-010-0152-x

Dang, K., Sassa, K., Konagai, K., Karunawardena, A., Bandara, R.M.S., Hirota, K., Tan, Q., Ha, N.D., 2019. Recent rainfall-induced rapid and long-traveling landslide on 17 May 2016 in Aranayaka, Kagelle District, Sri Lanka. Landslides 16, 155–164. https://doi.org/10.1007/s10346-018-1089-7

Danielson, J.J., Gesch, D.B., 2011. Global Multi-resolution Terrain Elevation Data 2010 (GMTED2010), U.S. Geological Survey Open-File Report 2011-1073.

Das, B., Bordoloi, R., Thungon, L.T., Paul, A., Pandey, P.K., Mishra, M., Tripathi, O.P., 2020. An integrated approach of GIS, RUSLE and AHP to model soil erosion in West Kameng watershed, Arunachal Pradesh. J. Earth Syst. Sci. 129, 94. https://doi.org/10.1007/s12040-020-1356-6

Das, B.S., Sarathjith, M.C., Santra, P., Sahoo, R.N., Srivastava, R., Routray, A., Ray, S.S., 2015. Hyperspectral remote sensing: Opportunities, status and challenges for rapid soil assessment in India. Curr. Sci. 108, 860–868. https://doi.org/10.18520/cs/v108/i5/860-868

De La Rosa, D., Mayol, F., Moreno, J.A., Bonsón, T., Lozano, S., 1999. An expert system/neural network model (ImpelERO) for evaluating agricultural soil erosion in Andalucia region, southern Spain. Agric. Ecosyst. Environ. 73, 211–226. https://doi.org/10.1016/S0167-8809(99)00050-X

De Rouw, A., Rajot, J.L., 2004. Soil organic matter, surface crusting and erosion in Sahelian farming systems based on manuring or fallowing, in: Agriculture, Ecosystems and Environment. pp. 263–276. https://doi.org/10.1016/j.agee.2003.12.020

de Silva, J., Sonnadara, D.U.J., 2016. Century scale climate change in the central

highlands of Sri Lanka. J. Earth Syst. Sci. 125, 75–84. https://doi.org/10.1007/s12040-015-0652-z

de Vente, J., Poesen, J., 2005. Predicting soil erosion and sediment yield at the basin scale: Scale issues and semi-quantitative models. Earth-Science Rev. 71, 95–125. https://doi.org/10.1016/j.earscirev.2005.02.002

Dissanayake, D., Morimoto, T., Ranagalage, M., 2019. Accessing the soil erosion rate based on RUSLE model for sustainable land use management: a case study of the Kotmale watershed, Sri Lanka. Model. Earth Syst. Environ. https://doi.org/10.1007/s40808-018-0534-x

Diyabalanage, S., Samarakoon, K.K., Adikari, S.B., Hewawasam, T., 2017. Impact of soil and water conservation measures on soil erosion rate and sediment yields in a tropical watershed in the Central Highlands of Sri Lanka. Appl. Geogr. 79, 103–114. https://doi.org/10.1016/j.apgeog.2016.12.004

Djeddou, M., Hameed, I.A., Mokhtari, E., 2019. Soil Erosion Rate Prediction using Adaptive Neuro-Fuzzy Inference System (ANFIS) and Geographic Information System (GIS) of Wadi Sahel-Soummam Watershed (Algeria), in: IEEE International Conference on Fuzzy Systems. Institute of Electrical and Electronics Engineers Inc. https://doi.org/10.1109/FUZZ-IEEE.2019.8858857

Drzewiecki, W., Wężyk, P., Pierzchalski, M., Szafrańska, B., 2014. Quantitative and Qualitative Assessment of Soil Erosion Risk in Małopolska (Poland), Supported by an Object-Based Analysis of High-Resolution Satellite Images. Pure Appl. Geophys. 171, 867–895. https://doi.org/10.1007/s00024-013-0669-7

Dube, H.B., Mutema, M., Muchaonyerwa, P., Poesen, J., Chaplot, V., 2020. A global analysis of the morphology of linear erosion features. Catena 190, 104542. https://doi.org/10.1016/j.catena.2020.104542

Durigon, V.L., Carvalho, D.F., Antunes, M.A.H., Oliveira, P.T.S., Fernandes, M.M., 2014. NDVI time series for monitoring RUSLE cover management factor in a tropical watershed. Int. J. Remote Sens. 35, 441–453. https://doi.org/10.1080/01431161.2013.871081

Dwivedi, R.S., Ravi Sankar, T., Venkataratnam, L., Karale, R.L., Gawande, S.P., Seshagiri Rao, K. V., Senchaudhary, S., Bhaumik, K.R., Mukharjee, K.K., 1997. The inventory and monitoring of eroded lands using remote sensing data. Int. J. Remote Sens. 18, 107–119. https://doi.org/10.1080/014311697219303

Eckstein, D., Winges, M., Marie-Lena, H., 2019. Global climate risk index 2019 [WWW Document]. URL https://germanwatch.org/en/16046 (accessed 5.8.21).

Edwards, A.C., Scalenghe, R., Freppaz, M., 2007. Changes in the seasonal snow cover of alpine regions and its effect on soil processes: A review. Quat. Int. https://doi.org/10.1016/j.quaint.2006.10.027

Elsheikh, R., Mohamed Shariff, A.R.B., Amiri, F., Ahmad, N.B., Balasundram, S.K., Soom, M.A.M., 2013. Agriculture Land Suitability Evaluator (ALSE): A decision and planning support tool for tropical and subtropical crops. Comput. Electron. Agric. 93, 98–110. https://doi.org/10.1016/j.compag.2013.02.003

Esham, M., Garforth, C., 2013. Climate change and agricultural adaptation in Sri Lanka: A review. Clim. Dev. https://doi.org/10.1080/17565529.2012.762333

Evans, J., Geerken, R., 2004. Discrimination between climate and human-induced dryland degradation. J. Arid Environ. 57, 535–554. https://doi.org/10.1016/S0140-1963(03)00121-6

FAO, 2020. FAO - Farming Systems [WWW Document]. URL http://www.fao.org/farmingsystems/description_en.htm (accessed 8.2.20).

FAO, 2019. Soil erosion: the greatest challenge to sustainable soil management, Food and Agriculture Organization of the United Nations. Rome.

Farhan, Y., Nawaiseh, S., 2015. Spatial assessment of soil erosion risk using RUSLE and GIS techniques. Environ. Earth Sci. 74, 4649–4669. https://doi.org/10.1007/s12665-015-4430-7

Fathizad, H., Karimi, H., Alibakhshi, S.M., 2014. The estimation of erosion and sediment by using the RUSLE model and RS and GIS techniques (Case study: Arid and semi-arid regions of Doviraj, Ilam province, Iran). Int. J. Agric. Crop Sci. 7, 303.

Fayas, C.M., Abeysingha, N.S., Nirmanee, K.G.S., Samaratunga, D., Mallawatantri, A., 2019. Soil loss estimation using rusle model to prioritize erosion control in KELANI river basin in Sri Lanka. Int. Soil Water Conserv. Res. 7, 130–137. https://doi.org/10.1016/j.iswcr.2019.01.003

Fensholt, R., Rasmussen, K., Kaspersen, P., Huber, S., Horion, S., Swinnen, E., 2013. Assessing land degradation/recovery in the african sahel from long-term earth observation based primary productivity and precipitation relationships. Remote Sens. 5, 664–686. https://doi.org/10.3390/rs5020664

Fenta, A.A., Tsunekawa, A., Haregeweyn, N., Tsubo, M., Yasuda, H., Kawai, T., Ebabu, K., Berihun, M.L., Belay, A.S., Sultan, D., 2021. Agroecology-based soil erosion assessment for better conservation planning in Ethiopian river basins. Environ. Res. 195, 110786. https://doi.org/10.1016/j.envres.2021.110786

Fernández, C., Vega, J.A., 2018. Evaluation of the rusle and disturbed wepp erosion models for predicting soil loss in the first year after wildfire in NW Spain. Environ. Res. 165, 279–285. https://doi.org/10.1016/j.envres.2018.04.008

Foster, Meyer, L.D., Onstad, C.A., 1977. Erosion equation derived from basic erosion principles. Trans. Am. Soc. Agric. Eng. 20, 678–682. https://doi.org/10.13031/2013.35627

Foulds, S.A., Warburton, J., 2007. Significance of wind-driven rain (wind-splash) in the erosion of blanket peat. Geomorphology 83, 183–192. https://doi.org/10.1016/j.geomorph.2006.07.001

Fu, S., Yang, Y., Liu, B., Liu, H., Liu, J., Liu, L., Li, P., 2020. Peak flow rate response to vegetation and terraces under extreme rainstorms. Agric. Ecosyst. Environ. 288. https://doi.org/10.1016/j.agee.2019.106714

Ganasri, B.P., Ramesh, H., 2016. Assessment of soil erosion by RUSLE model using remote sensing and GIS - A case study of Nethravathi Basin. Geosci. Front. 7, 953–961. https://doi.org/10.1016/j.gsf.2015.10.007

García-Ruiz, J.M., Beguería, S., Nadal-Romero, E., González-Hidalgo, J.C., Lana-Renault, N., Sanjuán, Y., 2015. A meta-analysis of soil erosion rates across the world. Geomorphology. https://doi.org/10.1016/j.geomorph.2015.03.008

García-Ruiz, J.M., Lana-Renault, N., 2011. Hydrological and erosive consequences of

farmland abandonment in Europe, with special reference to the Mediterranean region - A review. Agric. Ecosyst. Environ. https://doi.org/10.1016/j.agee.2011.01.003

García-Ruiz, J.M., Nadal-Romero, E., Lana-Renault, N., Beguería, S., 2013. Erosion in Mediterranean landscapes: Changes and future challenges. Geomorphology. https://doi.org/10.1016/j.geomorph.2013.05.023

Garosi, Y., Sheklabadi, M., Conoscenti, C., Pourghasemi, H.R., Van Oost, K., 2019. Assessing the performance of GIS- based machine learning models with different accuracy measures for determining susceptibility to gully erosion. Sci. Total Environ. 664, 1117–1132. https://doi.org/10.1016/j.scitotenv.2019.02.093

Garosi, Y., Sheklabadi, M., Pourghasemi, H.R., Besalatpour, A.A., Conoscenti, C., Van Oost, K., 2018. Comparison of differences in resolution and sources of controlling factors for gully erosion susceptibility mapping. Geoderma 330, 65–78. https://doi.org/10.1016/j.geoderma.2018.05.027

Gayen, A., Pourghasemi, H.R., Saha, S., Keesstra, S., Bai, S., 2019. Gully erosion susceptibility assessment and management of hazard-prone areas in India using different machine learning algorithms. Sci. Total Environ. 668, 124–138. https://doi.org/10.1016/j.scitotenv.2019.02.436

Gayen, A., Saha, S., 2017. Application of weights-of-evidence (WoE) and evidential belief function (EBF) models for the delineation of soil erosion vulnerable zones: a study on Pathro river basin, Jharkhand, India. Model. Earth Syst. Environ. 3, 1123–1139. https://doi.org/10.1007/s40808-017-0362-4

Gholizadeh, A., Žižala, D., Saberioon, M., Borůvka, L., 2018. Soil organic carbon and texture retrieving and mapping using proximal, airborne and Sentinel-2 spectral imaging. Remote Sens. Environ. 218, 89–103. https://doi.org/10.1016/j.rse.2018.09.015

Goodwin, N.R., Armston, J., Stiller, I., Muir, J., 2016. Assessing the repeatability of terrestrial laser scanning for monitoring gully topography: A case study from Aratula, Queensland, Australia. Geomorphology 262, 24–36. https://doi.org/10.1016/j.geomorph.2016.03.007

Gorrab, A., Zribi, M., Baghdadi, N., Mougenot, B., Fanise, P., Chabaane, Z.L., 2015. Retrieval of both soil moisture and texture using TerraSAR-X images. Remote Sens. 7, 10098–10116. https://doi.org/10.3390/rs70810098

Govender, M., Chetty, K., Bulcock, H., 2007. A review of hyperspectral remote sensing and its application in vegetation and water resource studies. Water SA. https://doi.org/10.4314/wsa.v33i2.49049

Gray, J.M., Chapman, G.A., Murphy, B.W., 2015. Land management within capability: A new scheme to guide sustainable land management in New South Wales, Australia, in: Soil Research. pp. 683–694. https://doi.org/10.1071/SR14196

Grebby, S., Cunningham, D., Tansey, K., Naden, J., 2014. The Impact of Vegetation on Lithological Mapping Using Airborne Multispectral Data: A Case Study for the North Troodos Region, Cyprus. Remote Sens. 6, 10860–10887. https://doi.org/10.3390/rs61110860

Guenang, G.M., Kamga, F.M., 2014. Computation of the standardized precipitation index (SPI) and its use to assess drought occurrences in Cameroon over recent decades. J.

Appl. Meteorol. Climatol. 53, 2310–2324. https://doi.org/10.1175/JAMC-D-14-0032.1

Guerra, A.J.T., Fullen, M.A., Jorge, M. do C.O., Bezerra, J.F.R., Shokr, M.S., 2017. Slope Processes, Mass Movement and Soil Erosion: A Review. Pedosphere 27, 27–41. https://doi.org/10.1016/S1002-0160(17)60294-7

Gunathilaka, R.P.D., Smart, J.C.R., Fleming, C.M., Hasan, S., 2018. The impact of climate change on labour demand in the plantation sector: the case of tea production in Sri Lanka. Aust. J. Agric. Resour. Econ. 62, 480–500. https://doi.org/10.1111/1467-8489.12262

Gunatilaka, A., 2007. Role of basin-wide landslides in the formation of extensive alluvial gemstone deposits in Sri Lanka. Earth Surf. Process. Landforms 32, 1863–1873. https://doi.org/10.1002/esp.1498

Gupta, H. V., Kling, H., Yilmaz, K.K., Martinez, G.F., 2009. Decomposition of the mean squared error and NSE performance criteria: Implications for improving hydrological modelling. J. Hydrol. 377, 80–91. https://doi.org/10.1016/j.jhydrol.2009.08.003

Gyssels, G., Poesen, J., Bochet, E., Li, Y., 2005. Impact of plant roots on the resistance of soils to erosion by water: A review. Prog. Phys. Geogr. https://doi.org/10.1191/0309133305pp443ra

Hajjar, R., Jarvis, D.I., Gemmill-Herren, B., 2008. The utility of crop genetic diversity in maintaining ecosystem services. Agric. Ecosyst. Environ. 123, 261–270. https://doi.org/10.1016/j.agee.2007.08.003

Hajkowicz, S., Young, M., 2005. Costing yield loss from acidity, sodicity and dryland salinity to Australian agriculture. L. Degrad. Dev. 16, 417–433. https://doi.org/10.1002/ldr.670

Hall, F.G., Strebel, D.E., Nickeson, J.E., Goetz, S.J., 1991. Radiometric rectification: Toward a common radiometric response among multidate, multisensor images. Remote Sens. Environ. 35, 11–27. https://doi.org/10.1016/0034-4257(91)90062-B

Han, J., Ge, W., Hei, Z., Cong, C., Ma, C., Xie, M., Liu, B., Feng, W., Wang, F., Jiao, J., 2020. Agricultural land use and management weaken the soil erosion induced by extreme rainstorms. Agric. Ecosyst. Environ. 301, 107047. https://doi.org/10.1016/j.agee.2020.107047

Hewawasam, T., 2010. Effect of land use in the upper Mahaweli catchment area on erosion landslides and siltation in hydropower reservoirs of Sri Lanka. J. Natl. Sci. Found. Sri Lanka 38, 3–14. https://doi.org/10.4038/jnsfsr.v38i1.1721

Hewawasam, T., Illangasinghe, S., 2015. Quantifying sheet erosion in agricultural highlands of Sri Lanka by tracking grain-size distributions. Anthropocene 11, 25–34. https://doi.org/10.1016/j.ancene.2015.11.004

Hewawasam, T., von Blanckenburg, F., Bouchez, J., Dixon, J.L., Schuessler, J.A., Maekeler, R., 2013. Slow advance of the weathering front during deep, supply-limited saprolite formation in the tropical Highlands of Sri Lanka. Geochim. Cosmochim. Acta 118, 202–230. https://doi.org/10.1016/j.gca.2013.05.006

Hewawasam, T., von Blanckenburg, F., Schaller, M., Kubik, P., 2003. Increase of human over natural erosion rates in tropical highlands constrained by cosmogenic nuclides.

Geology 31, 597–600. https://doi.org/10.1130/0091-7613(2003)031<0597:IOHONE>2.0.CO;2

Hoar, T., Nychka, D., 2008. Download NCAR Community Climate System Model (CCSM) projections in GIS formats | GIS Climate Change Scenarios [WWW Document]. Stat. Downscal. Community Clim. Syst. Model Mon. Temp. Precip. Proj. URL https://gisclimatechange.ucar.edu/gis-climatedata, (accessed 7.31.21).

Holzkämper, A., 2017. Adapting agricultural production systems to climate change—What's the use of models? Agric. https://doi.org/10.3390/agriculture7100086

Hou, J., Wang, H., Fu, B., Zhu, L., Wang, Y., Li, Z., 2016. Effects of plant diversity on soil erosion for different vegetation patterns. Catena 147, 632–637. https://doi.org/10.1016/j.catena.2016.08.019

Huang, S., Ding, J., Liu, B., Ge, X., Wang, J., Zou, J., Zhang, J., 2020. The capability of integrating optical and microwave data for detecting soil moisture in an oasis region. Remote Sens. 12, 1358. https://doi.org/10.3390/RS12091358

Huete, A., Didan, K., Miura, T., Rodriguez, E.P., Gao, X., Ferreira, L.G., 2002. Overview of the radiometric and biophysical performance of the MODIS vegetation indices. Remote Sens. Environ. 83, 195–213. https://doi.org/10.1016/S0034-4257(02)00096-2

Huete, A.R., 1988. A soil-adjusted vegetation index (SAVI). Remote Sens. Environ. 25, 295–309. https://doi.org/10.1016/0034-4257(88)90106-X

Hunt, N.D., Hill, J.D., Liebman, M., 2019. Cropping System Diversity Effects on Nutrient Discharge, Soil Erosion, and Agronomic Performance. Environ. Sci. Technol. 53, 1344–1352. https://doi.org/10.1021/acs.est.8b02193

Hurni, H., 1988. Degradation and conservation of the resources in the Ethiopian highlands. Mt. Res. Dev. 8, 123–130. https://doi.org/10.2307/3673438

Hutton, C., Brazier, R., 2012. Quantifying riparian zone structure from airborne LiDAR: Vegetation filtering, anisotropic interpolation, and uncertainty propagation. J. Hydrol. 442–443, 36–45. https://doi.org/10.1016/j.jhydrol.2012.03.043

Ibrahim, Y.Z., Balzter, H., Kaduk, J., Tucker, C.J., 2015. Land degradation assessment using residual trend analysis of GIMMS NDVI3g, soil moisture and rainfall in Sub-Saharan West Africa from 1982 to 2012. Remote Sens. 7, 5471–5494. https://doi.org/10.3390/rs70505471

IPCC, 2015. AR5 SYNTHESIS REPORT (LONG) Climate Change 2014 1–167.

Islam, M.R., Jaafar, W.Z.W., Hin, L.S., Osman, N., Hossain, A., Mohd, N.S., 2018. Development of an intelligent system based on ANFIS model for predicting soil erosion. Environ. Earth Sci. 77, 186. https://doi.org/10.1007/s12665-018-7348-z

Jacob, V.J., Alles, W.S., 1987. Kandyan gardens of Sri Lanka. Agrofor. Syst. 5, 123–137. https://doi.org/10.1007/BF00047517

Jain, S.K., Goel, M.K., 2002. Assessing the vulnerability to soil erosion of the Ukai Dam catchments using remote sensing and GIS. Hydrol. Sci. J. 47, 31–40. https://doi.org/10.1080/02626660209492905

Jayasinghe, G.J.M.S.R., Wijekoon, P., Gunatilake, J., 2017. Landslide susceptibility assessment using statistical models: A case study in Badulla district, Sri Lanka.

Ceylon J. Sci. 46, 27. https://doi.org/10.4038/cjs.v46i4.7466

Jayasinghe, S.L., Kumar, L., Sandamali, J., 2019. Assessment of potential land suitability for tea (Camellia sinensis (L.) O. Kuntze) in Sri Lanka using a gis-based multi-criteria approach. Agric. 9, 148. https://doi.org/10.3390/agriculture9070148

Jayawardena, I.M.S.P., Darshika, D.W.T.T., C. Herath, H.M.R., 2018. Recent Trends in Climate Extreme Indices over Sri Lanka. Am. J. Clim. Chang. 07, 586–599. https://doi.org/10.4236/ajcc.2018.74036

Jebur, M.N., Pradhan, B., Tehrany, M.S., 2014. Optimization of landslide conditioning factors using very high-resolution airborne laser scanning (LiDAR) data at catchment scale. Remote Sens. Environ. 152, 150–165. https://doi.org/10.1016/j.rse.2014.05.013

Jena, R., Pradhan, B., Beydoun, G., Nizamuddin, Ardiansyah, Sofyan, H., Affan, M., 2020. Integrated model for earthquake risk assessment using neural network and analytic hierarchy process: Aceh province, Indonesia. Geosci. Front. 11, 613–634. https://doi.org/10.1016/j.gsf.2019.07.006

John, R., Chen, J., Lu, N., Guo, K., Liang, C., Wei, Y., Noormets, A., Ma, K., Han, X., 2008. Predicting plant diversity based on remote sensing products in the semi-arid region of Inner Mongolia. Remote Sens. Environ. 112, 2018–2032. https://doi.org/10.1016/j.rse.2007.09.013

Jozdani, S.E., Johnson, B.A., Chen, D., 2019. Comparing deep neural networks, ensemble classifiers, and support vector machine algorithms for object-based urban land use/land cover classification. Remote Sens. 11, 1713. https://doi.org/10.3390/rs11141713

Kandel, D.D., Western, A.W., Grayson, R.B., 2005. Scaling from process timescales to daily time steps: A distribution function approach. Water Resour. Res. 41, 1–16. https://doi.org/10.1029/2004WR003380

Karimi, H., Amiri, S., Huang, J., Karimi, A., 2019. Integrating GIS and multi-criteria decision analysis for landfill site selection, case study: Javanrood County in Iran. Int. J. Environ. Sci. Technol. 16, 7305–7318. https://doi.org/10.1007/s13762-018-2151-7

Karydas, C.G., Panagos, P., Gitas, I.Z., 2014. A classification of water erosion models according to their geo-spatial characteristics. Int. J. Digit. Earth 7, 229–250. https://doi.org/10.1080/17538947.2012.671380

Kastridis, A., Kirkenidis, C., Sapountzis, M., 2020. An integrated approach of flash flood analysis in ungauged Mediterranean watersheds using post-flood surveys and unmanned aerial vehicles. Hydrol. Process. 34, 4920–4939. https://doi.org/10.1002/hyp.13913

Kayet, N., Pathak, K., Chakrabarty, A., Sahoo, S., 2018. Evaluation of soil loss estimation using the RUSLE model and SCS-CN method in hillslope mining areas. Int. Soil Water Conserv. Res. 6, 31–42. https://doi.org/10.1016/j.iswcr.2017.11.002

Keating, B.A., McCown, R.L., 2001. Advances in farming systems analysis and intervention, in: Agricultural Systems. Elsevier, pp. 555–579. https://doi.org/10.1016/S0308-521X(01)00059-2

Keesstra, S., Pereira, P., Novara, A., Brevik, E.C., Azorin-Molina, C., Parras-Alcántara,

L., Jordán, A., Cerdà, A., 2016. Effects of soil management techniques on soil water erosion in apricot orchards. Sci. Total Environ. 551–552, 357–366. https://doi.org/10.1016/j.scitotenv.2016.01.182

Khaledian, Y., Kiani, F., Ebrahimi, S., Brevik, E.C., Aitkenhead-Peterson, J., 2017. Assessment and Monitoring of Soil Degradation during Land Use Change Using Multivariate Analysis. L. Degrad. Dev. 28, 128–141. https://doi.org/10.1002/ldr.2541

Khaniya, B., Jayanayaka, I., Jayasanka, P., Rathnayake, U., 2019. Rainfall Trend Analysis in Uma Oya Basin, Sri Lanka, and Future Water Scarcity Problems in Perspective of Climate Variability. Adv. Meteorol. 2019. https://doi.org/10.1155/2019/3636158

Khoi, D.D., Murayama, Y., 2010. Delineation of suitable cropland areas using a GIS based multi-criteria evaluation approach in the tam Dao national park region, Vietnam. Sustainability 2, 2024–2043. https://doi.org/10.3390/su2072024

Kling, J.R., Mullainathan, S., Shafir, E., Vermeulen, L.C., Wrobel, M. V., 2012. Comparison friction: Experimental evidence from medicare drug plans. Q. J. Econ. 127, 199–235. https://doi.org/10.1093/qje/qjr055

Koh, L.P., Wich, S.A., 2012. Dawn of drone ecology: Low-cost autonomous aerial vehicles for conservation. Trop. Conserv. Sci. https://doi.org/10.1177/194008291200500202

Kuhnert, P.M., Henderson, A.K., Bartley, R., Herr, A., 2010. Incorporating uncertainty in gully erosion calculations using the random forests modelling approach. Environmetrics 21, 493–509. https://doi.org/10.1002/env.999

Kumarasiri, A.D., Sonnadara, U.J., 2008. Performance of an artificial neural network on forecasting the daily occurrence and annual depth of rainfall at a tropical site. Hydrol. Process. 22, 3535–3542. https://doi.org/10.1002/hyp.6964

Kundu, A., Patel, N.R., Saha, S.K., Dutta, D., 2017. Desertification in western Rajasthan (India): an assessment using remote sensing derived rain-use efficiency and residual trend methods. Nat. Hazards 86, 297–313. https://doi.org/10.1007/s11069-016-2689-y

Labrière, N., Locatelli, B., Laumonier, Y., Freycon, V., Bernoux, M., 2015. Soil erosion in the humid tropics: A systematic quantitative review. Agric. Ecosyst. Environ. 203, 127–139. https://doi.org/10.1016/j.agee.2015.01.027

Lal, R., 2014. Climate Strategic Soil Management. Challenges 5, 43–74. https://doi.org/10.3390/challe5010043

Lal, R., 2011. Climate of South Asia and the Human Wellbeing, in: Climate Change and Food Security in South Asia. Springer Netherlands, pp. 3–12. https://doi.org/10.1007/978-90-481-9516-9_1

Lal, R., 2004. Soil carbon sequestration impacts on global climate change and food security. Science (80-.). https://doi.org/10.1126/science.1097396

Lal, R., 2003. Soil erosion and the global carbon budget. Environ. Int. https://doi.org/10.1016/S0160-4120(02)00192-7

Lal, R., 2001. Soil degradation by erosion. L. Degrad. Dev. 12, 519–539. https://doi.org/10.1002/ldr.472

Lal, R., 1995. Erosion-Crop Productivity Relationships for Soils of Africa. Soil Sci. Soc. Am. J. 59, 661–667. https://doi.org/10.2136/sssaj1995.03615995005900030004x

Lal, R., 1988. Soil erosion by wind and water: problems and prospects. Soil Eros. Res. methods 1–6. https://doi.org/10.1201/9780203739358-1

Lal, R., Bouma, J., Brevik, E., Dawson, L., Field, D.J., Glaser, B., Hatano, R., Hartemink, A.E., Kosaki, T., Lascelles, B., Monger, C., Muggler, C., Ndzana, G.M., Norra, S., Pan, X., Paradelo, R., Reyes-Sánchez, L.B., Sandén, T., Singh, B.R., Spiegel, H., Yanai, J., Zhang, J., 2021. Soils and sustainable development goals of the United Nations: An International Union of Soil Sciences perspective. Geoderma Reg. https://doi.org/10.1016/j.geodrs.2021.e00398

Lal, R., Mokma, D., Lowery, B., 1999. Relation Between Soil Quality and Erosion, 1st Editio. ed, Soil Quality and Soil Erosion. CRC Press. https://doi.org/10.1201/9780203739266-14

Landmann, T., Dubovyk, O., 2014. Spatial analysis of human-induced vegetation productivity decline over eastern Africa using a decade (2001-2011) of medium resolution MODIS time-series data. Int. J. Appl. Earth Obs. Geoinf. 33, 76–82. https://doi.org/10.1016/j.jag.2014.04.020

Lee, S., Hong, S.M., Jung, H.S., 2017. A support vector machine for landslide susceptibility mapping in Gangwon Province, Korea. Sustain. 9. https://doi.org/10.3390/su9010048

Lee, S., Talib, J.A., 2005. Probabilistic landslide susceptibility and factor effect analysis. Environ. Geol. 47, 982–990. https://doi.org/10.1007/s00254-005-1228-z

Leh, M., Bajwa, S., Chaubey, I., 2013. IMPACT of land use change on erosion risk: AN integrated remote sensing, geographic information system and modeling methodology. L. Degrad. Dev. 24, 409–421. https://doi.org/10.1002/ldr.1137

Lelong, C.C.D., Burger, P., Jubelin, G., Roux, B., Labbé, S., Baret, F., 2008. Assessment of unmanned aerial vehicles imagery for quantitative monitoring of wheat crop in small plots. Sensors 8, 3557–3585. https://doi.org/10.3390/s8053557

Levin, N., Shmida, A., Levanoni, O., Tamari, H., Kark, S., 2007. Predicting mountain plant richness and rarity from space using satellite-derived vegetation indices. Divers. Distrib. 13, 692–703. https://doi.org/10.1111/j.1472-4642.2007.00372.x

Li, B., Zhang, F., Zhang, L.W., Huang, J.F., Jin, Z.F., Gupta, D.K., 2012. Comprehensive Suitability Evaluation of Tea Crops Using GIS and a Modified Land Ecological Suitability Evaluation Model. Pedosphere 22, 122–130. https://doi.org/10.1016/S1002-0160(11)60198-7

Li, H. bo, Li, X. wen, Li, W. zhou, Zhang, S. lin, Zhou, J. wen, 2019. Quantitative assessment for the rockfall hazard in a post-earthquake high rock slope using terrestrial laser scanning. Eng. Geol. 248, 1–13. https://doi.org/10.1016/j.enggeo.2018.11.003

Li, Y., Mo, P., 2019. A unified landslide classification system for loess slopes: A critical review. Geomorphology. https://doi.org/10.1016/j.geomorph.2019.04.020

Li, Z., Fang, H., 2016. Impacts of climate change on water erosion: A review. Earth-Science Rev. https://doi.org/10.1016/j.earscirev.2016.10.004

Li, Z., Zhang, Y., Zhu, Q., He, Y., Yao, W., 2015. Assessment of bank gully development

and vegetation coverage on the Chinese Loess Plateau. Geomorphology 228, 462–469. https://doi.org/10.1016/j.geomorph.2014.10.005

Liang, K., 2019. Spatio-temporal variations in precipitation extremes in the endorheic Hongjian Lake Basin in the Ordos Plateau, China. Water (Switzerland) 11. https://doi.org/10.3390/w11101981

Lin, B.B., 2011. Resilience in agriculture through crop diversification: Adaptive management for environmental change. Bioscience. https://doi.org/10.1525/bio.2011.61.3.4

Lisboa, U.N. De, Lal, M., Munasinghe, M., Deraniyagala, Y., Dassanayake, N., Karunarathna, H., Poesen, J., Nachtergaele, J., Verstraeten, G., Valentin, C., Huete, A.R., Kerr, Y.H., Sorooshian, S., Nearing, M.A., Gournellos, T., Evelpidou, N., Vassilopoulos, A., Dreibrodt, S., Busato, P., Moshou, D., Pearson, S., Bochtis, D., Dissanayake, D.M.S.L.B., Morimoto, T., Ranagalage, M., Rathnayake, V.S., Premaratne, H.L., Sonnadara, D.U.J., de Jong, R., de Bruin, S., Schaepman, M., Dent, D., Yang, X., Gray, J.M., Chapman, G.A., Zhu, Q., Tulau, M., McInnes-Clarke, S., Mishra, D., Singh, B.N., Perera, E.N.C.C., Jayawardana, D.T., Jayasinghe, P., Bandara, R.M.S., Alahakoon, N., de Silva, J., Gunarathna, M.H.J.P., Dissanayake, D.M.S.L.B., Murayama, Y., Simwanda, M., Ratnayake, U., Herath, S., Huete, A.R., Liu, H.Q., Batchily, K., Van Leeuwen, W., Jayawardena, I.M.S.P., Darshika, D.W.T.T., C. Herath, H.M.R., Wickramasinghe, L.A., Foody, G.M., Cutler, M.E.J., Pradhan, B., Lee, S., 2018. Quantitative mapping of global land degradation using earth observations. Agric. Ecosyst. Environ. 5, 6823–6853. https://doi.org/10.1080/01431161.2010.512946

Liu, J., Gao, G., Wang, S., Jiao, L., Wu, X., Fu, B., 2018. The effects of vegetation on runoff and soil loss: Multidimensional structure analysis and scale characteristics. J. Geogr. Sci. 28, 59–78. https://doi.org/10.1007/s11442-018-1459-z

Liu, Y., Li, Y., Li, S., Motesharrei, S., 2015. Spatial and temporal patterns of global NDVI trends: Correlations with climate and human factors. Remote Sens. 7, 13233–13250. https://doi.org/10.3390/rs71013233

Liu, Yue, Zhao, W., Liu, Yanxu, Pereira, P., 2020. Global rainfall erosivity changes between 1980 and 2017 based on an erosivity model using daily precipitation data. Catena 194, 104768. https://doi.org/10.1016/j.catena.2020.104768

Loch, R.J., Slater, B.K., Devoil, C., 1998. Soil erodibility (K(m)) values for some Australian soils. Aust. J. Soil Res. 36, 1045–1055. https://doi.org/10.1071/S97081

Lozano-García, D.F., Fernández, R.N., Johannsen, C.J., 1991. Assessment of Regional Biomass-Soil Relationships Using Vegetation Indexes. IEEE Trans. Geosci. Remote Sens. 29, 331–339. https://doi.org/10.1109/36.73676

LPDAAC, 2021. Land Processes Distributed Active Archive Center [WWW Document]. NASA EOSDIS L. Process. DAAC, USGS Earth Resour. Obs. Sci. Center, Sioux Falls, South Dakota. URL https://lpdaac.usgs.gov/ (accessed 6.20.21).

Lu, C., Barr, D.B., Pearson, M., Bartell, S., Bravo, R., 2006. A longitudinal approach to assessing urban and suburban children's exposure to pyrethroid pesticides. Environ. Health Perspect. 114, 1419–1423. https://doi.org/10.1289/ehp.9043

Lucas, K.L., Carter, G.A., 2008. The use of hyperspectral remote sensing to assess vascular plant species richness on Horn Island, Mississippi. Remote Sens. Environ.

112, 3908–3915. https://doi.org/10.1016/j.rse.2008.06.009

Maitima, J.M., Mugatha, S.M., Reid, R.S., Gachimbi, L.N., Majule, A., Lyaruu, H., Pomery, D., Mathai, S., Mugisha, S., 2009. The linkages between land use change, land degradation and biodiversity across East Africa. African J. Environ. Sci. Technol. 3, 310–325. https://doi.org/10.5897/AJEST08.173

Malczewski, J., 1999. GIS and Multicriteria Decision Analysis, The Journal of the Operational Research Society. John Wiley & Sons, Inc., Canada., Canada. https://doi.org/10.2307/254268

Maltsev, K., Yermolaev, O., 2020. Assessment of soil loss by water erosion in small river basins in Russia. Catena 195. https://doi.org/10.1016/j.catena.2020.104726

Masoudi, M., Jokar, P., Pradhan, B., 2018. A new approach for land degradation and desertification assessment using geo-spatial techniques. Nat. Hazards Earth Syst. Sci. 18, 1133–1140. https://doi.org/10.5194/nhess-18-1133-2018

Masoudi, M., Patwardhan, A.M., Gore, S.D., 2006. Risk assessment of water erosion for the Qareh Aghaj subbasin, southern Iran. Stoch. Environ. Res. Risk Assess. 21, 15–24. https://doi.org/10.1007/s00477-006-0040-y

McLeod, A., McLeod, M., 2014. Package "Kendall," cran.microsoft.com.

Meena, S.R., Ghorbanzadeh, O., Blaschke, T., 2019. A comparative study of statistics-based landslide susceptibility models: A case study of the region affected by the Gorkha earthquake in Nepal. ISPRS Int. J. Geo-Information 8. https://doi.org/10.3390/ijgi8020094

Mendicino, G., 1999. Sensitivity analysis on GIS procedures for the estimate of soil erosion risk, in: Natural Hazards. Springer Netherlands, pp. 231–253. https://doi.org/10.1023/a:1008120231103

Menne, M.J., Durre, I., Vose, R.S., Gleason, B.E., Houston, T.G., 2012. An overview of the global historical climatology network-daily database. J. Atmos. Ocean. Technol. 29, 897–910. https://doi.org/10.1175/JTECH-D-11-00103.1

Merritt, W.S., Letcher, R.A., Jakeman, A.J., 2003. A review of erosion and sediment transport models, in: Environmental Modelling and Software. Elsevier BV, pp. 761–799. https://doi.org/10.1016/S1364-8152(03)00078-1

Mitra, B., Scott, H.D., Dixon, J.C., McKimmey, J.M., 1998. Applications of fuzzy logic to the prediction of soil erosion in a large watershed. Geoderma 86, 183–209. https://doi.org/10.1016/S0016-7061(98)00050-0

Mizuochi, H., Hayashi, M., Tadono, T., 2019. Development of an operational algorithm for automated deforestation mapping via the Bayesian integration of long-term optical and microwave satellite data. Remote Sens. 11, 2038. https://doi.org/10.3390/rs11172038

Moeini, A., Zarandi, N.K., Pazira, E., Badiollahi, Y., 2015. The relationship between drainage density and soil erosion rate: a study of five watersheds in Ardebil Province, Iran, in: River Basin Management VIII. WIT Press, pp. 129–138. https://doi.org/10.2495/rm150121

Mondal, P., McDermid, S.S., Qadir, A., 2020. A reporting framework for Sustainable Development Goal 15: Multi-scale monitoring of forest degradation using MODIS, Landsat and Sentinel data. Remote Sens. Environ. 237.

https://doi.org/10.1016/j.rse.2019.111592

Montanarella, L., Pennock, D.J., McKenzie, N.J., Badraoui, M., Chude, V., Baptista, I., Mamo, T., Yemefack, M., Singh Aulakh, M., Yagi, K., Young Hong, S., Vijarnsorn, P., Zhang, G.-L., Arrouays, D., Black, H., Krasilnikov, P., Sobocká, J., Alegre, J., Henriquez, C.R., Mendonça-Santos, M.L., Taboada, M., Espinosa-Victoria, D., AlShankiti, A., AlaviPanah, S.K., Elsheikh, E.A.E., Hempel, J., Camps Arbestain, M., Nachtergaele, F., Vargas, R., 2015. World's soils are under threat. SOIL Discuss. 2, 1263–1272. https://doi.org/10.5194/soild-2-1263-2015

Montgomery, B., Dragićević, S., Dujmović, J., Schmidt, M., 2016. A GIS-based Logic Scoring of Preference method for evaluation of land capability and suitability for agriculture. Comput. Electron. Agric. 124, 340–353. https://doi.org/10.1016/j.compag.2016.04.013

Moore, I.D., Burch, G.J., 1986. Physical Basis of the Length-slope Factor in the Universal Soil Loss Equation. Soil Sci. Soc. Am. J. 50, 1294–1298. https://doi.org/10.2136/sssaj1986.03615995005000050042x

Moore, I.D., Wilson, J.P., 1992. Length-slope factors for the revised universal soil loss equation: simplified method of estimation. J. Soil Water Conserv. 47, 423–428.

Morgan, R.P.C., Morgan, D.D.V., Finney, H.J., 1984. A predictive model for the assessment of soil erosion risk. J. Agric. Eng. Res. 30, 245–253. https://doi.org/10.1016/S0021-8634(84)80025-6

Moriasi, D.N., Arnold, J.G., Van Liew, M.W., Bingner, R.L., Harmel, R.D., Veith, T.L., 2007. Model evaluation guidelines for systematic quantification of accuracy in watershed simulations. Trans. ASABE 50, 885–900.

Morisette, J.T., Jarnevich, C.S., Ullah, A., Cai, W., Pedelty, J.A., Gentle, J.E., Stohlgren, T.J., Schnase, J.L., 2006. A tamarisk habitat suitability map for the continental United States. Front. Ecol. Environ. 4, 11–17. https://doi.org/10.1890/1540-9295(2006)004[0012:ATHSMF]2.0.CO;2

Mosadeghi, R., Warnken, J., Tomlinson, R., Mirfenderesk, H., 2015. Comparison of Fuzzy-AHP and AHP in a spatial multi-criteria decision making model for urban land-use planning. Comput. Environ. Urban Syst. 49, 54–65. https://doi.org/10.1016/j.compenvurbsys.2014.10.001

Mosavi, A., Sajedi-Hosseini, F., Choubin, B., Taromideh, F., Rahi, G., Dineva, A.A., 2020. Susceptibility mapping of soil water erosion using machine learning models. Water (Switzerland) 12. https://doi.org/10.3390/w12071995

Mukherjee, F., Singh, D., 2020. Assessing Land Use–Land Cover Change and Its Impact on Land Surface Temperature Using LANDSAT Data: A Comparison of Two Urban Areas in India. Earth Syst. Environ. 4, 385–407. https://doi.org/10.1007/s41748-020-00155-9

Mulder, V.L., de Bruin, S., Schaepman, M.E., Mayr, T.R., 2011. The use of remote sensing in soil and terrain mapping - A review. Geoderma. https://doi.org/10.1016/j.geoderma.2010.12.018

Mullan, D., Favis-Mortlock, D., Fealy, R., 2012. Addressing key limitations associated with modelling soil erosion under the impacts of future climate change. Agric. For. Meteorol. 156, 18–30. https://doi.org/10.1016/j.agrformet.2011.12.004

Mwaniki, M.W., Agutu, N.O., Mbaka, J.G., Ngigi, T.G., Waithaka, E.H., 2015. Landslide scar/soil erodibility mapping using Landsat TM/ETM+ bands 7 and 3 Normalised Difference Index: A case study of central region of Kenya. Appl. Geogr. 64, 108–120. https://doi.org/10.1016/j.apgeog.2015.09.009

Myeong, S., Nowak, D.J., Duggin, M.J., 2006. A temporal analysis of urban forest carbon storage using remote sensing. Remote Sens. Environ. 101, 277–282. https://doi.org/10.1016/j.rse.2005.12.001

Nagendra, H., 2002. Opposite trends in response for the Shannon and Simpson indices of landscape diversity. Appl. Geogr. 22, 175–186. https://doi.org/10.1016/S0143-6228(02)00002-4

Nagendra, H., Rocchini, D., Ghate, R., Sharma, B., Pareeth, S., 2010. Assessing plant diversity in a dry tropical forest: Comparing the utility of landsat and ikonos satellite images. Remote Sens. 2, 478–496. https://doi.org/10.3390/rs2020478

Nampak, H., Pradhan, B., Mojaddadi Rizeei, H., Park, H.J., 2018. Assessment of land cover and land use change impact on soil loss in a tropical catchment by using multitemporal SPOT-5 satellite images and Revised Universal Soil Loss Equation model. L. Degrad. Dev. 29, 3440–3455. https://doi.org/10.1002/ldr.3112

Nearing, M.A., Jetten, V., Baffaut, C., Cerdan, O., Couturier, A., Hernandez, M., Le Bissonnais, Y., Nichols, M.H., Nunes, J.P., Renschler, C.S., Souchère, V., Van Oost, K., 2005. Modeling response of soil erosion and runoff to changes in precipitation and cover, in: Catena. Elsevier, pp. 131–154. https://doi.org/10.1016/j.catena.2005.03.007

Nearing, M.A., Lane, L.J., Lopes, V.L., 1994. Modeling soil erosion., in: Lal, R. (Ed.), Modeling Soil Erosion. Soil and Water Conservation Society (SWCS).Ankeny, IA, USA., Ankeny, IA, USA, pp. 127-156. https://doi.org/10.1002/9781118351475.ch22

NRMC, 2015. Crop Suitability [WWW Document]. Nat. Resour. Manag. Center, Dep. Agric. Sri lanka. https://doi.org/10.7312/schw92626-007

Oldeman, L.R., 1992. Global Extent of Soil Degradation, Soil resilience and sustainable land use.

Olofsson, P., Foody, G.M., Stehman, S. V., Woodcock, C.E., 2013. Making better use of accuracy data in land change studies: Estimating accuracy and area and quantifying uncertainty using stratified estimation. Remote Sens. Environ. 129, 122–131. https://doi.org/10.1016/j.rse.2012.10.031

Olsoy, P.J., Glenn, N.F., Clark, P.E., Derryberry, D.W.R., 2014. Aboveground total and green biomass of dryland shrub derived from terrestrial laser scanning. ISPRS J. Photogramm. Remote Sens. 88, 166–173. https://doi.org/10.1016/j.isprsjprs.2013.12.006

Orhan, U., Hekim, M., Ozer, M., 2011. EEG signals classification using the K-means clustering and a multilayer perceptron neural network model. Expert Syst. Appl. 38, 13475–13481. https://doi.org/10.1016/j.eswa.2011.04.149

ORNL DAAC, 2018. MODIS and VIIRS Land Products Global Subsetting and Visualization Tool [WWW Document]. ORNL DAAC, Oak Ridge, Tennessee, USA. URL https://daac.ornl.gov/cgi-bin/dsviewer.pl?ds_id=1379 (accessed 6.25.21).

Orwig, D.A., Boucher, P., Paynter, I., Saenz, E., Li, Z., Schaaf, C., 2018. The potential to characterize ecological data with terrestrial laser scanning in Harvard Forest, MA. Interface Focus. https://doi.org/10.1098/rsfs.2017.0044

Oštir, K., Veljanovski, T., Podobnikar, T., Stančič, Z., 2003. Application of satellite remote sensing in natural hazard management: The Mount Mangart landslide case study. Int. J. Remote Sens. 24, 3983–4002. https://doi.org/10.1080/0143116031000103826

Ouma, Y.O., Cheruyot, R., Wachera, A.N., 2021. Rainfall and runoff time-series trend analysis using LSTM recurrent neural network and wavelet neural network with satellite-based meteorological data: case study of Nzoia hydrologic basin. Complex Intell. Syst. 1, 3. https://doi.org/10.1007/s40747-021-00365-2

Panabokke, C.R., 1996. Soils and Agro-Ecological Environments of Sri Lanka, Natural Resources, Energy and Science Authority of Sri Lanka. Natural Resources, Energy and Science Authority, Colombo 07, Sri Lanka.

Panagos, P., Ballabio, C., Himics, M., Scarpa, S., Matthews, F., Bogonos, M., Poesen, J., Borrelli, P., 2021. Projections of soil loss by water erosion in Europe by 2050. Environ. Sci. Policy 124, 380–392. https://doi.org/10.1016/j.envsci.2021.07.012

Panagos, P., Borrelli, P., Meusburger, K., Yu, B., Klik, A., Jae Lim, K., Yang, J.E., Ni, J., Miao, C., Chattopadhyay, N., Sadeghi, S.H., Hazbavi, Z., Zabihi, M., Larionov, G.A., Krasnov, S.F., Gorobets, A. V., Levi, Y., Erpul, G., Birkel, C., Hoyos, N., Naipal, V., Oliveira, P.T.S., Bonilla, C.A., Meddi, M., Nel, W., Al Dashti, H., Boni, M., Diodato, N., Van Oost, K., Nearing, M., Ballabio, C., 2017a. Global rainfall erosivity assessment based on high-temporal resolution rainfall records. Sci. Rep. 7, 4175. https://doi.org/10.1038/s41598-017-04282-8

Panagos, P., Borrelli, P., Meusburger, K., Yu, B., Klik, A., Lim, K.J., Yang, J.E., Ni, J., Miao, C., Chattopadhyay, N., Sadeghi, S.H., Hazbavi, Z., Zabihi, M., Larionov, G.A., Krasnov, S.F., Gorobets, A. V, Levi, Y., Erpul, G., Birkel, C., Hoyos, N., Naipal, V., Oliveira, P.T.S., Bonilla, C.A., Meddi, M., Nel, W., Al Dashti, H., Boni, M., Diodato, N., Van Oost, K., Nearing, M., Ballabio, C., 2017b. Global rainfall erosivity assessment based on high-temporal resolution rainfall records. Sci. Rep. 7. https://doi.org/10.1038/s41598-017-04282-8

Panagos, P., Borrelli, P., Poesen, J., Ballabio, C., Lugato, E., Meusburger, K., Montanarella, L., Alewell, C., 2015. The new assessment of soil loss by water erosion in Europe. Environ. Sci. Policy 54, 438–447. https://doi.org/10.1016/j.envsci.2015.08.012

Panagos, P., Katsoyiannis, A., 2019. Soil erosion modelling: The new challenges as the result of policy developments in Europe. Environ. Res. https://doi.org/10.1016/j.envres.2019.02.043

Patakamuri, S.K., Muthiah, K., Sridhar, V., 2020. Long-Term homogeneity, trend, and change-point analysis of rainfall in the arid district of ananthapuramu, Andhra Pradesh State, India. Water (Switzerland) 12. https://doi.org/10.3390/w12010211

Pau, S., Gillespie, T.W., Wolkovich, E.M., 2012. Dissecting NDVI-species richness relationships in Hawaiian dry forests. J. Biogeogr. 39, 1678–1686. https://doi.org/10.1111/j.1365-2699.2012.02731.x

Penadés-Plà, V., García-Segura, T., Martí, J. V., Yepes, V., 2016. A review of multi-

criteria decision-making methods applied to the sustainable bridge design. Sustain. https://doi.org/10.3390/su8121295

Perera, E.N.C., Jayawardana, D.T., Jayasinghe, P., Bandara, R.M.S., Alahakoon, N., 2018. Direct impacts of landslides on socio-economic systems: a case study from Aranayake, Sri Lanka. Geoenvironmental Disasters 5, 1–12. https://doi.org/10.1186/s40677-018-0104-6

Perera, E.N.C., Jayawardana, D.T., Jayasinghe, P., Ranagalage, M., 2019. Landslide vulnerability assessment based on entropy method: a case study from Kegalle district, Sri Lanka. Model. Earth Syst. Environ. 5, 1635–1649. https://doi.org/10.1007/s40808-019-00615-w

Perotto-Baldiviezo, H.L., Thurow, T.L., Smith, C.T., Fisher, R.F., Wu, X.B., 2004. GIS-based spatial analysis and modeling for landslide hazard assessment in steeplands, southern Honduras. Agric. Ecosyst. Environ. 103, 165–176. https://doi.org/10.1016/j.agee.2003.10.011

Persichillo, M.G., Bordoni, M., Meisina, C., 2017. The role of land use changes in the distribution of shallow landslides. Sci. Total Environ. 574, 924–937. https://doi.org/10.1016/j.scitotenv.2016.09.125

Pham, B.T., Prakash, I., Khosravi, K., Chapi, K., Trinh, P.T., Ngo, T.Q., Hosseini, S. V, Bui, D.T., 2019. A comparison of Support Vector Machines and Bayesian algorithms for landslide susceptibility modelling. Geocarto Int. 34, 1385–1407. https://doi.org/10.1080/10106049.2018.1489422

Pham, T.G., Degener, J., Kappas, M., 2018. Integrated universal soil loss equation (USLE) and Geographical Information System (GIS) for soil erosion estimation in A Sap basin: Central Vietnam. Int. Soil Water Conserv. Res. 6, 99–110. https://doi.org/10.1016/j.iswcr.2018.01.001

Pimentel, D., 2006. Soil erosion: A food and environmental threat. Environ. Dev. Sustain. https://doi.org/10.1007/s10668-005-1262-8

Pimentel, D., Burgess, M., 2013. Soil erosion threatens food production. Agric. 3, 443–463. https://doi.org/10.3390/agriculture3030443

Poesen, J., 2018. Soil erosion in the Anthropocene: Research needs. Earth Surf. Process. Landforms 43, 64–84. https://doi.org/10.1002/esp.4250

Poesen, J., Nachtergaele, J., Verstraeten, G., Valentin, C., 2003. Gully erosion and environmental change: Importance and research needs, in: Catena. Elsevier, pp. 91–133. https://doi.org/10.1016/S0341-8162(02)00143-1

Pohl, M., Alig, D., Körner, C., Rixen, C., 2009. Higher plant diversity enhances soil stability in disturbed alpine ecosystems. Plant Soil 324, 91–102. https://doi.org/10.1007/s11104-009-9906-3

Pour, S.H., Wahab, A.K.A., Shahid, S., 2020. Physical-empirical models for prediction of seasonal rainfall extremes of Peninsular Malaysia. Atmos. Res. 233, 104720. https://doi.org/10.1016/j.atmosres.2019.104720

Pouteau, R., Gillespie, T.W., Birnbaum, P., 2018. Predicting tropical tree species richness from normalized difference vegetation index time series: The devil is perhaps not in the detail. Remote Sens. 10, 698. https://doi.org/10.3390/rs10050698

Pradhan, B., 2013. A comparative study on the predictive ability of the decision tree,

support vector machine and neuro-fuzzy models in landslide susceptibility mapping using GIS. Comput. Geosci. 51, 350–365. https://doi.org/10.1016/j.cageo.2012.08.023

Pradhan, B., 2011. Use of GIS-based fuzzy logic relations and its cross application to produce landslide susceptibility maps in three test areas in Malaysia. Environ. Earth Sci. 63, 329–349. https://doi.org/10.1007/s12665-010-0705-1

Pradhan, B., Abokharima, M.H., Jebur, M.N., Tehrany, M.S., 2014. Land subsidence susceptibility mapping at Kinta Valley (Malaysia) using the evidential belief function model in GIS. Nat. Hazards 73, 1019–1042. https://doi.org/10.1007/s11069-014-1128-1

Pradhan, B., Chaudhari, A., Adinarayana, J., Buchroithner, M.F., 2012. Soil erosion assessment and its correlation with landslide events using remote sensing data and GIS: A case study at Penang Island, Malaysia. Environ. Monit. Assess. 184, 715–727. https://doi.org/10.1007/s10661-011-1996-8

Pradhan, B., Lee, S., 2010a. Landslide susceptibility assessment and factor effect analysis: backpropagation artificial neural networks and their comparison with frequency ratio and bivariate logistic regression modelling. Environ. Model. Softw. 25, 747–759. https://doi.org/10.1016/j.envsoft.2009.10.016

Pradhan, B., Lee, S., 2010b. Delineation of landslide hazard areas on Penang Island, Malaysia, by using frequency ratio, logistic regression, and artificial neural network models. Environ. Earth Sci. 60, 1037–1054. https://doi.org/10.1007/s12665-009-0245-8

Prince, S.D., Colstoun, E.B.D., Kravitz, L.L., 1998. Evidence from rain-use efficiencies does not indicate extensive Sahelian desertification. Glob. Chang. Biol. 4, 359–374. https://doi.org/10.1046/j.1365-2486.1998.00158.x

Puente, C., Olague, G., Trabucchi, M., Arjona-Villicaña, P.D., Soubervielle-Montalvo, C., 2019. Synthesis of Vegetation Indices using genetic programming for soil erosion estimation. Remote Sens. 11, 156. https://doi.org/10.3390/rs11020156

Punyawardena, B.V.., Bandara, T.M.., Munasinghe, M.A.., Banda, N.J., 2003. Agro-Ecological Regions of Sri Lanka [WWW Document]. Nat. Resour. Manag. Center, Dep. Agric. Sri Lanka. URL https://doa.gov.lk/images/weather_climate/Krushi_parisarika.jpg (accessed 12.20.20).

Qi, J., Chehbouni, A., Huete, A.R., Kerr, Y.H., Sorooshian, S., 1994. A modified soil adjusted vegetation index. Remote Sens. Environ. 48, 119–126. https://doi.org/10.1016/0034-4257(94)90134-1

Qi, Z., Yeh, A.G.O., Li, X., Lin, Z., 2012. A novel algorithm for land use and land cover classification using RADARSAT-2 polarimetric SAR data. Remote Sens. Environ. 118, 21–39. https://doi.org/10.1016/j.rse.2011.11.001

Rahman, M.R., Shi, Z.H., Chongfa, C., 2009. Soil erosion hazard evaluation-An integrated use of remote sensing, GIS and statistical approaches with biophysical parameters towards management strategies. Ecol. Modell. 220, 1724–1734. https://doi.org/10.1016/j.ecolmodel.2009.04.004

Rahman, M.R., Shi, Z.H., Chongfa, C., Dun, Z., 2015. Assessing soil erosion hazard -a raster based GIS approach with spatial principal component analysis (SPCA). Earth

Sci. Informatics 8, 853–865. https://doi.org/10.1007/s12145-015-0219-1

Rahmati, O., Tahmasebipour, N., Haghizadeh, A., Pourghasemi, H.R., Feizizadeh, B., 2017. Evaluation of different machine learning models for predicting and mapping the susceptibility of gully erosion. Geomorphology 298, 118–137. https://doi.org/10.1016/j.geomorph.2017.09.006

Raman, M.A.E., Shalaby, A., Essa, E.F., 2018. Quantitative land evaluation based on fuzzy-multi-criteria spatial model for sustainable land-use planning. Model. Earth Syst. Environ. 4, 1341–1353. https://doi.org/10.1007/s40808-018-0478-1

Ranasinghe, A.K.R.N., Bandara, R., Puswewala, U.G.A., Dammalage, T.L., 2019. Efficacy of using Radar Induced Factors in Landslide Susceptibility Analysis: case study of Koslanda, Sri Lanka. Nat. Hazards Earth Syst. Sci. Discuss. 1–22. https://doi.org/10.5194/nhess-2018-335

Ratnayake, U., Herath, S., 2005. Changing rainfall and its impact on landslides in Sri Lanka. J. Mt. Sci. 2, 218–224. https://doi.org/10.1007/bf02973195

Regmi, A., Meade, B., 2013. Demand side drivers of global food security. Glob. Food Sec. https://doi.org/10.1016/j.gfs.2013.08.001

Remley, P.A., Bradford, J.M., 1989. Relationship of Soil Crust Morphology to Inter-rill Erosion Parameters. Soil Sci. Soc. Am. J. 53, 1215–1221. https://doi.org/10.2136/sssaj1989.03615995005300040038x

Renard, K.G., Foster, G.R., Weesies, G., McCool, D., Yoder, D., 1997. Predicting soil erosion by water: a guide to conservation planning with the Revised Universal Soil Loss Equation (RUSLE). Agric. Handb. No. 703. https://doi.org/DC0-16-048938-5 65–100.

Rinot, O., Levy, G.J., Steinberger, Y., Svoray, T., Eshel, G., 2019. Soil health assessment: A critical review of current methodologies and a proposed new approach. Sci. Total Environ. 648, 1484–1491. https://doi.org/10.1016/j.scitotenv.2018.08.259

Rizeei, H.M., Pradhan, B., Saharkhiz, M.A., 2018. Surface runoff prediction regarding LULC and climate dynamics using coupled LTM, optimized ARIMA, and GIS-based SCS-CN models in tropical region. Arab. J. Geosci. 11, 1–16. https://doi.org/10.1007/s12517-018-3397-6

Rizeei, H.M., Saharkhiz, M.A., Pradhan, B., Ahmad, N., 2016. Soil erosion prediction based on land cover dynamics at the Semenyih watershed in Malaysia using LTM and USLE models. Geocarto Int. 31, 1158–1177. https://doi.org/10.1080/10106049.2015.1120354

Rodrigo-Comino, J., López-Vicente, M., Kumar, V., Rodríguez-Seijo, A., Valkó, O., Rojas, C., Pourghasemi, H.R., Salvati, L., Bakr, N., Vaudour, E., Brevik, E.C., Radziemska, M., Pulido, M., Di Prima, S., Dondini, M., de Vries, W., Santos, E.S., Mendonça-Santos, M. de L., Yu, Y., Panagos, P., 2020. Soil Science Challenges in a New Era: A Transdisciplinary Overview of Relevant Topics. Air, Soil Water Res. 13, 117862212097749. https://doi.org/10.1177/1178622120977491

Rodríguez Sousa, A.A., Barandica, J.M., Sanz-Cañada, J., Rescia, A.J., 2019. Application of a dynamic model using agronomic and economic data to evaluate the sustainability of the olive grove landscape of Estepa (Andalusia, Spain). Landsc. Ecol. 34, 1547–1563. https://doi.org/10.1007/s10980-019-00773-3

Rogan, J., YooL, S.R., 2001. Mapping fire-induced vegetation depletion in the Peloncillo Mountains Arizona and New Mexico. Int. J. Remote Sens. 22, 3101–3121. https://doi.org/10.1080/01431160152558279

Rondeaux, G., Steven, M., Baret, F., 1996. Optimization of soil-adjusted vegetation indices. Remote Sens. Environ. 55, 95–107. https://doi.org/10.1016/0034-4257(95)00186-7

Rouse, J.W., Haas, R.H., Schell, J.A., Deering, D.W., 1974. Monitoring Vegetation Systems in the Great Plains with Erts, in: Stanley C. Freden, Enrico P. Mercanti, and M.A.B. (Ed.), Third Earth Resources Technology Satellite-1 Symposium-Volume I: Technical Presentations. NASA SP. published by NASA, Washington, D.C., Washington, D.C., USA, p. 309.

Rozos, D., Skilodimou, H.D., Loupasakis, C., Bathrellos, G.D., 2013. Application of the revised universal soil loss equation model on landslide prevention. An example from N. Euboea (Evia) Island, Greece. Environ. Earth Sci. 70, 3255–3266. https://doi.org/10.1007/s12665-013-2390-3

Saaty, T.L., 2002. Decision making with the Analytic Hierarchy Process. Sci. Iran. 9, 215–229. https://doi.org/10.1504/ijssci.2008.017590

Saaty, T.L., Vargas, L.G., 2013. The analytic network process, in: International Series in Operations Research and Management Science. Springer New York LLC, pp. 1–40. https://doi.org/10.1007/978-1-4614-7279-7_1

Sadeghi, M., Nguyen, P., Naeini, M.R., Hsu, K., Braithwaite, D., Sorooshian, S., 2021. PERSIANN-CCS-CDR, a 3-hourly 0.04° global precipitation climate data record for heavy precipitation studies. Sci. Data 8. https://doi.org/10.1038/s41597-021-00940-9

Saha, S., Gayen, A., Pourghasemi, H.R., Tiefenbacher, J.P., 2019. Identification of soil erosion-susceptible areas using fuzzy logic and analytical hierarchy process modeling in an agricultural watershed of Burdwan district, India. Environ. Earth Sci. 78, 649. https://doi.org/10.1007/s12665-019-8658-5

Salari, M., Shariat, S.M., Rahimi, R., Dashti, S., 2019. Land capability evaluation for identifying industrial zones: combination multi-criteria decision-making method with geographic information system. Int. J. Environ. Sci. Technol. 16, 5501–5512. https://doi.org/10.1007/s13762-018-1925-2

Samui, P., 2008. Slope stability analysis: A support vector machine approach. Environ. Geol. 56, 255–267. https://doi.org/10.1007/s00254-007-1161-4

Sanchis, M.P.S., Torri, D., Borselli, L., Poesen, J., 2008. Climate effects on soil erodibility. Earth Surf. Process. Landforms 33, 1082–1097. https://doi.org/10.1002/esp.1604

Sankey, T., Donager, J., McVay, J., Sankey, J.B., 2017. UAV lidar and hyperspectral fusion for forest monitoring in the southwestern USA. Remote Sens. Environ. 195, 30–43. https://doi.org/10.1016/j.rse.2017.04.007

Santos, L., Thirel, G., Perrin, C., 2018. Technical note: Pitfalls in using log-transformed flows within the KGE criterion. Hydrol. Earth Syst. Sci. 22, 4583–4591. https://doi.org/10.5194/hess-22-4583-2018

Sarmah, S., Jia, G., Zhang, A., 2018. Satellite view of seasonal greenness trends and

controls in South Asia. Environ. Res. Lett. 13. https://doi.org/10.1088/1748-9326/aaa866

Scaioni, M., Longoni, L., Melillo, V., Papini, M., 2014. Remote sensing for landslide investigations: An overview of recent achievements and perspectives. Remote Sens. https://doi.org/10.3390/rs6109600

Schmidt, K.S., Skidmore, A.K., 2003. Spectral discrimination of vegetation types in a coastal wetland. Remote Sens. Environ. 85, 92–108. https://doi.org/10.1016/S0034-4257(02)00196-7

Şen, Z., 2017. Innovative trend significance test and applications. Theor. Appl. Climatol. 127, 939–947. https://doi.org/10.1007/s00704-015-1681-x

Şen, Z., 2012. Innovative Trend Analysis Methodology. J. Hydrol. Eng. 17, 1042–1046. https://doi.org/10.1061/(asce)he.1943-5584.0000556

Senanayake, S., Pradhan, B., Huete, A., Brennan, J., 2022. Spatial modeling of soil erosion hazards and crop diversity change with rainfall variation in the Central Highlands of Sri Lanka. Sci. Total Environ. 806, 150405. https://doi.org/10.1016/j.scitotenv.2021.150405

Senanayake, S., Pradhan, B., Huete, A., Brennan, J., 2020a. Assessing Soil Erosion Hazards Using Land-Use Change and Landslide Frequency Ratio Method: A Case Study of Sabaragamuwa Province, Sri Lanka. Remote Sens. 12, 1483. https://doi.org/10.3390/rs12091483

Senanayake, S., Pradhan, B., Huete, A., Brennan, J., 2020b. A Review on Assessing and Mapping Soil Erosion Hazard Using Geo-Informatics Technology for Farming System Management. Remote Sens. 12, 4063. https://doi.org/10.3390/rs12244063

Senanayake, S.S., Munasinhe, M.A.K., W.M.A.D.B. Wickramasinghe, 2013. Use of erosion hazard assessments for regional scale crop suitability mapping in the Uva province. Ann. Sri Lanka Dep. Agric. 127–141.

Seo, S.N.N., Mendelsohn, R., Munasinghe, M., 2005. Climate change and agriculture in Sri Lanka: A Ricardian valuation. Environ. Dev. Econ. 10, 581–596. https://doi.org/10.1017/S1355770X05002044

Sepuru, T.K., Dube, T., 2018. An appraisal on the progress of remote sensing applications in soil erosion mapping and monitoring. Remote Sens. Appl. Soc. Environ. https://doi.org/10.1016/j.rsase.2017.10.005

Sertel, E., Topaloğlu, R., Şallı, B., Yay Algan, I., Aksu, G., 2018. Comparison of Landscape Metrics for Three Different Level Land Cover/Land Use Maps. ISPRS Int. J. Geo-Information 7, 408. https://doi.org/10.3390/ijgi7100408

Seutloali, K.E., Dube, T., Mutanga, O., 2017. Assessing and mapping the severity of soil erosion using the 30-m Landsat multispectral satellite data in the former South African homelands of Transkei. Phys. Chem. Earth 100, 296–304. https://doi.org/10.1016/j.pce.2016.10.001

Shahabi, H., Hashim, M., 2015. Landslide susceptibility mapping using GIS-based statistical models and Remote sensing data in tropical environment. Sci. Rep. 5, 1–15. https://doi.org/10.1038/srep09899

Shannon, C.E., 1948. A Mathematical Theory of Communication. Bell Syst. Tech. J. 27, 379–423. https://doi.org/10.1002/j.1538-7305.1948.tb01338.x

Shinde, V., Tiwari, K.N., Singh, M., 2010. Prioritization of micro watersheds on the basis of soil erosion hazard using remote sensing and geographic information system. Int. J. Water Resour. Environ. Eng. 2, 130–136. https://doi.org/10.5897/IJWREE.9000046

Shrestha, R.P., Schmidt-Vogt, D., Gnanavelrajah, N., 2010. Relating plant diversity to biomass and soil erosion in a cultivated landscape of the eastern seaboard region of Thailand. Appl. Geogr. 30, 606–617. https://doi.org/10.1016/j.apgeog.2010.01.005

Shruthi, R.B.V., Kerle, N., Jetten, V., Abdellah, L., Machmach, I., 2015. Quantifying temporal changes in gully erosion areas with object oriented analysis. Catena 128, 262–277. https://doi.org/10.1016/j.catena.2014.01.010

Singh, J., Knapp, H.V., Arnold, J.G., Demissie, M., 2005. Hydrological modeling of the Iroquois River watershed using HSPF and SWAT. J. Am. Water Resour. Assoc. 41, 343–360. https://doi.org/10.1111/j.1752-1688.2005.tb03740.x

Singh, S., Dhote, P.R., Thakur, P.K., Chouksey, A., Aggarwal, S.P., 2020. Identification of flash-floods-prone river reaches in Beas river basin using GIS-based multi-criteria technique: validation using field and satellite observations. Nat. Hazards 1–23. https://doi.org/10.1007/s11069-020-04406-w

Singh, S.K., Srivastava, P.K., Gupta, M., Thakur, J.K., Mukherjee, S., 2014. Appraisal of land use/land cover of mangrove forest ecosystem using support vector machine. Environ. Earth Sci. 71, 2245–2255. https://doi.org/10.1007/s12665-013-2628-0

Sinshaw, B.G., Belete, A.M., Tefera, A.K., Dessie, A.B., Bizuneh, B.B., Alem, H.T., Atanaw, S.B., Eshete, D.G., Wubetu, T.G., Atinkut, H.B., Moges, M.A., 2021. Prioritization of potential soil erosion susceptibility region Using fuzzy Logic and Analytical Hierarchy process, Upper Blue Nile Basin, Ethiopia. Water-Energy Nexus 4, 10–24. https://doi.org/10.1016/j.wen.2021.01.001

Smith, M.L., Ollinger, S. V., Martin, M.E., Aber, J.D., Hallett, R.A., Goodale, C.L., 2002. Direct estimation of aboveground forest productivity through hyperspectral remote sensing of canopy nitrogen. Ecol. Appl. 12, 1286–1302. https://doi.org/10.1890/1051-0761(2002)012[1286:DEOAFP]2.0.CO;2

Somasiri, I.S., Hewawasam, T., Rambukkange, M.P., 2021. Adaptation of the revised universal soil loss equation to map spatial distribution of soil erosion in tropical watersheds: a GIS/RS-based study of the Upper Mahaweli River Catchment of Sri Lanka. Model. Earth Syst. Environ. 1, 3. https://doi.org/10.1007/s40808-021-01245-x

Sommer, R., Fölster, H., Vielhauer, K., Carvalho, E.J.M., Vlek, P.L.G., 2003. Deep Soil Water Dynamics and Depletion by Secondary Vegetation in the Eastern Amazon. Soil Sci. Soc. Am. J. 67, 1672–1686. https://doi.org/10.2136/sssaj2003.1672

Sousa, A.A.R., Barandica, J.M., Sanz-Cañada, J., Rescia, A.J., 2019. Application of a dynamic model using agronomic and economic data to evaluate the sustainability of the olive grove landscape of Estepa (Andalusia, Spain). Landsc. Ecol. 34, 1547–1563. https://doi.org/10.1007/s10980-019-00773-3

Sumfleth, K., Duttmann, R., 2008. Prediction of soil property distribution in paddy soil landscapes using terrain data and satellite information as indicators. Ecol. Indic. 8, 485–501. https://doi.org/10.1016/j.ecolind.2007.05.005

Sun, Q., Miao, C., Duan, Q., Ashouri, H., Sorooshian, S., Hsu, K.L., 2018. A Review of

Global Precipitation Data Sets: Data Sources, Estimation, and Intercomparisons. Rev. Geophys. 56, 79–107. https://doi.org/10.1002/2017RG000574

Symstad, A.J., Jonas, J.L., 2011. Incorporating biodiversity into rangeland health: Plant species richness and diversity in great plains grasslands. Rangel. Ecol. Manag. 64, 555–572. https://doi.org/10.2111/REM-D-10-00136.1

Tarboton, D.G., Bras, R.L., Rodriguez-Iturbe, I., 1992. A physical basis for drainage density. Geomorphology 5, 59–76. https://doi.org/10.1016/0169-555X(92)90058-V

Tarolli, P., 2014. High-resolution topography for understanding Earth surface processes: Opportunities and challenges. Geomorphology. https://doi.org/10.1016/j.geomorph.2014.03.008

Tarolli, P., Borga, M., Chang, K.T., Chiang, S.H., 2011. Modeling shallow landsliding susceptibility by incorporating heavy rainfall statistical properties. Geomorphology 133, 199–211. https://doi.org/10.1016/j.geomorph.2011.02.033

Tarolli, P., Preti, F., Romano, N., 2014. Terraced landscapes: From an old best practice to a potential hazard for soil degradation due to land abandonment. Anthropocene. https://doi.org/10.1016/j.ancene.2014.03.002

Tehrany, M.S., Shabani, F., Javier, D.N., Kumar, L., 2017. Soil erosion susceptibility mapping for current and 2100 climate conditions using evidential belief function and frequency ratio. Geomatics, Nat. Hazards Risk 8, 1695–1714. https://doi.org/10.1080/19475705.2017.1384406

Teng, H., Liang, Z., Chen, S., Liu, Y., Viscarra Rossel, R.A., Chappell, A., Yu, W., Shi, Z., 2018. Current and future assessments of soil erosion by water on the Tibetan Plateau based on RUSLE and CMIP5 climate models. Sci. Total Environ. 635, 673–686. https://doi.org/10.1016/j.scitotenv.2018.04.146

Termeh, S.V.R., Kornejady, A., Pourghasemi, H.R., Keesstra, S., 2018. Flood susceptibility mapping using novel ensembles of adaptive neuro fuzzy inference system and metaheuristic algorithms. Sci. Total Environ. 615, 438–451. https://doi.org/10.1016/j.scitotenv.2017.09.262

Thanh Noi, P., Kappas, M., 2017. Comparison of Random Forest, k-Nearest Neighbor, and Support Vector Machine Classifiers for Land Cover Classification Using Sentinel-2 Imagery. Sensors (Basel). 18, 18. https://doi.org/10.3390/s18010018

Thornton, P.K., Ericksen, P.J., Herrero, M., Challinor, A.J., 2014. Climate variability and vulnerability to climate change: A review. Glob. Chang. Biol. https://doi.org/10.1111/gcb.12581

Tien Bui, D., Pradhan, B., Lofman, O., Revhaug, I., Dick, O.B., 2012. Landslide susceptibility mapping at Hoa Binh province (Vietnam) using an adaptive neuro-fuzzy inference system and GIS. Comput. Geosci. 45, 199–211. https://doi.org/10.1016/j.cageo.2011.10.031

Tien Bui, D., Tuan, T.A., Hoang, N.D., Thanh, N.Q., Nguyen, D.B., Van Liem, N., Pradhan, B., 2017. Spatial prediction of rainfall-induced landslides for the Lao Cai area (Vietnam) using a hybrid intelligent approach of least squares support vector machines inference model and artificial bee colony optimization. Landslides 14, 447–458. https://doi.org/10.1007/s10346-016-0711-9

Tiwari, A.K., Risse, L.M., Nearing, M.A., 2000. Evaluation of WEPP and its comparison

with USLE and RUSLE. Trans. Am. Soc. Agric. Eng. 43, 1129–1135. https://doi.org/10.13031/2013.3005

Tiwari, D.N., Loof, R., Paudyal, G.N., 1999. Environmental-economic decision-making in lowland irrigated agriculture using multi-criteria analysis techniques. Agric. Syst. 60, 99–112. https://doi.org/10.1016/S0308-521X(99)00021-9

Tralli, D.M., Blom, R.G., Zlotnicki, V., Donnellan, A., Evans, D.L., 2005. Satellite remote sensing of earthquake, volcano, flood, landslide and coastal inundation hazards, in: ISPRS Journal of Photogrammetry and Remote Sensing. Elsevier, pp. 185–198. https://doi.org/10.1016/j.isprsjprs.2005.02.002

Turner, W., Spector, S., Gardiner, N., Fladeland, M., Sterling, E., Steininger, M., 2003. Remote sensing for biodiversity science and conservation. Trends Ecol. Evol. https://doi.org/10.1016/S0169-5347(03)00070-3

Udayakumara, E.P.N., Shrestha, R.P., Samarakoon, L., 2011. People ' s perception and socioeconomic determinants of soil erosion : A case study of Samanalawewa watershed , Sri Lanka. Int. J. Sediment Res. 25, 323–339. https://doi.org/10.1016/S1001-6279(11)60001-2

Udayakumara, E.P.N., Shrestha, R.P., Samarakoon, L., Schmidt-Vogt, D., 2012. Mitigating soil erosion through farm-level adoption of soil and water conservation measures in Samanalawewa Watershed, Sri Lanka. Acta Agric. Scand. Sect. B Soil Plant Sci. 62, 273–285. https://doi.org/10.1080/09064710.2011.608708

Udayakumara, E.P.N., Shrestha, R.P., Samarakoon, L., Schmidt-Vogt, D., 2010. People's perception and socioeconomic determinants of soil erosion: A case study of Samanalawewa watershed, Sri Lanka. Int. J. Sediment Res. 25, 323–339. https://doi.org/10.1016/S1001-6279(11)60001-2

ul Haq, S., Boz, I., 2020. Measuring environmental, economic, and social sustainability index of tea farms in Rize Province, Turkey. Environ. Dev. Sustain. 22, 2545–2567. https://doi.org/10.1007/s10668-019-00310-x

UNISDR, 2021. Inventar [WWW Document]. Desaster Inf. Syst. URL http://www.desinventar.lk:8081/DesInventar/ (accessed 5.14.21).

Valavanis, K.P., Vachtsevanos, G.J., 2015. Handbook of unmanned aerial vehicles, Handbook of Unmanned Aerial Vehicles. Springer Netherlands. https://doi.org/10.1007/978-90-481-9707-1

van der Knijff, J.M., Jones, R.J.A., Montanarella, L., 2000. Soil erosion risk assessment in Europe, Luxembourg: Office for Official Publications of the European Communities.

Vergari, F., 2015. Assessing soil erosion hazard in a key badland area of Central Italy. Nat. Hazards 79, 71–95. https://doi.org/10.1007/s11069-015-1976-3

Verheijen, F.G.A., Jones, R.J.A., Rickson, R.J., Smith, C.J., 2009. Tolerable versus actual soil erosion rates in Europe. Earth-Science Rev. https://doi.org/10.1016/j.earscirev.2009.02.003

Vermeulen, S.J., Campbell, B.M., Ingram, J.S.I., 2012. Climate change and food systems. Annu. Rev. Environ. Resour. https://doi.org/10.1146/annurev-environ-020411-130608

Vermote, E.F., El Saleous, N.Z., Justice, C.O., 2002. Atmospheric correction of MODIS

data in the visible to middle infrared: First results. Remote Sens. Environ. 83, 97–111. https://doi.org/10.1016/S0034-4257(02)00089-5

Vrieling, A., 2006. Satellite remote sensing for water erosion assessment: A review. Catena. https://doi.org/10.1016/j.catena.2005.10.005

Vrieling, A., Sterk, G., de Jong, S.M., 2010. Satellite-based estimation of rainfall erosivity for Africa. J. Hydrol. 395, 235–241. https://doi.org/10.1016/j.jhydrol.2010.10.035

Wang, C., Zhang, Z., Paloscia, S., Zhang, H., Wu, F., Wu, Q., 2018. Permafrost soil moisture monitoring using multi-temporal TerraSAR-X data in Beiluhe of Northern Tibet, China. Remote Sens. 10, 1577. https://doi.org/10.3390/rs10101577

Wang, X., Xie, H., Guan, H., Zhou, X., 2007. Different responses of MODIS-derived NDVI to root-zone soil moisture in semi-arid and humid regions. J. Hydrol. 340, 12–24. https://doi.org/10.1016/j.jhydrol.2007.03.022

Wang, Z., Hou, Y., Fang, H., Yu, D., Zhang, M., Xu, C., Chen, M., Sun, L., 2012. Effects of plant species diversity on soil conservation and stability in the secondary succession phases of a semihumid evergreen broadleaf forest in China. J. Soil Water Conserv. 67, 311–320. https://doi.org/10.2489/jswc.67.4.311

Waring, R.H., Coops, N.C., Fan, W., Nightingale, J.M., 2006. MODIS enhanced vegetation index predicts tree species richness across forested ecoregions in the contiguous U.S.A. Remote Sens. Environ. 103, 218–226. https://doi.org/10.1016/j.rse.2006.05.007

Warren, S.D., Alt, M., Olson, K.D., Irl, S.D.H., Steinbauer, M.J., Jentsch, A., 2014. The relationship between the spectral diversity of satellite imagery, habitat heterogeneity, and plant species richness. Ecol. Inform. 24, 160–168. https://doi.org/10.1016/j.ecoinf.2014.08.006

Wessels, K.J., Prince, S.D., Malherbe, J., Small, J., Frost, P.E., VanZyl, D., 2007. Can human-induced land degradation be distinguished from the effects of rainfall variability? A case study in South Africa. J. Arid Environ. 68, 271–297. https://doi.org/10.1016/j.jaridenv.2006.05.015

Wessels, K.J., Prince, S.D., Reshef, I., 2008. Mapping land degradation by comparison of vegetation production to spatially derived estimates of potential production. J. Arid Environ. 72, 1940–1949. https://doi.org/10.1016/j.jaridenv.2008.05.011

Wessels, K.J., van den Bergh, F., Scholes, R.J., 2012. Limits to detectability of land degradation by trend analysis of vegetation index data. Remote Sens. Environ. 125, 10–22. https://doi.org/10.1016/j.rse.2012.06.022

West, T.O., Post, W.M., 2002. Soil Organic Carbon Sequestration Rates by Tillage and Crop Rotation. Soil Sci. Soc. Am. J. 66, 1930–1946. https://doi.org/10.2136/sssaj2002.1930

Westra, S., Alexander, L. V., Zwiers, F.W., 2013. Global increasing trends in annual maximum daily precipitation. J. Clim. 26, 3904–3918. https://doi.org/10.1175/JCLI-D-12-00502.1

Whitlow, R., 1988. Soil erosion and conservation policy in Zimbabwe. Past, present and future. Land use policy 5, 419–433. https://doi.org/10.1016/0264-8377(88)90076-2

Wibowo, A., Ismullah, I.H., Dipokusumo, B.S., Wikantika, K., 2012. Land degradation

model based on vegetation and erosion aspects using remote sensing data. ITB J. Sci. 44 A, 19–34. https://doi.org/10.5614/itbj.sci.2012.44.1.3

Wicaksono, P., Hafizt, M., 2018. Dark target effectiveness for dark-object subtraction atmospheric correction method on mangrove above-ground carbon stock mapping. IET Image Process. 12, 582–587. https://doi.org/10.1049/iet-ipr.2017.0295

Wickramagamage, P., 2016. Spatial and temporal variation of rainfall trends of Sri Lanka. Theor. Appl. Climatol. 125, 427–438. https://doi.org/10.1007/s00704-015-1492-0

Wijesekera, N.T.S., Samarakoon, L., 2013. Extraction of Parameters and Modelling Soil Erosion Using Gis in a Grid Environment. J. Chem. Inf. Model. 53, 1689–1699.

Wijesundara, N.C., Abeysingha, N.S., Dissanayake, D.M.S.L.B., 2018. GIS-based soil loss estimation using RUSLE model: a case of Kirindi Oya river basin, Sri Lanka. Model. Earth Syst. Environ. 4, 251–262. https://doi.org/10.1007/s40808-018-0419-z

Wilby, A., Thomas, M.B., 2002. Natural enemy diversity and pest control: Patterns of pest emergence with agricultural intensification. Ecol. Lett. 5, 353–360. https://doi.org/10.1046/j.1461-0248.2002.00331.x

Wilkinson, S.N., Kinsey-Henderson, A.E., Hawdon, A.A., Hairsine, P.B., Bartley, R., Baker, B., 2018. Grazing impacts on gully dynamics indicate approaches for gully erosion control in northeast Australia. Earth Surf. Process. Landforms 43, 1711–1725. https://doi.org/10.1002/esp.4339

Willers, J.L., Wu, J., O'Hara, C., Jenkins, J.N., 2012. A categorical, improper probability method for combining NDVI and LiDAR elevation information for potential cotton precision agricultural applications. Comput. Electron. Agric. 82, 15–22. https://doi.org/10.1016/j.compag.2011.11.010

Wind, Y., Saaty, T.L., 1980. Marketing applications of the analytic hierarchy process. Manage. Sci. 26, 641–658. https://doi.org/10.1287/mnsc.26.7.641

Wischmeier, W., Smith, D., 1978. Predicting rainfall erosion losses: a guide to conservation planning. U.S. Dep. Agric. Handb. No. 537 62–7. https://doi.org/10.1029/TR039i002p00285

Wu, Q., Wang, M., 2007. A framework for risk assessment on soil erosion by water using an integrated and systematic approach. J. Hydrol. 337, 11–21. https://doi.org/10.1016/j.jhydrol.2007.01.022

Wu, X., Niu, R., Ren, F., Peng, L., 2013. Landslide susceptibility mapping using rough sets and back-propagation neural networks in the Three Gorges, China. Environ. Earth Sci. 70, 1307–1318. https://doi.org/10.1007/s12665-013-2217-2

Xue, J., Su, B., 2017. Significant remote sensing vegetation indices: A review of developments and applications. J. Sensors. https://doi.org/10.1155/2017/1353691

Xue, R., Wang, C., Liu, M., Zhang, D., Li, K., Li, N., 2019. A new method for soil health assessment based on Analytic Hierarchy Process and meta-analysis. Sci. Total Environ. 650, 2771–2777. https://doi.org/10.1016/j.scitotenv.2018.10.049

Yan, H., Wang, L., Wang, T.W., Wang, Z., Shi, Z.H., 2020. A synthesized approach for estimating the C-factor of RUSLE for a mixed-landscape watershed: A case study in the Gongshui watershed, southern China. Agric. Ecosyst. Environ. 301. https://doi.org/10.1016/j.agee.2020.107009

Yang, H., Li, S., Chen, J., Zhang, X., Xu, S., 2017. The Standardization and harmonization of land cover classification systems towards harmonized datasets: A review. ISPRS Int. J. Geo-Information. https://doi.org/10.3390/ijgi6050154

Yang, X., Gray, J., Chapman, G., Zhu, Q., Tulau, M., McInnes-Clarke, S., 2018a. Digital mapping of soil erodibility for water erosion in New South Wales, Australia. Soil Res. 56, 158–170. https://doi.org/10.1071/SR17058

Yang, X., Zhang, M., Oliveira, L., Ollivier, Q.R., Faulkner, S., Roff, A., 2020. Rapid assessment of hillslope erosion risk after the 2019–2020 wildfires and storm events in sydney drinking water catchment. Remote Sens. 12, 1–20. https://doi.org/10.3390/rs12223805

Yang, X., Zhu, Q., Tulau, M., McInnes-Clarke, S., Sun, L., Zhang, X., 2018b. Near real-Time monitoring of post-fire erosion after storm events: A case study in Warrumbungle National Park, Australia. Int. J. Wildl. Fire 27, 413–424. https://doi.org/10.1071/WF18011

Yengoh, G.T., Dent, D., Olsson, L., Tengberg, A.E., Tucker, C.J., 2014. The use of the Normalized Difference Vegetation Index (NDVI) to assess land degradation at multiple scales: a review of the current status, future trends, and practical considerations, SpringerBriefs in Environmental Science. Springer International Publishing, Cham. https://doi.org/10.1007/978-3-319-24112-8

Yohannes, H., Soromessa, T., 2019. Integration of Remote Sensing, GIS and MCDM for Land Capability Classification in Andit Tid Watershed, Ethiopia. J. Indian Soc. Remote Sens. 47, 763–775. https://doi.org/10.1007/s12524-019-00949-z

Youssef, A.M., Pourghasemi, H.R., Pourtaghi, Z.S., Al-Katheeri, M.M., 2016. Landslide susceptibility mapping using random forest, boosted regression tree, classification and regression tree, and general linear models and comparison of their performance at Wadi Tayyah Basin, Asir Region, Saudi Arabia. Landslides 13, 839–856. https://doi.org/10.1007/s10346-015-0614-1

Zabihi, H., Alizadeh, M., Langat, P.K., Karami, M., Shahabi, H., Ahmad, A., Said, M.N., Lee, S., 2019. GIS multi-criteria analysis by orderedweighted averaging (OWA): Toward an integrated citrus management strategy. Sustain. 11. https://doi.org/10.3390/su11041009

Zappa, L., Forkel, M., Xaver, A., Dorigo, W., 2019. Deriving field scale soil moisture from satellite observations and ground measurements in a Hilly Agricultural Region. Remote Sens. 11, 2596. https://doi.org/10.3390/rs11222596

Zeng, Z.Y., Cao, J.Z., Gu, Z.J., Zhang, Z.L., Zheng, W., Cao, Y.Q., Peng, H.Y., 2013. Dynamic Monitoring of Plant Cover and Soil Erosion Using Remote Sensing, Mathematical Modeling, Computer Simulation and GIS Techniques. Am. J. Plant Sci. 04, 1466–1493. https://doi.org/10.4236/ajps.2013.47180

Zhang, K., Yu, Y., Dong, J., Yang, Q., Xu, X., 2019. Adapting & testing use of USLE K factor for agricultural soils in China. Agric. Ecosyst. Environ. 269, 148–155. https://doi.org/10.1016/j.agee.2018.09.033

Zhang, X., Srinivasan, R., Van Liew, M., 2009. Approximating SWAT model using artificial neural network and support vector machine. J. Am. Water Resour. Assoc. 45, 460–474. https://doi.org/10.1111/j.1752-1688.2009.00302.x

Zheng, H., Chiew, F.H.S., Charles, S., Podger, G., 2018. Future climate and runoff

projections across South Asia from CMIP5 global climate models and hydrological modelling. J. Hydrol. Reg. Stud. 18, 92–109. https://doi.org/10.1016/j.ejrh.2018.06.004

Zhu, A.X., Miao, Y., Wang, R., Zhu, T., Deng, Y., Liu, J., Yang, L., Qin, C.Z., Hong, H., 2018. A comparative study of an expert knowledge-based model and two data-driven models for landslide susceptibility mapping. Catena 166, 317–327. https://doi.org/10.1016/j.catena.2018.04.003

Zhu, A.X., Wang, R., Qiao, J., Qin, C.Z., Chen, Y., Liu, J., Du, F., Lin, Y., Zhu, T., 2014. An expert knowledge-based approach to landslide susceptibility mapping using GIS and fuzzy logic. Geomorphology 214, 128–138. https://doi.org/10.1016/j.geomorph.2014.02.003